CONTROLLING STEERING USING VISION

Callum David Mole

Submitted in accordance with the requirements for the degree of

Doctor of Philosophy

The University of Leeds

School of Psychology

October 2015

INTELLECTUAL PROPERTY AND PUBLICATIONS

The candidate confirms that the work submitted is his own, except where work which has formed part of jointly-authored publications has been included. The contribution of the candidate and the other authors to this work has been explicitly indicated below. The candidate confirms that appropriate credit has been given within the thesis where reference has been made to the work of others

Three publications have been produced from research that was undertaken as part of this thesis. Each publication is listed below with a full reference and details of its location within this thesis. In all publications where the candidate is the first author the candidate was solely responsible for the production of the content, with named authors providing support through review and modification only unless otherwise stated.

*Wilkie, R., Mole, C.***,** *Kountouriotis, G., Billington, J. (2015). Prospective steering control is influenced by retinal flow.* Journal of Vision*. 15(12):414*

Poster presented at Vision Sciences Society 2015, by Richard M. Wilkie, based on the data presented in **Chapter 5**. Only material produced by Callum D. Mole has been used in the thesis.

Mole, C., Kountouriotis, G., Billington, J., & Wilkie, R.M. (2015). Steering control using feedback from near road edges does not rely upon retinal flow. Journal of Vision*. 15(12):415*

Poster presented at Vision Sciences Society 2015, based on data presented in **Chapter 7**.

Mole, C., Kountouriotis, G., Billington, J. & Wilkie, R. M. (2014). Going with the flow when driving with road edges? Perception. *43(5):475-476.*

Poster presented at the Applied Vision Association Annual Meeting 2014 (York) and Vision Leads to Action 2014 (Birmingham), based on data from **Chapters 3-4.**

Kountouriotis, G.K., Shire, K.A., Mole, C.D., Gardner, P.H., Merat, N., & Wilkie, R.M. (2013). Optic flow asymmetries bias high-speed steering. Journal of Vision. 13(10):23, 1-9.

&

Kountouriotis, G., Mole, C., Merat, N., Gardner, P., & Wilkie, R. (2015). Steering along curved paths is influenced by global flow speed not speed asymmetry. Journal of Vision. 15 (12):416

The flow manipulation used in **Chapters 2-4** was adapted from libraries developed by Richard M. Wilkie & Kountouriotis, G. K. These libraries have led to a published manuscript and a poster presented at Vision Sciences Society 2015 by Kountouriotis, G. K.

ACKNOWLEDGEMENTS

I would not have conducted research of any sort, let alone finished a Thesis, were it not for Richard Wilkie's tremendous guidance, patience and insight. Thanks must also go to Georgios Kountouriotis for programming advice and moral support, and to Mark Mon-Williams and Jac Billington for general guidance and passion. All members of the Perception, Action and Cognition Laboratory must also receive thanks for creating an environment where it is a pleasure to work, and I am indebted to Mark Hullah and Rob Bromley whom I have relied on extensively to fix my bumbling technical mishaps.

Special thanks must also go to the postgraduate cohort at Leeds for providing impeccable social support over coffee, beers, and whisky, but in particular to my office mates, Oscar, Radka, Bex, Katy, Dharsh, Emma, and Helen, who have provided interminable cheer to buoy my spirits despite invariably being rewarded with a grunt and a furrowed brow.

Lastly, heartfelt thanks go to friends and family, both North and South of the Watford Gap, for giving me inspiration and energy over the last three years through all manner of adventures.

ABSTRACT

The Two-level model is a popular account of how humans use visual information to successfully control steering within road edges. A guidance component uses information from far regions to preview upcoming steering requirements, and a compensatory component uses information from near regions to stabilise position-in-lane. Researchers who have considered the case of driving often treat road edges as the sole informational input for controlling steering, but this approach is not consistent with the notion that the human visual system adaptively uses multiple inputs to maintain robust control of steering. A rich source of information which may also be useful for steering control is optic flow. Chapter 2 demonstrates that optic flow *speed* is used to control steering even with road edges present. Chapters 3-5 develop a framework to examine how use of flow speed changes depending on the availability of guidance or compensatory road edge information, and demonstrate that use of flow speed increases only when guidance level information (*far* road edges) is present. Chapters 6-7 go on to examine the contribution of flow *direction* to controlling steering within road edges, and demonstrate that the use of flow direction appears to be yoked to the presence of compensatory information (*near* road edges). Together, these experiments demonstrate that the contribution of flow information to controlling steering within road edges can be understood within the context of two-level steering, and show that an approach which emphasise robust control through combining multiple informational inputs is vital if we are to fully understand how the visual-motor system solves the problem of steering along constrained paths.

CONTENTS

LIST OF FIGURES

LIST OF TABLES

LIST OF ABBREVIATIONS

FoE	-	Focus of Expansion
ED	-	Egocentric Direction
RD	-	Retinal Direction
ERD	-	Extra-retinal Direction
REs	-	Road-Edges
VR	-	Virtual Reality
NHST	-	Null-hypothesis significance testing
SB	-	Steering Bias
RMSE	-	Root-mean-squared error
SWJ	-	Steering Wheel Jerk
FISB	-	Flow-Induced Steering Bias
H1	-	Modulation Hypothesis
H2	-	Weighted Combination Hypothesis

CHAPTER 1

GENERAL INTRODUCTION

1.1 Introduction

A hunting hawk, a swimming salmon, a migrating moth: for all these animals, survival rests on their ability to control self-motion through their environment. Locomotion – the controlled movement of an organism through their environment – has been recognised as the most important behaviour in determining the morphology and physiology of animals (Dickinson et al., 2000). However, solving the problem of locomotor control is not simple. Successful locomotion relies on generating a collision-free course through the environment to a goal, exerting mechanical forces to propel the organism down the chosen route, and using sensory feedback to dynamically respond to any errors or disturbances which may occur. Humans routinely achieve this task with apparent ease and little conscious thought, and across a variety of modes of transport – from cycling to wingsuit proximity flying – propelling humans at speeds beyond that experienced during the time-course of recent evolutionary pressures. Vehicular locomotion requires the learning of novel sensorimotor mappings and dynamic forces peculiar to each device (e.g. the rate of change controller that is a steering wheel), but it is sensible to assume that much of the underlying neural circuitry supporting locomotor tasks generalises from walking, to running, to cycling, or driving a car. Driving is now commonplace, with 36.3 million license vehicles (30 million cars) in the UK at the end of June 2015 (Department for Transport, 2015b), and whilst on average 175.4 million miles were travelled without a fatality, there were still 1,775 reported deaths on UK roads in 2014 (Department for Transport, 2015a) demonstrating that there are important safety implications for

improving our understanding of how humans steer successfully. Understanding how humans successfully steer is therefore not only of fundamental scientific interest, but also has direct implications for safety in the modern world.

The problem of controlling locomotion can be understood through a control-theoretic approach. This approach attempts to uncover the sensory inputs for locomotor tasks, and the *control strategies* that govern them. A control strategy is a set of principles or mathematical rules that allow goal directed behaviour given variation in the quality or nature of sensory inputs. For locomotor tasks, human control is predominantly driven by visual inputs (Gibson, 1958). Gibson (1958) proposed some general laws of control that could underpin biological locomotion which has inspired many attempts to capture complex locomotor behaviour with simple laws of control (e.g. Fajen & Warren, 2003; Kim & Turvey, 1999; Land & Lee, 1994; Lee & Lishman, 1977; Salvucci & Gray, 2004; Wann & Swapp, 2000; Warren, Kay, Zosh, Duchon, & Sahuc, 2001; Wilkie & Wann, 2003). The primary thrust of this thesis is to build on these models to better describe the visual inputs needed for successful locomotion and the control strategies which govern their use. This introduction will first discuss the information sources that are available to a locomoting agent throughout any environment, before turning attention towards the specific control problems presented by having to generate trajectories that are constrained by defined road edges.

1.2 Optic Flow (on straight paths)

It is useful to start with a description of the visual world presented to a moving observer. Light propagates rectilinearly and reflects off surfaces. This means that at any point of observation in an illuminated environment the eye receives a unique distribution of light rays. The nature of this distribution can give the viewer information about the layout of their environment. If the observer moves forward they will be faced with a different distribution of light rays, and surfaces will appear to translate towards the observer at a rate proportional to the observer's movement, and

inversely proportional to their distance from the observer (Gibson, Olum, & Rosenblatt, 1955). This continuous transformation of texture elements due to self-motion is called *optic flow*, and was first introduced by Gibson (Gibson et al., 1955; Gibson, 1950, 1958) as a potential means of controlling locomotion. If one was to follow a single texture element (imagine, for example, a white dot in an otherwise black room) over successive transformations (i.e. over time), the resultant vector's directional displacement could give information about observer's direction of travel. If the texture element was displaced leftwards the observer would be heading to the right of the target (and vice versa), with a magnitude proportional to heading offset. If the observer was heading on a collision course with the texture element, it would not be displaced leftwards or rightwards. With multiple texture elements, their relative displacement can also give depth information (farther away elements will displace less). Remarkably, these properties mean that they will appear to radiate from a single point that coincides with instantaneous direction of travel (heading; Figure 1.1). This point has been named *focus of expansion* (FoE) – a possible control solution for locomoting towards a goal would be to align the FoE with the desired object or direction (Gibson, 1958).

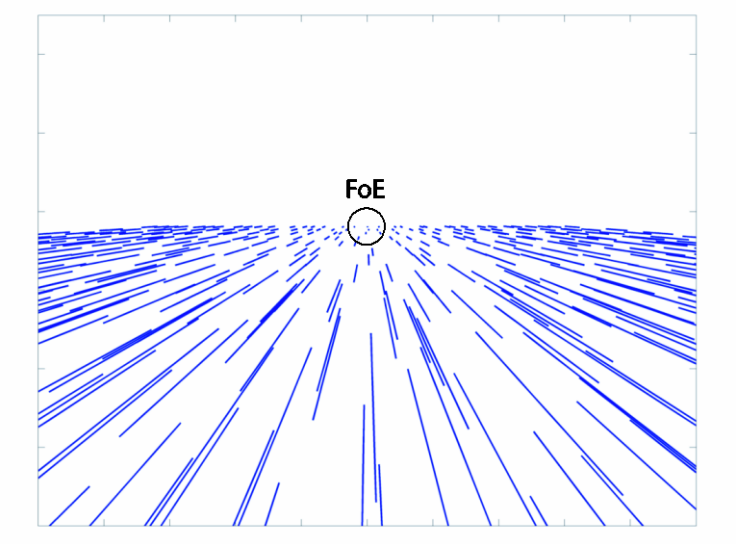

Figure 1.1 Simulation of a linear trajectory across a textured ground plane generating a straight line flow pattern, with the focus of expansion (FoE) at horizon.

The case considered in Figure 1.1 is oversimplified since it requires the eye to be in a fixed direction whilst travelling forward on a linear path. In reality humans do not always fixate straight ahead. Like many other animals humans have evolved mobile eyes that allow adaptive sampling of a visual scene, and although we tend to look where we are going (Hollands, Patla, & Vickers, 2002) we routinely use eye-movements to look at objects within the scene. Furthermore, humans do not always move in straight lines. When travelling at slow speeds (i.e. walking) it is hypothetically possible to stop and pivot to face one's destination then approach directly. At higher speeds (e.g. running, cycling), momentum precludes this strategy and curved trajectories are necessary – additionally many vehicles have a wheelbase which introduces a turning arc. At a more fundamental level, humans have developed locomotor control systems through evolutionary pressure to successfully navigate complex natural terrains, where straight paths (e.g. man-made motorways) are rare. A general theory of locomotive control therefore must account for travelling along curved paths, as Wilkie & Wann (2006, p. 91) surmise:

> *"The general task of locomotion is maintaining a (curved) trajectory and predicting future path, of which a straight trajectory is the limit case of zero curvature".*

Movement of the eyes, head, or body all change the optic flow field stimulus available to the retina (what will from hereon in be referred to as retinal flow). Eye movements add a global rotation to the texture elements in the visual field, which can obfuscate the FoE (Regan & Beverley, 1982). Research evidence suggests that when travelling along linear paths, heading perception remains reliable if the extra-retinal signals (e.g. from the muscles controlling the eye) are known (Royden, Banks, & Crowell, 1992; Royden, Crowell, & Banks, 1994), presumably because the rotation component can be partialled out using the eye-movement signal. Curving trajectories add rotations that are not easily distinguishable from eye movements, creating potentially ambiguous flow fields whereby a single retinal flow snapshot containing translation and rotation elements could potentially represent a number of trajectories ranging from a linear trajectory with eye, head or body rotations through to a curved path without gaze rotations. Given the complexity of computationally resolving this ambiguity (Longuet-Higgins & Prazdny, 1980) there has been much debate over the extent to which flow uniquely provides sufficient information to control steering along complex trajectories – the next section will review this literature.

1.3 Optic Flow travelling along Curved Paths

It is straightforward to observe how heading may be used to control steering on straight paths. If instantaneous heading aligns with the goal, then the observer is on the desired path (Gibson, 1958). However, it is less clear how instantaneous heading may be used to control steering along a curved trajectory. On a curved trajectory, instantaneous heading corresponds with the tangent of the curve (straight ahead) instead of future direction of travel (in the literature, this is usually referred to as *future path;* see Figure 1.2). Steering towards a goal whilst avoiding obstacles requires

anticipatory control (Higuchi, 2013), which is provided by future path, not heading. It is generally agreed that path information is essential for locomotor control, and that path can be reliably estimated (Cheng & Li, 2011; Kim & Turvey, 1998; Warren, Mestre, Blackwell, & Morris, 1991; Wilkie & Wann, 2006)*. The key question (as identified by Lappe, Bremmer, & van den Berg, 1999), remains "*how* is path information obtained from retinal flow and extra retinal signals and *how* is the path predicted" (p. 335).

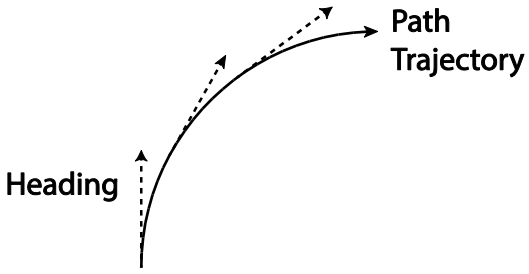

Figure 1.2 An illustration of the difference between heading and path whilst steering a curve.

Some have suggested that path can be perceived by decomposing the retinal flow to retrieve heading information in order to estimate path (Cheng & Li, 2011). Cheng & Li (2011) asked participants to estimate future path trajectory 10m ahead using a post-trial probe, where a trial consisted of viewing a circular path (duration of 1s) over a ground-plane that was either textured, dotted, or populated with life-limited dots. In principle, perceiving future path trajectory requires integrating velocity vectors over time therefore it should not be detectable from life-limited dots, whereas heading perception should be available from all these displays (Cheng & Li, 2011). Cheng & Li

* Confusingly, both Warren et al. (1991) and Kim & Turvey (1998) use the term *heading,* but 'heading' was calculated by forced-choice judgements of *future path* relative to a reference object, not tangential heading. Warren et al. (1991) do propose a method using *vector normals*, which can be calculated by two elements over two frames, thereby providing an instantaneous method of judging path. This is evidenced by accurate circular heading perception when only two elements were in the scene. However, Warren et al. (1991) has been criticised for using low radii bends (Wilkie & Wann, 2006) and an ecologically low threshold for their heading judgments (this latter criticism also applies to Kim & Turvey, 1998; Wann & Land, 2000). On a heading task using tighter bends with a higher heading threshold, circular heading perception may not be as robust (Warren et al., 1991, themselves found that performance dropped off sharply for small radii).

(2011) found that participants were able to estimate future path trajectory just as accurately for life-limited dot displays as for textured- or dot-flow. Similarly, Li, Sweet, & Stone, (2006) and Li, Chen, & Peng, (2009) claim to show accurate heading perception (estimated by aligning virtual line of sight with perceived heading) of curvilinear self-motion on life-limited displays. However, participants determined their own trial length because judgements were only submitted when they were certain. Longer viewing times may have allowed the observer to combine successive estimates of heading therefore produce a more accurate estimate than would have been manageable under short viewing times. Furthermore, both studies (Li et al., 2009, 2006) use a 3D cloud display which could be considered artificially rich compared to the usual viewing conditions during terrestrial locomotion.

Interestingly, Cheng & Li (2011) also found that path perception was most accurate when gaze was fixed along the heading direction, rather than at a point along the future path. This prompted the authors to conclude that one should "look where you are going but not where you want to go" (p. 13). In a recent attempt to provide a neurophysiological basis combined heading and path perception, Layton & Browning (2014) simulated Cheng & Li's (2011) experiment using a computational neuronal model which simultaneously codes heading and path. They find that the results are comparable; suggesting that Cheng & Li's (2011) hypothesis of heading-dependent-path might be computationally viable. In support of their findings, Layton & Browning (2014) claim that "directing gaze in the direction of heading naturally occurs in many activities, such as locomotion and driving" (p. 18). This is certainly not the consensus view, however, with evidence suggesting that this gaze behaviour is not typical of natural locomotion. When asked to saccade to path or heading, observers saccade more accurately to future path (Wilkie & Wann, 2006). Furthermore, it has been consistently shown that drivers prefer to fixate their future path when steering bends (Itkonen, Pekkanen, & Lappi, 2015; Lappi, Pekkanen, & Itkonen, 2013; Lappi & Pekkanen, 2013; Lehtonen, Lappi, Kotkanen, & Summala, 2013; Robertshaw & Wilkie,

2008; Wilkie, Kountouriotis, Merat, & Wann, 2010), and fixating elsewhere for extended periods can actually bias steering trajectories in the direction of fixation (Kountouriotis, Floyd, Gardner, Merat, & Wilkie, 2012).

Studies that monitor eye-movements during active steering control (e.g. Lappi & Pekkanen, 2013; Robertshaw & Wilkie, 2008) demonstrate that gaze behaviours which enhance heading perception (i.e. looking tangential to the curve; Cheng & Li, 2011; Layton & Browning, 2014) are generally not observed in active control of steering, which questions whether the mechanisms involved in perceptual judgments of heading transfer to steering tasks. Unfortunately, none of the psychophysical studies that imply heading perception helps path perception (Li et al., 2009, 2006; Li & Cheng, 2011) assess active control of steering so it is unclear whether display conditions which support accurate heading perception also support accurate steering control. Kountouriotis & Wilkie (2013) attempted to address this issue by directly comparing steering and heading accuracy, and found performance to be comparable with dense flow displays or displays with a textured ground-plane, but degrading the flow information caused steering accuracy to decrease whilst heading judgements remained fairly accurate (although dropped off at lower levels, see Figure 1.3). They conclude that "control of steering curved paths may not solely rely on heading perception" (p. 344). As highlighted by Wann & Land (2000), it may be the case that:

> *"heading may be a post-hoc percept: one that can be recovered by observers if they are required to do so, but that is not actually used in active naturalistic tasks". (p. 324).*

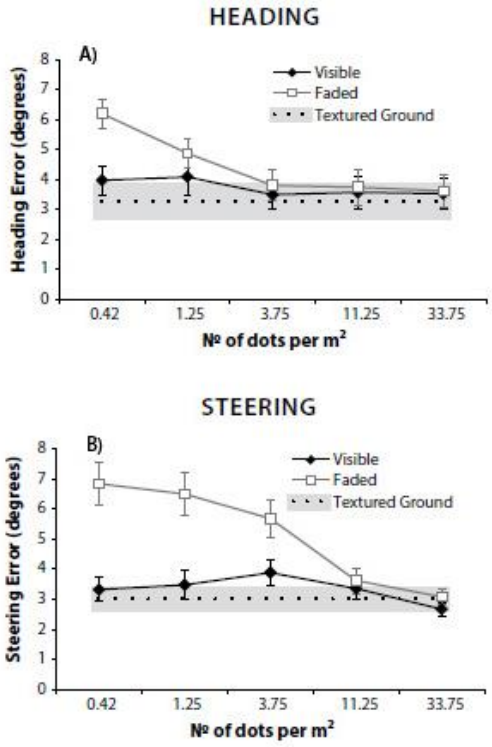

Figure 1.3. A) Heading errors for the different levels of flow visibility (open symbols='faded'; filled symbols='visible') and different numbers of dots on the ground. For a comparison, the error for the texture and ground condition is shown by the dotted line ± standard error of the mean (grey rectangle). B) matches A) but depicts steering error. Figure and caption adapted from Kountouriotis and Wilkie (2013).

Alternatively, *direct path perception* theories circumvent the need to decompose flow to retrieve heading. Wann & Swapp (2000) and Kim & Turvey (1999; see also Wann & Land, 2000) both present an elegant solution to the heading problem through a control law using curvature properties of retinal flow. If one was to fixate on or near the target, the shape of curvature can inform the driver of their course relative to the target (Figure 1.4). If the observer was on course to intercept the target (in a path of constant bearing, be it linear or curved), flow vectors would have minimal curvature (Figure 1.4), and a remarkable property of retinal flow is that all vectors aligned with the course of travel will be straight (Figure 1.4A). Understeering will cause flow vectors

to curve in the direction of oversteering (Figure 1.4B), proportional to the magnitude of the error, and oversteering will cause flow vectors to curve in the opposite direction (Figure 1.4C).

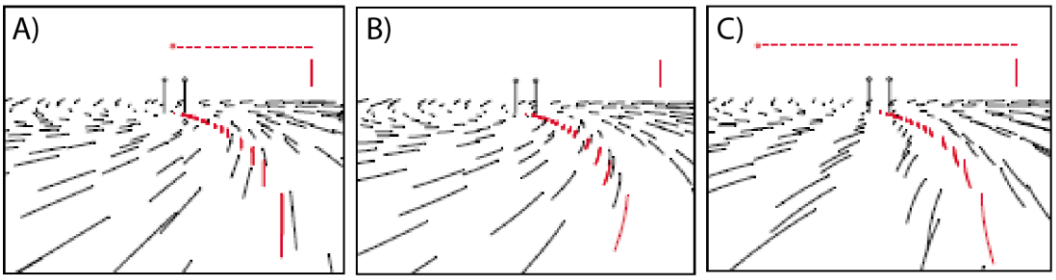

Figure 1.4 Retinal flow patterns during steering whilst fixating between the target poles. The red vertical line indicates initial heading, and the horizontal red line indicates change of heading. A) If the observer is steering appropriately, flow lines on course to the target will remain straight. B) If the observer is understeering, the flow pattern will be centred around the fixation point, but flow lines curve in a direction opposite to the steering error. C) If the observer is oversteering, the curve of flow lines is opposite to B). Figure adapted from Wann & Swapp (2000).

A locomotor strategy involving looking where one wants to go has advantages other than being able to harness 'raw' retinal flow, notwithstanding the obvious advantage of being able to see oncoming obstacles. Fixating a future point on the path gives the driver the egocentric direction (see section 1.4) of the target with respect to the locomotor axis. On a path of constant curvature, keeping the rate of change of egocentric direction to zero means one has matched the curvature of the bend. Wann & Land (2000) proposed that robust locomotor steering around a bend of variable curvature can be achieved through splining together various sections of constant curvature, fixating a future point, and using vertical vectors in retinal flow or egocentric direction, or a combination of the two, as a control input.

The support for this model comes indirectly through a large body of gaze behaviour literature, showing that gaze is generally directed towards the future path during locomotive tasks (Itkonen et al., 2015; Lappi et al., 2013; Lappi & Pekkanen, 2013;

Robertshaw & Wilkie, 2008; Wilkie et al., 2010). Although it is debatable whether retinal flow is actually used in this manner (for a critical view see Saunders & Ma, 2011, and Li & Cheng, 2011), the importance of this framework is that it emphasises that mobile gaze should not be treated as a problem but instead that it can be used directly as a control signal and indirectly to process and alter retinal flow in a useful way.

1.4 Steering without flow

Flow information is often treated as a ubiquitous source of information, but there are many locomotor scenarios where flow is unreliable or unavailable. For example, when driving through rain or snow in the presence of wind, flow may be subject to transformations that are independent of eye, head, or body motion, potentially rendering flow unreliable. Additionally, when in fog, or at night, flow information will be degraded. In conditions of complete darkness (where no flow is available) humans can steer successfully to a target (Wilkie & Wann, 2002). This shows human locomotion may use other information sources of information apart from flow to steer effectively.

The participants in Wilkie & Wann's (2002) study exhibited accurate steering because they were able to perceive the direction of the target relative to their body. This percept can be specified both retinally and non-retinally. Often terminology is confusing, for example, the term *visual direction* has been used to refer both to the general percept of target direction (e.g. Harris & Rodgers, 1999; Harris, 2001; Wann & Wilkie, 2004; Wood, Harvey, & Young, 2000) and specifically the retinal counterpart (e.g. Wilkie & Wann, 2003). Throughout this thesis the general percept of the direction of target relative to the observer's body will be referred to as *egocentric direction* (ED; Howard, 1982; Rushton & Salvucci, 2001), the retinal information will be *retinal direction* (RD), and the extra-retinal information will be *extra-retinal direction* (ERD).

Both RD and ERD can be recovered without reliance on vector patterns, therefore are relatively independent of flow. RD can be specified with respect to a visible marker attached to the locomotor axis[†]. Such visual markers are often very clear in vehicular locomotion. A car often has a windscreen frame, or a bonnet, which can provide visual references for steering. The same can be said for one's arms and handlebars when cycling, or for skis when skiing. A simple strategy to orient to a goal would be to move the target so the angle between visual marker and the target was zero[‡]. Although RD is a powerful source when available, it can be argued that its availability is limited. When running or walking, visual markers are less obvious, although it is possible that peripheral information of nose, orbital ridges, feet and torso may be used (Howard, 1982)[§].

ERD can be specified by eye-in-head and head-on-body orientation information. Eye-in-head orientation is predominantly specified through efferent copies of signals sent to extra-ocular muscles, but also through proprioceptive feedback from those muscles (Bridgeman & Stark, 1991; Howard, 1982). Head-on-body orientation can be specified through proprioceptive feedback from the neck muscles, but also through efference copies and indirectly from vestibular semi-circular canals (although the vestibular system has been shown to contribute little to steering control, Wilkie & Wann, 2005). Whilst RD is only available if there is a suitable visual marker, ERD is always available and can offer valuable information about the eccentricity of a target relative to one's body. The accuracy of ERD alone is hard to assess (attempts are generally confounded

---

[†] There is also the preceding issue of spatially resolving the point of interest from a retinal image (Howard, 1982).This is only an issue when points are in the peripheral field, where acuity is less, and since humans generally foveate the object or point they wish to locomote to the possible error in spatially resolving the image will not be discussed (and is generally taken for granted in the literature).

[‡] Relationships between visual markers and desired angles can be learnt. There is no need for a visual marker to match with the body's midline, this is simply the extreme case (see Wilkie & Wann, 2002). The marker merely needs to be the same orientation as the body so the RD which specifies straight ahead can be learnt. It is possible that multiple estimates of RD can be corroborated to provide a better estimate of target direction (as in with a windscreen frame).

[§] Judgements of straight ahead have been shown to be improved by adding an external visual marker attached to locomotor axis, suggesting the eccentricity of peripheral body parts alone might be too large for use in specifying RD (Howard, 1982).

by having to hold a previous eye position in memory, e.g. Blouin, Gauthier, & Vercher, 1995), since it is very rare to have ERD without some retinal information, for example, in Wilkie & Wann's (2002) study where drivers steer to a target in darkness, ERD is accompanied by retinal drift of the target. Whilst there are cases where ERD can be biased, such as after a prolonged eccentric fixation, or during a prolonged fixation without any additional visual information (the *autokinetic* effect), it is generally accepted that ERD is accurate and precise enough to strongly contribute to ED (Howard, 1982). Grasso, Prévost, Ivanenko, & Berthoz (1998) showed that visual look-ahead was displayed even when turning corners without visual information (eyes closed), a finding Bernardin et al. (2012) replicated with participants mentally simulating complex trajectories. Both these studies strongly suggest the utility of ERD information in specifying egocentric direction.

Both RD and ERD give rise to the percept of ED. Some control strategies for locomoting using ED are relatively straightforward. If there were no turning constraints (e.g. momentum or wheelbase) an animal could simply pivot so the angle between the locomotor axis and the target was nulled, then move forward. A strategy such as this can be observed in the jumping spider (salticidae), where it turns to face a target before jumping towards it (Land, 1971). When an animal is not moving, there is no flow. In principle, flow may be used during the pivoting movement of the spider, but it has been shown that the pivot of this creature is an open-loop mechanism (Land, 1971). Therefore, the jumping spider is an example of an animal that relies little on flow information, and navigates through ED (specifically, RD). In situations where there are turning constraints, the egocentric direction angle could be nulled over time with the rate of change of angle dependent on the turning constraints. This would produce a curved path to a target.

In most natural locomotion settings it is hard to distinguish between steering using ED and retinal flow information, since both can be used to independently explain linear and curved trajectories. Rushton, Harris, Lloyd, & Wann (1998) report an

innovative experimental design to disentangle the two sources of information using prisms. Prisms can displace light sideways, so if an observer views the world through a prism the entire visual scene will appear retinally displaced with respect to its veridical position. This means that when viewing a target, the perceived ED of that target will be offset. However, since all light coming into the eye is shifted by the same amount, the properties of the flow field do not change. To illustrate this fact, consider walking straight towards the real-world location of the target whilst wearing prisms. Since the real-world direction of visible surfaces is still straight ahead (the prism simply translates the entire flow field), the FoE would still be centred on the target, but the target would be offset. If one proceeded to the target using ED they would walk with a constant heading offset because they would orient themselves towards the retinally displaced target position instead of the real-world target position: which would result in a curved trajectory. However, if one was to walk by positioning the FoE over the target, a straight line trajectory would be taken. Rushton et al. (1998) had participants walk to a straight-ahead target while wearing prisms that displaced the target by 16 degrees, and observed that participants generally took curved paths to the target, with a constant heading error of approximately 85% of prismatic displacement[**]. It was concluded that observers may rely little on flow, instead using ED of objects and fixation points to navigate through the world.

This sparked a flurry of research and debate on whether humans predominantly use flow (Fajen & Warren, 2000) or ED (Harris & Bonas, 2002; Harris & Rodgers, 1999; Harris, 2001; Rushton & Salvucci, 2001; Wann & Land, 2000). There is now strong evidence that humans can utilise either cue. Both Wood et al. (2000) and Warren et al. (2001) demonstrated that walking trajectories evident of an ED strategy are observed when the quality of flow information is poor, but straighter trajectories (indicative of walking using flow information) are taken if flow information is rich (these studies are

[**] A heading error of less than the prismatic displacement is consistent with an 'immediate correction' effect when wearing prisms (Rock, Goldberg, & Mack, 1966; Rushton & Salvucci, 2001). This found in most prism studies, and is discussed further in Harris and Bonas (2002).

reviewed in more detail in Chapter 6). The combinatorial approach to ED and flow has been strongly supported by empirical data from Wilkie & Wann (2002, 2003) suggesting humans combine ERD, RD and flow information weighted by their relative strength.

1.5 Steering with Road Edges

The tasks considered so far have predominantly involved steering to (or being steered to) a single target, or viewing simulated self-motion using an open-field display with no visible target. However, it is routinely the case that locomotor trajectories are constrained by a variety of obstacles and/or boundaries: be it forest trail, pavement, country lane or motorway. Investigations of how humans drive when there are visible road edges (REs) seem to have developed relatively independently of literature investigating the more general case of steering to a goal.

Consider steering down a single track road. This task may be achieved by simple feedback control. To start, the driver needs to merely move themselves forward. At the next moment, the driver can perceive their current position using splay rate (e.g. Beall & Loomis, 1996) or egocentric direction (Salvucci & Gray, 2004) relative to the near road edges and compare that to their ideal position (e.g. centre of the road). The third step requires the driver to produce a motor command that reduces the error signal to zero. This could be a continuous loop, enabling the driver to correct for internal disturbances (e.g. signalling noise, Faisal, Selen, & Wolpert, 2008) or external disturbances (e.g. crosswind) in order to reduce trajectory error to acceptable limits.

A feedback control strategy requires the driver to continuously monitor the road. In real world scenarios dedicated monitoring is unlikely, with the driver's attention distributed across the scene (e.g. to monitor road signs, passengers, pedestrians and other cars) and the driver may look at the road only intermittently. There are also inherent delays between perception and action with additional system delays due to

second-order control[††]. At slow driving speeds errors develop only gradually, therefore feedback mechanisms can be used at a low gain to smoothly correct for errors. As driving speeds increase, however, there comes a point at which errors develop so quickly that gradual correction is not possible. The driver now has to make large corrections to compensate for the rapid error growth at each moment. Under these conditions a feedback control strategy results in oscillatory trajectories and jerky steering, so compensatory feedback based on lane position is no longer sufficient to provide adequate control (Land & Horwood, 1995).

Fortunately, there are alternatives to pure compensatory control. Humans have a mobile gaze system that allows distant information to be sampled in order to anticipate future steering requirements. In principle such prospective information could be sufficient to steer (without need for immediate error feedback), however, these prospective signals tend to be less indicative of the immediate positional error. Optimal motor control would therefore make use of both feedforward and feedback control systems, with the feedforward component reducing delays and error thus allowing feedback control to operate successfully (cf. Desmurget & Grafton, 2000).

A form of this two-stage framework has been applied to steering control. Donges (1978) stipulated that steering consisted of both an anticipatory process and a compensatory, error correction process. The anticipatory mechanism specifies future steering requirements, and the compensatory mechanism monitors positional error (Figure 1.5).

[††] Second order control, or *acceleration control*, means there are two integrations between the control input and device output. Change in steering wheel angle corresponds to a change in lateral acceleration (heading velocity), which integrates to specify lateral velocity (heading), which integrates to specify position. Therefore, there is a delay inherent in the control system between input (change in steering wheel angle) and device output (Jagacinski & Flach, 2003).

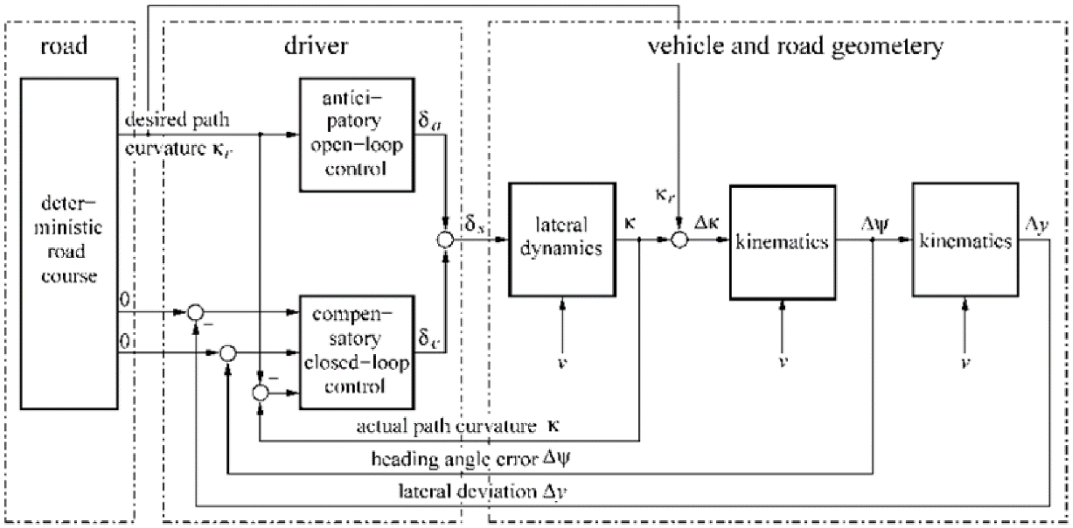

Figure 1.5 Two-level model, comprising of anticipatory 'open-loop' controls which previews desired path curvature, and a compensatory 'closed-loop' control which stabilises lateral deviation. Figure taken from Donges (1978).

The 'two-level' framework is conceptually similar to feedforward and feedback control, and often the terms feedforward, open-loop, prospective, anticipatory and guidance are used interchangeably (Donges, 1978; Land, 1998). As a result, feedforward (open-loop) control is often conflated with feedback (closed-loop) control using information from a far point. This is a non-trivial confusion. Although some two-level models treat guidance control as a parallel, open-loop, process (e.g. Markkula, Benderius, & Wahde, 2014; for reviews see Plöchl & Edelmann, 2007, or Steen, Damveld, Happee, van Paassen, & Mulder, 2011), evidence suggests that the internal models needed for open-loop control are poor (Cloete & Wallis, 2009; Macuga, Beall, Kelly, Smith, & Loomis, 2007). On the other hand, there is extensive visual science literature looking at how perceptual variables are 'picked up' from the scene and used to adjust steering towards a goal under the tacit framework of feedback control (e.g. Salvucci & Gray, 2004; Wilkie, Wann, & Allison, 2008; see also Mars, 2011; Saleh, Chevrel, Mars, Lafay, & Claveau, 2011; Sentouh, Chevrel, Mars, & Claveau, 2009). To avoid confusion, this thesis uses the terms originally proposed by Donges (1978) of "guidance control" to describe control mechanisms that use

information from a far point, and "compensatory control" to describe control mechanisms using information from a near point.

The most commonly cited two-level steering model in the vision science literature is Salvucci & Gray's two point visual control model (2004). Salvucci and Gray (2004) reformulated Donges's (1978) two-level approach into a simple 'Proportional-Integral' feedback controller using egocentric direction for a (fixated) far point and a (peripherally picked up) near point. This model (Equation 1.1) acts to keep the egocentric direction angle of a near and a far point stable (the proportional part) whilst simultaneously reducing error of a near point relative to some ideal reference point (e.g. centre of the road; the integral part). The continuous form of the model can be expressed as:

$$\varphi = k_f\theta_f + k_n\theta_n + k_I\theta_n \tag{1.1}$$

Whereby θ_n and θ_f represent the egocentric direction angle of a near point and a far point respectively, k_f and k_n are constant values scaling the proportional terms, and k_I is a constant scaling the integral term. Salvucci & Gray (2004) demonstrate that by simply changing the location of the near or far point, or changing the weights attributed to k_f, k_n, or k_I, this simple model can account for various steering behaviours, such as curve negotiation, corrective steering, lane changing, and also individual differences in steering strategy. Consistent with the two-level predictions, the far point acts to smoothly guide steering but not necessarily maintain position in the centre of the road. The near point acts to keep the vehicle in the lane centre, but without the far region to provide anticipatory information about changing steering requirements it would be expected that "bang-bang" steering would occur (Salvucci & Gray, 2004).

A highly influential source of empirical support for the two-level model comes from Land & Horwood (1995). Land and Horwood (1995) used a basic driving simulator to investigate how varying RE information affected steering along a winding road (displayed as white road edges super-imposed onto a black background). Participants

were asked to steer a central trajectory whilst RE information was restricted to one or two 1° viewing 'windows' (Figure 1.6A). Crucially, equal performance to a full road could be achieved with one viewing window placed in a far region (1-2° down from horizon), and one viewing window in the near region (placed 7-8° down from the true horizon; Figure 1.6B). This suggests that steering can be accurate as long as there is a guidance and compensatory signal available. When only one viewing window was available, an optimum region was identified midway between the far and near regions, at 5.5° down from the true horizon (Figure 1.6B), suggesting that having either a compensatory or guidance signal alone is not sufficient for accurate steering. Additionally, Figure 1.6C shows that steering became more unstable with one viewing window as it was moved lower in the scene (effectively removing guidance information). However, if guidance information was provided by a viewing window fixed to a far region, steering was often as stable as when a full road was available (Figure 1.6C). The results can be summarised thus: when only near road was available, steering became jerky, characterised by 'bang-bang' control. When only far road was available, steering was smoother, but less accurate. This provides crucial support for Donges' (1978) proposal that the provision of guidance information allows for smooth steering, and that a switch to compensatory control would be identified by an increase in jerky steering behaviours.

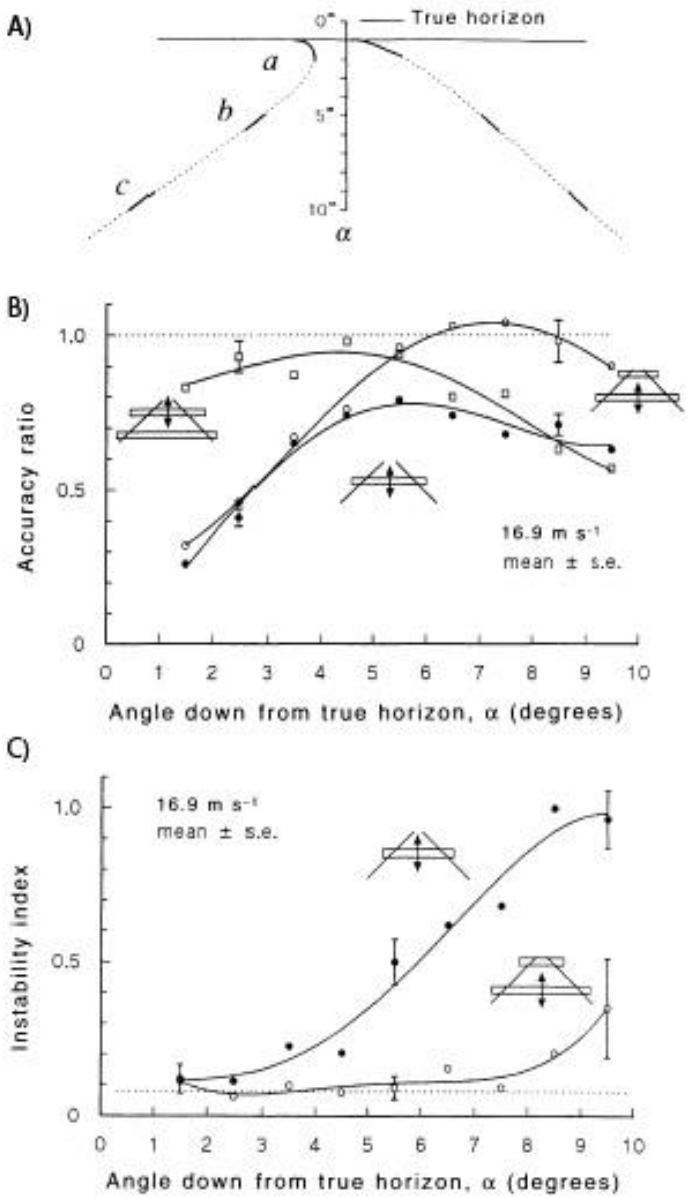

Figure 1.6 Empirical support for two-level model. A) Locations of viewing windows relative to true horizon. B) Accuracy of steering as a ratio of the standard deviation of lane position with a full road divided by the standard deviation (an accuracy ratio of one indicates steering just as accurate to full road conditions) when only one or two 1° viewing windows are visible. C) Instability index was a product of the number and amplitude of spike-like steering movements. In both B) and C) performance of steering with a full road is shown by a dotted line. Figures adapted from Land & Horwood (1995).

Whilst the two-level narrative of Land & Horwood (1995) is appealing, other papers have failed to replicate some of its key conclusions. Chatziastros, Wallis, & Bülthoff (1999) used Land and Horwood's (1995) road manipulations to investigate the effect of field of view and surface texture on steering performance (the results relating to field of view and surface texture are covered in Chapter 3). With one viewing window, Chatziastros et al. (1999) found that steering position was highly variable when the viewing window is at 1-2° or 2-3° down from the horizon, but between 3°-10° there was little difference in steering accuracy. This contrasts with Land and Horwood's (1995) reported half-way optimum. Additionally, Chatziastros et al. (1999) found that the addition of a fixed far region did not improve steering accuracy nor decrease instability – this is in direct contrast to Land & Horwood's (1995) findings (Figure 1.6B-C), and disagrees with the notion that guidance information allows for smoother steering. However, when a near region was added to a far region steering behaviour was greatly affected – reducing steering error but increasing jerky behaviour – which agrees with the notion that the near region allows for compensatory control characterised by increased jerk but more accurate steering (Land & Horwood, 1995; Land, 1998). Chatziastros et al.'s results (1999) appear to suggest that steering control is predominantly determined by the presence of near road information. The road sections in Chatziastros et al.'s (1999) study ranged from 1.06°/s to 8.45°/s, which are fairly shallow bends. Land & Horwood (1995) do not report the road characteristics of "Queens Drive", but describe it as 'tortuous' or 'twisting'. It is possible that the roads in Chatziastros et al.'s (1999) study were less demanding, thus guidance information may not have been weighted highly.

Land & Horwood's findings were also criticised by Cloete & Wallis (2011). Cloete and Wallis (2011) suggested that the low refresh rate in Land & Horwood's study (7Hz) may have exacerbated some of the observed steering effects. Cloete and Wallis (2011) replicated Land and Horwood's (1995) experiment using two refresh rates: 7.2Hz and 72Hz. They found that steering behaviour was less accurate (measured by standard

deviation of the deviation from the road centre) and jerkier at the lower refresh rate, and that this effect was especially pronounced when only a near road segment was viewed. With a 72Hz update rate Cloete & Wallis (2011) failed to find evidence of either i) a mid-road optimum, ii) a decrease in steering accuracy when near road information was removed, and iii) equivalent performance to full road conditions when road edge visibility is restricted to one viewing window in the far region and one in the near region (as per Land & Horwood, 1995). They do, however, replicate the finding that steering behaviour becomes increasingly jerkier as guidance level information is removed (this interaction is reduced in 72Hz displays compared with the 7.2Hz refresh rate, but still consistent across participants; Cloete & Wallis, 2011).

Although both Chatziastros et al. (1999) and Cloete & Wallis (2011) question Land & Horwood's (1995) findings of a mid-road optimum and that adding guidance level information improves steering performance, their studies support the two-level prediction that compensatory control (using information from near regions) leads to accurate steering at the expense of jerky behaviour. More recent support for the two-level model comes from Frissen & Mars (2014), who applied an opacity mask (20%, 40%, 60%, 80%, or 100% opaque) to either the top half or bottom half of the visual field, thus systematically degraded guidance or compensatory information respectively. Removing compensatory information led to an increase in steering variability (measured by standard deviation of lane position) although mean lane position and steering smoothness were no different to baseline performance. This agrees with the two-level proposal that steering with guidance level information tends to be smooth but imprecise (Land, 1998). Removing guidance information, however, led to jerkier steering which was also more variable and less accurate (i.e. there were large errors in mean lane position) than baseline. Frissen & Mars (2014) suggest that error increased when guidance information was degraded because of the higher speeds used ($25ms^{-1}$ vs $16.9ms^{-1}$ used in Chatziastros et al., 1999; Cloete & Wallis, 2011; Land

& Horwood, 1995) which will require more anticipatory information for successful control (Land, 1998; Salvucci & Gray, 2004).

Although the two-level model still lacks definitive empirical support, Frissen & Mars (2014) have provided recent evidence in favour of the approach. Additionally, there is also convergent fMRI evidence that suggests near (MT+) and far (superior parietal lobe and medial intraparietal sulcus) road edges may be processed by different functional brain regions (Billington, Field, Wilkie, & Wann, 2010). A two-level approach to explaining steering control is now commonplace amongst computational models of steering behaviour (Markkula et al., 2014; Plöchl & Edelmann, 2007), and appears to be a useful way of describing the nature of the control task of driving when road edges are present.

1.6 Modelling gaze and steering behaviour.

Two-level models usually posit that the driver looks at a far point to retrieve anticipatory information, but two-level models generally do not make specific predictions about *where* a driver should look to obtain the anticipatory information. Candidate models for where gaze falls during curve driving have broadly been grouped into tangent point (TP) fixation or future path (FP) fixation (Lappi, 2014; Figure 1.7).

The tangent point is a point on the inside lane edge where the line of sight is tangential to the lane edge, which corresponds with the point of reversal of the visual projection of the inside edge (Figure 1.7). Land & Lee (1994) recorded eye-movements of participants driving a real-world car along Queens Drive in Edinburgh (a skeletal model of this road was used in Land & Horwood's, 1995, study), and found that participants stereotypically made saccades to the tangent point 1-2s before bend entry, then during the bend drivers fixated on the TP 80% of the time.

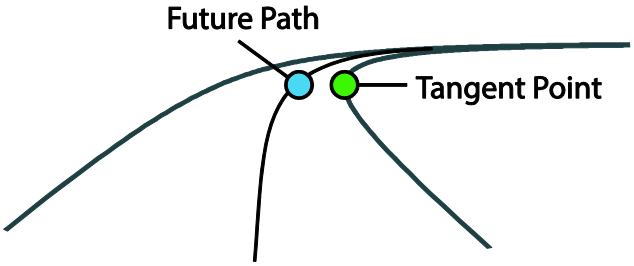

Figure 1.7 Some steering models suggest the tangent point (green) is where gaze predominantly falls during steering curved bends (Land & Lee, 1994), whereas others suggest that the future path (blue) is where gaze predominantly falls (Wilkie, Wann & Allison, 2008).

Land & Lee (1994) propose a simple control law that may explain why the TP was fixated throughout the bend. Since the placement of the TP is determined by the optical properties of the bend relative to the observer (i.e. it is not fixed in the world), if the angle (θ) between the observer and the TP remains stable during a bend then the observer has matched the curvature of the bend. Additionally, assuming the driver knows the distance from the inside edge (d), bend curvature can be simply calculated as follows:

$$Curvature = \frac{1}{r} = \frac{\theta^2}{2d} \tag{1.2}$$

The TP model is a seductively parsimonious account of curve driving. However, accurate estimation of curvature is necessary for drivers to plan steering using TP orientation, and it has been demonstrated that observers are generally poor at estimating curvature of bends (Fildes & Triggs, 1985; Shinar, 1977). Alternatively, a driver could keep the angle of TP stable during a bend, which does not require estimation of curvature. However, this would require the driver to maintain a constant lateral distance to the inside edge. Again, this is not usually observed, instead, drivers typically 'cut the corner' in natural steering conditions (Lappi, 2014).

An alternative model of gaze behaviour during steering is Wilkie et al.'s (2008) Active Gaze Model. Wilkie et al. (2008) developed a model based on the principles of using the fixation as a point-attractor that supplies multiple sources of information (Wilkie & Wann, 2002) to maintain robust steering control. The model originally used only the perceptual inputs of the rotation of retinal flow (RF; described in Wann & Swapp, 2000), and the rate of change of extra-retinal direction ($E\dot{R}D$) and retinal direction ($\dot{RD}$; e.g. specified by the windscreen of a car), and was expressed as follows:

$$\ddot{\theta} = k(\beta_1 RF + \beta_2 E\dot{R}D + \beta_3 \dot{RD}) - b\dot{\theta} \quad (1.3)$$

where θ is the angle between an observer and the point of fixation. $\ddot{\theta}$ denotes the acceleration of steering response and $\dot{\theta}$ is the current response rate. k and b are scaling and response rate parameters, respectively, whilst $\beta_1 - \beta_3$ are weights that sum to one. The model conceptually acts as a spring, drawing steering position towards the point of fixation at a controlled rate. Wilkie et al. (2008) found that humans generally turn more rapidly than Equation 1.3 predicts, so they added an extra term (Equation 1.4), essentially creating a 'quickened' second-order system (Jagacinski & Flach, 2003):

$$\ddot{\theta} = k_1(\beta_1 RF + \beta_2 E\dot{R}D + \beta_3 \dot{RD}) + k_2(\beta_4 ERD + \beta_5 RD) - b\dot{\theta} \quad (1.4)$$

If a driver attempts to steer a course at the centre of the road, the TP model would predict that gaze would fall on the TP region, whereas Wilkie et al.'s (2008) Active Gaze Model would predict that gaze would fall on the region along the desired future path. A number of on-road studies have reported evidence of TP orientation (Chattington, Wilson, Ashford, & Marple-Horvat, 2007; Kandil, Rotter, & Lappe, 2009, 2010; Underwood, Chapman, Crundall, Cooper, & Wallen, 1999). However, these have generally evaluated gaze data in terms of area of interest (AoI) – Lappi (2014) has raised a number of shortcomings of this approach. One issue is that the conclusion of TP orientation over FP fixation requires the desired FP to be made explicit. Under natural driving circumstances drivers tend to oversteer, therefore if no instructions to 'keep to the middle of the road' are given, FP and TP models may

predict similar gaze behaviour. These instructions were not given in any of the cited studies (Chattington et al., 2007; Kandil et al., 2009, 2010; Land & Lee, 1994; Underwood et al., 1999) nor were there sufficient information given on the lateral position of steering trajectories, therefore it is hard to disentangle FP vs TP predictions. Indeed, Robertshaw and Wilkie (2008) have demonstrated that participants fixate centrally if they are asked to maintain a trajectory in the centre of the roadway, and forcing participants to look at the tangent point caused participants to 'cut the corner' (i.e. they steered toward the point of fixation).

A second issue is that even with different trajectories being specified the degree of overlap between a tangent point AoI and FP AoI may be large (Lappi & Pekkanen, 2013), and fixations may have been falsely included as TP fixations when participants are actually fixating the FP next to, or beyond, the TP. Indeed, gaze distribution in naturalistic driving is often further ahead than the TP (Itkonen et al., 2015; Lappi et al., 2013; Lappi & Pekkanen, 2013), which complicates localising fixations as these fixations are often in the direction of the TP.

Lappi and colleagues (Itkonen et al., 2015; Lappi et al., 2013) have developed a more sophisticated method of localising gaze during naturalistic driving by looking at the pattern of optokinetic nystagmus (OKN). OKN is a reflexive eye-movement pattern characterised by alternating slow-phase drift away from fixation and a fast-phase saccade to reset the eye movement (Authié & Mestre, 2011). This type of eye-movement is powerfully experienced if one was to look out the window at the passing scenery whilst on a moving train. It is also elicited during curvilinear flow patterns (Authie & Mestre, 2011), whereby the texture pattern 'drags' the eye in the direction of local flow. Importantly, different OKN patterns would be predicted depending upon whether the observer looks at the TP or at a point beyond the TP which lies on the FP (Figure 1.8A). The TP is a region of low optic flow speed (Figure 1.8A) – indeed it has been claimed that this property makes it the ideal location with which to discriminate between flow fields of different curvatures (Authié & Mestre, 2012). To

assess whether drivers look to the TP or the FP, Itkonen et al. (2015) monitored eye-movements during real-world car driving, with participants driving i) without any instructions given, ii) instructed to 'drive normally', or iii) instructed to look at the TP. Crucially, the OKN patterns were identical in the uninstructed (Figure 1.8B) and 'drive normally' (Figure 1.8C) conditions, and matched the direction of local flow on the desired FP (Figure 1.8A). TP fixations exhibited a much diminished pattern of OKN (Figure 1.8D), which was markedly different from the uninstructed control condition and was consistent with the local flow surrounding the TP (Figure 1.8A). Although the diminished OKN at the TP location is consistent with Authié & Mestre's (2012) predictions, this does not appear to be a characteristic that is determining gaze location for Itkonen et al.'s (2015) participants. This provides fresh evidence that the anticipatory information required for high-speed steering tends to come from the FP rather than the TP (Itkonen et al., 2015).

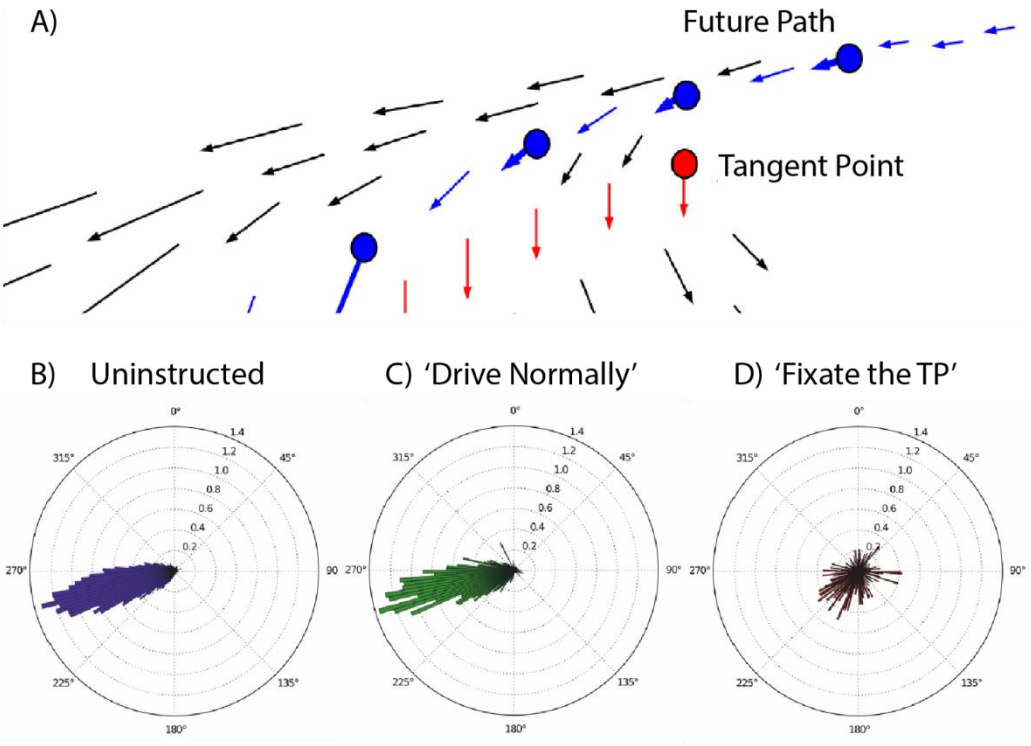

Figure 1.8 A) A simulated optic flow pattern of curvilinear motion, showing horizontal local flow at points on the FP beyond the TP, which is diminished at the TP. B) Pattern of OKN observed in uninstructed driving conditions is consistent with the local flow present beyond the TP, this is also the case when drivers were asked to 'Drive Normally' – shown in C). D) This pattern was not observed when participants were asked to fixate the TP. Figures modified from Itkonen et al., 2015.

It appears that the Active Gaze Model does fairly well at explaining gaze behaviour during steering curved trajectories (Wilkie et al., 2008). Additionally, the founding principle of using a weighted combination of multiple sources of information to maintain robust control fits well with literature on how the visual-motor system usefully combines sensory information (Ernst & Banks, 2002). However, the Active Gaze Model was conceived to explain behaviour in unconstrained situations (Wilkie & Wann, 2002, 2003b). The differences between unconstrained and constrained trajectory steering has already been outlined (section 1.5) and it is unclear how the Active Gaze Model could explain some key behaviours of two-level steering without being developed to incorporate monitoring of lateral position with reference to REs

(Salvucci & Gray, 2004). The Active Gaze Model was adjusted in Kountouriotis et al. (2012) to include a RE component which acted to push the trajectory to the centre of the road, but this conception of the model did not include flow information – from the originally proposed perceptual inputs (RD, ERD, and RF) only ERD was retained in that particular form of the model.

1.8. Thesis Structure

In their current form, two-level steering models (Saleh et al., 2011; Salvucci & Gray, 2004) do not adequately incorporate multiple sources of information that are available and used by the observer (see sections 1.2-1.4). However, flow-inspired models such as the Active Gaze Model (Wilkie et al., 2008) do not adequately explain steering when visible road edges are present. This thesis will investigate how flow information interacts with road edge information in order to identify key avenues how two-level steering models might incorporate multiple sources of information. The experiments will use a virtual reality driving simulator because systematic and controlled variation of road edge information (Chatziastros et al., 1999; Cloete & Wallis, 2011; Land & Horwood, 1995), or precise manipulation of flow information (e.g. Kountouriotis et al., 2013; Wilkie & Wann, 2002) is almost impossible using on-road methods.

Chapter 2 will develop and validate a novel flow manipulation to allow predictable steering biases through the manipulation of flow *speed*. Chapters 3-4 will use this flow manipulation to develop a framework for assessing the contribution of flow speed to two-level steering control. Chapter 3 will monitor eye movements to see how manipulating RE information can affect gaze behaviours, whereas Chapter 4 will control gaze behaviours using a constrained gaze paradigm. Chapter 5 will expand the framework developed during Chapters 2-4 to test key findings in relation to the contribution of road edges and flow speed information to steering.

In Chapter 6 a different manipulation of flow is developed which generates predictable steering biases by manipulating flow *direction*, rather than flow *speed*. The framework developed in Chapter 4 is adapted to probe how flow direction might interact with road edge information. Chapter 7 uses an expanded design (similar to Chapter 5) to test key findings emerging from Chapter 6 in relation to how flow direction is combined with road edge information to support steering control.

CHAPTER 2

INDEPENDENTLY MANIPULATING FLOW AND ROAD EDGES

2.1 Introduction

Smooth steering of winding roads using road edge information can be achieved using a far point to preview changes in direction in order to estimate upcoming steering requirements, and a near point to stabilise position-in-lane (Donges, 1978; Saleh et al., 2011; Salvucci & Gray, 2004). Accurate steering using a far point and a near point have been observed using displays without flow information (Land & Horwood, 1995; Neumann & Deml, 2011), suggesting that road edge (RE) information is sufficient to support steering control. However, REs are not the only source of information when steering bends. In an illuminated environment, there is often optic flow available from, for example, the texture of the road or borders (e.g. hedges). A number of control strategies for using optic flow to govern steering control (e.g. starting, stopping, and changing direction) were outlined by Gibson (1958), and since then numerous studies have examined the conditions under which optic flow influences steering control. Although there is evidence to suggest that in some cases optic flow does not contribute to steering control (Harris & Bonas, 2002; Rushton et al., 1998), there is much evidence to suggest that when flow information is particularly rich (Warren et al., 2001), or when alternative sources of information are weak (Wilkie & Wann, 2002), optic flow is useful for steering control. It seems, then, that rich optic flow information (e.g. from a textured ground plane) may be useful even when road edge information is available (Kountouriotis et al., 2013), particularly when road edge information is weak.

The possible control strategies for controlling steering using either optic flow or road edges *independently* have been well-researched (see sections 1.2-1.5), but studies investigating control strategies governing their *combined* usage are relatively sparse.

To examine the situations under which both information sources are used, they can be put into conflict and the resultant steering behaviours observed (Wilkie & Wann, 2002): if two information sources conflict, preferential use of either source can be inferred by the resultant trajectory (e.g. Warren et al., 2001). Virtual Reality (VR) techniques have massively advanced the field of visually-guided locomotion (Kemeny & Panerai, 2003). VR allows isolated manipulation of an information source, whilst other sources remain veridical or absent. This Chapter introduces and validates a display paradigm for independently manipulating flow and road edges. A core thread of the thesis will be assessing how the magnitude of response to one variable (flow) changes across another variable (road). The standard method of reporting is null-hypothesis significance testing (NHST), which is useful for assessing the presence of effects, but limited in assessing patterns of magnitude changes across conditions. This Chapter will contrast NHST with an Estimation Approach (Cumming, 2012, 2014) in an attempt to settle on a suitable standard of reporting for the remainder of the thesis.

2.1.1 Manipulating Flow

In order to examine use of flow, manipulating the information to look for behavioural consequences is desirable. The question, then, is how to introduce a systematic bias to flow when travelling on a curved path. In the past, flow has been biased by manipulating the nature (size, or presence) of texture elements (Kountouriotis et al., 2013). Kountouriotis et al. (2013) independently manipulated the textured regions outside and inside of a curved pathway to create asymmetric flow patterns (Figure 2.1). Experiments 1 and 2 showed steering was biased towards regions with smaller (Figure 2.2A), or absent (Figure 2.2B), texture elements. Experiment 3 replicated these steering biases by simply keeping either the inside or outside of the bend apparently static, therefore controlling for texture size (Experiment 1) and presence (Experiment 2). The authors raised the possibility that some of the observed steering biases may have been due to asymmetries in the optic flow field (Kountouriotis et al., 2013), and proposed two underlying mechanisms: *flow equalisation*, or *global averaging*.

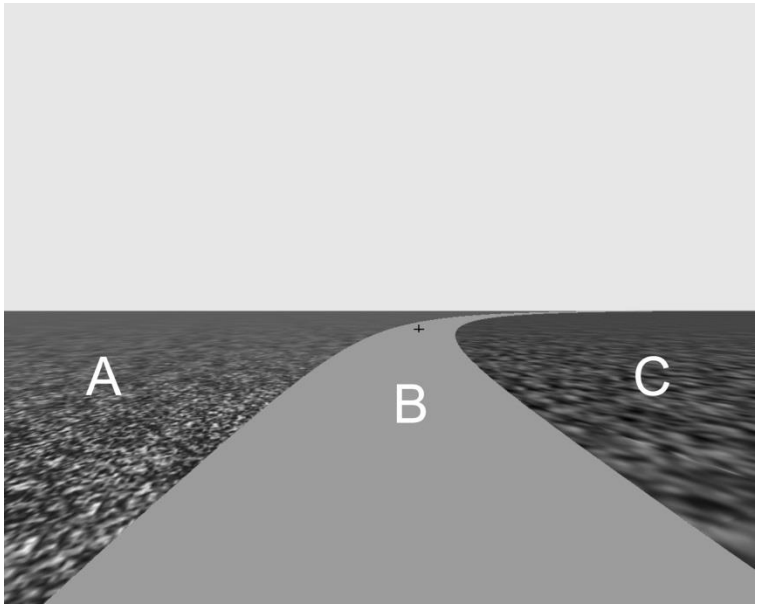

Figure 2.1 Sample stimuli from Kountouriotis et al. (2013). The flow field is separated into an 'outside' region (A), the untextured road (B), and an 'inside' region (C). Regions A and C were independently manipulated to create asymmetric flow fields. Figure taken from Kountouriotis et al. (2013).

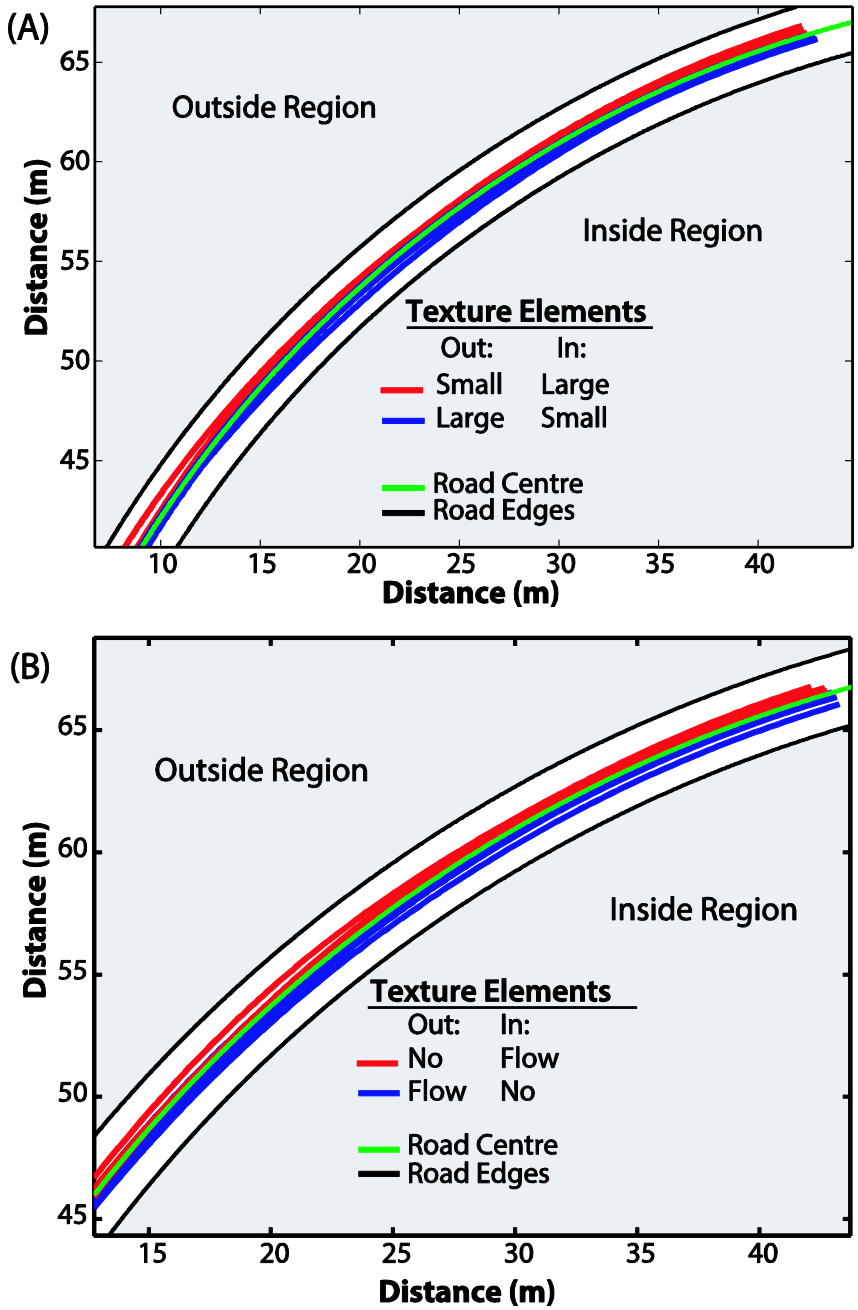

Figure 2.2 A) Trajectories for a sample participant in Experiment 1, showing steering towards the inside when the inside region is smaller, and steering towards the outside region when the outside region is smaller. B) Trajectories from a sample participant in Experiment 2, showing oversteering when the inside was blank, and understeering when the outside was blank. Graphs taken from Kountouriotis et al. (2013).

Flow equalisation proposes that animals adjust steering position so that the properties of either side of the flow field are equalised (Duchon & Warren, 2002). Duchon &

Warren (2002) asked participants to walk down a VR corridor with identically textured walls either side. They found that walking trajectories could be biased by increasing or decreasing either the flow speed or texture size of one wall but not the other wall (although the bias induced by texture scale was small). Supporting this, Kountouriotis et al. (2013) found participants steer towards regions of smaller elements to increase their optical size whilst decreasing the optical size of the larger region (thereby appearing to equalise texture element size). Similarly, when there was a region of static flow drivers steered towards the region of *zero* flow which would reduce the perceived speed of the region *with* flow (thereby appearing to equalise flow speed).

Alternatively, an animal could extract locomotor speed from averaging flow speed vectors across the entire scene. In Kountouriotis et al. (2013) drivers consistently showed greater understeering when texture was 'static' rather than 'blank' (or absent), irrespective of whether the texture was on the inside or outside region. Global flow averaging can potentially explain this steering behaviour. In 'static' conditions, speed may be estimated by averaging veridical length flow vectors with zero length flow vectors (from the static texture), therefore speed is estimated to be slower-than-veridical. Slower locomotor speeds need less rapid steering responses, so a slower-than-veridical percept of speed might cause understeering. In 'blank' texture conditions it is possible that only the veridical length flow vectors are used to estimate speed (because the blank texture is omitted from the averaging process) so there is no consistent understeering.

These mechanisms are not mutually exclusive, and the Kountouriotis et al. (2013) results are likely a combination of the two. The predominance of each strategy could depend on the given steering task. Flow Equalisation would be most beneficial when travelling on a straight trajectory down a corridor with identically textured walls either side. In this scenario, equalising flow speed results in a trajectory centred between the two walls (Duchon & Warren, 2002). However, on a curved path flow vectors have

different lengths depending on their proximity to the centre of rotation (Figure 2.3A), so Flow Equalisation may be a poor strategy for staying in the middle of the road. To assess which strategy was predominant when steering a curved path, Kountouriotis, Mole, Merat, Gardner, & Wilkie (2015) kept locomotor speed constant but independently manipulated the flow speed of inside or outside regions (see Figure 2.1) to induce either asymmetric flow speeds, or an average global speed that was faster or slower than the actual locomotor speed. Crucially, the steering patterns observed varied depending upon the global speed, not the direction or magnitude of asymmetries present in the scene (Figure 2.3B). It seems that global flow speed averaging, rather than flow speed equalisation, was predominantly used to inform steering on curved paths.

There is a paucity of studies that investigate how the steering system responds to altering global flow speed patterns. Indirect evidence comes from Pretto, Bresciani, Rainer, & Bülthoff (2012) who demonstrated that introducing fog (where the far scene is occluded, but not near information) or anti-fog (where the near road is occluded, but not the far scene) to a straight road altered perceived speed in a manner consistent with global flow averaging. On a straight road with gaze placed forward, flow vectors from the far region have lower vector length than flow vectors from the near region. A global flow averaging strategy would predict that occluding the larger vectors from the near scene *decreases* perceived flow speed (because only small vectors remain), whereas occluding the smaller vectors from the far scene would *increase* perceived flow speed (because only larger vectors remain from the near region). This corresponds with the pattern of results in Pretto et al. (2012) where they observed that perceived speed was reduced in the anti-fog conditions (where larger vectors are removed), but increased in the fog conditions (where smaller vectors are removed). Pretto et al. (2012) describe their results in terms of contrast reduction (see also Owens, Wood, & Carberry, 2010), whereby the high-contrast nearer region causes overestimation of

speed but the low contrast farther region causes underestimation. However, global flow averaging also provides an explanation for the observed pattern of results.

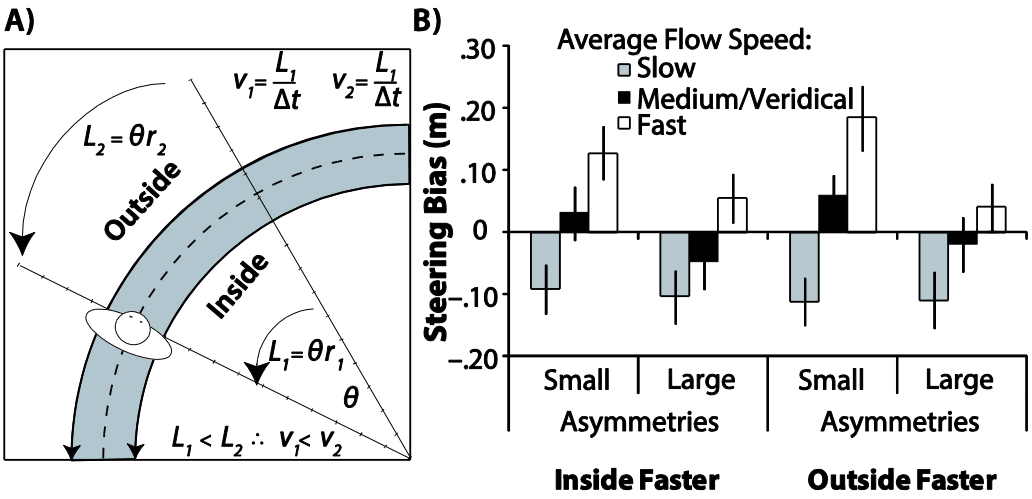

Figure 2.3 A) Geometry of a bend of constant curvature showing smaller flow vectors closer to the curve origin, and larger flow vectors farther away. B) Steering Bias for conditions of asymmetric or symmetric speed for varying average speeds. Participants oversteered or understeered dependent on the global average speed, rather than asymmetries. Figures adapted from Kountouriotis et al. (in preparation), presented at Vision Sciences Society 2015 (Kountouriotis et al., 2015).

It seems then that humans steering curved trajectories are sensitive to global flow speed, and exhibit systematic directional steering biases depending whether flow speed is faster or slower than veridical. Altering global flow speed could, therefore, act as a useful manipulation for examining the original issue of determining the extent to which flow is used in the presence of a demarcated pathway. A virtual environment with REs and ground texture has two sources of speed information: flow speed and rate of approach to REs. These two sources of information can be put into conflict (Figure 2.4). When the camera moves on a curved path the observer experiences counter-movement of texture elements which gives rise to the percept of self-motion. The same flow pattern can be simulated by keeping the camera stationary but rotating the ground-plane counter-clockwise (when steering a right-hand bend; Figure 2.4A). Using these principles, it is possible to produce a flow pattern indicative of any given

velocity whilst keeping the actual driver velocity constant, because flow vector length is an additive result of the driver velocity and ground-plane rotation (Figure 2.4B & C). If the rate that the positional error develops is kept constant the requirements of the steering task (of keeping to the middle of the road) are the same across flow conditions, therefore any steering bias across flow conditions can be attributed to manipulating global flow speed.

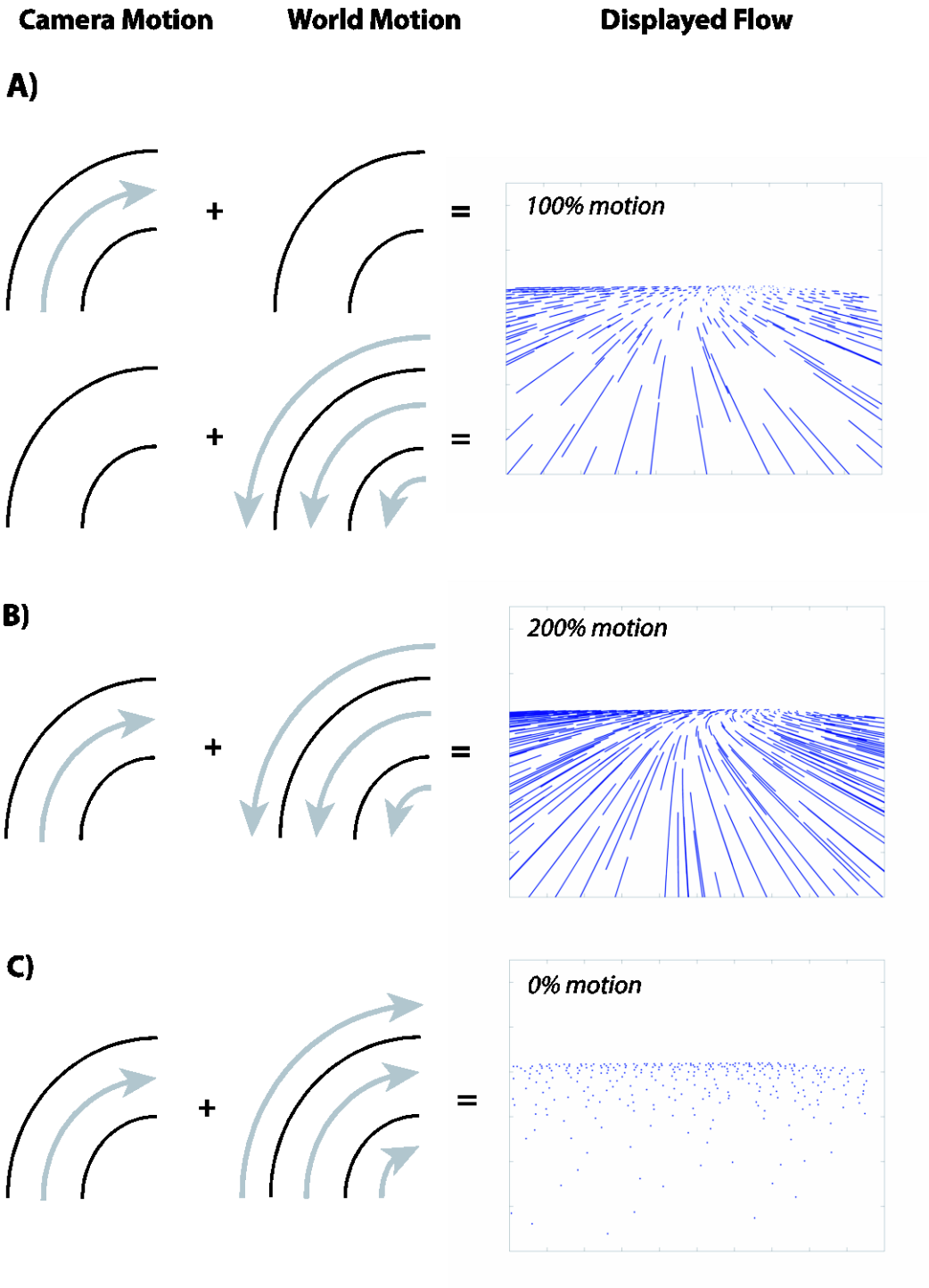

Figure 2.4 Schematic depicting methods of simulating perceived motion in a virtual environment. A) Given a trajectory of constant curvature, it is possible to generate identical flow patterns by either moving the camera or counter-rotating the ground plane. B) A faster flow can be generated by combining camera motion with ground

plane counter rotation. C) A slower flow pattern can be induced if the ground plane is rotated in the direction of camera movement (clockwise in right-hand bends). The flow pattern presented is the extreme case of rotating the ground plane with the observer at the same rate as the camera, therefore cancelling out texture motion and giving an illusory 'static' flow display (as per Kountouriotis et al., 2013).

2.1.2 Manipulating Road Edges

The previous work by Kountouriotis et al. (2013, 2015) used an untextured road, where lane boundaries are denoted by the point where the grey untextured road finishes and the green textured region starts (Figure 2.1). This was appropriate since they did not attempt to manipulate the presence or quality of road edge (RE) information in their experiments. Previous studies that have aimed to vary the extent of RE information have opted for explicitly drawing curvilinear markings that are super-imposed on top of a ground plane (Billington et al., 2010; Cloete & Wallis, 2011; Land & Horwood, 1995; Neumann & Deml, 2011). This method allows RE information to be manipulated without altering the underlying ground texture (hence the flow patterns are also unaffected).

2.1.3 Pilot testing of the paradigm

It was important to assess whether increasing or decreasing the global flow speed, independent of locomotor speed (relative to the road edges), resulted in predictable biases. Additionally, the artificially induced flow patterns were compared with actual alterations in locomotor speed (where both flow and RE information are veridical to programmed velocity). This was performed to gain some indication of how strongly the visual-motor system weights RE information compared to Flow information.

2.2 Methods

2.2.1 Participants

A sample of 13 University students (9 females, 4 males, ages ranged from 20 to 31, mean 24.7 years), all having normal (participants did not need glasses) or corrected-to-normal vision (participants wore glasses), took part in Chapter 2. All held a full driving license (average time since test was 5.7 years). All participants were naïve as to the purpose of the experiment. All participants gave written informed consent and the study was approved by the University of Leeds, School of Psychology Research Ethics Committee (Ref 13-0221), and complied with all guidelines as set out in the declaration of Helsinki.

2.2.2 Apparatus

Using a driving simulator, participants steered along a series of bends. Virtual environments were created using WorldViz Vizard 3.0 (WorldViz, Santa Barbara, CA) on a PC with Intel i7 3770 (3.40 GHz). Images were generated at 60Hz and were back projected using a Sanyo Liquid Crystal Projector (PLC-XU58, Sanyo, Watford, UK) onto a screen with dimensions of 1.98 x 1.43m in a matte-black viewing booth (the projector was the sole source of light). Images were perspective correct from a viewing distance of 1m from the screen with eye-height of 1.2m (total field of view 89.42° × 71.31°). Participants sat in a height-adjustable driving seat. Participants controlled steering using a force-feedback wheel (Logitech G27, Logitech, Fremont, CA) and steering wheel angle was linearly mapped onto rate of change of heading (i.e. vehicle dynamics were not simulated so as to reduce the amount of practice needed to achieve stable performance, this is often the case in vision science e.g. Cloete & Wallis, 2011; Land & Horwood, 1995) through a minimum step size of .36°/s. Steering data was recorded at a rate of 60Hz.

2.2.3 Stimuli

The simulated virtual environment consisted of a green tinted texture, with a 3m wide road of constant curvature (60m radius) demarcated with white road edges (as per Kountouriotis et al., 2012; see Figure 2.5b). The road had an initial straight section

which was 9m in length. Participants fixated a cross 16.1m (~1.2s) ahead in the road centre (to control for eye-movements which have been shown to be an important influence over steering in some conditions). It is worth highlighting the importance of terminology when describing the nature of constraining gaze. Participants were asked to keep gaze focussed on the cross, which moved across the display in accordance with the driver's movement. Therefore, gaze was not *fixed* in a manner which prohibited movement of the eyes (as is sometimes the case in psychophysical experiments), but instead gaze was *constrained* to a point but free to move as the point moved across the display. Throughout this thesis, the terms fixated and constrained are used interchangeably to refer to mobile gaze focussed on a point on the future path. Participants started each trial in the road centre and were asked to keep to the centre of the road and to steer as smoothly and as accurately as they could.

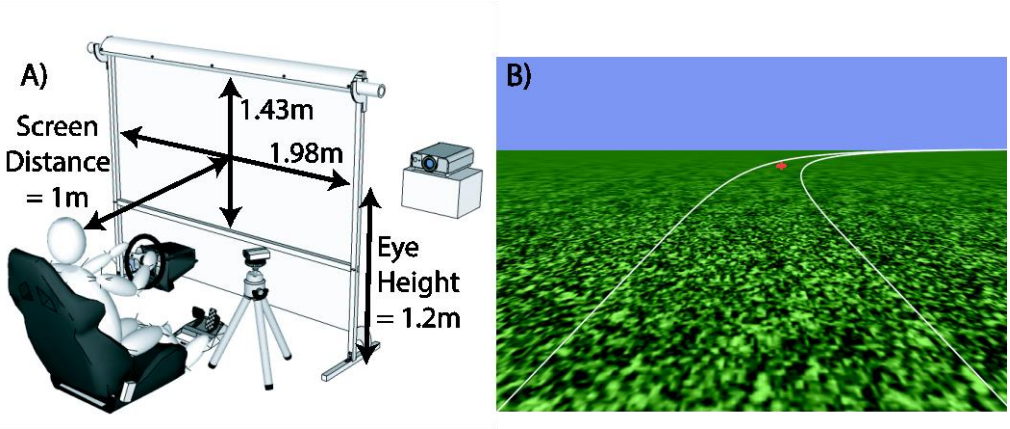

Figure 2.5 A) Schematic of Driving Simulator Layout. B) Screenshot of right-hand bend stimuli, with the red fixation cross.

Simulated locomotor speeds were either 8.94ms^{-1} (~20mph), 13.38ms^{-1} (~30mph), or 17.88ms^{-1} (~40mph). In all conditions, movement of the road on the display was veridical to driver speed. In some conditions the rate the ground texture moved on the display was manipulated independently of driver speed, so that optic flow speed could be faster or slower than veridical with the actual locomotor speed remaining

unaffected (actual locomotor speed refers to the speed of motion with respect to the road edges, not optic flow, so that the driver approached the road edges at the same rate across non-veridical flow conditions).

2.2.4 Procedure

Participants were instructed to steer as smoothly and as accurately as they could, and to fixate the red cross. Firstly, the seat was adjusted so the participant's viewing characteristics matched the dimensions shown in Figure 2.5. Participants were then given five practice trials to familiarise themselves with the simulator dynamics. For the control condition, locomotor speed was 30mph, and flow was VEridical: VE_{30}. When the locomotor speed was altered (to 20mph or 40mph), flow remained veridical: VE_{20}, VE_{40} (Table 2.1). Conversely, there were also conditions where locomotor speed did not match flow speed. In these conditions locomotor speed was kept at 30mph, but flow was rotated either to simulate the flow pattern experienced when travelling at slower (20mph) or faster (40mph) than the locomotor speed: these were the 'SLow Flow' (SL_{30}) and 'FaSt Flow' (FS_{30}) conditions respectively (Table 2.1). The presence of the fixation cross served to stabilise gaze across all trials, ensuring that steering biases across flow manipulations could not be explained by different gaze patterns. Note that participants were asked to steer in the middle of the lane. Whilst this steering behaviour could be considered unrealistic (Lappi, 2014), it does allow precise measurement of steering error, especially steering biases such as oversteering or understeering (see section 2.2.5) with reference to the 'ideal' trajectory. Trials were 6 seconds long with a .83s (50 frame) pause at the start of trials to give participants time to re-centre the wheel before motion commenced: the driving time was therefore 5.17s. There were six trials of each condition. Total experiment time, including practice, was 3.5 minutes.

Table 2.1 The four experimental conditions, with the subscript denoting locomotor speed. The control condition, VE_{30}, is not displayed.

Flow Speed	Flow Type	Veridical Flow	Non-Veridical Flow (locomotor speed was 30mph)
20mph		VE_{20}	SL_{30}
40mph		VE_{40}	FS_{30}

2.2.5 Analysis

Position in the world and steering wheel angle were recorded each frame (60 Hz). Position-in-lane over time is a continuous signal that can be used to quantify steering behaviour over the course of a trial. Steering behaviour was captured by quantifying positional error with reference to the ideal path (the lane centre). It is useful to capture both the direction and magnitude of steering errors. Error direction can be measured using a constant error measure such as Steering Bias (section 2.2.5.1). However, simply calculating average positional error can mask other information: one can have a trajectory with an average steering bias of zero because half of the trial lies to one side of the midline and half on the other side (Figure 2.6). It is, therefore, also useful to have a measure of the variable error such as Root-Mean-Squared Error to indicate the total deviation away from the midline, regardless of direction (section 2.2.5.2; Figure 2.6). These two measures can capture important aspects of steering behaviour within a trial with respect to the instruction 'stay as close to the centre of the road as possible'. Since participants are also asked to steer 'as *smoothly* and as *accurately* as they can', a measure of smoothness is required. To capture smoothness, the rate of change of movement of the steering wheel can be used: namely Steering Wheel Jerk.

	Steering Bias	RMSE	Steering Jerk
Blue	oversteering	medium	low
Green	negligible	high	high
Red	understeering	medium	low

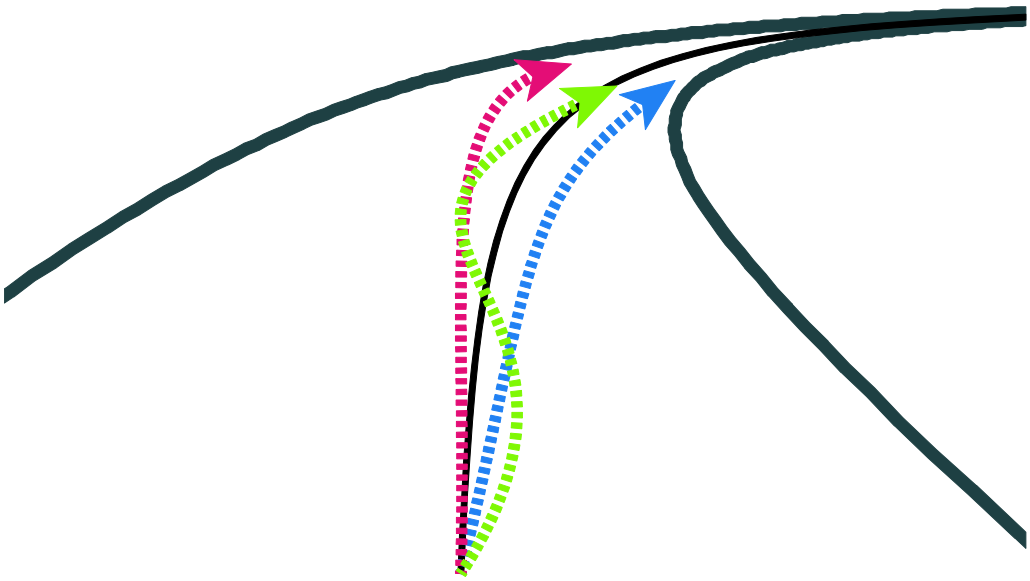

Figure 2.6 A schematic of hypothetical trajectories and the resultant values of Steering Bias, RMSE, and Jerk. The red arrow shows understeering (negative bias) developing from the driver turning too late. The blue arrow shows oversteering (positive bias) developing from the driver turning too early. The green arrow shows oversteering from turning too early, which is quickly corrected for but the steering correction which overshoots, resulting in understeering later in the trajectory before the trajectory is brought back to the midline. The table shows how these different steering behaviours are captured by patterns across Steering Bias, RMSE, and Steering Jerk.

2.2.5.1 Steering Bias (SB)

Steering Bias (SB) was calculated to measure positional deviation from the lane centre for every frame, providing a signed directional measure of steering error (whereby

positive bias denotes 'oversteering' and negative bias denotes 'understeering' with respect to the middle of the road). For a set of n (in this case, number of frames), with x representing the signed distance from the closest point on the road midline – $\{x_1, x_2, \ldots, x_n\}$ – SB can be expressed as follows:

$$\frac{1}{n}\sum_{i=1}^{n} x_i \tag{2. 5}$$

It should be noted that the thesis adopts the terms 'oversteering' and 'understeering' to denote a participant steering more towards the inside edge of the bend or outside edge of the bend respectively (Figure 2.6). These terms are distinct from the labels 'oversteer' and 'understeer' used to describe the response of real vehicles (since somewhat confusingly they describe the inherent tendencies of a particular vehicle to turn more or less than required given an identical steering input).

The findings from Kountouriotis et al. (2015) suggest that under full road view conditions systematic changes in directional error occur when flow speed is manipulated. Steering bias, then, will be the primary measure of interest. The extent that systematic shifts in steering bias are observed under specific road conditions will indicate whether flow is used for steering control with that particular road section.

2.2.5.2 Root-mean-squared Steering Error (RMSE)

Root-mean squared steering error (RMSE) was calculated from the magnitude of steering error (relative to the lane centre) at every frame, and measures both deviation and consistency of steering (but not systematic directional error). First, the positional error for each frame is squared. This is then averaged before the root is taken to return the measure into the original units (m). For a set of n (number of frames), with x representing the signed distance from closest point on the road midline – $\{x_1, x_2, \ldots, x_n\}$ – RMSE can be expressed as follows:

$$\sqrt{\frac{1}{n}\sum_{i=1}^{n} x_i^2} \tag{2. 6}$$

Squaring the error means that extreme error scores have a proportionally larger impact on the outcome measure. Given two trajectories of equal steering bias, the more variable trajectory will generally result in a larger RMSE than the constant offset (Figure 2.6). In this way RMSE incorporate both variability and position error into a single unsigned error measure.

2.2.5.3 Steering Wheel Jerk (SWJ)

Angular jerk (deg.s^{-3}) is the change in angular acceleration of the steering wheel, and can be used to indicate steering smoothness. Because a fixed position of the steering wheel causes a change in heading angle (i.e. an angular velocity), jerk reflects accelerated turning of the steering wheel. Large jerk values will, therefore, correspond to rapid steering corrections. For a set of n (number of frames), with w representing wheel angle – $\{w_1, w_2, \ldots, w_n\}$ – and t representing time, SWJ can be expressed as follows:

$$\frac{1}{n}\sum_{i=1}^{n} \frac{d^3 w}{dt^3} \tag{2. 7}$$

It can be seen that this measure does not explicitly relate to the requirement to maintain a position near the road midline so it is possible to steer very smoothly but completely erroneously.

2.3 Results

2.3.1 Investigating an appropriate reporting method: Difference between the Mean Plots

The method of reporting results will be kept consistent throughout the experimental Chapters of this thesis, so requires some investigation and validation. The traditional way of reporting continuous parametric data (and that used in much of the literature cited) is null-hypothesis significance testing (NHST). If $p<.05$, the null hypothesis – that the two estimates are equal – can be rejected. However, despite its widespread use in psychological literature, there are some well-documented problems with NHST (Kline, 2004). This section does not give a full overview of the issues surrounding NHST (but see Kline, 2004); rather it focusses on the issues informing the choice of results presentation for this thesis. Firstly, there is the issue that NHST tends to overestimate evidence against the null hypothesis. Before even running an experimental study, it is fairly easy to demonstrate that the null hypothesis (that two estimates of behaviour gained from two experimental conditions are identical) is unlikely to be true. Fidler & Loftus (2009) use a quote from Meehl (1967) that illustrates why this is the case:

> *"Considering…that everything in the brain is connected with everything else, and that there exist several "general state-variables" (such as arousal, attention, anxiety, and the like) which are known to be at least slightly influenceable by practically any kind of stimulus input, it is highly unlikely that any psychologically discriminable situation which we apply to an experimental subject would exert literally zero effect on any aspect of performance." (p. 109).*

Therefore $p<.05$ tells the reader that, if the null hypothesis were true, the probability that the observed data would occur is below 5%. This is not particularly illuminating,

because the alternative hypothesis is *anything other than absolute equality*. For the experiments conducted in this thesis, the focus is not merely the *presence* of a difference, but in the magnitude and direction of any differences.

Thus follows the second issue: the dichotomous nature of (mis)interpreting *p* values. NHST allows a binary decision of whether there is an effect or not. It does not allow estimation of the magnitude, direction, or uncertainty of the difference, and thus whether this difference is practically meaningful. However, if one adopts an estimation approach with an emphasis on uncertainty (confidence intervals) and magnitude, a fuller, more nuanced interpretation can be achieved (Cumming, 2012, 2014; Fidler & Loftus, 2009). With this in mind, the thesis will report each measure with an accompanied difference-between-the-means plots (DBTM; e.g. Figure 2.8). These plots give a fuller depiction of data trends than merely reporting *p* values and effect sizes (η_p^2). To create these plots the *paired difference* (because every study in the thesis is repeated measures) between the experimental condition and the control condition (in all experiments in this thesis, the control condition is veridical flow, a complete road, and ~30mph locomotor speed) is calculated for every participant. This allows an estimate of the magnitude of the difference and an estimate of uncertainty associated with the effect via the presentation of confidence intervals. 95% CIs are preferable to representing uncertainty instead of standard error of the mean (SEM) because SEM bars often underestimate uncertainty, being approximately equivalent to 68% CIs for the experimental situations tested here (Figure 2.7). Whenever the paired difference of the means is reported as opposed to a group mean, M, it will be labelled as M_{diff} to avoid confusion.

It is important that these plots are interpreted correctly. It is tempting to use CIs in a similar way to T-tests, concluding that if the CI does not overlap zero then it can be concluded that there is a difference. This interpretation is common, but wrong (Hoekstra, Morey, Rouder, & Wagenmakers, 2014). CIs provide information about the uncertainty of the *procedure* of obtaining that estimate (e.g. consistency of

participant behaviour), it does not provide information about the uncertainty surrounding the *estimated parameter* (for which a Bayesian approach is needed to obtain credibility regions; Hoekstra et al., 2014). Instead, the DBTM plots are to be used to interpret the magnitude of differences between conditions, and the variability of this magnitude across participants. Nevertheless, it has been pointed out that "imperfectly understood confidence intervals are more useful and less dangerous than imperfectly understood *p* values and hypothesis tests" (Hoenig & Heisey, 2001, p. 23).

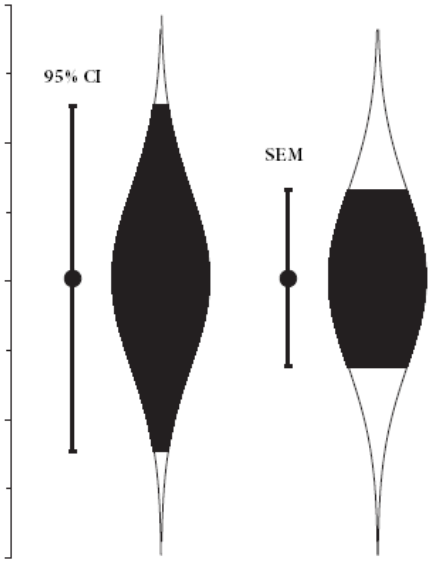

Figure 2.7 Example 95% CIs and SEM bars. The curved *Cat-eye* pictures (to use Cumming's, 2014, terminology) are centred on the sample mean and indicate the relative likelihood of the true value of the mean. The black areas match about 95% and 68% of the area between the curves. Adapted from Cumming (2014).

The purpose of this style of reporting is to make trends in the data easier for the reader to identify. Having said this, line graphs that represent group data for each condition (Figure 2.9) are very hard to read when they include 95% CIs because they are so large and overlapping, therefore SEM bars will be used in these figures to indicate the uncertainty in the estimate (approximately half the size of 95% CIs). In this Chapter the results of traditional NHST will also be reported. This enables the relative merits of NHST vs. Estimation to be evaluated, so that the approach which is better able to

navigate a course of clarity through the data is chosen as the standard for the remainder of the thesis.

2.3.2 Results: Steering Behaviour

2.3.2.1 Steering Bias

Figure 2.9A displays condition averages positional bias. Under control conditions (VE_{30}) participants were able to keep to the midline successfully, on average only 1.7cm of oversteer (M=.017 [-.054, .087], SEM=.032). It is sometimes useful to consider bias magnitude values in terms of percentage of road width, since the ultimate goal is to stay on the road. Under veridical visual conditions participants were able to steer to keep within 1% Road Width (RW). Increasing the locomotor speed (VE_{40}) resulted in increased understeering, whereas slowing locomotor speed (VE_{20}) induced oversteering. Conversely (when locomotor speed was veridical), increasing global flow speed (FS_{30}) resulted in oversteering, and decreasing global flow speed (SL_{30}) resulted in understeering.

2.3.2.1.1 *NHST*

A 2 (Flow Type: Veridical vs Non-Veridical) x 2 (Speed: 20mph vs 40mph) Repeated Measures ANOVA assessed whether there were any systematic trends in the data. The control condition, VE_{30}, was removed from the ANOVA because it was only present for the veridical level of Flow Type. There was not a significant main effect of Flow type, but there was a significant main effect of Speed and a significant interaction (results shown in Table 2.2).

The main effect of Speed occurred because 40mph caused significantly more understeering than 20mph. The interaction was due to the main effect of Speed reversing across Flow Types: in Veridical flow conditions VE_{40} causes understeering compared VE_{20}; in non-Veridical flow conditions FS_{30} causes oversteering compared to SL_{30}.

2.3.2.1.2 DBTM plots

Differences were explored with DBTM plots (as suggested by Cummings, 2012; Figure 2.8). When driver speed was constant, increasing Flow speed (independently of driver speed; FS_{30}) by 33% caused oversteering by ~3%RW (M_{diff} =.091 [.045, .138], SEM=.021), and decreasing flow speed by 33% (SL_{30}) caused understeering by ~3%RW (M_{diff}=-.094 [-.158, -.029], SEM=.03). This trend is reversed, with a larger magnitude, for changes in locomotor speed. VE_{40} caused understeering by ~6%RW (M_{diff} =-.179 [-.265, -.092], SEM=.04) and VE_{20} caused oversteering by ~6%RW (M_{diff} =.18 [.106, .255], SEM=.034).

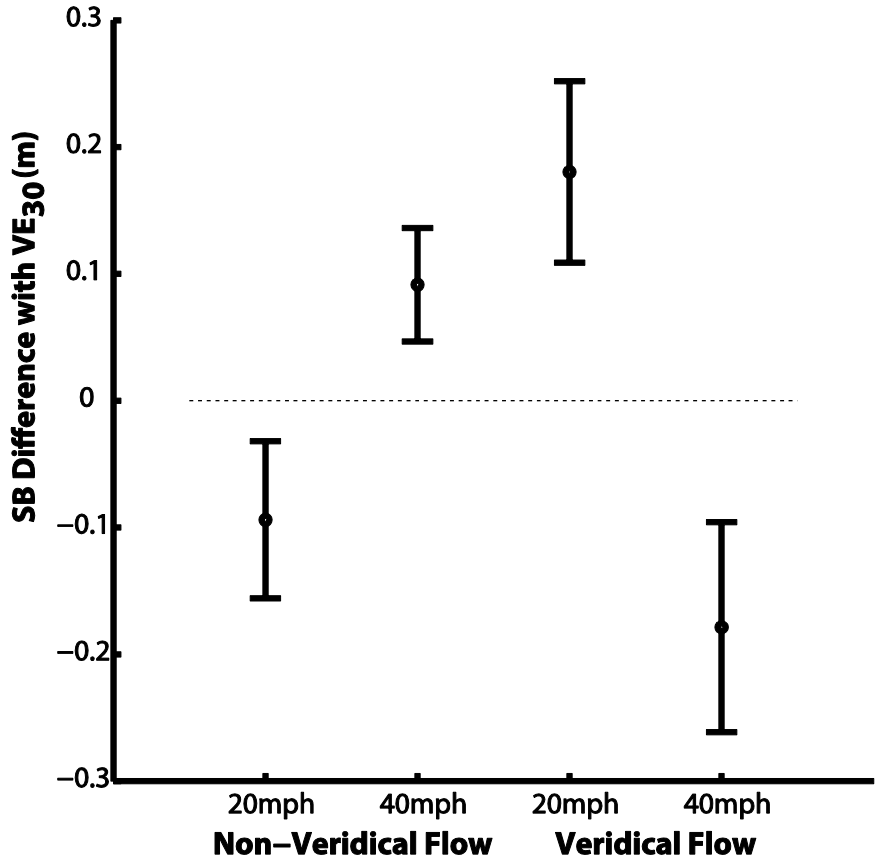

Figure 2.8 Paired differences between condition means and the control condition. Non-veridical flow (constant driver speed) conditions are shown on the left-hand side; Veridical flow (changes in locomotor and flow speed) conditions are shown on the right-hand side. A positive magnitude indicates oversteering relative to VE_{30}.

The dotted line indicates zero difference. Error bars represent 95% confidence intervals.

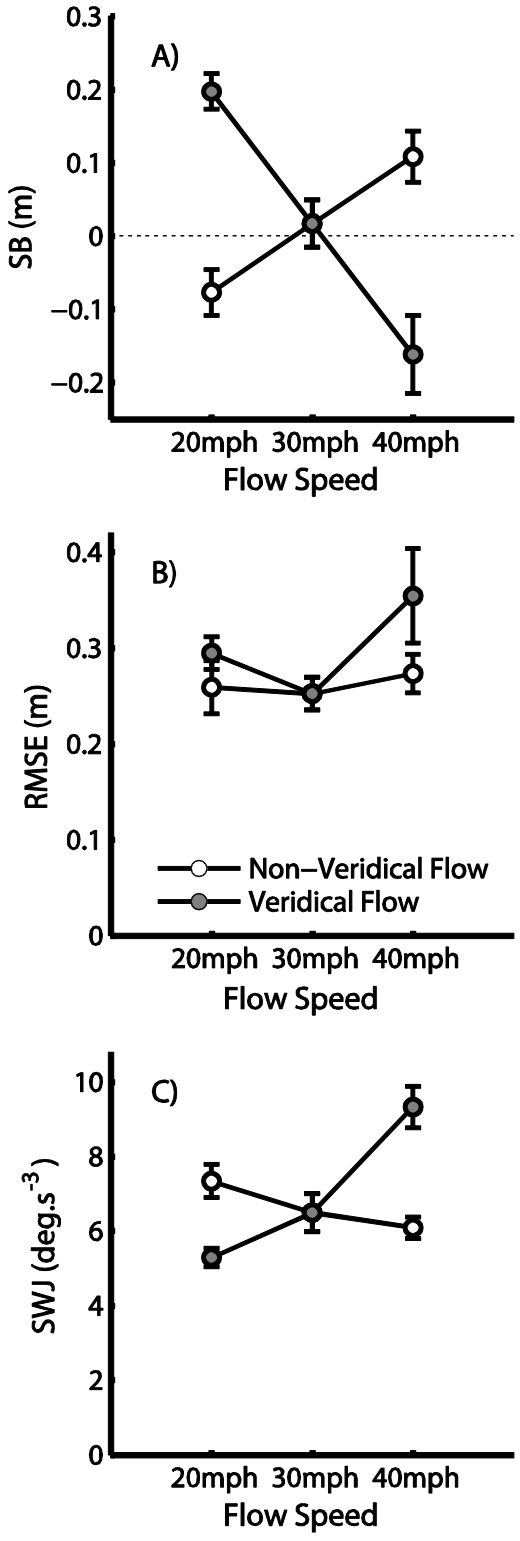

Figure 2.9 All steering performance measures across non-veridical (empty markers) and veridical (filled markers) flow conditions, showing A) Steering Bias, B) Root-mean-squared error, and C) Steering Wheel Jerk. Error bars represent standard error of the mean (SEM).

Table 2.2 Table showing NHST results for steering measures.

	Steering Bias				RMSE				Steering Wheel Jerk			
	F	df	p	η_p^2	F	df	p	η_p^2	F	df	p	η_p^2
Flow Type	.012	1,12	.916	.001	23.825	1,12	<.001	.665	11.272	1,12	.006	.484
Speed	13.15	1,12	.003	.523	5.198	1,12	.042	.302	36.446	1,12	<.001	.752
Flow Type x Speed	37.363	1,12	<.001	.757	.436	1,12	.521	.035	88.041	1,12	<.001	.88

2.3.2.2 RMSE

Figure 2.9B shows RMSE scores, which give an indication of total deviation from the midline. In VE_{30} participant's error was .25m [.21, .29], meaning that, on average, the participant was ~25cm (8.3%RW) away from the road centre at any particular moment. This value changes little when driver speed is constant but flow speed is altered (the line is flat), however, error increases for both VE_{20} and VE_{40} conditions.

2.3.2.2.1 NHST

A 2 (Flow Type) x 2 (Speed) repeated measures ANOVA was conducted, with the results shown in Table 2.2. There were significant main effects of Flow Type and Flow Speed, but there was no significant interaction. The main effect of Flow Type is due to veridical changes in locomotor speed causing larger errors than non-veridical flow changes (this is also reflected in the magnitude of steering biases observed in section 2.3.2.1) but bear in mind that the direction of error in veridical and non-veridical flow is in the opposite direction, which is not picked up by the RMS error measure. The main effect of Flow Speed occurs because faster flow causes more error than slower flow, regardless of Flow Type.

2.3.2.2.2 DBTM plots

Figure 2.10 shows the paired differences of each experimental condition compared to the control condition. The difference in steering error between VE_{30} and the non-veridical flow conditions, SL_{30} and FS_{30}, is minimal – the upper limit of 95% CI on both is only ~5cm. The increase in steering error in VE_{20} is still small, only 1.4%RW (M_{diff} =.042 [.004, .081], SEM=.018), but this value doubles in VE_{40}, although so does variability (M_{diff} =.102 [.018, .186], SEM=.039).

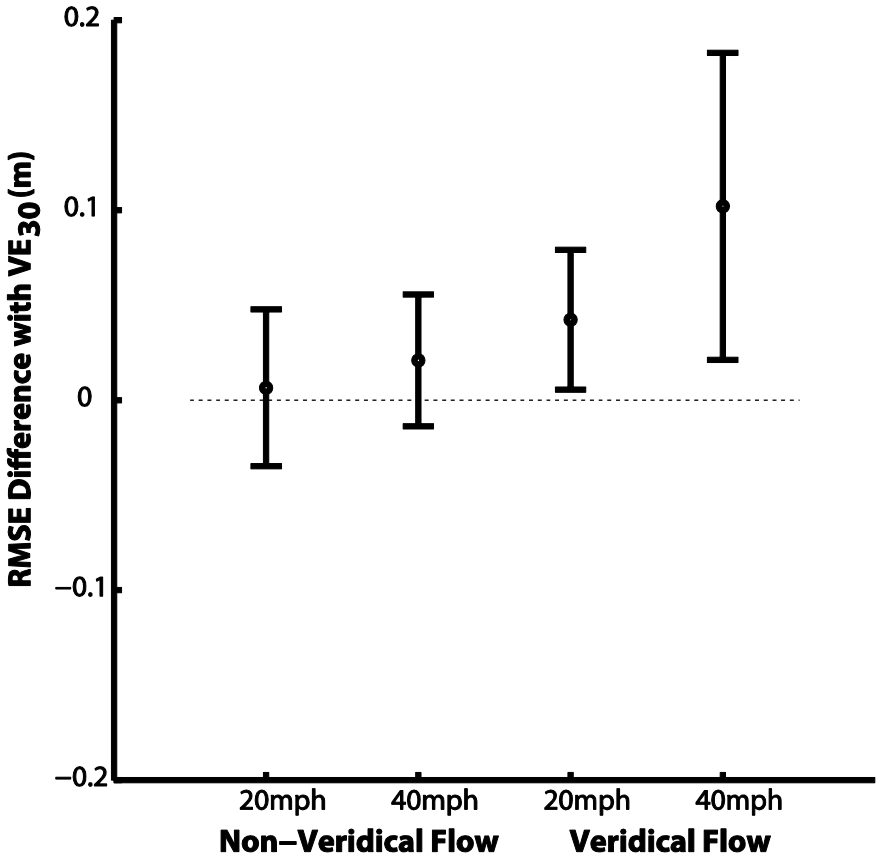

Figure 2.10 RMSE paired differences compared to VE_{30}, with error bars representing 95% confidence intervals. Non-veridical flow (constant driver speed) conditions are shown on the left-hand side; veridical flow (changes in driver speed) conditions are shown on the right-hand side. A positive magnitude indicates greater deviation from the midline relative to VE_{30}.

2.3.2.3 Steering Wheel Jerk

Figure 2.9C shows SWJ, which can be used as a proxy for steering smoothness. Instructions were to steer as *smoothly* and as accurately as you can, therefore, lower SWJ indicates better performance. However, it is not easy to determine a priori what value of SWJ constitutes 'good' performance, since there is not an 'ideal' threshold (for SB and RMSE one can compare performance to real-world distances on the road, with an ideal placed at zero). Rather, we can only compare the relative changes in SWJ

between conditions. Average SWJ under control conditions is 6.5deg.s^{-3} [5.4, 7.6]. SWJ is affected by every manipulation (Figure 2.9C), but there appear to be larger increases due to veridical changes in locomotor speed.

2.3.2.3.1 NHST

A 2 (Flow Type) x 2 (Flow Speed) Repeated Measures ANOVA was conducted (shown in Table 2.2). There were significant main effects for Flow type and Flow Speed, as well as a significant interaction. Participants were jerkier at higher flow speeds than slower speeds (main effect of Flow Speed); jerkier when locomotor speed was altered (VE_{20} and VE_{40}) compared to when it was kept constant (main effect of Flow Type); and the effect of Flow Speed was reversed and diminished for SL_{30} and FS_{30} (interaction).

2.3.2.3.2 DBTM plots

Figure 2.11 shows the paired differences. Slowing locomotor speed by 10mph (VE_{20}) reduced SWJ by ~18.5% (M_{diff}=-1.2deg.s^{-3} [-2.06, -.34], SEM=.4) and increasing locomotor speed by 10mph (VE_{40}) increased SWJ by ~43.6% (M_{diff}=2.83deg.s^{-3} [2.12, 3.55], SEM=.33). This demonstrates that increasing driver speed requires more steering corrections and therefore produces consistently jerkier behaviour, whilst slowing driver speed enabled smoother steering. In contrast SL_{30} caused a slight (~13%), but consistent, *rise* in SWJ (M_{diff}=.85deg.s^{-3} [.204, 1.49], SEM=.3) whilst FS_{30} produced a very slight (~6%) reduction (M_{diff} =-.4deg.s^{-3} [-1.09, .28], SEM=.32). Manipulating locomotor speed (VE_{40} and VE_{20}) caused much larger changes in steering smoothness than manipulating perceived speed (FS_{30} and SL_{30}), with VE_{40} causing the largest change and the jerkiest steering.

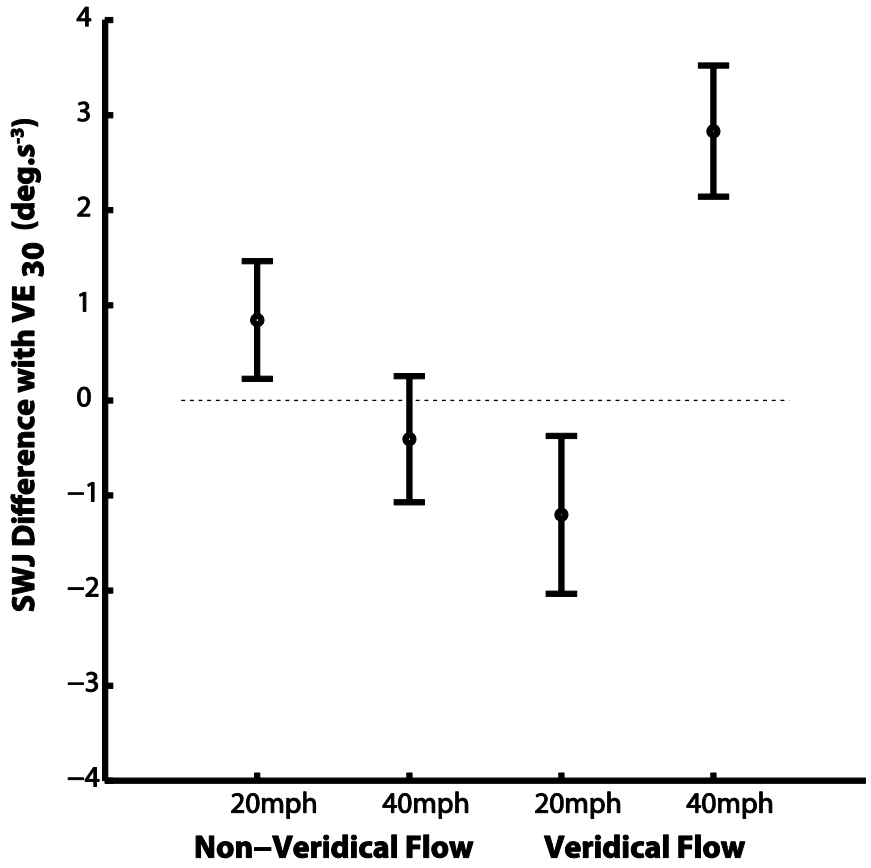

Figure 2.11 Jerk paired differences with VE_{30}. Non-veridical flow (constant driver speed) conditions are shown on the left-hand side; veridical flow (changes in driver speed) conditions are shown on the right-hand side. A positive magnitude indicates greater steering corrections relative to VE_{30}. Error bars represent 95% confidence intervals

2.3.2.4 Steering Measures Summary

Whilst every experimental condition caused systematic changes in steering bias relative to VE_{30}, the magnitude of change was larger for VE_{40} and VE_{20} than for FS_{30} and SL_{30}. This is reflected in RMSE scores, which did not increase for FS_{30} and SL_{30} but increased slightly for VE_{20} and were especially large for VE_{40}. The increase in RMSE for VE_{40} was also accompanied by jerkier steering; however for VE_{20} steering actually became slightly smoother (despite a slight increase in RMSE).

SB, RMSE, and SWJ all capture different aspects of performance (Figure 2.6), so one only builds a complete picture of steering behaviour by utilising all three. For example, SL_{30} and FS_{30} both cause systematic changes in SB (Figure 2.8), but this is not reflected in substantial increases in RMSE (Figure 2.10). It is possible that SL_{30} and FS_{30} might cause drivers to exhibited understeering or oversteering consistently throughout a trial whereas VE_{30} might cause drivers to spend some time either side of the midline (Figure 2.6). Whilst the hypothetical trajectories shown in Figure 2.6 are exaggerated, they are useful at depicting how these behaviours might result in different SB values but similar RMSE values.

Similarly, jerkier steering does not necessarily mean poor positional performance – SWJ is increased in SL_{30} (Figure 2.11), but this is not accompanied by an increase in RMSE (Figure 2.10). An increase in steering corrections that is not accompanied by an increase in error suggests that there is enough information in the task for the driver to compensate successfully. However, an increase in jerk accompanied by an increase in error (such as is the case in VE_{40}) suggests that the visual-motor system cannot successfully compensate for the changing task demands.

2.3.3 Results: Analysing Trajectory Development

Whilst the previous steering measures are useful for quantifying steering behaviour, they are average measures of the entire trial therefore are limited in scope because they do not give information about how a trajectory develops throughout the trial. Figure 2.12 represents the bias trajectories of an average participant by generating an averaged trajectory per participant (from their 6 trials for each condition), then averaging these trajectories across participants for every frame. Although there is some information lost in this approach, the inclusion of shaded error bounds helps clarify where in the trajectory participants' behaviour was more or less consistent. This is a good way of developing a qualitative understanding of trajectory development without looking at each individual trajectory plot.

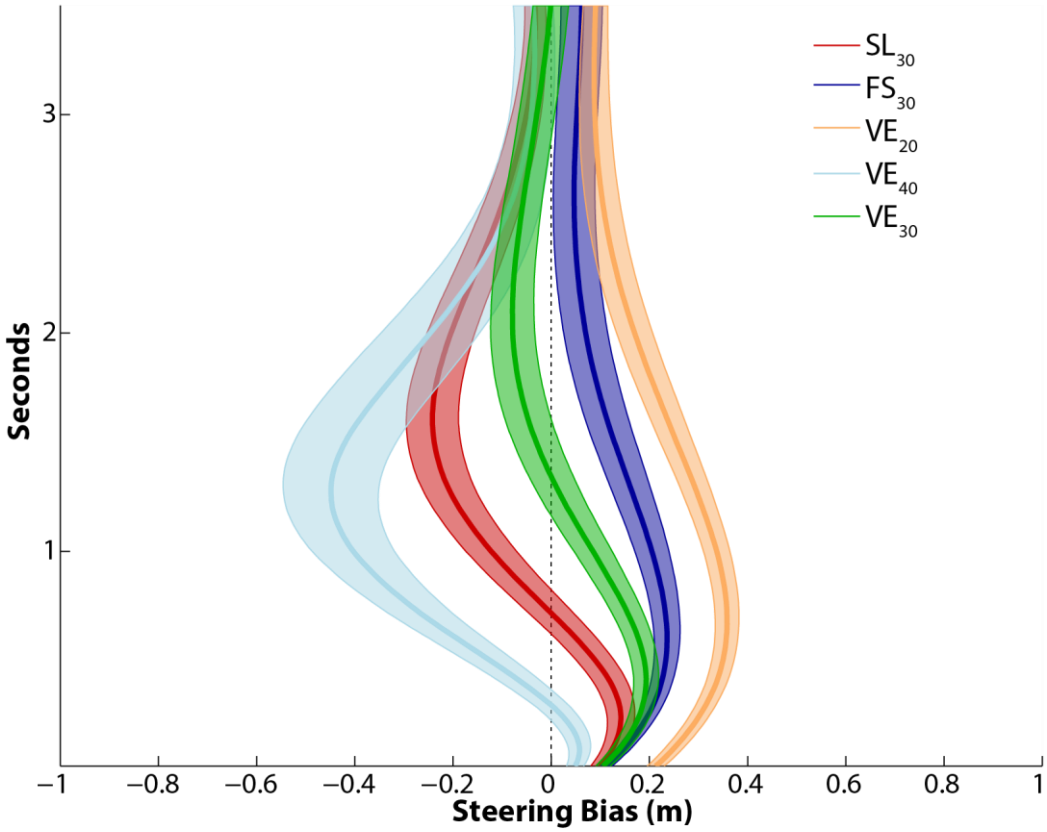

Figure 2.12 Plots showing how steering bias develops over a trial. Signed error for each frame is calculated by averaging across the trials for a participant, then averaging across participants and using this inter-individual variability for the shaded standard error bounds. For all conditions the first 3.5s after the straight road is shown, this means that they correspond temporally but not spatially (changing locomotor speed alters the rate at which the bend is approached). The control condition is shaded green: Faster Flow conditions are shaded dark and light blue; Slower Flow conditions are shaded red and orange; veridical conditions are light; non-veridical conditions are dark.

In Figure 2.12, the control condition, VE_{30}, is shaded green. Participants enter the bend oversteering, i.e. they appear to turn too early. This is corrected for by ~1s after bend initiation, but participants typically overshoot with the steering correction, placing themselves towards the outside road edge ~2s into the bend. As the trajectory progresses, steering settles around the road midline. Figure 2.12 demonstrates that the negligible bias observed in VE_{30} (Figure 2.9A) is due to spending some time either side

of the midline, which acts to 'cancel out' constant error. This behaviour is accurately reflected in a non-zero RMSE score (Figure 2.9B).

The two non-veridical flow conditions are shown in red (SL_{30}) and blue (FS_{30}). These two conditions have the same levels of oversteering as VE_{30} on bend entry, indicating premature turning. Differences develop in the early stages of the bend: SL_{30} sees a rapid positional change towards the outside edge with some correction later on, resulting in negative overall bias (Figure 2.9A); whereas FS_{30} stays closer to the inside road edge and gradually drifts back towards the midline, resulting in positive bias (Figure 2.9A). Even though SL_{30} and FS_{30} have qualitatively different trajectories, they have similar RMSE scores (Figure 2.9B) since the cumulative area between the trajectories and the midline is broadly equivalent. However, the extra corrective steering responses in SL_{30} manifests in higher SWJ (Figure 2.9C), compared to the flatter trajectories in VE_{30} and FS_{30}.

When locomotor speed is increased (VE_{40}; light blue) drivers enter the bend oversteering slightly. However, understeering develops quickly before steering is sharply brought back towards the midline. This manifests in a variable average trajectory (Figure 2.12), characterised by high understeering, high RMSE, and high SWJ (Figure 2.9).

On the other hand, when locomotor speed is decreased (VE_{20}; orange) drivers respond faster than required, entering the bend oversteering greatly. This oversteering persists throughout the trajectory, but is gradually, and smoothly, reduced by the end of the trial. This manifests in a large, positive, bias, middling RMSE, and low SWJ compared to the other conditions (Figure 2.9). Overall then, Figure 2.12 demonstrates that the differences in averaged steering measures reported on sections 2.3.2.1, 2.3.2.2 & 2.3.2.3 capture qualitative differences in steering behaviour between the conditions.

2.4 Discussion

This discussion consists of two parts. The first part evaluates the reporting frameworks of NHST vs. Estimation. The second part discusses what can be learnt from the current experiment's results.

2.4.1 NHST vs. Estimation

In section 2.3.1 it was argued that an estimation approach emphasising uncertainty and magnitude allows a fuller, more nuanced interpretation than the dichotomous reporting of NHST. In this Chapter both methods were used and reported in the results. A summary of each approach is outlined below:

NHST:

> *Statistical analyses revealed that increasing locomotor speed caused significantly more understeering, significantly higher error, and significantly jerkier steering, than decreasing locomotor speed. However, manipulating Flow speed independent of rate of approach to REs generally caused the opposite trend to occur: increasing Flow speed caused significantly more oversteering, and lower jerk, than decreasing Flow speed, but RMSE was not significantly altered.*

Estimation:

> *Altering locomotor speed generally caused larger, and more variable, changes in steering behaviour than simply manipulating Flow speed. Increasing locomotor speed from 30mph to 40mph caused steering position to shift towards the outside edge by ~.18m, and RMSE to rise by ~.1m, although there was high variability between individuals. These changes were accompanied by a large and consistent increase in SWJ. Decreasing locomotor speed caused an equal and opposite shift in steering Bias, and a small increase in RMSE, but these changes were*

> *accompanied by a reduction in SWJ (of smaller magnitude than VE_{40}). In contrast manipulating Flow speed independently of REs caused smaller positional shifts (about half the magnitude compared to when locomotor speed was changed), and very little change in total error, with much smaller changes in SWJ. Increasing Flow speed caused oversteering and marginally smoother steering, whereas decreasing Flow speed caused understeering and slightly jerkier steering.*

Both approaches identify that the experimental manipulations caused systematic trends in the data. However, it is clear that the NHST framework is limited since any further description, for example the magnitude and consistency of the difference, is not readily available from NHST because the author is restricted to explaining whether something is *significantly different* or not. On the other hand, an Estimation approach does equally well at identifying consistent trends, but also allows magnitudes and direction of differences to be compared between manipulations and the reliability of these estimates assessed. Such comparisons will be very useful for the remainder of the thesis since a core thread of the experimental Chapters of this thesis will be assessing how altering REs influences the use of Flow information. A key measure of flow influence will be the extent that steering bias alters in the predicted directions (e.g. oversteering for faster than veridical flow). As such, it is essential to easily detect changes in the magnitude *and* direction of flow effects across different RE displays. An estimation approach suits this purpose well (and also supports the pooling of data across multiple experiments through meta-analytic methods). For the purposes of this thesis, then, an estimation approach meets, and surpasses, the capabilities of NHST, therefore will be the primary form of analysis and reporting throughout the remaining experimental Chapters.

2.4.2 Global Flow vs. Road Edges

This experiment assessed whether manipulating global flow speed in the presence of veridical RE information caused predictable steering biases. This was found to be the case: faster-than-veridical flow caused oversteering; slower-than-veridical flow caused understeering. A global flow bias has been shown before with displays containing an untextured road (Kountouriotis et al., 2015), but this Chapter replicates the findings when the road edges are demarcated using explicitly rendered white lines. This method allows greater flexibility for manipulating RE properties, which is exploited in later Chapters.

The current experiment asked participants to keep to the middle of the road (of a constant curvature bend). Participants were given two potential cues to estimate locomotor speed: REs and Flow. In some conditions REs and Flow were congruent, i.e. the rate of movement of both was matched to the same specified speed (20mph, 30mph, or 40mph). In other conditions REs and Flow were incongruent: RE movement (and locomotor speed) was kept at 30mph, but Flow movement was matched to either 20mph or 40mph. Since the task of keeping to the middle of the road is specified by the lane boundaries, the movement of the REs is the prime determinant of task performance. Maintaining a centre-line on a 60m radius bend at 30mph is a challenging, but manageable, task (see Kountouriotis et al., 2013, 2012; Wilkie et al., 2010). Faster locomotor speeds means error relative to the road centre develops quickly, and larger and more rapid steering movements are required. In VE_{40} steering becomes less accurate and less smooth, indicating that drivers start to reach performance limits, understeering early in the bend suggests participants fail to meet the more rapid steering requirements (Figure 2.12). This error needs a correcting movement, which needs to be larger than at slower speeds. In motor control variability generally scales with movement magnitude (Jagacinski & Flach, 2003), so it makes sense that participant's trajectories are more variable in VE_{40} compared to other conditions, and specifically between .5-2s in the trajectory as this is when large corrections for initial errors are being made.

On the other hand, it might be expected that error is reduced at slower speeds, where error develops slowly therefore can be corrected for at a lower gain. Slowing speed enabled smoother steering, but, surprisingly, increased positional error. At slow speeds steering does not need to be as rapid because the REs are approached slowly. However, the large oversteering on bend entry (Figure 2.12) demonstrates that participants are not delaying steering enough to compensate for the slow speed. Due to the slow speed, however, positional errors can be corrected for smoothly, so the large oversteering is accompanied by reduced jerk.

In VE_{20}, steering is initiated too early; in VE_{40}, it is too late. In the three conditions where RE movement was veridical to 30mph – SL_{30}, $VE_{30,}$ and FS_{30} – steering is initiated at similar times, as demonstrated by equivalent levels of oversteering on bend entry (Figure 2.12). If the timing was influenced by Flow speed there would be differences between SL_{30}, VE_{30}, and FS_{30}. However, if the timing was based on rate of approach of REs, there would not be differences (as is the case). In 60% of all trials the REs corresponded to 30mph. It follows that the timing failures in VE_{20} and VE_{40} might be in part due to participants being conservative in their steering adjustments because the 30mph steering task was the most frequently encountered.

Choosing the appropriate time to initiate the movement is not sufficient for good performance. The driver also needs to choose the appropriate gain (rapidity) of turning the wheel. A driver may initiate steering 'on-time', but if the gain is too low understeering will develop quickly; if the gain is too large, oversteering will develop. Although Figure 2.12 suggests the time of initiation in SL_{30}, VE_{30}, and FS_{30}, is uniform, the *gain* of the wheel turn is not. In FS_{30} the gain of the wheel is too large, leading to oversteering as the bend develops. In SL_{30}, the gain of the wheel is too small, leading to understeering. It seems that, in the current displays, the gain of the wheel turn can be modulated by flow speed, but the timing of the wheel turn is relatively unaffected. This is evidence that flow information contributes to some aspects of steering control, but not others. More generally, it supports the idea that steering control can be

separated into sub-components, each with their own preferential inputs (e.g. Donges, 1978).

One final observation concerns the prevalence of oversteering. In all conditions, participants entered the bend biased towards the inside edge (Figure 2.12). In the current steering task the participant starts in the middle of the road. If the participant does not steer sufficiently, understeering would develop quickly on bend entry (Figure 2.6). Additionally, the force feedback of the steering wheel acts to return the wheel to centre (effectively no steering input) which would also result in understeering. Because the maximum steering response is fixed, insufficient steering early on in the trial could (in principle) lead to impossible steering requirements later in the trial. It seems that participants try to guard against this by actively employing oversteering to provide a safety margin (a similar point is made by Robertshaw & Wilkie, 2008). Relaxing oversteering should smoothly move the trajectory back towards the middle of the lane, whereas initial understeering will require large increases in steering to make sufficient correction to reach the lane centre. This qualitative description is backed up by quantitative measures: conditions that have the largest understeering, SL_{30} and VE_{40}, also have the largest jerk (greater corrective steering actions); conversely, conditions that have the high oversteering, FS_{30} and VE_{20}, have low jerk (smooth adjustment of position).

On the basis of the experiment in this Chapter it is possible to suggest that global flow speed modulates some aspects of steering control (e.g. rapidity of wheel gain), rather than others (e.g. timing of initiation of wheel turn). This indicates that the way in which flow contributes to steering when RE information is available may well be complex. Steering control changes dynamically depending on the amount of guidance or compensatory RE information present in the scene (Salvucci & Gray, 2004), and it is worth investigating whether the contribution of flow to steering alters along with the nature of the steering control task. Future Chapters will use this two-level

framework to assess further how the contribution of Flow varies across different steering control tasks.

CHAPTER 3

FLOW SPEED AND TWO-LEVEL STEERING: UNCONSTRAINED GAZE

3.1 Introduction

In the previous Chapter it was suggested that to fully capture steering behaviour one may need to incorporate flow speed into steering models. Many steering models that seek to explain path following behaviour work on a principle of 'two-level control' (Salvucci & Gray, 2004; Figure 3.1A): Guidance level control that utilises information picked up for far regions in space, and Compensatory level control that utilises information from nearer regions. Chapter 2 shows that people's steering is affected when flow speed is biased (Chapter 2), but it is unknown which mode of steering control is influenced.

One way of assessing how flow may contribute to each level of control is by varying the amount of road edge information present in the scene. Only one study has tested the influence of added road texture (i.e. flow information) across different road presentation conditions. Chatziastros et al. (1999) used Land & Horwood's (1995) method of moving 1° windows (see section 1.5) to measure steering performance with road texture or without road texture (i.e. white lines on a black background). The presence of road texture reduced lateral deviation uniformly across all viewing segment conditions (there was not an interaction), suggesting that flow information contributes equally to both levels of steering control. However, this was only observed on a high resolution monitor, and Chatziastros et al. (1999) fail to replicate this effect on a projector screen, which they suppose is down to the lower resolution compared to the computer monitor (14 pixels/° for the projector screen; ~34 pixels/° for the monitor). Disregarding low quality optic flow in favour of more reliable RE information supports a weighted cue combination approach (e.g. Wilkie & Wann,

2002). However, it seems that Chatziastros et al. (1999) added texture *only* to the road, not to the entire scene (they refer to the added texture as 'road surface texture', but do not provide an image of the stimuli). This would omit peripheral flow which is used for steering control (Kountouriotis et al., 2013; 2015). Additionally, Chatziastros et al. (1999) only tested the *presence* of flow, they did not manipulate the flow in any other way, so it is difficult to know what flow components were being used. This means that the contribution of global flow speed to each level of control remains unclear.

To test the role of global flow speed in two-level steering control, Chapter 2's displays were used to manipulate near and far RE visibility alongside optic flow information. The pattern of flow influence across visibility conditions will reveal how flow contributes to control of curved driving. It is predicted that some flow bias will be observed in full road viewing conditions (see Chapter 2). It is unknown how this flow bias will change across different visibility conditions. Two mutually exclusive frameworks are proposed to aid predictions of the pattern of results (see Figure 3.1):

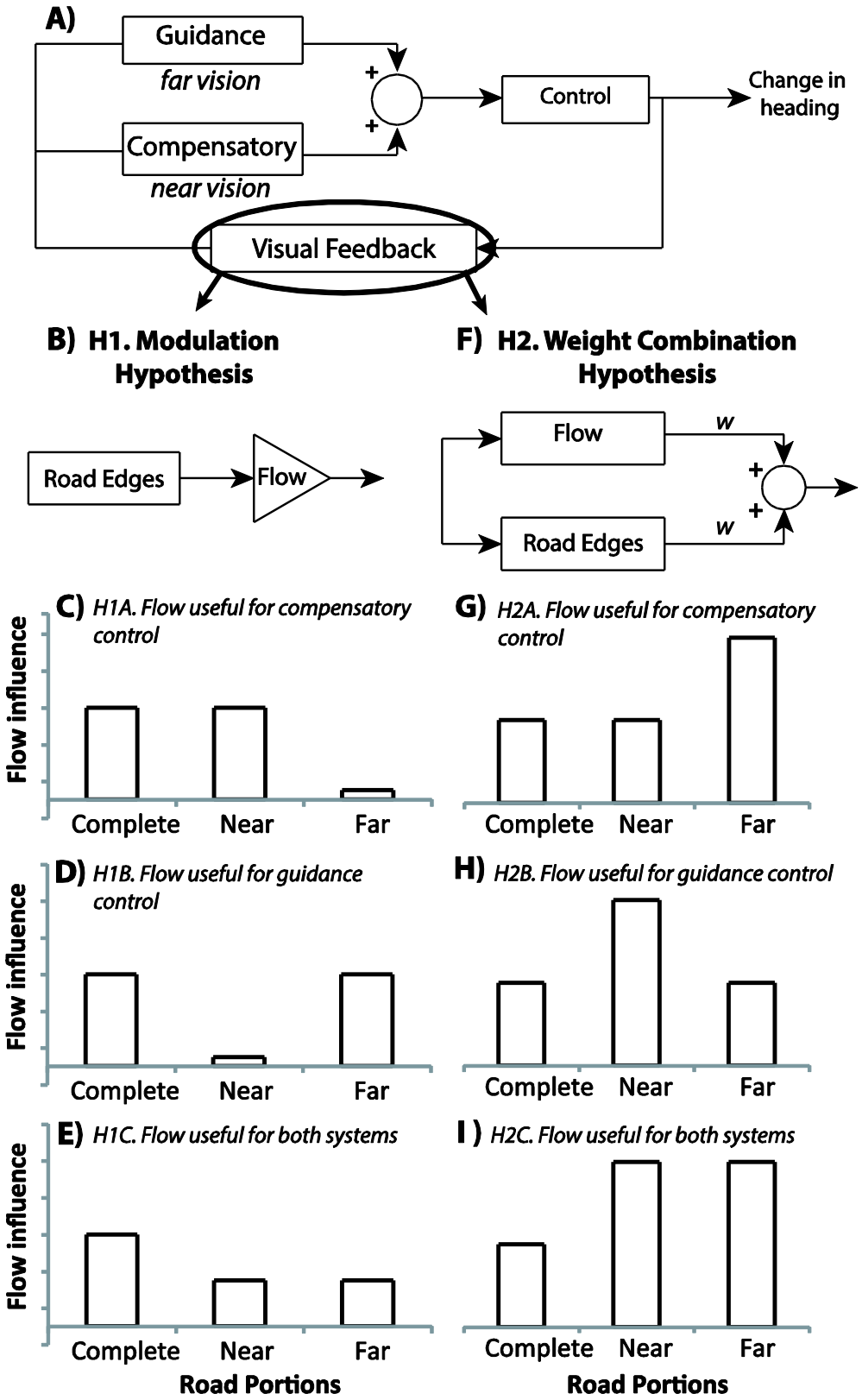

Figure 3.1 A) The Two-Level framework for steering control. B) The Modulation Hypothesis proposes that flow modulates an existing control signal supplied by road edges. C) – E) Possible patterns of results under the Modulation Hypothesis (for

explanation see text). F) The Weighted Combination Hypothesis proposes that flow and edge information could be augmented in a weighted combinatory manner to provide a control solution. G) – I) possible patterns of results under the Weighted Combination Hypothesis (for further explanation see sections 3.1.1-3.1.2).

3.1.1 Modulation Hypothesis (H1): Flow modulates a control signal provided by REs

The *Modulation Hypothesis* is based on the assumption that the distribution of control across guidance and compensatory levels is determined by availability of task-relevant information (road edges). If far road guidance level information is unavailable, the control solution will be dominated by compensatory control; if compensatory (near road) information is unavailable, the control solution will be dominated by guidance level control (Land & Horwood, 1995). Within this framework, the flow influences steering by modulating an existing road edge control signal (Figure 3.1B). The nature of how flow contributes to steering control can be observed from an influence of flow *when the corresponding road edge information is present.* This leads to three hypotheses:

H1A) *Flow useful for compensatory level control only:* There is some evidence that, on curved paths, flow information is *not* useful for perceiving future path (Saunders & Ma, 2011), but that it can provide information about immediate heading (Warren et al., 1991). It could be argued that instantaneous heading is not necessarily useful for specifying future steering requirements because it does not provide information about future path (see section 1.3), but could be useful for compensatory level control in relation to the near road edges. Removing near road edges means that compensatory control is only available through an uncertain estimate of where the near road edges might be. Therefore, when near road edge information is removed from the display, H1A would predict flow influence to diminish as guidance level control takes over (see Figure 3.1D).

H1B) *Flow useful for guidance level control only:* Whilst Saunders & Ma (2011) contend that retinal flow does not support future circular path perception, there is some evidence that humans can gauge future path (from flow) adequately enough to steer (Cheng & Li, 2011), and theories have been proposed that use properties of the *retinal* flow pattern to 'directly perceive' path (Wann & Swapp, 2000; Kim & Turvey, 1999). If flow contributes to estimating future path, H1B would predict an interaction with far road information. When far road edge information is removed from the scene, information about future steering requirements of the task becomes uncertain, therefore the control solution would rely on compensatory control (near road edges; Land & Horwood, 1995) and flow influence will decrease (see Figure 3.1E).

H1C) *Flow ubiquitously useful for control:* There is evidence that humans are able to judge future path from flow (Kim & Turvey, 1998; Wilkie & Wann, 2006; Cheng & Li, 2011) so flow might contribute to guidance level control. However, there is also evidence that flow is useful for gauging instantaneous direction (Li et al., 2009, 2006), which could be useful for compensatory control. Additionally, Chatziastros et al. (1999) observed improved performance across all road viewing conditions when a strong flow signal was added (to a high contrast road surface). If flow is useful for both control systems flow should influence steering in all road conditions (Figure 3.1C).

3.1.2 Weighted Combination Hypothesis (H2): Flow and REs provide independent control signals that are flexibly combined

The *Modulation Hypothesis* (section 3.1.1) is inspired by Land and Horwood's (1995) observations that steering control strategies were largely provided by RE availability. However, Land & Horwood's (1995) displays did not include optic flow. It is possible that optic flow could provide information to supplement uncertain task information. In the *Weighted Combination Hypothesis*, flow and RE information are treated as two (potentially) competing sources of information that combine to provide inputs to a control solution (e.g. Wilkie & Wann, 2002; Figure 3.1F). Road edges are weighted highly by the visual system during curved trajectory driving (Kountouriotis et al.,

2012), therefore when RE information is strong, and/or flow information weak, flow may only contribute little to steering control. Supporting this, Chatziastros et al. (1999) found that adding a weak flow signal (low resolution road texture) to black-background displays did not improve steering performance (similar results are reported by Kountouriotis & Wilkie, 2013, for degraded dot flow displays). Using a strong optic flow signal (large, high resolution projector screen with global flow manipulations), Chapter 2 demonstrates a predictable amount of flow bias under full-road viewing conditions. H2 offers three competing hypotheses to predict how this bias will change when RE information is removed:

H2A) *Flow is useful for compensatory level control only:* If flow is treated as a weighted input to *compensatory* control, removing *near* road edges will cause more weight to be attributed to flow information. Therefore, flow influence will increase when *near* road edge information is removed, but remain unchanged when *far* information is removed (because the 'near only' condition provides the same compensatory control information as a complete road; Figure 3.1H).

H2B) *Flow is useful for guidance level control only:* If flow is treated as a weighted input into *guidance* level control, removing *far* edges will cause more weight to be attributed to flow information. Therefore, flow influence will increase when *far* road edge information is unavailable, but remain constant when *near* road information is removed (Figure 3.1I).

H2C) *Flow ubiquitously useful for control:* If flow is useful for both compensatory and guidance level control, flow will influence steering more whenever road edge information is removed: the RE signal is weaker and less reliable, therefore is down-weighted (Ernst & Banks, 2002). One would expect to see a pattern similar to Figure 3.1G.

These frameworks will be useful throughout this thesis for assessing how the influence of flow on steering bias alters between road conditions. However, road edge

information may not be the sole determinant of flow use. Where a driver looks in the scene may affect how they utilise flow (Authié & Mestre, 2012), and road edges appear inextricably linked to eye-movements (Land & Lee, 1994). The next section provides a brief review on the relevant literature of how manipulating road edges may affect gaze patterns.

3.1.3 Eye-movements and steering control

Gaze patterns are heavily influenced by steering requirements (Wilkie et al., 2008), and steering behaviour can conversely be biased by gaze patterns (Wilkie et al., 2010). Importantly, gaze distributions are influenced by RE availability: fading or removing one RE caused horizontal relocation of gaze closer, towards the remaining RE (Kountouriotis et al., 2012). It might be predicted, therefore, that removing near or far road segments will cause vertical relocation of gaze. This will change the available extra-retinal information, often used as a guidance signal (Salvucci & Gray, 2004), and also the visual flow patterns (e.g. Wann & Swapp, 2000), therefore it may have ramifications for steering control. Unfortunately, most studies that manipulate near and far RE information do not record eye-movements (e.g. Chatziastros et al., 1999; Cloete & Wallis, 2011; Frissen & Mars, 2014; Neumann & Deml, 2011; van Leeuwen, Happee, & de Winter, 2014), or do not sufficiently report gaze behaviour (Land & Horwood, 1995). Land & Horwood (1995) only report gaze data for full road viewing conditions. Additionally, two of the three participants in Land & Horwood's study were non-naïve authors. Eye-movements are often influenced by prior experience (Mourant & Rockwell, 1972), therefore this represents a major confound for interpreting the gaze data reported in Land & Horwood's study. The effect of removing near or far RE information upon gaze behaviour will be examined here to document how gaze patterns change when REs are manipulated.

3.2 Methods

3.2.1 Participants

The same participants as Chapter 2 took part in the experiment. To avoid confounding the participant's gaze sampling behaviour (e.g. the participants may look at where the fixation cross was previously), the free gaze experiment was conducted before the experiments reported in Chapters 2 & 4. All participants gave written informed consent and the study was approved by the University of Leeds, School of Psychology Research Ethics Committee (Ref 13-0221).

3.2.2 Apparatus

The same driving simulator setup as Chapter 2 was used. Eye tracking was conducted using an ASL remote eye tracker to calibrate and record eye movements and a magnetic head tracker recorded head movements (Flock of Birds). The system can be accurate to within ±.6° in active steering tasks (Kountouriotis et al., 2012; Wilkie et al., 2010). Participants' gaze was calibrated using a custom calibration procedure (Figure 3.3) using WorldViz Vizard 3.0 (WorldViz, Santa Barbara, CA). Recording of eye, head and steering data was synchronised with display update rate at 60Hz. Post-experiment, it emerged that the RE manipulations were computationally demanding, reducing the update rate to 51Hz for 'Near' road conditions and 35Hz for 'Far' road conditions. The possibility of any confounding effects of reduced frame rates is discussed later.

3.2.3 Stimuli

The same flow manipulation as Chapter 2 was used, with an additional road edge manipulation (see Figure 3.2). Roads were cropped at 6m (11.3° below horizon; .45s) and 12m (5.7° below horizon; .91s), as per Billington et al. (2010). In these displays the road up to 6m does not give any indication of future direction of travel (i.e. no curvature) but indicates immediate position relative to road edges (the initial straight road section, as described in Chapter 2, was also shortened to 6m), whilst 12m to horizon allows preview for upcoming steering requirements but not information

relative to immediate steering corrections. Additionally, .45s and .91s are similar to the near and far optima reported in Land (1998).

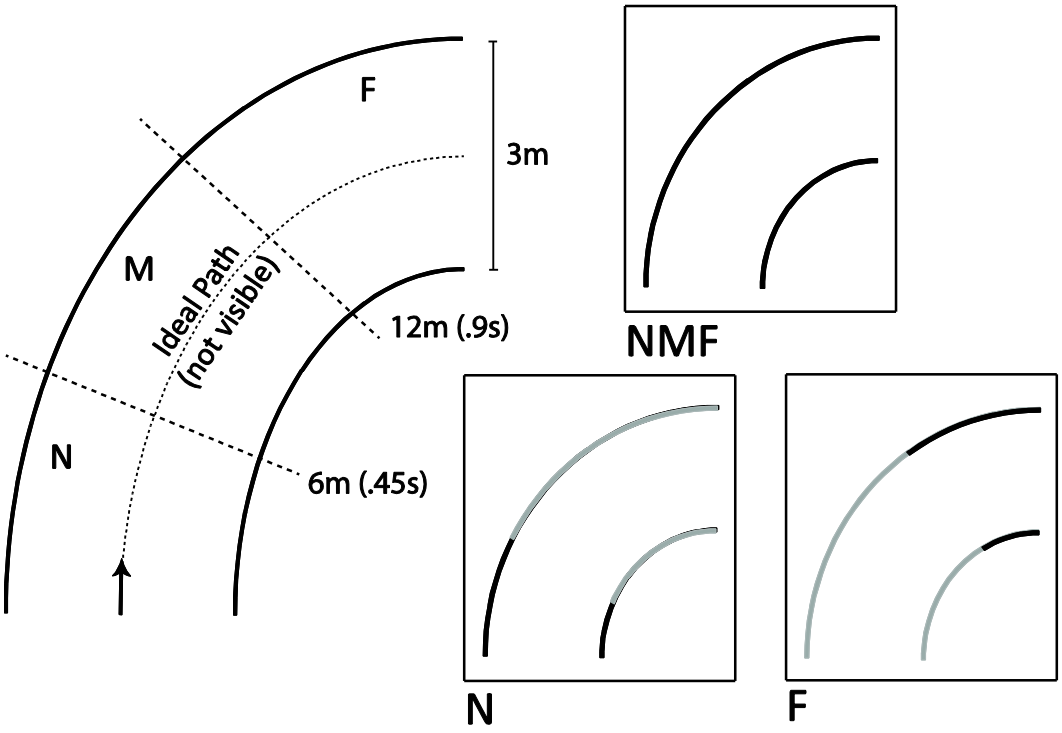

Figure 3.2 Birdseye view of road manipulations. Three conditions were used, denoted by the combinations of three segments, (N)ear, (M)iddle, or (F)ar: NMF, N, and F.

3.2.4 Procedure

For eye tracking purposes, all participants were calibrated using a 9-point custom calibration procedure (described in section 3.2.4.1). Participants then completed 8 practice trials (veridical flow speed, each road visibility condition, for left and right bends) to familiarise themselves with the simulator dynamics. Participants were instructed to 'attempt to steer a central trajectory, keeping to the middle of the road'; to steer 'as smoothly and as accurately as you can'; and to 'centre the wheel after each trial'. There were three flow manipulations: slower-than-veridical (8.9ms^{-1}; ~20mph), veridical (13.41ms^{-1}; ~30mph) and faster-than-veridical (17.9ms^{-1}; ~40mph), abbreviated to SL_F ('SLower Flow'), VE_F ('VEridical Flow'), and FS_F ('FaSter Flow'). There were also three road manipulations: 'Complete Road', 'Near Road', and 'Far

Road' (Figure 3.2), abbreviated to NMF_{Rd}, N_{Rd}, and F_{Rd}. Although the notation of NMF_{Rd} may appear odd at this stage, it facilitates comparison with later Chapters (where the M segment is also manipulated). Participants completed all trials with unconstrained (free) gaze. Trials were 6 seconds long with a .83s (50 frame) pause at the start of trials to give participants time to re-centre the wheel before motion commenced: the driving time was therefore 5.17s. There were six trials of each condition.

3.2.4.1 Eye Calibration Procedure

A custom eye calibration procedure was created for this experiment, shown in Figure 3.3. The calibration grid was shown with the same (but static) background as the trials to match luminosity to trial characteristics. Once calibrated (Step 1), the calibration was visually inspected (Step 2). Gaze data was then recorded for fixation points at the True Horizon (Step 3), and also at various fixation distances (Step 4). This process allowed assessment of eye-height and calibration precision during post-processing, and adjustment of the horizontal and vertical parameters of the 'centre' of the display per individual to ensure maximum accuracy of gaze recordings.

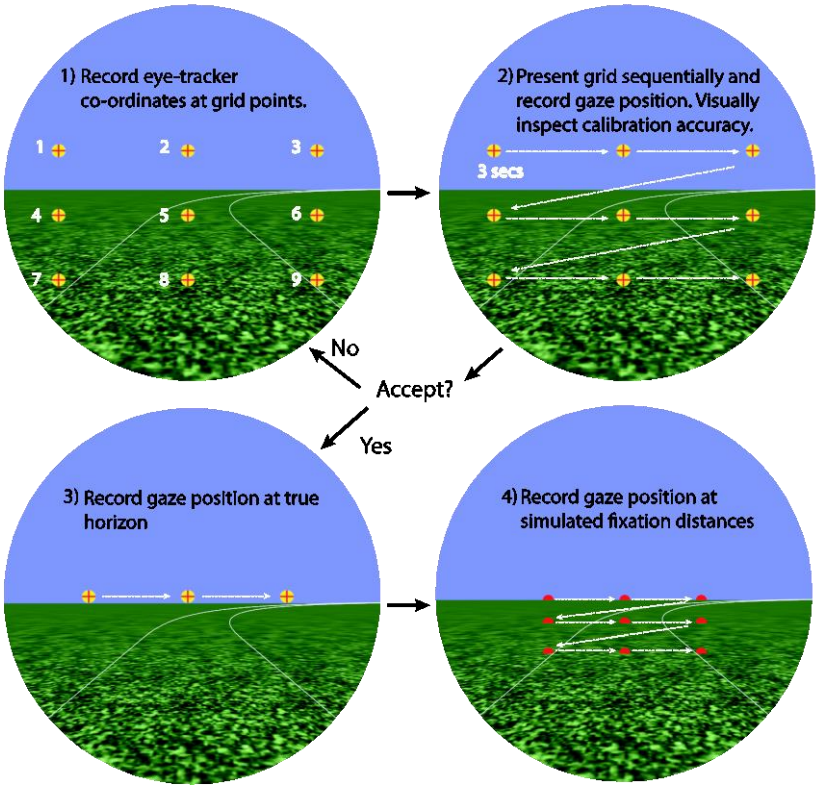

Figure 3.3 The eye calibration process. 1) The 9 point calibration grid. Fixation points were presented one-at-a-time, under complete control of the experimenter, whilst the eye-tracking parameters were adjusted, and the pupillary and corneal reflex characteristics were recorded at each point. 2) The grid was presented sequentially, 3 seconds for each point, and gaze position was recorded. The experimenter could visually inspect the calibration accuracy at each point from the eye-tracker control panel. 3) If the calibration was within acceptable tolerances (if the gaze crosshair rested on the points the participant was asked to look at), gaze at true horizon was recorded so eye-height could be validated at processing. 4) Gaze position was then directed to different simulated distances, so calibration accuracy could be validated during post-processing.

3.3.5 Analysis

The participant's head was left unconstrained to allow natural gaze behaviours, which could have affected gaze recording accuracy, but the average head rotation throughout a trial was in the range of only ±1°. The same steering measures as Chapter 2 were

used: Steering Bias (SB), Root-mean-squared error (RMSE), and Steering Wheel Jerk (SWJ). There are many ways to analyse gaze data, but the focus of this experiment was whether different conditions caused gaze distribution to differ vertically, horizontally, or to be more or less concentrated within a particular region. Therefore, the following metrics were calculated: *Lookahead Distance, Angular Road Offset,* and *Focal Area.*

3.3.5.1 Quantifying steering behaviour: Flow Induced Steering Bias (FISB)

This Chapter sets out to examine whether the magnitude of steering bias changes due to flow manipulations varied depending on road component availability. Results from Chapter 2 suggest that (under complete road conditions) the observed change in steering bias would be proportional (linear) to the change in flow speed. Therefore, the gradient of a line fitted between SB estimates in SL_F, VE_F, and FS_F, indicates how heavily drivers rely on flow: Flow-Induced-Steering-Bias (FISB). For three estimates, the gradient can be simply approximated by taking half the difference between steering bias in FS_F and SL_F conditions: $(FS_F - SL_F)/2$. The greater the FISB score, the more sensitive steering is to the flow manipulations in the predicted direction (oversteering in FS_F, understeering in SL_F). A negative FISB score would indicate steering in the opposite direction of the predictions, and a zero FISB score would indicate that steering was unaffected by the flow manipulations.

3.3.5.2 Quantifying gaze behaviour: Lookahead Distance, Angular Road Offset, and Focal Area.

Eye movement recordings of gaze coordinates for each condition, for each individual, were placed into spatial bins of .89° × .71° (100 x 100 bins). A 2D Gaussian low pass filter of size 10 x 10 and σ=.3 was then applied to these bins for smoothing. The bin of highest fixation density was identified per trial, from this point the *Lookahead Distance* (LD; depth in metres) and the *Angular Road Offset* (ARO; signed angular deviation from the road centre) was calculated. The bin of highest fixation density was

used instead of the average point because averaging across all the data makes the point estimate susceptible to bias from occasional eccentric fixations or noise in the eye-movement signal (e.g. blinks). Finally, Focal Area (FA) is a measure of gaze concentration. The binned data was used to determine the 'catchment area' around the point of highest density where 25% of gaze fixation points fall. The size of this area (in degrees^2) provides a measure of how concentrated gaze fixations were during a trial. A schematic of how the gaze measures are derived is shown in Figure 3.4.

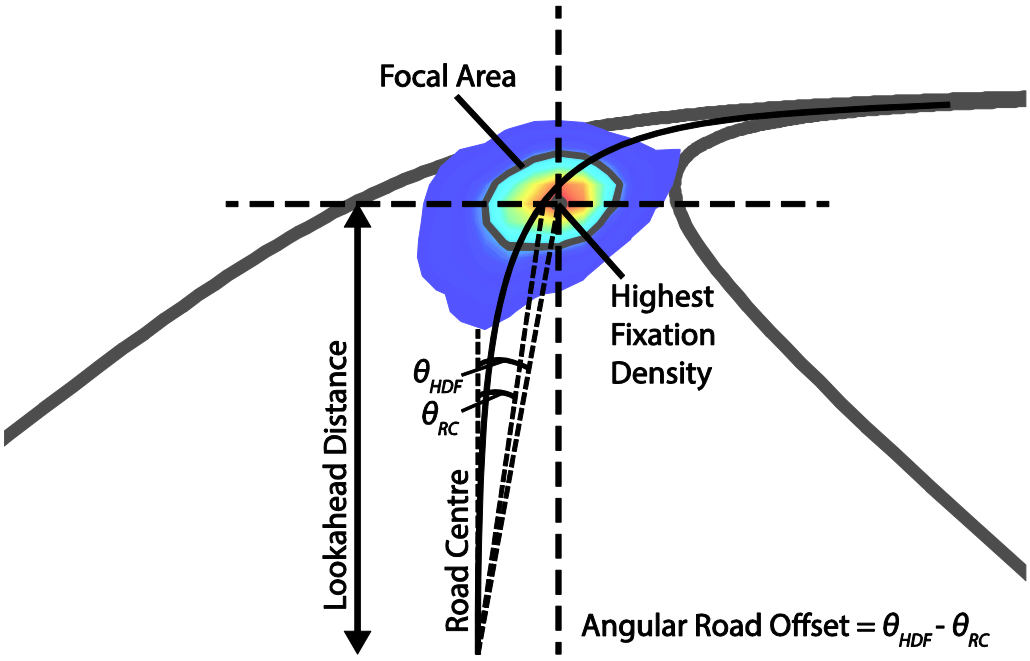

Figure 3.4 Schematic showing how gaze measures are derived.: Lookahead Distance, Angular Road Offset, and Focal Area.

3.4 Results

In Chapter 2 it was argued that an Estimation approach is more intuitive way than NHST to assess steering behaviour across many levels. Here, independent variables are explored by taking the paired difference (for each individual) between each flow level and the control condition, so that each flow level (e.g. FS_F) has two paired difference estimates (N_{Rd}-NMF_{Rd}; F_{Rd}-NMF_{Rd}). 95% Confidence Intervals are

constructed around each estimate so that the consistency of the effect can be evaluated. Each difference-between-the-mean plot is shown with a dotted line representing zero. For example, an estimate on this dotted line for the paired difference F_{Rd} – NMF_{Rd} indicates that removing near road information did not change steering behaviour. The 95% CIs are then used to weight the reliability of this estimate. Main effects are indicated by paired difference estimates of a similar magnitude across all levels (e.g. NMF_{Rd}, N_{Rd}, and F_{Rd}) within a factor (e.g. Road). Interactions are indicated by variable paired difference magnitudes. Crucially, instead of simply identifying the presence of main effects and interactions (as in NHST), these plots give information about which combination of levels drive the effect or interaction, and how large the behavioural difference is.

Averaged group data are shown in single plots for each dependent variable (Figure 3.6 & Figure 3.11). These plots are shown with errors bars representing standard error of the mean (when many close estimates are shown on a single graph, 95% CIs can overlap and be hard to read).

3.4.1 Steering Behaviour

3.4.1.1 Steering Bias (SB)

Figure 3.6A shows SB scores. Under complete road conditions (NMF_{Rd}) participants show negligible SB in VE_F (M=.021m [-.021, .064], SEM=.04). FS_F causes oversteering by ~4%RW (M_{diff}=.13m [.078, .18], SEM=.02) and SL_F causes understeering by ~5%RW (M_{diff}=-.14m [-.22, -.056], SEM=.04; Figure 3.5D). However, this flow induced steering bias interacts with REs. The clear dichotomy observed in NMF_{Rd} (Figure 3.5D) diminishes in F_{Rd}, where FS_F fails to induce oversteering (Figure 3.5F), and in N_{Rd} (Figure 3.5E) there is no consistent flow induced steering bias.

This experiment also sought to examine how Road presentation affected steering bias. Within every flow level, removing far road information caused understeering (Figure

3.5A-C), shifting, on average, ~.35m away from the midline (Figure 3.6A). Removing near information does not seem to have caused systematic positional biases. In VE_F (Figure 3.5B) and SL_F (Figure 3.5C), SB for F_{Rd} was broadly equivalent to NMF_{Rd}. Within FS_F, removing near road information caused a small amount of understeering (Figure 3.5A).

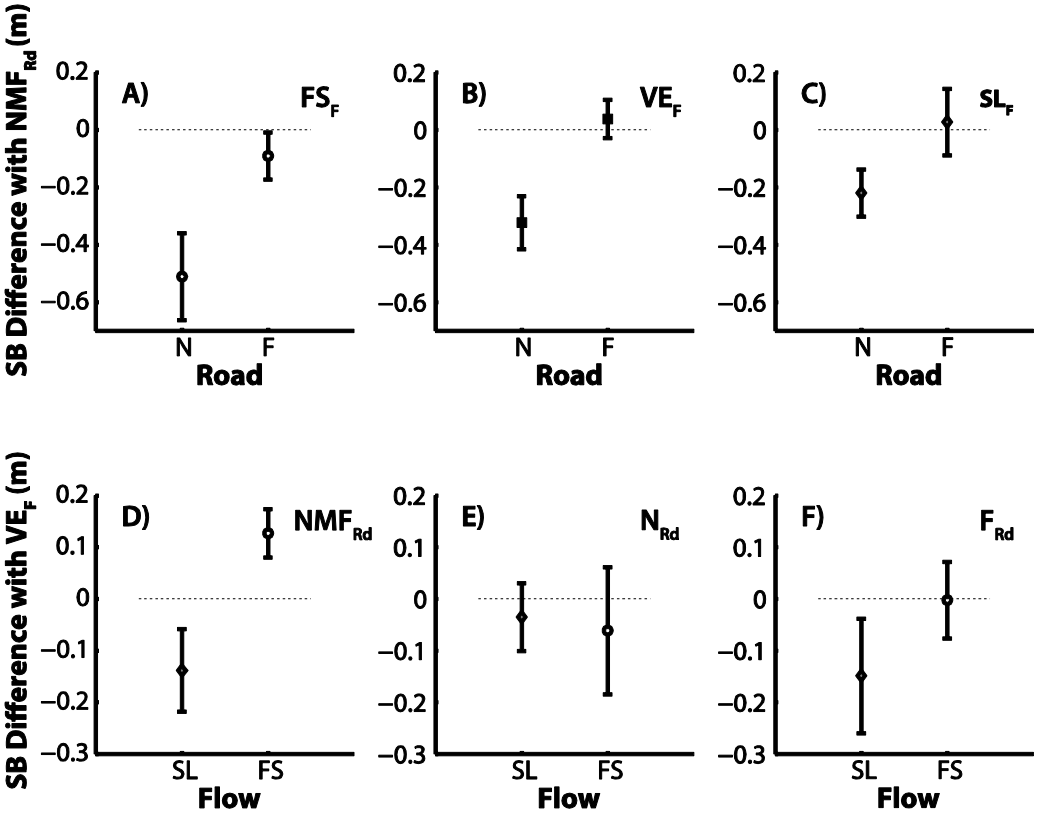

Figure 3.5 Steering Bias difference between means plots. Top Row: paired difference estimates compared to NMF_{Rd} for A) FS_F, B) VE_F, and C) SL_F. Bottom Row: paired difference estimates compared to VE_F for D) NMF_{Rd}, E) N_{Rd}, and F) F_{Rd}. For all graphs a negative magnitude means more understeering than the respective comparison condition, NMF_{Rd} or VE_F. The dotted line represents zero difference between the experimental condition and the control. Note the change of scales between the Top Row and the Bottom Row. Error bars are 95% confidence intervals.

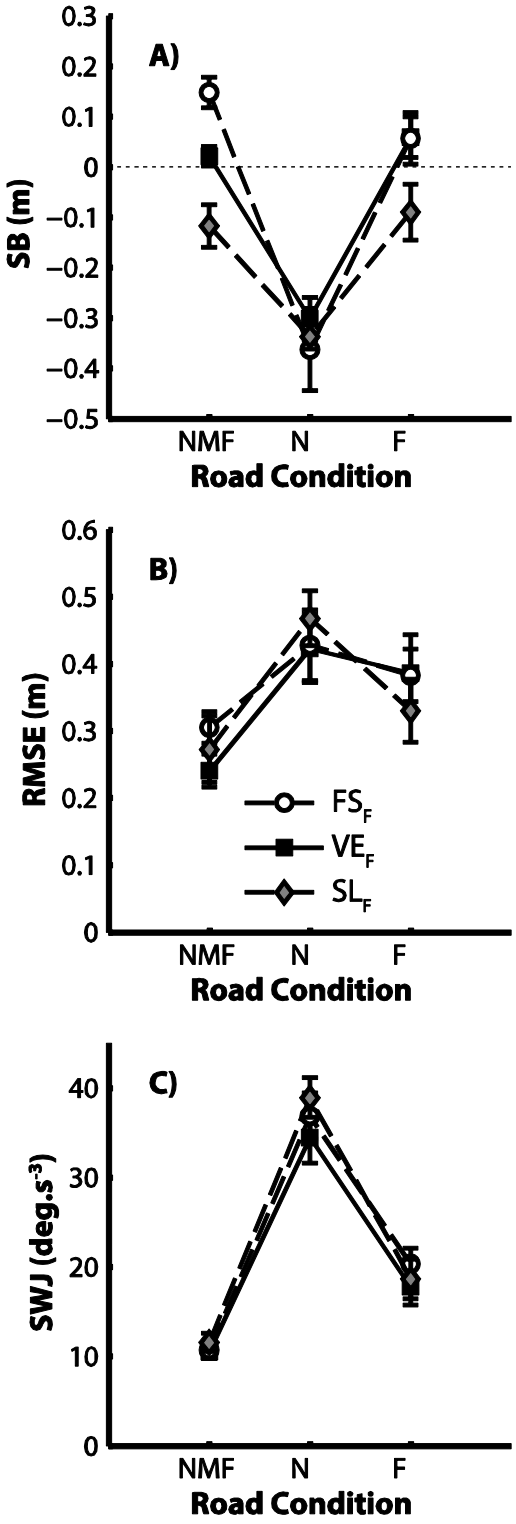

Figure 3.6 All steering performance measures across FS_F (empty circles, dashed line), VE_F (filled squares, solid line), and SL_F (grey diamonds, dashed line), showing A) Steering Bias, B) Root-mean-squared error, and C) Steering Wheel Jerk. Error bars represent standard error of the mean (SEM).

3.4.1.2 Flow Induced Steering Bias (FISB)

FISB highlights 'use' of Flow across Road conditions (Figure 3.7A). FISB was largest for NMF_{Rd}, showing that a 10mph shift in Flow speed resulted in approximately 13cm positional change in steering (M=.13 [.095, .17], SEM=.02). This reduced to approximately 7cm for F_{Rd} conditions (M=.074 [.03, .12], SEM=.02). In N_{Rd} participants did not respond consistently to alterations in Flow (there is large uncertainty in the estimate), but on average FISB sits around zero (M=-.013, [-.089, .062], SEM=.03). The paired difference plot (Figure 3.7B) gives a good indication of how consistent these trends are across participants. Participants consistently exhibit a smaller FISB for F_{Rd} than NMF_{Rd} (Figure 3.7B). The magnitude that FISB reduces between N_{Rd} and NMF_{Rd} is much greater, but varies between participants, indicating that there may be individual differences in how participants use flow when there is no guidance level RE information available.

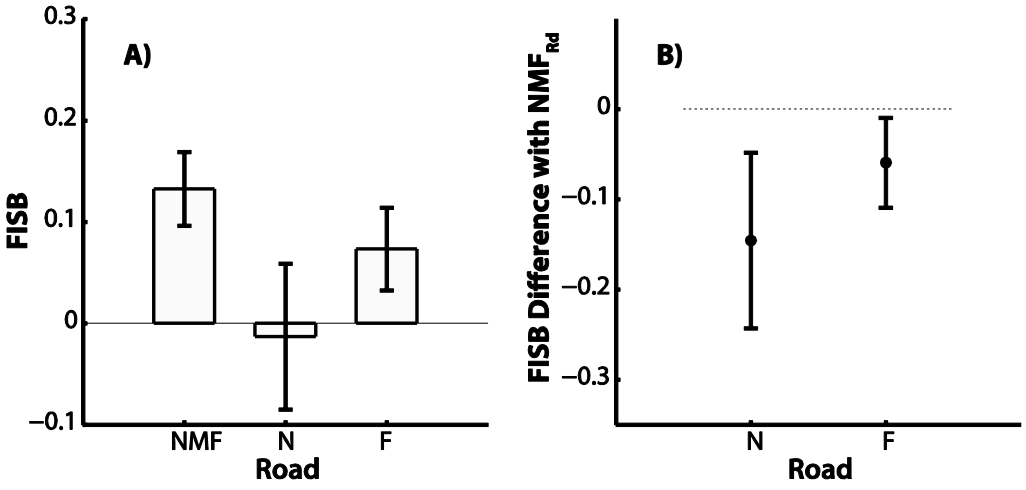

Figure 3.7 A) Average FISB scores for each Road Condition, a positive FISB indicates steering behaviour in line with predictions (oversteering for FS_F; understeering for SL_F). B) Difference between NMF and the other road conditions. All error bars are 95% confidence intervals.

3.4.1.3 Root Mean Squared Error (RMSE)

RMSE scores for all conditions are shown in Figure 3.6B. Changes in Flow speed do cause differences in steering error for some conditions (Figure 3.8D-F), but on the whole the estimated magnitude of these differences are small (.034m on average) and not systematic. When driving with a full road (Figure 3.8D), faster flow speed caused small and consistent increases in steering error. This increase is not replicated within N_{Rd} (Figure 3.8E) and F_{Rd} (Figure 3.8F), where the paired difference between FS_F and VE_F sits around zero. In NMF_{Rd}, the response to slower flow speed was variable, on average causing a marginal increase in steering error (Figure 3.8D). This marginal increase was replicated in N_{Rd} (Figure 3.8E), but not in F_{Rd}, where slowing flow speed causes a marginal decrease (Figure 3.8F).

RMSE altered more systematically for changes in Road component availability (Figure 3.6B). RSME was least for NMF_{Rd} (M=.27m [.21, .33], SEM=.027), but increases by ~62% in N_{Rd} (M=.44m [.34, .54], SEM=.046): this increase is true across all flow conditions (Figure 3.8A-C). F_{Rd} (M=.37 [.27, .47], SEM=.046) also consistently caused greater error than NMF_{Rd}, although to a lesser extent than N_{Rd}. This effect is similar for FS_F (Figure 3.8A) and VE_F (Figure 3.8B), where the F_{Rd} – NMF_{Rd} paired difference sits just lower than the N_{Rd} – NMF_{Rd} paired difference. Within SL_F, however, the response of removing near road information is more variable, although the average estimate exhibits a small increase in error (Figure 3.8C).

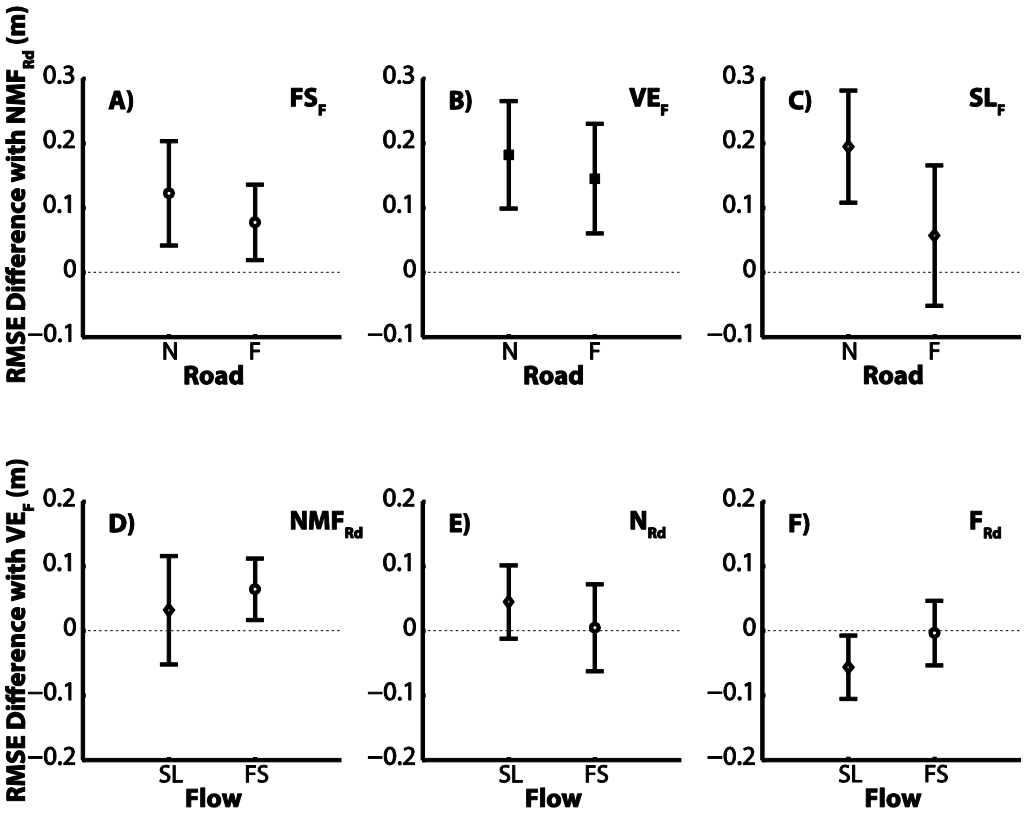

Figure 3.8 RMSE difference between means plots. Top Row: difference between means compared to NMF_{Rd} for A) FS_F, B) VE_F, and C) SL_F. Bottom Row: difference between means compared to VE_F for D) NMF_{Rd}, B) N_{Rd}, and C) F_{Rd}. For all graphs a negative magnitude means more less deviation from the midline than the respective comparison condition, NMF_{Rd} or VE_F. Error bars are 95% confidence intervals.

3.4.1.4 Steering Smoothness (SWJ)

It is clear from Figure 3.6C that SWJ varies greatly when Road is manipulated, but, as with RMSE, differences across Flow conditions are not evident. SWJ for NMF_{Rd} sits around 10.93deg.s^{-3} [9.25, 12.62]. Removing compensatory information increases jerky behaviour (M=18.92deg.s^{-3} [14.68, 23.15], SEM=1.94), but the largest increase is observed when guidance information is removed where SWJ more than triples (M=38.75deg.s^{-3} [31.66, 41.83], SEM=2.33). Both these differences are of roughly equivalent magnitude across Flow levels (Figure 3.9A-C).

Manipulating flow speed has a tendency to cause more steering corrections rather than fewer (Figure 3.9D-F), irrespective of the direction of manipulation, but these changes are nowhere near the magnitudes observed for the Road manipulations (and the estimates for N_{Rd}, where the magnitudes are highest, are also more uncertain).

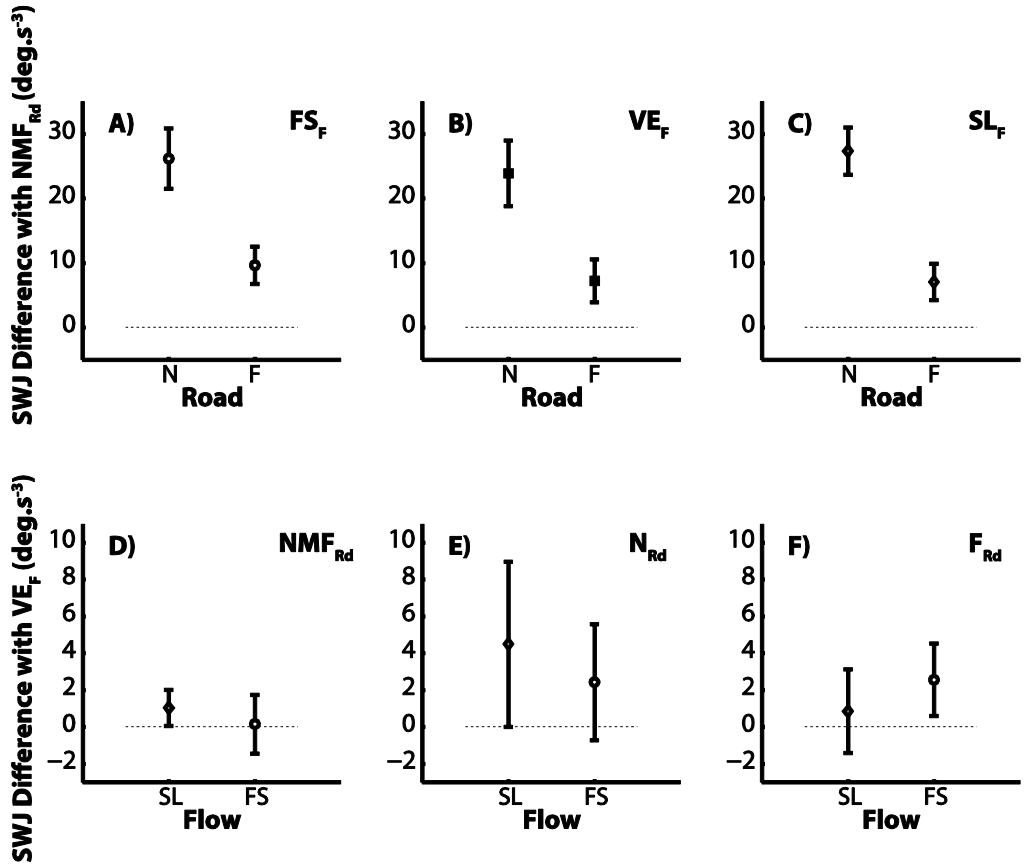

Figure 3.9 SWJ difference between means plots. Top Row: difference between means compared to NMF_{Rd} for A) FS_F, B) VE_F, and C) SL_F. Bottom Row: difference between means compared to VE_F for D) NMF_{Rd}, B) N_{Rd}, and C) F_{Rd}. For all graphs a positive magnitude means jerkier steering behaviour, indicative of more steering corrections, than the respective comparison condition, NMF_{Rd} or VE_F. Note the change of scales between the Top Row and Bottom Row. Error bars are 95% confidence intervals.

3.4.2 Gaze Behaviour

Eye tracking data was successfully obtained for 9 out of the 13 participants: three participants wore glasses, making it difficult for the eye tracker to pick up the pupil and corneal reflex; a fourth participant was excluded because head tracking data failed to record.

3.4.2.1 Binned Data

The individual data from which LD, ARO, and FA were calculated (see section 3.3.5.2) was averaged across all participants and displayed in Figure 3.10. Heat-maps are an intuitive way of assessing how gaze distribution varies between road conditions. Under complete road conditions, gaze seems concentrated between 10-20m ahead, in the centre of the road, with some dispersion around this focal point. An equivalent gaze distribution is observed in F_{Rd}. However, when far road information is removed gaze is 'pulled' downwards towards the near REs and is dispersed more widely, without the same concentrated region of high density (there is no red in any N_{Rd} plots). This trend is reflected in the averaged group data, displayed in Figure 3.11. The LD is closer (Figure 3.11A), and the Focal Area larger (Figure 3.11C), for N_{Rd} than either NMF_{Rd} or F_{Rd}.

Changes in Flow speed do not seem to cause large changes in gaze patterns, demonstrated by similar pooled distribution maps across flow levels (Figure 3.10). However, the group measures (Figure 3.11) show there may be subtle flow and road trends that are difficult to pick out from the pooled distribution maps; F_{Rd} and NMF_{Rd} do not appear equivalent across all measures, and there may be consistent differences between Flow conditions in ARO and FA (Figure 3.11B & C).

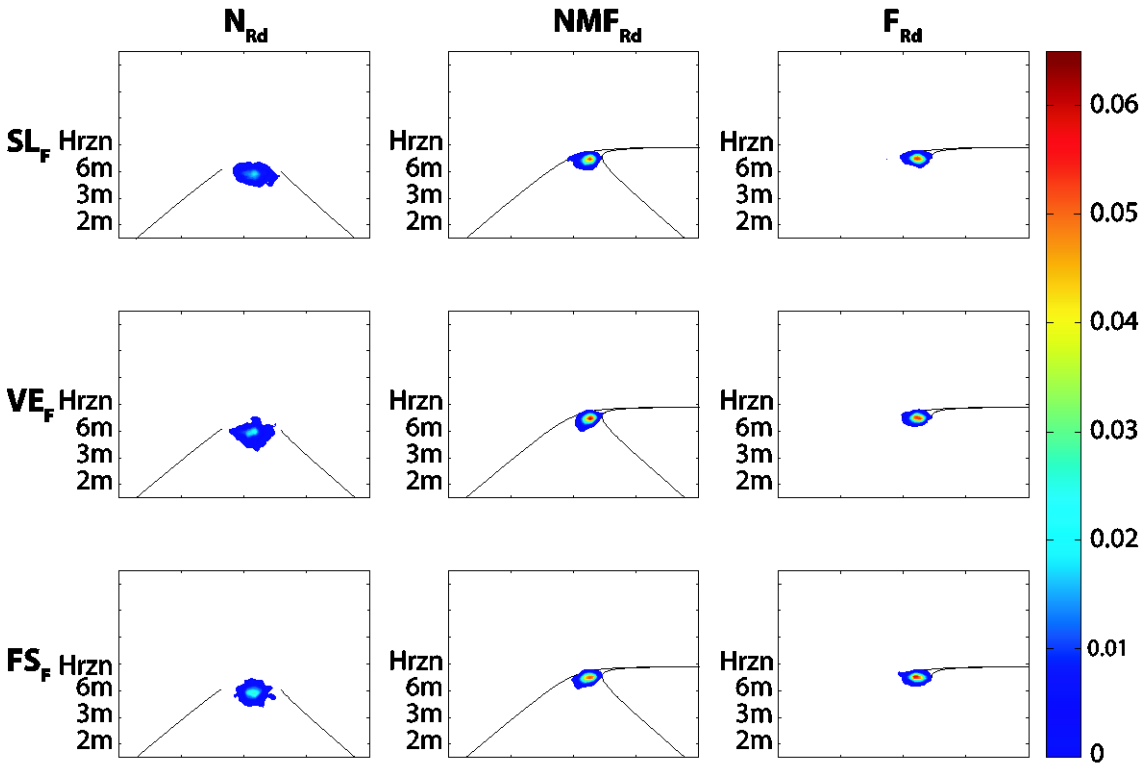

Figure 3.10 Eye tracking data was converted into real-world co-ordinates, binned, and smoothed. This data was then converted into a fixation density map for every participant, which was subsequent summed across participants. Finally, these real-world bins were converted in perspective correct windows though projective geometry adhering to the viewing characteristics of the driving simulator. The results are super-imposed onto perspective correct road edges.

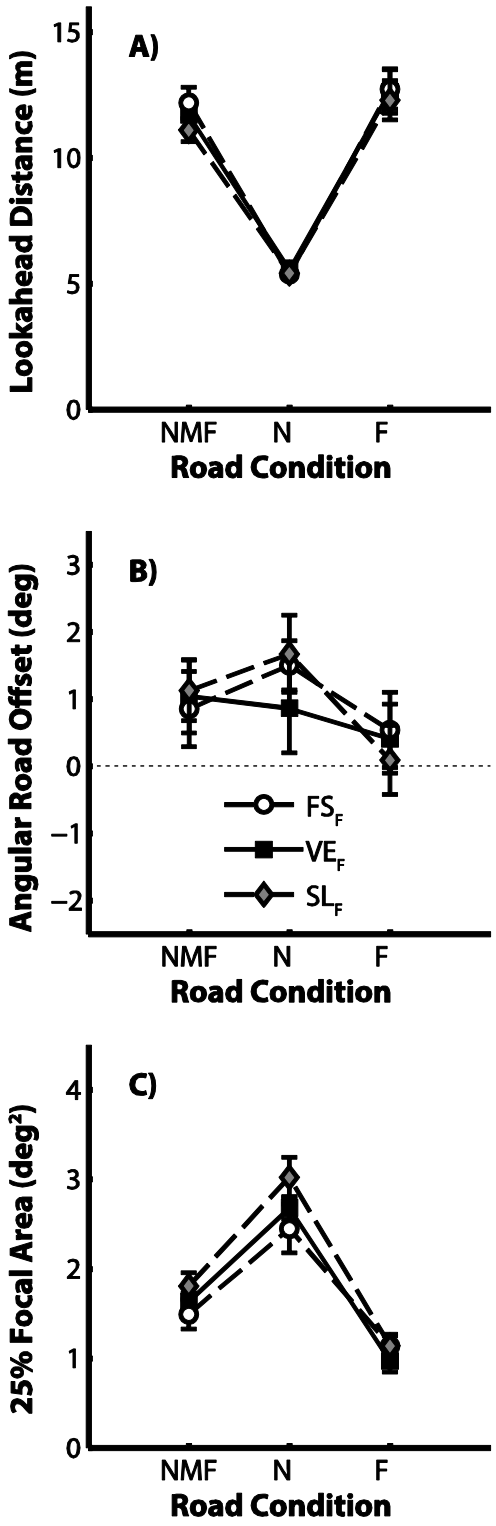

Figure 3.11 All gaze performance measures across FS_F (empty circles, dashed line), VE_F (filled squares, solid line), and SL_F (grey diamonds, dashed line), showing A) Lookahead distance, B) Gaze Offset from Midline, and C) Focal Area where 25% of Gaze falls. Error bars represent standard error of the mean (SEM).

3.4.2.2 Lookahead Distance

Average LD for all conditions is shown in Figure 3.11A. LD varied with road edges, but not with flow. In NMF_{Rd} participants looked ~.87s ahead (M=11.66m [10.47, 12.85], SEM=.52). Participants looked marginally further ahead in F_{Rd}, around .94s (M=12.55m [10.68, 14.41], SEM=.81), but gaze dropped to ~.41s ahead in N_{Rd} (M=5.45m [5.06, 5.83], SEM= .17). The magnitude of these changes was fairly consistent across all Flow levels (Figure 3.12A-C).

Conversely, there are no large, systematic, differences in vertical gaze caused by changes in Flow speed. SL_F caused marginally closer LDs than VE_F in NMF_{Rd} (Figure 3.12D) and F_{Rd} (Figure 3.12F), but this was diminished in N_{Rd}; FS_F caused marginally farther LDs than VE_F in NMF_{Rd} (although the estimate of the paired difference in uncertain), but the FS_F – VE_F paired difference sits around zero in F_{Rd} and N_{Rd}. Altogether, the magnitudes of any changes due to Flow are generally within 1m of VE_F, which equates to a very small time window (.07s).

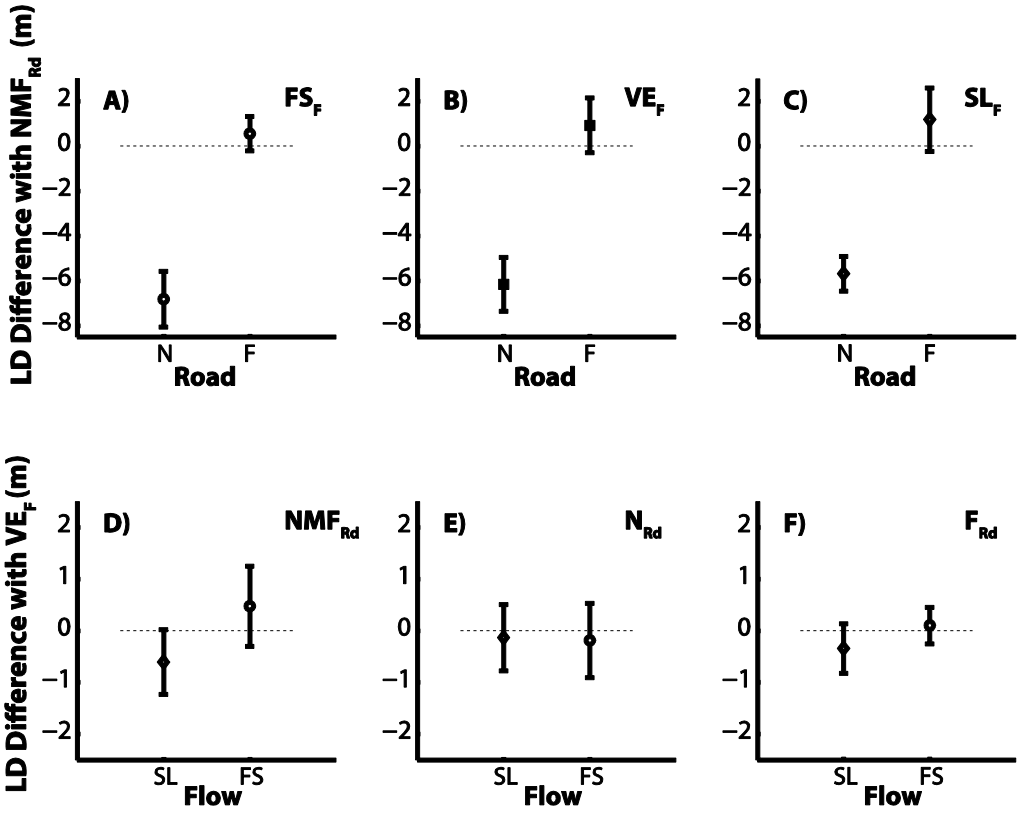

Figure 3.12 Lookahead Distance difference plots. Top Row: difference between means compared to NMF_{Rd} for A) FS_F, B) VE_F, and C) SL_F. Bottom Row: difference between means compared to VE_F for D) NMF_{Rd}, B) N_{Rd}, and C) F_{Rd}. For all graphs a positive magnitude means looking further ahead in the scene, than the respective comparison condition, NMF_{Rd} or VE_F. Note the difference in scales between the Top Row and Bottom Row. Error bars are 95% confidence intervals.

3.4.2.3 Angular Road Offset

This measure assessed where drivers looked relative to the road-centre (Figure 3.4). A positive ARO indicates gaze offset in the direction of the inside edge (a zero offset indicates looking to the road centre). Figure 3.11B shows that generally participants looked very close to the centre of the road (within 2°), even though gaze was unconstrained and there was no explicit visual marker for this location. The grand mean was under 1° away from the road centre (M=.9°, [-.017, 1.82], SEM=.4).

ARO was not greatly altered by changes in Flow speed. When viewing a complete road or only a far road, the paired flow differences (SL_F – VE_F; FS_F – VE_F) both sit around zero (Figure 3.13D & F). In N_{Rd}, AROs for both Flow manipulations are marginally more positive, but the estimates are uncertain (Figure 3.13E). Removing the far road causes marginally higher AROs (in this case, indicative of looking towards the inside edge) than NMF_{Rd} in FS_F (Figure 3.13A) and SL_F (Figure 3.13B), but not in VE_F (Figure 3.13B), where the paired difference sits around zero, and is uncertain. Removing the near road component causes a small reduction in ARO (compared to a complete road) for VE_F and SL_F (Figure 3.13B & C), but this is diminished in FS_F (Figure 3.13A). Across all flow levels the average paired difference between F_{Rd} and NMF_{Rd} is just -.66° [-1.23, -.093], which at 12m (the combined mean LD for F_{Rd} and NMF_{Rd} is 12.1m) equates to only a 10cm difference on the road. Generally, the difference plots reveal few ARO differences between conditions, and show that any potential differences are of small magnitude (<2°).

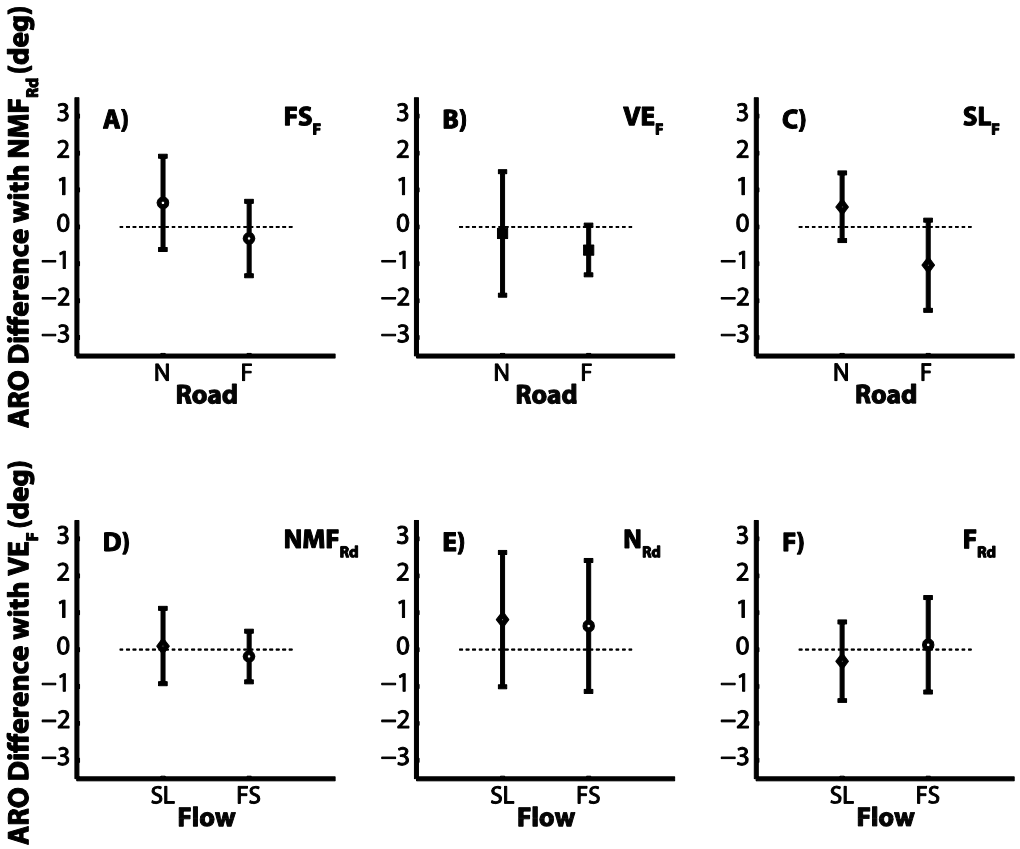

Figure 3.13 Angular Road Offset difference plots. Top Row: difference between means compared to NMF_{Rd} for A) FS_F, B) VE_F, and C) SL_F. Bottom Row: difference between means compared to VE_F for D) NMF_{Rd}, B) N_{Rd}, and C) F_{Rd}. For all graphs a positive magnitude means looking further towards the inside edge and a negative magnitude indicates looking further towards the outside edge. Error bars are 95% confidence intervals.

3.4.2.4 Focal Area

Figure 3.11C displays the group averages of the contoured area which captured 25% of gaze fixations. FA in NMF_{Rd} was small, only ~1.6deg^2 [1.43, 1.87], which at 12m corresponds to a region ~33cm^2 in size on the ground. FA increases in N_{Rd} conditions to, on average, 2.7deg^2 [2.3, 3.14], but diminished to ~1.1deg^2 [.87, 1.3] in F_{Rd} conditions. Figure 3.14A-C shows that these trends due to road are fairly consistent across Flow levels. On the other hand, manipulating Flow speed caused smaller differences (Figure 3.14D-F). FA is marginally larger in SL_F than VE_F across every Road condition, but estimates of the difference are small (<1deg^2).

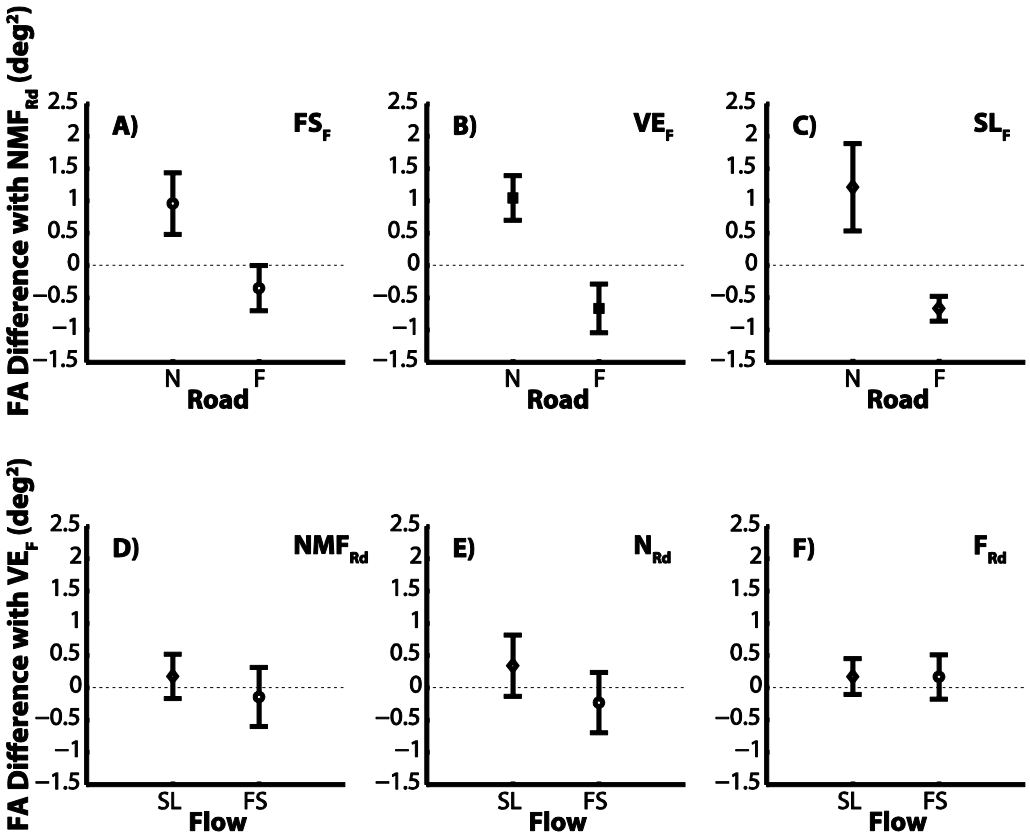

Figure 3.14 FA contrast plots. Top Row: difference between means compared to NMF_{Rd} for A) FS_F, B) VE_F, and C) SL_F. Bottom Row: difference between means compared to VE_F for D) NMF_{Rd}, B) N_{Rd}, and C) F_{Rd}. For all graphs a positive magnitude indicates more dispersed gaze patterns, and a negative magnitude indicates more concentrated gaze. Error bars are 95% confidence intervals.

3.5 Discussion

This experiment assessed whether use of flow speed depended on road component availability, and whether eye movements interacted with flow or road properties. Removing near or far RE information caused systematic changes in FISB scores, suggesting that use of flow is in part determined by the availability of road segments. These changes were accompanied by differences in gaze behaviour. This discussion will firstly discuss the implications for how flow and REs might be combined, before assessing the potential role of gaze in modulating this interaction.

Under full road conditions consistent FISB was observed (Figure 3.7). This would be expected from Chapter 2's results, and previous research (Kountouriotis et al., 2015). How FISB changes across road conditions has implications for the way in which Flow contributes to steering control (see section 3.1). Two frameworks were presented, depending on whether flow *modulates* (H1) or *competes with* (H2) a RE signal, each with three competing hypotheses that predict mutually exclusive patterns of FISB (Figure 3.1). A crucial difference between H1 and H2 is whether FISB increases or decreases when the RE signal is made weaker by removing RE components. Under a weighted combination framework, a less reliable RE signal would be down-weighted, and flow information would be up-weighted (Ernst & Banks, 2002; Wilkie & Wann, 2002). In the current experiment, there is no evidence for FISB increasing when RE components were removed, allowing H2 to be rejected. Instead, FISB reduced, indicating that the utility of flow speed is boosted by the presence of REs, which is the framework presented under H1.

Importantly, FISB reduced by different amounts depending on whether near or far road edges were removed: FISB diminished during F_{Rd}, but disappeared altogether in N_{Rd}. This suggests that the contribution of flow speed to steering control is selective and depends on the nature of the control task, which is in contrast with previous research suggesting that a strong flow signal is ubiquitously useful for control

(Chatziastros et al., 1999) and allows H1C to be rejected. When only guidance information was available (F_{Rd}), FISB reduced to around 55% of NMF_{Rd}. The two-levels of steering control are often treated as additive combinations (Saleh et al., 2011; Salvucci & Gray, 2004); on this basis one might predict FISB to reduce to around 45% (which is the approximate difference between NMF_{Rd} and F_{Rd}) when only compensatory information is available, with NMF_{Rd} representing the additive result of both signals. This did not happen; instead FISB was approximately zero for N_{Rd}. This creates a pattern of FISB that is most similar to that predicted by H1B: where flow speed is useful for guidance level control only. However, H1B does not fully capture the results. If flow speed was exclusively useful for guidance level control, equivalent FISB would be predicted (for NMF_{Rd} and F_{Rd}). Instead, it seems that combining near road and far road signals increases FISB, but providing near road information in isolation does not cause FISB.

A critical behavioural difference between NMF_{Rd} and N_{Rd}, which might help explain this interaction, is where participants directed gaze. In both NMF_{Rd} and F_{Rd}, gaze was generally located around 1 second ahead. This temporal distance is similar to that previously found for guidance control (Land, 1998; Wilkie et al., 2008). In N_{Rd} conditions, gaze was shifted closer to around half a second ahead. This temporal distance is similar to that previously found for compensatory control (Land, 1998); although it is often assumed that this information would naturally be sampled through peripheral vision (Salvucci & Gray, 2004). The obvious advantage of re-orienting gaze is to obtain task-relevant information (gauging lateral distance from REs). However, looking closer in the scene will impair the guidance cues that are available, such as extra-retinal direction (Authié, Hilt, N'Guyen, Berthoz, & Bennequin, 2015; Wilkie & Wann, 2003a). Under N_{Rd} conditions, driving becomes jerkier and more errorful. Jerkier steering is a predictable consequence of removing anticipatory information, and reflects a switch to compensatory control: drivers cannot anticipate movements, so need to operate with a large gain to keep positional error within acceptable limits

(Land & Horwood, 1995; Land, 1998). The increased error suggests that a locomotor speed of 13.41ms^{-1} on a 60m radius (12.81°/s) bend was too fast and tight a bend for compensatory control to successfully 'take over' guidance control. Frissen & Mars (2014) similarly found both increased error and less smooth steering when removing guidance level information, at a locomotor speed of 25ms^{-1} on a road with bends of radii 100 or 200m (14.32°/s and 7.16°/s respectively). These results appear to go against other studies where instability is increased but positional error is maintained (Chatziastros et al., 1999; Cloete & Wallis, 2011; Land & Horwood, 1995). These experiments were conducted at speeds around 16.9ms^{-1} (Chatziastros et al., 1999; Cloete & Wallis, 2011; Land & Horwood, 1995) and on a variety of bends, ranging from a sharp bend of 37.1m (26.1°/s; Cloete & Wallis, 2011), to a very gradual sweep of 916.7m (1.06°/s; Chatziastros et al., 1999). It is highly likely that ability to compensate for a lack of anticipatory information depends on the difficulty of the task, and that the conflicts in the literature between successfully compensating (Chatziastros et al., 1999; Cloete & Wallis, 2011; Land & Horwood, 1995), or not (Frissen & Mars, 2014; the current experiment) arises from the differing speeds and/or bend sharpness.

It has been highlighted that steering was jerkier for N_{Rd} than NMF_{Rd}, and that this could be a predicted from an assumed switch to compensatory control (Land, 1998). However, jerk also increased for F_{Rd} compared to NMF_{Rd} (Figure 3.5B), although to a smaller extent than for N_{Rd}. This is not predicted under the framework of two-level steering, where reduced position-in-lane information reduces the amount of steering corrections (Land, 1998), thus makes for smoother steering but greater lane deviation. It was observed post-experiment that the method of continuously updating the far road edges was computationally demanding, and caused the update rate to reduce to around 35Hz in F_{Rd} and 51Hz for N_{Rd}. Cloete & Wallis (2011) have demonstrated that a slow refresh rate can lead to less accurate and less stable steering responses, an effect which is exacerbated by removing anticipatory information (i.e. they do not find an

interaction between steering accuracy and aperture position with a fast update rate). This may potentially explain some of the increased jerk and less accurate steering in F_{Rd} and N_{Rd}. However, Cloete & Wallis (2011) compared refresh rates with a tenfold difference (7.2Hz vs. 72Hz), and the refresh rate difference here is considerably smaller (35Hz or 51Hz vs. 60Hz). Additionally, here the refresh rate difference was greatest for F_{Rd}, but the effects in the Cloete & Wallis (2011) study were less pronounced when only far road was viewed. The effects in Cloete & Wallis (2011) were greater when only near road was viewed, but here the refresh rate drop between N_{Rd} is only small. There is also no evidence from the Cloete & Wallis (2011) study to expect a low refresh rate to confound directional error. Unfortunately, the next Chapter still contains the potential low refresh rate confound (due to the experiments being conducted concurrently; see section 4.4.2.1), but this issue is addressed in Chapter 5 (section 5.4.3).

It has been proposed that the strongest hypothesis is H1B (Figure 3.1H). H1B suggests that the low FISB observed in N_{Rd} is because Flow speed does not inform compensatory control. However, it is also possible that the reduction in flow use was caused by looking lower in the scene, not by a switch to compensatory control per se. At lower vertical gaze angles optic flow moves at a faster rate. It has been suggested that the visual-motor system prefers sampling regions of low flow speed, in order to reduce optokinetic nystagmus and better discriminate between flow vectors (Authié & Mestre, 2012). Authié & Mestre (2012) put forward the tangent point as a candidate fixation region of low flow speed – there is no evidence for in the current experiment[‡‡]. However, more widely dispersed gaze patterns in N_{Rd}, compared to NMF_{Rd} and F_{Rd}, suggests that looking nearer caused greater optokinetic nystagmus (Authié & Mestre, 2011; Vansteenkiste, Cardon, D'Hondt, Philippaerts, & Lenoir, 2013), and it also is

[‡‡] Across all conditions, the maximum upper limit of ARO 95% CIs is 3°. The tangent point (~13m away from the viewer in these displays) is ~ 6.5° away from the road centre. However, the instructions were to keep to the lane centre, which is different from natural driving where there is a propensity to 'cut the corner', a behaviour that produces TP fixations (Robertshaw & Wilkie, 2008).

possible that the higher rate of flow caused flow to be down-weighted because less reliable direction estimates could be obtained (Authié & Mestre, 2012) which would impair perceiving path-related cues from flow (Kim & Turvey, 1999; Wann & Swapp, 2000). Chapter 4 goes on to assess whether diminished FISB in N_{Rd} is due to a low vertical gaze angle or the removal of guidance RE information to further test H1B.

Chapter 3 has presented preliminary evidence that Flow speed is selectively useful for guidance control, rather than compensatory control, but there are nuances that suggest the combination of compensatory and guidance signals may be more complex than a simple additive combination. The current experiment has also highlighted the importance of controlling for gaze when manipulating REs (Kountouriotis et al., 2012), or flow information (Regan & Beverley, 1982). The extent that the changes in steering behaviour in N_{Rd} compared to NMF_{Rd} and F_{Rd} (characterised by increased jerk, increased error, and decreased FISB), is solely due to RE component availability is unclear, due to the accompanying changes in gaze behaviour. This confound is prevalent amongst driving simulator studies that have investigated two-level steering control (Chatziastros et al., 1999; Cloete & Wallis, 2011; Frissen & Mars, 2014; Land & Horwood, 1995; van Leeuwen et al., 2014), and will be controlled for in future Chapters using constrained gaze.

CHAPTER 4

FLOW SPEED AND TWO-LEVEL STEERING: CONSTRAINED GAZE

4.1 Introduction

Where one looks is usually determined by the task to be performed (Ballard & Hayhoe, 2009). During many forms of locomotion it is important for the agent to anticipate upcoming changes in motor requirements, with fixations often being made to the desired future path (e.g. Higuchi, 2013; Patla & Vickers, 2003). It has been suggested that the placement of gaze is determined by a trade-off between a need for anticipation (where gaze is directed to distant regions), and a need for direct control of position (where gaze is directed to closer regions; Vansteenkiste et al., 2013).

When travelling at slow speeds, increasing task difficulty – for example making the pathway uneven whilst walking (Pelz & Rothkopf, 2007), or narrowing the cycle lane whilst cycling slowly (Vansteenkiste et al., 2013) – can cause gaze to be directed toward near regions. However, during high-speed locomotion the need for anticipation is greater, and gaze is stereotypically directed 1-2s ahead of the driver, with near regions rarely looked at (Land & Lee, 1994; Lehtonen et al., 2013; Wilkie et al., 2008). Position-in-lane information is generally not fixated (although potentially could be), but instead monitored through peripheral vision of either road edge (Kountouriotis et al., 2012). This behaviour seems to represent a good trade-off between the need for anticipation and need for direct control, and also seems to be a behaviour that separates experts from novices, who look nearer in the scene (Mourant & Rockwell, 1972).

Studies which have disrupted stereotypical gaze patterns demonstrate the importance of gaze direction in steering control. On a straight road lane-keeping task, Readinger,

Chatziastros, Cunningham, Bülthoff, & Cutting (2002) forced participants to look at eccentric fixations. This caused steering to be biased in the direction of fixation. Importantly, this effect persisted when the steering wheel mapping was reversed, thus ruling out a biomechanical explanation of biasing steering in the direction the head and eyes are pointing. Kountouriotis et al. (2012) demonstrated similar effects on curved paths. In this experiment, the degree of bias induced by offset gaze was modulated by RE availability, in that participants were more affected by offset gaze when REs were faded. These papers show that if gaze is disrupted in the horizontal domain steering can be biased, especially if RE signals are weak.

Disrupting gaze in the vertical domain may also cause steering biases. Occlusion studies demonstrate that using an opaque mask to occlude anticipatory road information caused increased lane departures on 5m wide lanes at self-selected speeds (van Leeuwen et al., 2014) and increased positional error on 3.5m wide lanes at 25ms^{-1} (Frissen & Mars, 2014). Whilst neither of these studies record eye-movements, it is reasonable to assume that gaze was relocated to lower in the scene because there was no information in the top half. A criticism of these occlusion studies is that they remove *all* information from the top half of the visual scene, so the observed results are not simply due to the relocation of gaze in the vertical domain. Summala, Nieminen, & Punto (1996) assessed whether drivers could monitor road position using peripheral vision of the upper half of the visual field. They asked drivers to fixate on an in-car task placed either 7°, 23°, or 38° lower than the horizon, whilst simultaneously performing a lane-keeping task on a 3m wide straight road. For novice participants, performance was impaired for both 23° and 38° vertical eccentricity positions. Experienced drivers, however, were able to keep in lane in the 23° position but performance was impaired for the 38° condition. This is often cited as evidence that successful monitoring of road position through peripheral vision can be improved through experience. However, their performance measure was the percentage of total run completed before leaving the lane. This is a crude measure, and only penalises

performance when lane deviation reaches potentially fatal levels (i.e. leaving the lane, which on their undemanding straight lane keeping task is incredibly poor performance). Other studies investigating offset gaze have found robust effects using more precise measures of positional performance (Frissen & Mars, 2014; Kountouriotis et al., 2012; Readinger et al., 2002). Moreover, the results of the previous Chapter show that looking lower in the scene on a curved road is associated with large increases in positional error (although well within the boundaries of a 3m wide road). Since Summala et al. (1996) did not precisely measure position over time they may have underestimated the negative impact of not looking in the direction one is going.

Looking where one is going does not simply allow guidance and monitoring of the road edges, but there is evidence that suggests looking where you are going could allow path to be directly perceived from the curvature of flow vectors (Kim & Turvey, 1999; Wann & Swapp, 2000). In the previous Chapter, evidence was presented that suggests flow may interact selectively with far road components over near road components. However, this result is potentially confounded by gaze differences between the two road viewing conditions. In particular, presenting only near road regions caused gaze to be shifted and directed closer. A possible interpretation for the observed pattern of results is that flow speed is selectively used when people are looking ~1s ahead, rather than ~.5s ahead.

The following study replicates Chapter 3's experimental design, with the additional constraint of participants looking at a fixation cross on the future path. This serves to control extra-retinal direction and changes in perceived retinal flow that would accompany gaze shifts. In Chapter 3, flow-induced-steering-bias (FISB) was greatest for the complete road condition, halved when only far road was presented, and reduced to around zero when just the near road component was visible (Figure 4.1A). The current experiment tests whether the absence of FISB when only near road is presented is due to Far road being removed, or the lowered gaze. Two patterns of results are predicted, in light of Chapter 3's results, under the framework of flow speed

modulating RE control signals (Chapter 3, H1). Figure 4.1B displays predictions that arise from assuming flow use is dependent upon gaze, therefore FISB is present whenever gaze is forward (in every condition in this experiment), but this hypothesis leaves room for selective use of Flow dependent on Road component availability. Complete road represents 'maximum' bias, with flow speed apportioned into flow-for-guidance control and flow-for-compensatory control. The relative magnitude of FISB will determine which level of steering control the flow speed signal is *most useful* for. The motivation for this approach is that previously FISB was reduced in far road conditions (see section 3.5). Importantly, it is assumed that the bias observed in complete road is roughly the sum of the bias observed in the other two road viewing conditions. Conversely, if FISB is independent of gaze but dependent on Far road availability, the pattern depicted in Figure 4.1C would be expected: Flow use with only near road information would remain minimal, with larger FISB magnitudes whenever far road was present.

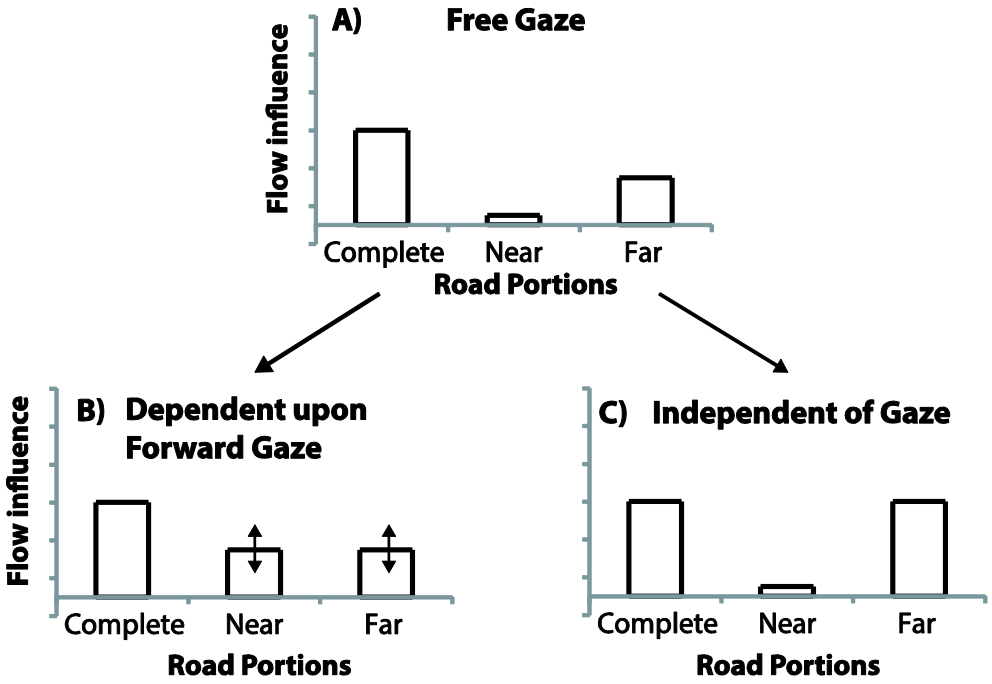

Figure 4.1 Predicted Patterns of FISB. A) The pattern observed in Chapter 3 with unconstrained gaze. B) If FISB was dependent on forward gaze, FISB would be expected in both Near and Far conditions, with the relative magnitude indicating the usefulness with either road segment. C) If FISB is independent of gaze direction, but dependent on Far Road availability, diminished FISB would be observed in Near Road, but higher FISB in Far Road and Complete Road.

4.2 Methods

4.2.1 Participants

The same participants as Chapters 2 & 3 took part in the current experiment. All participants gave written informed consent and the study was approved by the University of Leeds, School of Psychology Research Ethics Committee (Ref 13-0221).

4.2.2 Apparatus

The same apparatus as Chapter 2 was used.

4.2.3 Stimuli

Similar stimuli as Chapter 3 were used. This time, however, participants fixated a red cross positioned 16m ahead on the future path (Figure 4.3). This value was chosen because it corresponds to 1.2s ahead on the future path, which is similar to where participants look under free gaze conditions viewing similar displays (Wilkie & Wann, 2003b). The fixation position was based on previous research, rather than the gaze coordinates reported in Chapter 3 (which suggest a slightly lower lookahead distance of ~.9s), because the experiments were conducted concurrently. Reported lookahead distances vary between individuals (Wilkie & Wann, 2003b) and between studies (Land, 1998, reports a lookahead distance of ~1s, whereas Lehtonen et al., 2013, report lookahead distances of ~2s), and nevertheless the retinal difference between a fixation at .9s and a fixation at 1.2s is only 1.4° in these displays. Therefore, it is highly unlikely that a fixation placed at 1.2s rather than .9s would be unnaturally far enough to confound steering behaviour. The fixation cross served to stabilise gaze across all trials, ensuring that steering biases across flow manipulations could not be explained by different gaze patterns. The cross also allowed an extra condition, the 'Invisible' Road (INV_{Rd}), to be included (Figure 4.3D). In this condition, road edges are completely removed, so all the information made available for the participants to control steering is the flow field and the fixation. The INV_{Rd} condition was included to assess the influence of flow based purely on the position of the fixation cross indicating the direction of the future path, without road edge information (participants were always exposed to full road viewing conditions before the 'invisible' road condition to ensure had knowledge of where the road edge would have been if visible).

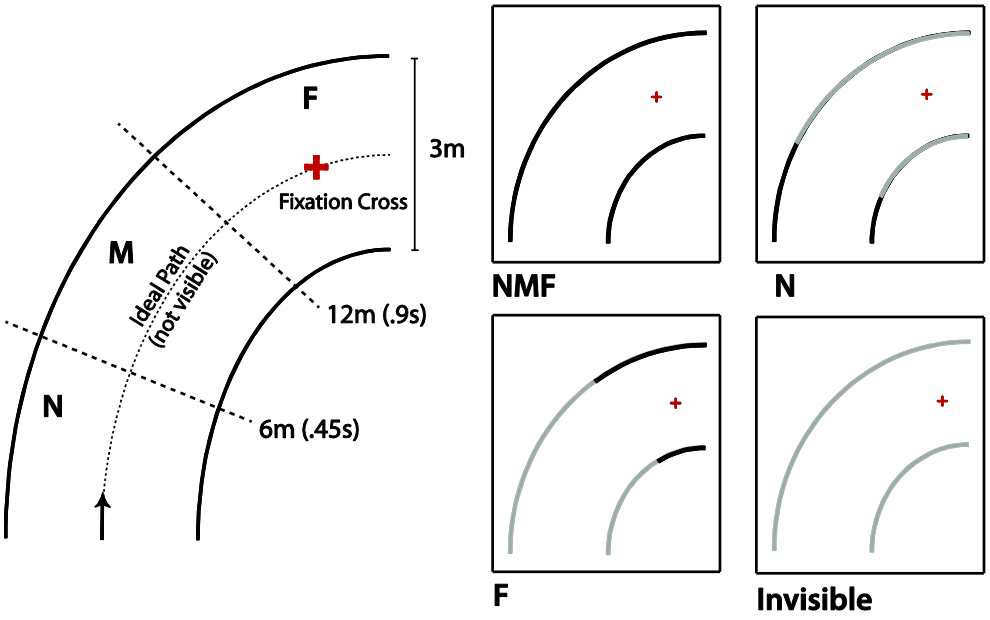

Figure 4.2 Birds-eye schematic of different road edge combinations. Four conditions were used, denoted by the combinations of three segments, (N)ear, (M)iddle, (F)ar, or (INV)isible: NMF, N, F, and INV.

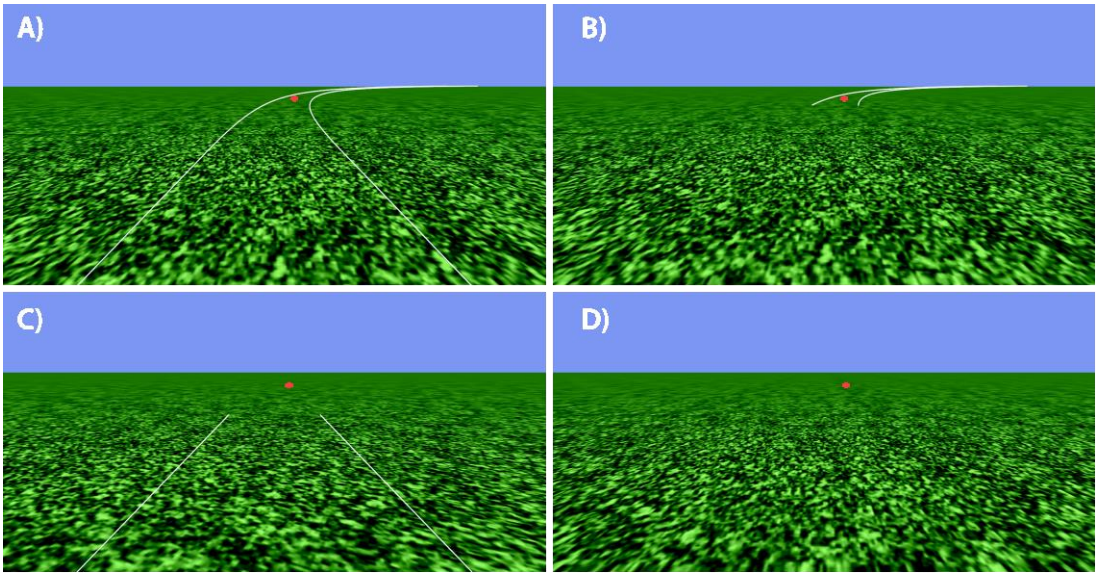

Figure 4.3 Screenshots of Stimuli for Right hand bends, with the red fixation cross 16m ahead on the future path. A) Complete Road. B) Far road, cropped at 12m. B) Near Road, cropped at 6m. D) Invisible Road.

4.2.4 Procedure

Participants completed 8 practice trials to familiarise themselves with the simulator dynamics. Participants were instructed to 'attempt to steer a central trajectory, keeping to the middle of the road', to steer 'as smoothly and as accurately as you can', to 'centre the wheel after each trial', and to 'fixate on the fixation cross'. There were three flow manipulations (SL_F, 8.9ms^{-1}; VE_F, 13.41ms^{-1}; FS_F, 17.9ms^{-1}) and four road conditions (NMF_{Rd}, N_{Rd}, F_{Rd}, and INV_{Rd}). Trial duration remained identical to Chapter 3 (6 seconds), meaning the whole experiment duration was 7.2mins.

4.2.5 Analysis

Positional data over time was recorded at 60Hz and the measures Steering Bias, RMSE, and SWJ were calculated. FISB was calculated using SB (FS_F – SL_F / 2).

4.3 Results

The results are reported as per Chapter 3. Trends are analysed through plots showing paired difference estimates between the means of experimental conditions and the control condition (VE_F + NMF_{Rd}), with the precision of each estimate captured through 95% CIs. Additionally, the grouped and average measures are shown with standard error bars (Figure 4.5).

4.3.1 Steering Bias

Average SB scores are displayed in Figure 4.5A (as per Chapter 3). There are clear positional differences caused by manipulating Flow. In NMF_{Rd}, participants exhibited negligible bias in VE_F (M=.034m [-.064, .13], SEM=.04). Faster flow produced consistent oversteering of ~1%RW (M_{diff}=.037 [-.03, .1], SEM=.03); Slower flow produced consistent understeering of ~5%RW (M_{diff}=-.156 [-.09, -.22], SEM=.03; Figure 4.4D). Similar SB values were obtained for F_{Rd}, although FS_F produced a slightly larger oversteering shift of than during NMF_{Rd} (~4%RW), and the estimate for the

paired difference of SL_F -VE_F is considerably more variable (M_{diff}=-.14m [-.26, -.02], SEM=.06; Figure 4.4F). In $N_{Rd,}$ the small oversteering bias caused by FS_F persists (M_{diff}=-.05m [-.05, .15], SEM=.04) although it is less consistent across participants than for F_{Rd} and NMF_{Rd} (Figure 4.4E). However, the levels of understeer caused by reducing flow speed is reduced compared to NMF_{Rd} and F_{Rd}, and sits around zero. In INV_{Rd} the steering response due to manipulating flow speed is more variable (Figure 4.4G). During INV_{Rd}, the estimate for FS_F – VE_F is similar to the other road conditions (M_{diff}=-.06m [-.11, .23], SEM=.08) though it is far less precise, suggesting that for many participants increasing flow speed did not increase oversteering. On the other hand, during INV_{Rd} the magnitude of understeering shift produced by slowing Flow speed is much greater than the other road conditions, around 10.5%RW; however, this estimate is also characterised by high variability (Figure 4.4G).

Figure 4.5A shows clear differences caused by manipulating Road. Under veridical flow conditions (Figure 4.4B), removing near road does not cause a systematic shift in steering position, whereas removing far road, or removing RE information altogether, caused understeering by around 6%RW. A similar trend can be observed in FS_F (Figure 4.4A). In SL_F, however, the pattern is a little different: the amount of understeer induced by removing far road is reduced, whereas the understeer induced by removing all REs is increased to ~10%RW, and more variable (Figure 4.4A; M_{diff}=-.32 [-.53, -.11], SEM=.1)

In summary, in all conditions the oversteering response to increasing flow speed is small. The understeering response to decreasing flow speed is larger, but diminished in N_{Rd}. In general, removing prospective road information caused understeering. In VE_F and FS_F, removing near road information did not cause any additional understeer, but in SL_F it did.

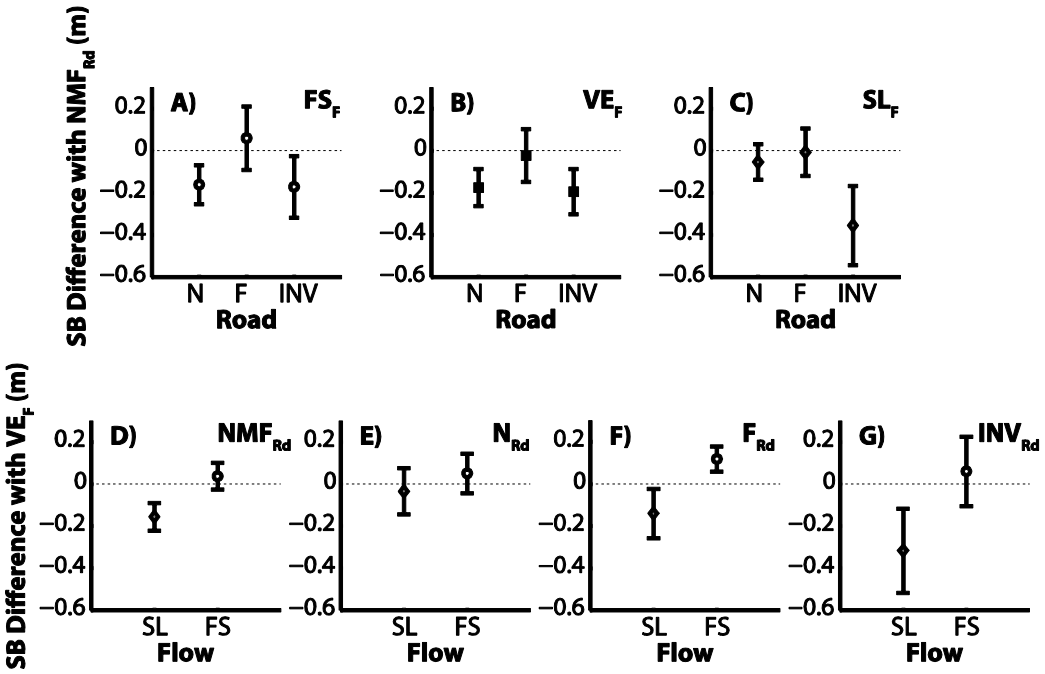

Figure 4.4 Steering Bias difference plots. Top Row: difference between means compared to NMF_{Rd} for A) FS_F, B) VE_F, and C) SL_F. Bottom Row: difference between means compared to VE_F for D) NMF_{Rd}, B) N_{Rd}, and C) F_{Rd}. For all graphs a negative magnitude means steering further towards the outside edge (understeering) than the respective comparison condition, NMF_{Rd} or VE_F. Error bars are 95% confidence intervals.

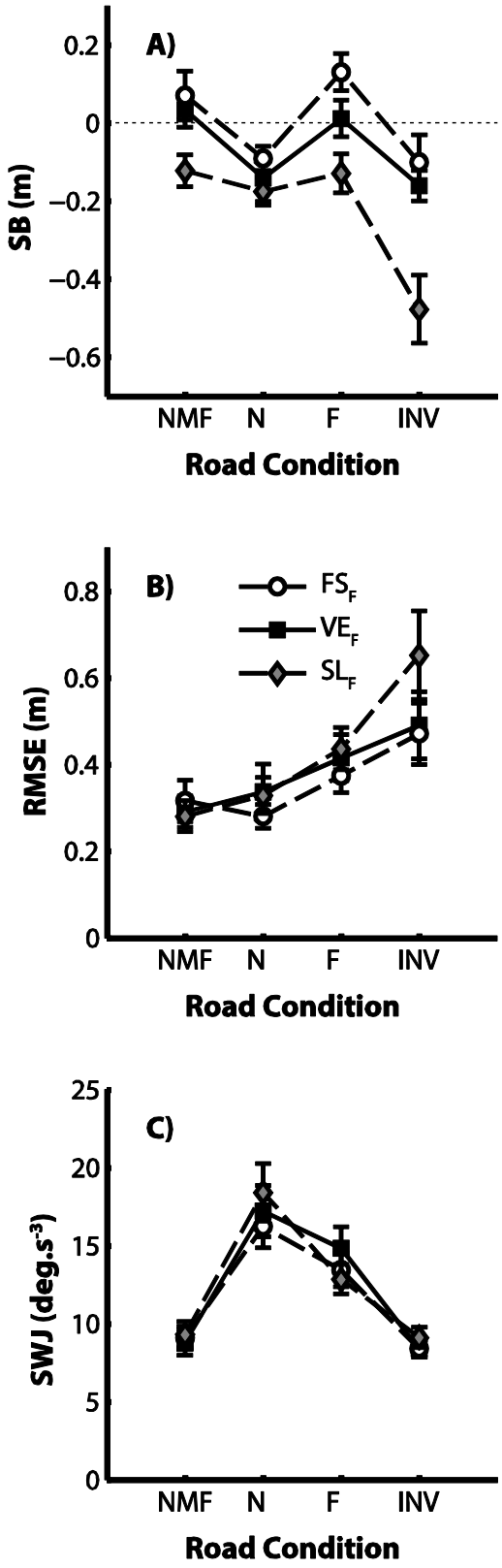

Figure 4.5 All steering performance measures across FS_F (empty circles, dashed line), VE_F (filled squares, solid line), and SL_F (grey diamonds, dashed line), showing A)

Steering Bias, B) Root-mean-squared error, and C) Steering Wheel Jerk. Error bars represent standard error of the mean (SEM).

4.3.2 Flow Induced Steering Bias

Average FISB scores are shown in Figure 4.6A. FISB captures how 'use of flow' changes across road conditions. In every road condition FISB was greater than zero (Figure 4.6A), showing that under constrained gaze conditions steering was biased by non-veridical changes in Flow speed. However, the magnitude of this change varies across road conditions. Figure 4.6B shows the paired differences between each road condition compared to the control (NMF_{Rd}). FISB is consistently reduced in N_{Rd} compared to NMF_{Rd}, sitting around a 54% reduction. The point estimates for F_{Rd} and INV_{Rd} indicate that FISB increased relative to NMF_{Rd}, but the uncertainty around the estimates are high and both 95% CI incorporate zero, so the precise magnitude of the increase is hard to estimate (Figure 4.6B).

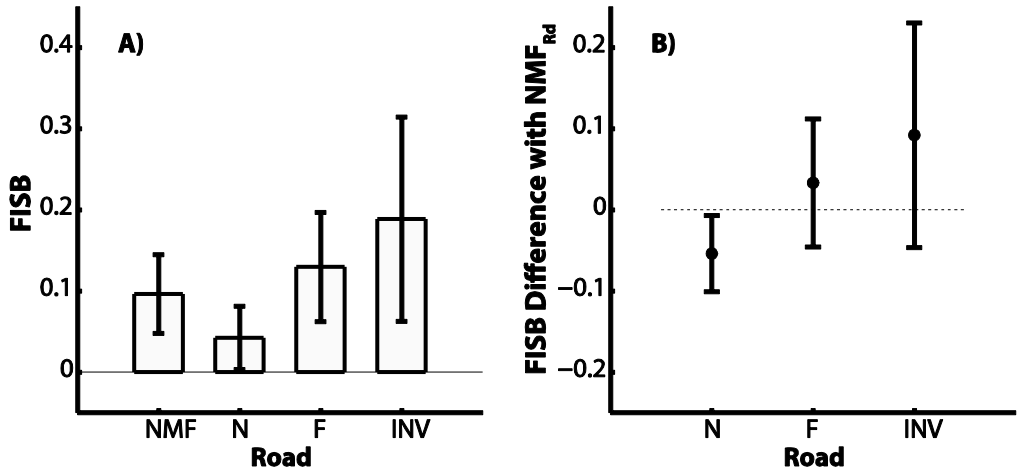

Figure 4.6 A) Average FISB scores for each Road Condition, a positive FISB indicates steering behaviour in line with predictions (oversteering for FS_F; understeering for SL_F). B) Difference between NMF and the other road conditions. All error bars are 95% confidence intervals.

4.3.3 Root Mean Squared Steering Error

Figure 4.5B shows average RMSE scores for all conditions. There is a clear trend from left-right in the graph, indicating that steering error varies systematically when REs are removed. For both NMF_{Rd} and N_{Rd}, total positional deviation is approximately 10%RW from the midline. This deviation increases to ~13%RW in F_{Rd}, and to ~18%RW in INV_{Rd}. Figure 4.7A-C shows that this trend is fairly consistent across Flow levels: the paired difference between N_{Rd} and NMF_{Rd} generally sits around zero, with a consistent increase in error in F_{Rd}, and a larger increase in error in INV_{Rd}. This trend seems most pronounced when flow speed is slowed (Figure 4.7C), where removing all RE information causes a large, but variable, increase in error.

Manipulating Flow did not alter steering as systematically as varying road edge presentation. Under full road conditions, manipulating flow in either direction failed to induce substantial steering responses, with both paired difference estimates sitting around zero (Figure 4.7A). In N_{Rd}, the steering response was more variable, but as with NMF_{Rd} flow manipulations failed to produce consistent biases (Figure 4.7B). F_{Rd} too did not have large RMSE differences between flow speeds (Figure 4.7C). On the other hand, steering behaviour in INV_{Rd} was considerably more variable, and slowing flow speed appears to have generally increased error (Figure 4.7G), although the high uncertainty requires the paired difference magnitude estimate of .16m [.0, .32], to be treated with caution.

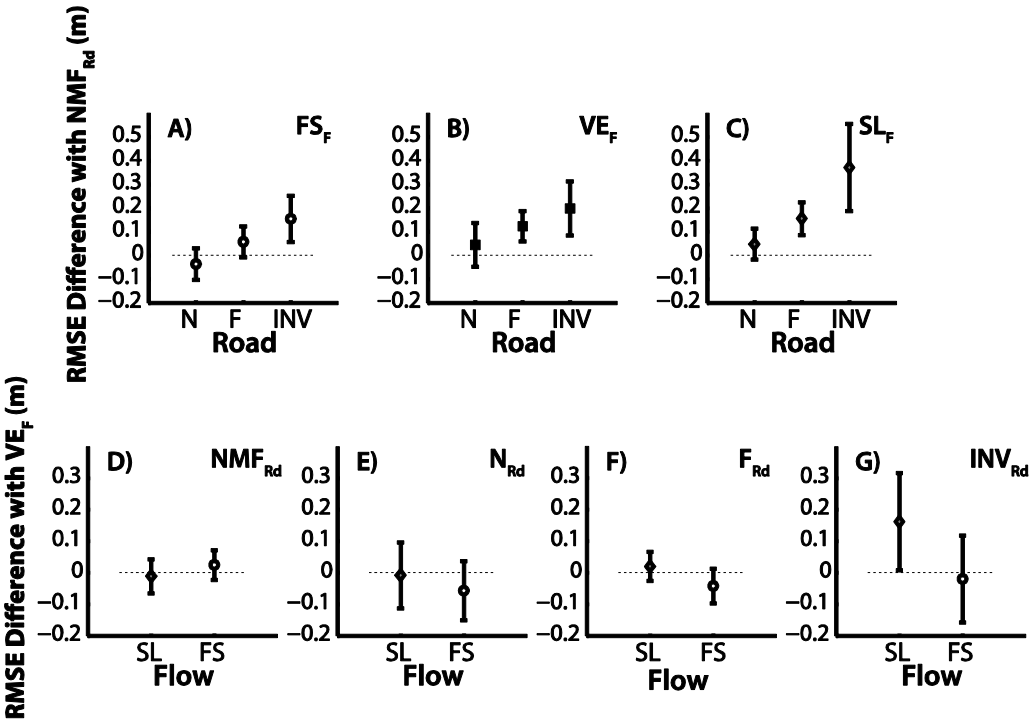

Figure 4.7 RMSE difference plots. Top Row: difference between means compared to NMF_{Rd} for A) FS_F, B) VE_F, and C) SL_F. Bottom Row: difference between means compared to VE_F for D) NMF_{Rd}, B) N_{Rd}, and C) F_{Rd}. For all graphs a negative magnitude indicates less deviation from the midline, compared to the control comparison (NMF_{Rd} or VE_F), and a positive magnitude indicates greater deviation from the midline. Note that the scales on the Top Row and the Bottom Row are different. Error bars are 95% confidence intervals.

4.3.4 Steering Wheel Jerk

Steering Wheel Jerk is displayed in Figure 4.5C. It is clear that there are systematic changes to steering smoothness when road components are removed. In NMF_{Rd} SWJ is ~9.1deg.s^{-3} [7.43, 10.7]. This increases by about 50% in F_{Rd} (M=13.7deg.s^{-3} [11.45, 15.96], SEM=1.03), and approximately doubles in N_{Rd} (M=17.2deg.s^{-3} [13.61, 20.81], SEM=1.65). When both RE components are removed (INV_{Rd}), SWJ is comparable to NMF_{Rd} (M=8.64deg.s^{-3} [7.68, 9.69], SEM=.48). This trend is consistent and systematic across all flow conditions (Figure 4.8A-C).

Systematic changes in steering smoothness in response to manipulating flow speed are less clear. In NMF_{Rd} (Figure 4.8D) and INV_{Rd} (Figure 4.8G), where steering is smoothest, changes in steering smoothness due to flow speed are minimal and the paired difference estimates mostly sit around zero. In F_{Rd}, manipulating flow speed in either direction seems to make steering smoother by around 2deg.s^{-3}, although the estimates are variable. In N_{Rd}, where steering is jerkiest, changes in flow speed cause the most variable responses in SWJ. Whilst slowing flow speed is estimated to cause jerkier steering ($M_{diff=}$1.21deg.s^{-3} [-1.28, 3.69], SEM=1.14) and increasing flow speed is estimated to cause smoother steering (M_{diff}=-.98deg.s^{-3}, [-3.1, 1.14], SEM=.97), there is large variability in responses and the 95% CIs span both positive and negative changes in SWJ, so the estimates must be treated with caution.

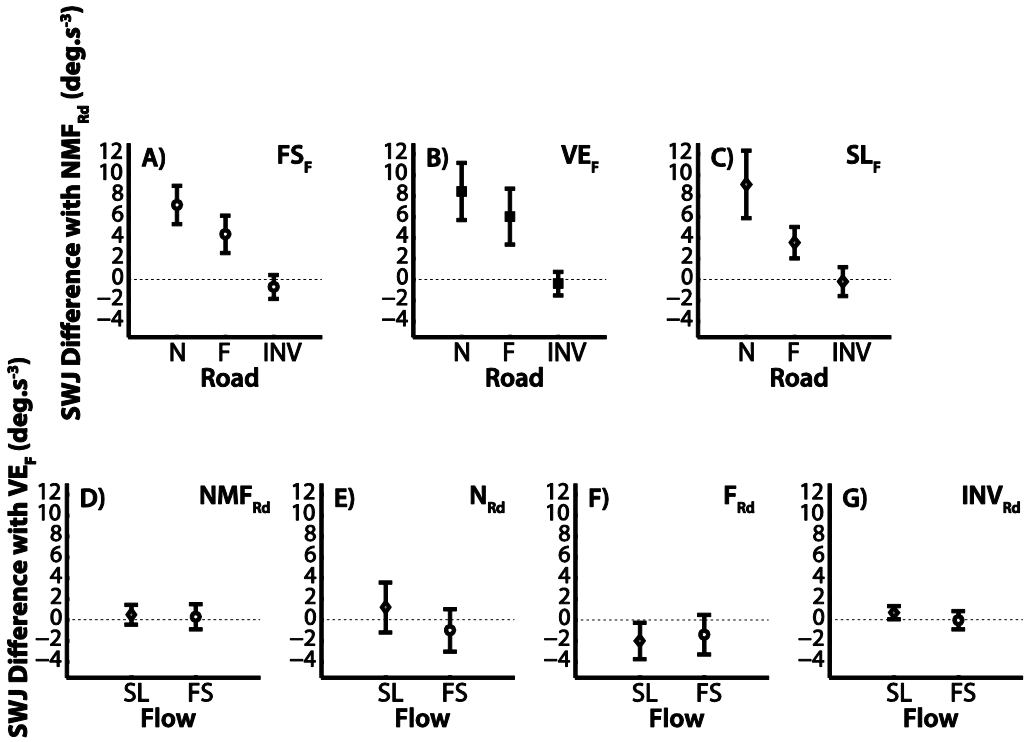

Figure 4.8 SWJ difference plots. Top Row: difference between means compared to NMF_{Rd} for A) FS_F, B) VE_F, and C) SL_F. Bottom Row: difference between means compared to VE_F for D) NMF_{Rd}, B) N_{Rd}, and C) F_{Rd}. For all graphs negative and positive magnitudes indicates less and more steering corrections, respectively,

compared to the control comparison (NMF_{Rd} or VE_F) Error bars are 95% confidence intervals.

4.4 Discussion

Chapter 3 suggested that the usefulness of flow speed depended on road component availability. However, there were accompanying changes in gaze behaviour that could have explained the observed steering differences. The current experiment used Chapter 3's design, but controlled gaze. This discussion forms two parts. The first part attempts to address the question of how flow is used; the second part explores what the current results say about steering behaviour in general.

4.4.1 Combining Flow speed with Road Edges.

H1B (Chapter 3: Figure1E) suggests that flow modulates a guidance signal supplied by the road edges. Under this framework, FISB would be predicted for both NMF_{Rd} and F_{Rd} where there is far road information, but not for N_{Rd}, where guidance RE information is removed. In line with these predictions, Chapter 3 observed no FISB for N_{Rd}, and greater FISB for F_{Rd} and NMF_{Rd}. However, concerns were raised that the diminished flow use might be due to differences in gaze behaviour. In the current experiment, with gaze constrained across conditions, the same basic patterns were observed: the least FISB was in the N_{Rd} condition and greater FISB in the F_{Rd} and NMF_{Rd} conditions. This confirms that flow speed biases steering more when a far road edge component is present.

In both N_{Rd} and F_{Rd}, FISB is increased when gaze is constrained compared to unconstrained gaze. There are two differences between constrained and unconstrained N_{Rd} conditions: forward gaze and the fixation cross. In order to interpret the impact of these two cues on steering control it is worth considering how the fixation cross could be used to control position in INV_{Rd} conditions, where the cross is the sole source of information. If the cross remains stationary on the display (i.e. the driver moves so as to cancel *target drift*) then the driver has matched the curvature of the bend, which is generally considered to be a guidance task (Donges, 1978; Land, 1998). It is less clear that the cross provides any usable position-in-lane

information that would be needed for compensatory control. Supporting this, the low jerk in INV_{Rd} suggests steering control was characterised by guidance level control, rather than compensatory control (Chatziastros et al., 1999; Frissen & Mars, 2014; Land & Horwood, 1995). Therefore, it can be assumed that the cross primarily provides guidance level information. It is worth noting that SWJ for N_{Rd} was approximately half as much in constrained Gaze as unconstrained gaze. Smoother steering is a characteristic of guidance, rather than compensatory control (Land, 1998). It is reasonable to assume the two cues of forward gaze and the fixation cross increased the guidance level information present in the scene, which might have led to an increase in FISB (compared to free gaze).

The increased FISB in F_{Rd} (fixated vs. free) is harder to explain. One possible explanation is that the increased guidance level information provided by the fixation cross causes an increase in the use of flow speed. However, if this was the case, one would also expect increased FISB in NMF_{Rd}, which was not observed. The magnitude of FISB during constrained gaze F_{Rd} varies across participants and more precise estimates are provided in later Chapters (see section 5.4.1).

4.4.2 Constrained Gaze and Two-level Steering: The effect of Road Component availability

Constraining gaze means that steering differences across road conditions are solely due to changes in road component availability. The task instructions were 'to steer in the middle of the road as *smoothly* and as *accurately* as you can'. Steering behaviour was smoothest and most accurate when a full road was available. Removing guidance RE information caused steering behaviour to become jerkier, but positional error remained the same as when a full road was available. The maintenance of position-in-lane at the expense of smooth steering is a characteristic of compensatory control (Land & Horwood, 1995). This is in contrast with the previous Chapter, where removing far road information caused both increased jerk and increased positional error. It seems that forcing participants to look 1.2s ahead on the path makes steering

smoother (N_{Rd} jerk is about half as much as in free gaze) by introducing two additional sources of guidance information: extra-retinal direction (Wilkie & Wann, 2002), and target drift from the fixation cross. The extent that extra-retinal direction or the fixation cross independently contributes to guidance control is unclear, and assessing this is beyond the scope of the current experiment because there is not a near road condition where participants look 1-2s ahead but the fixation cross is not present.

It appears that additional guidance information reduced the demands on compensatory control, thus compensatory control was sufficient to keep performance accurate. This successful 'switching' to compensatory control has been observed in previous studies (Chatziastros et al., 1999; Cloete & Wallis, 2011; Land & Horwood, 1995), but not in others (Frissen & Mars, 2014; Chapter 3 of this thesis). The difference between 'unsuccessful' compensation for lack of anticipatory information in Chapter 3, compared to the 'successful' compensation in the current Chapter, could be due to directing gaze forwards in the current Chapter. In Frissen & Mars (2014) there is a large increase in both jerk and positional error from an 80% upper-field mask and a 100% upper-field mask whereas the same increase in opacity of a lower-field mask does not cause damage performance so markedly. Their conclusion is that the 'compensatory process is more robust to visual degradation than the anticipatory process'. However, it is entirely possible that in the 80% upper-field mask condition drivers still made saccades into the upper mask (because weak guidance level information could be obtained) but that they did not make similar saccades in the 100% upper-field mask condition (as there is nothing to see). Based on the evidence presented in this Chapter, a relocation of gaze to lower regions may have precipitated the observed decrease in both steering smoothness and steering accuracy. An alternative explanation for their results could be 'as long as you have some guidance information from looking where you are going, you will perform OK'. Whilst gaze behaviour during slow-speed locomotion can be captured by a trade-off between the need for direct control (close gaze) and the need for anticipation (distant gaze;

Vansteenkiste et al., 2013), the evidence presented here suggests that this model does not adequately generalise to high-speed driving, where the need for anticipation is great (Lehtonen et al., 2013) and close gaze can be detrimental to performance. Instead, the evidence suggests that a driver has a better chance of adapting to changes in RE availability if they maintain a gaze strategy of looking toward the desired future path approximately 1-2s ahead (Wilkie et al., 2008).

4.4.2.1 Refresh rates and Steering Control

It was highlighted in Chapter 3 (section 3.5) that some of the increased error and jerk observed in N_{Rd} and F_{Rd} could be attributed to low refresh rates (51Hz for N_{Rd}; 35Hz for F_{Rd}; 60Hz for NMF_{Rd} and INV_{Rd}). The refresh rates observed in this experiment are the same as in Chapter 3, yet the RMSE and SWJ for N_{Rd} is much reduced (and equivalent to NMF_{Rd} which has a 60Hz refresh rate), demonstrating that all of the increased error and much of the increased jerk observed during N_{Rd} was due to gaze (looking closer in the scene than for the other road conditions), not low refresh rates. However, the drop in refresh rate for F_{Rd} is greater (35Hz, compared to 51Hz for N_{Rd}), and the pattern of jerkier and more errorful steering than NMF_{Rd} (observed in Chapter 3) is replicated in the current experiment (although the magnitude of the increase for jerk is reduced). The next Chapter uses a less computationally demanding road manipulation to investigate whether increased error and jerk in F_{Rd} is due to low refresh rates or due to inherent differences in the way road edge information is utilised to control steering.

4.4.3. Conclusions

Two competing predictions were made (Figure 4.1), based on whether Flow use depended on forward gaze (Figure 4.1B), or whether Flow use depended on far road edges (Figure 4.1C). The observed pattern of FISB falls somewhere in between. It

appears that FISB is not solely determined by RE presentation; rather it is also dependent on Forward Gaze. The results are best captured by the assumption that flow speed modulates a general guidance level control signal which may have multiple inputs (i.e. extra-retinal direction in the form of forward gaze, or a visual marker in the form of a fixation cross), not simply far road edge information. The next Chapter will test this hypothesis by systematically degrading the amount of compensatory and guidance level information present in the scene.

CHAPTER 5

EXPLORING THE INTERACTION BETWEEN FLOW SPEED AND ROAD EDGES

5.1 Introduction

Chapters 3 and 4 examined whether use of flow information when steering can be understood in the context of two-level control (Salvucci & Gray, 2004). These Chapters show that adding far road information and/or enforcing forward gaze through a fixation cross both increase the extent that flow influences steering (faster-than-veridical flow causes oversteering, and slower-than-veridical flow causes understeering). Based on these results, it would seem that flow speed information contributes to two-level steering by *modulating* the guidance signal. This insight is new: current two-level steering models (e.g. Mars, 2011; Salvucci & Gray, 2004) do not refer to flow information, and current flow-inspired steering models do not account for two-level steering control (Wilkie et al., 2008).

Whilst the previous Chapters reveal an association between utility of flow speed and the presence of guidance level information in the scene, there are some obvious unanswered questions. One outstanding issue is that it is unclear how flow speed magnitude is mapped on to guidance control. Humans are bad at estimating objective velocity of self-motion; perception of velocity is subjective (Brown, 1931) and is subject to adaptation (Denton, 1976) or changes in scene structure (Denton, 1980). This has direct implications to performing successful actions, with evidence that participants initiate overtaking manoeuvres later when they are adapted to high speeds, thus overestimate time-to-contact (Gray & Regan, 2000, 2005). Giving this changeable and imprecise perception of speed, it is unclear whether participants are responding to changes in flow speed in a manner proportional to the magnitude of change, or whether participants are responding in a more imprecise manner. (Wilkie

& Wann, 2003a) showed that smooth, curved trajectories can be modelled using inputs of retinal flow and visual direction that are crudely quantized on a 0-3 point scale, showing that high sensitivity to changes in perceptual input is not essential for smooth steering. It is possible that the observed flow induced steering biases in Chapters 2, 3, and 4 are caused by a general impression of going 'faster', or 'slower', than the previous trial, thus the steering response is adjusted accordingly. Since the previous experiments only use one magnitude of flow speed in either direction, they cannot tackle this issue. The current experiment examines this issue by adding an extra two levels of flow speed magnitudes. If participants are responding to a general impression of perceptual change than precise modulation of steering response according to flow speed magnitude will not be observed. On the other hand, if participants are responding in a manner proportional to flow speed magnitude, the extent that flow influences steering will be yoked to flow speed magnitude.

A second outstanding issue is that it is unclear how guidance and compensatory road edge signals are combined to provide a steering solution. Two-level models generally propose that separate angular inputs are obtained for both compensatory and anticipatory modes of control, which are additively combined (Donges, 1978; Mars, 2011; Salvucci & Gray, 2004). Degradation of either signal could be accommodated by redistributing weights (Salvucci & Gray, 2004). Supporting the idea that signals from each level are weighted according to their availability, Land & Horwood (1995) show smooth, bell-shaped, transitions in steering measures when they systematically increased or decreased the availability of an anticipatory (future curvature information) or compensatory (position-in-lane information) RE information. Two observations in particular support an additive combination: two independent viewing windows, if appropriately placed in near and far regions (therefore providing 'strong' signals), can cause steering behaviour similar to a full road; with one viewing window best performance was achieved when the segment was half-way between near and far 'optima', suggesting that two weakly informative signals can be combined to produce

acceptable performance. Unfortunately, both the bell-shaped transitions, and the middle 'optima', have not been subsequently replicated (Chatziastros et al., 1999; Cloete & Wallis, 2011). Cloete & Wallis (2011) also failed to find similar performance to a full road with two independent viewing windows. Frissen & Mars (2014) attempted to assess how two-level steering coped with degraded visual inputs by masking either the top or bottom visual fields, at different opacities (20%-100%). They found that high opacity levels of the top mask caused large understeering, presumably due to failing to anticipate the bend curvature, but the equivalent opacity of the full mask causes oversteering (despite the same level of anticipatory information available). They suggest that the results demonstrate that the combination of compensatory and anticipatory is more complex than a simple additive process.

The previous Chapters have demonstrated that the availability of REs strongly determines gaze direction, which may modulate how guidance and compensatory RE signals are combined. This modulation of steering control with gaze direction is likely to have played a role in all the studies reported here (Chatziastros et al., 1999; Cloete & Wallis, 2011; Frissen & Mars, 2014; Land & Horwood, 1995). As yet, there has not been a systematic assessment of how anticipatory and compensatory RE signals are combined, when gaze is constrained. The current Chapter addresses this issue by expanding the previous Chapter's design (which only assesses the presence or absence of a RE signal) by introducing four new road conditions which have various amounts of compensatory or anticipatory information available.

5.2 Methods

5.2.1 Participants

Twenty participants (10 females, 10 males, ages 20 to 35, mean 25.7yrs), all having normal or corrected-to-normal vision, took part the experiment. None of these participants took part in any of the other experiments. 18 participants held driving

licenses (average time since test=6.6yrs), and the remaining two had limited driving experience (go-karting and driving lessons). All participants gave informed consent and the studies was approved by the University of Leeds, School of Psychology Research Ethics Committee (Ref 14-0225), and complied with all guidelines as set out in the declaration of Helsinki.

5.2.2 Stimuli

The same method of flow manipulation as the previous three Chapters was used, however for this experiment there were five levels of flow manipulations, labelled by their speed proportional to veridical ($FL_{.5}$, $FL_{.75}$, FL_{1}, $FL_{1.25}$, and $FL_{1.5}$). With this notation the previous flow manipulations would be $FL_{.66}$ and $FL_{1.33}$. More sophisticated programming techniques than Chapters 2-4 meant greater control over the road edges. It should also be noted that the improved programming removed the impact of some road edge manipulations on refresh rate, resulting in a consistent 60Hz refresh rate throughout all conditions. The road was divided into three 'segments'. 'Near' road (N) was classified as the region from 0-.5s (6.71m) ahead, 'Mid' road (M) as the segment between .5s and 1s (13.41m), and 'Far' (F) road as the segment beyond 1s ahead (Figure 5.1). A fixation point was placed at 1.2s (16m) ahead on the future path to match the displays in Chapter 4 in order to facilitate comparisons (see discussion on fixation point placement in section 4.2.3; Figure 5.2).

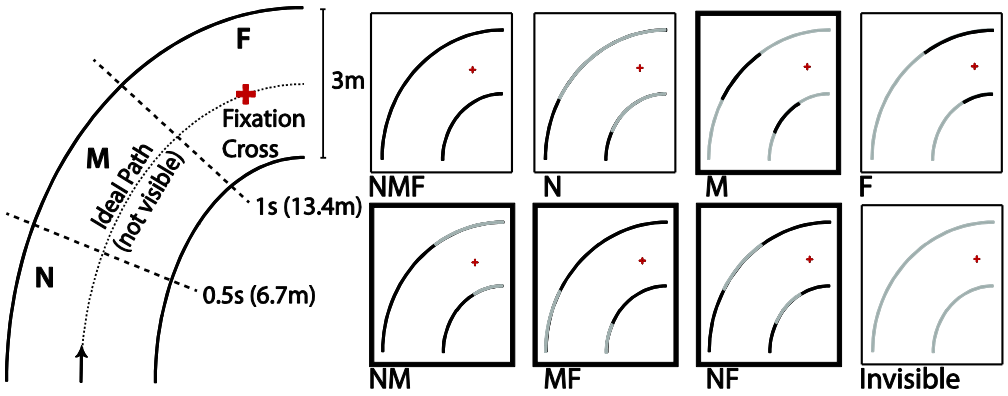

Figure 5.1 Birdseye schematic of all road conditions. Road display conditions are denoted by their constituent parts. The conditions of M, NM, MF, NF (thickened box) were not present in earlier studies.

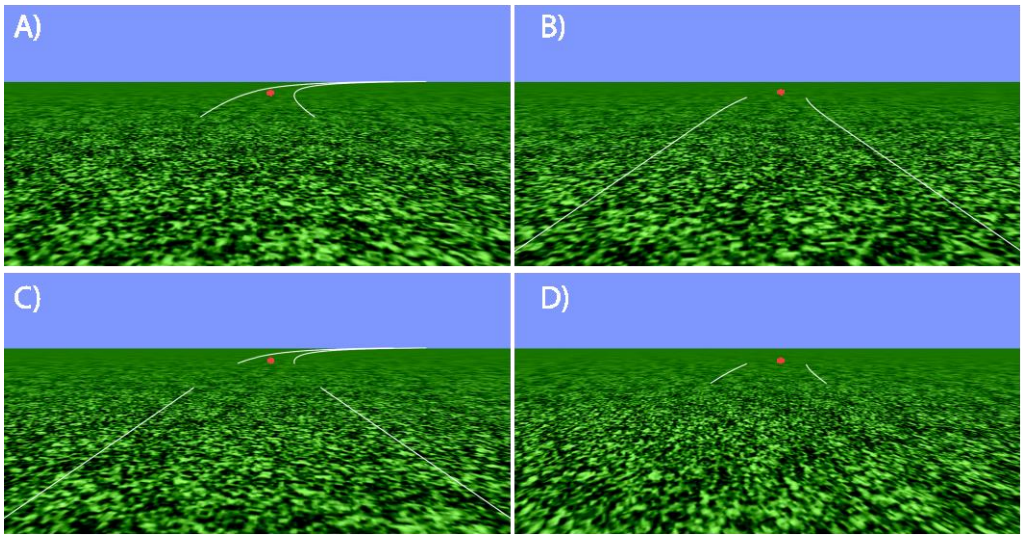

Figure 5.2 Screenshots of Road Conditions not included in Chapter 4. A) MF_{Rd}, from .5s to horizon. B) NM_{Rd}: cropped up to 1s. C) NF_{Rd}, showing road up to .5s, and from 1s. D) M_{Rd}: showing the road between .5s and 1s ahead.

5.2.3 Procedure

All participants received the same written instructions, to 'attempt to steer a central trajectory, keeping to the middle of the road', to steer 'as smoothly and as accurately as you can', to 'centre the wheel after each trial', and to 'fixate on the fixation cross'. Participants completed 20 practice trials (2 minutes) of veridical flow, starting with

four complete road trials and then being exposed to each road conditions for both left and right bends. There were six trials in each condition, each six seconds long, resulting in an experiment running time of 24 minutes. A brief (un-timed) rest break was inserted at the half-way point to alleviate fatigue.

5.2.4 Analysis

The same steering measures as used in Chapters 2-4 are calculated: SB, RMSE and SWJ. The current experiment expanded the experimental design to include more levels of flow, so an improved FISB metric could be calculated to measure overall sensitivity and reliance on flow under each road edge condition.

5.2.4.1 Fitting Slopes across Flow Levels: Assessing Linear Fit.

Instead of approximating the gradient of the slope ($(FS_F - SL_F)/2$; as per Chapters 3-4), FISB scores were calculated by finding the slope of the linear regression fitted to the steering bias estimates across the five flow speeds for each road condition. In Chapter 2 it was observed that a 33% increase in Flow speed biased steering to the same magnitude as a 33% decrease (but in the opposite direction), i.e. there was a linear relationship between flow speed and steering bias. This led to the linear slope across flow levels being approximated during Chapters 3 and 4 by the simple formula $(FS_F - SL_F)/2$. In the current experiment, it quickly emerged that this linear relationship did not fit well across five flow levels. In particular, the shift in SB from $FL_{.5}$ to $FL_{.75}$ was clearly greater than the shift from $FL_{1.25}$ to $FL_{1.5}$, meaning that a simple linear fit did not capture the data well (Figure 5.3), with R^2 values ranging from around .4 in N_{Rd}, to around .75 in NMF_{Rd}. The next section investigates different approaches to obtaining an acceptable fit across flow levels.

5.2.4.2 Fitting Slopes across Flow Levels: Logarithmic Transform

It has been argued that Flow Speed perception follows a Weber relationship (Authié & Mestre, 2012). Weber's law stipulates that perceived differences between two signals of difference magnitudes is determined by the ratio between the two signals, rather than the absolute difference. Therefore, given the same separation interval, two values of higher magnitude will have a smaller perceived difference than two values of smaller magnitudes.

In the current experiment, the ratio for $FL_{.75}$ and $FL_{.5}$ is 1.5, but the ratio for $FL_{1.5}$ and $FL_{1.25}$ is 1.2. The larger ratio between lower flow speeds might explain why a greater shift in steering behaviour is observed than for higher levels. With this in mind, the flow levels were logarithmically transformed, so that .5, .75, 1, 1.25, and 1.5 became -.301,-.125, 0, .097, and .176. A major advantage of doing a logarithmic transform on the flow values is that they can still be used to carry out linear regression. Whilst this led to minor improvements in R^2 (Figure 5.3), the R^2 values indicated that this may still be a sub-optimal approach to capturing the true extent of FISB.

5.2.4.3 Fitting Slopes across Flow Levels: Weighted Linear Regression

An assumption of linear regression is that every data point contributes equally to the regression line (i.e. it assumes that every data point is equally reliable). In the present case, linear regression is conducted on 5 data points (the flow levels), each representing an average of 6 trials per person. If a participant was particularly variable in one condition, this would be weighted equally with a condition where the participant's behaviour was highly precise, even though the precise condition's estimate should really be trusted more. A Weighted Least Squares procedure takes into account the uncertainty in participant bias estimates (Ryan, 2009), and can be expressed mathematically as follows:

$$\beta 1 = \frac{\sum w_i x_i y_i - \frac{(\sum w_i x_i)(\sum w_i y_i)}{\sum w_i}}{\sum w_i x_i^2 - \frac{(\sum w_i x_i)^2}{\sum w_i}} \tag{5.8}$$

Using a weighted least squares regression approach improved the fit of FISB for every condition (Figure 5.3). However, an additional minor improvement was obtained from logarithmically transforming the scale. Therefore, a weighted least squares regression on a logarithmically transformed flow scale was the method chosen to calculate FISB scores for the current Chapter. Since a large slope value indicates that participants were biased by flow in the predicted direction (oversteering for faster-than-veridical, understeering for slower-than-veridical), the β1 estimate was taken as the FISB score.

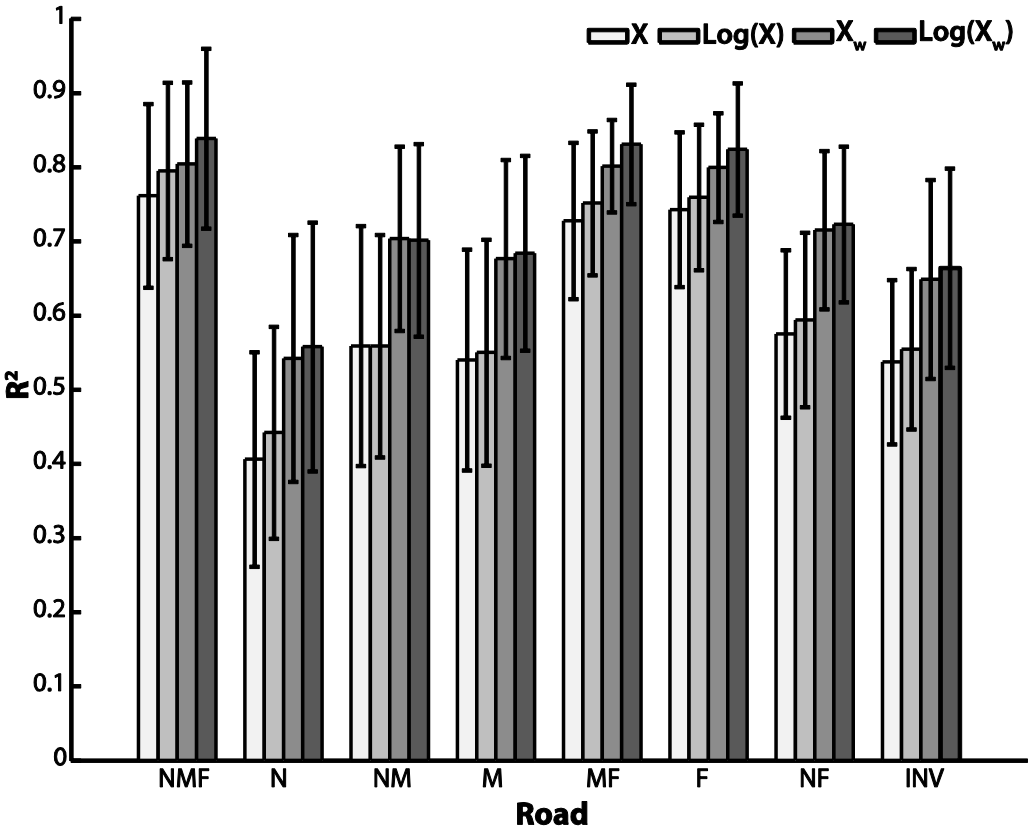

Figure 5.3 R^2 estimates are calculated per person, per condition, and then subsequently averaged. The graph compares average explained variance for a 1) linear fit, a 2) linear fit on logarithmically transformed data, a 3) weighted linear fit, and a 4) weighted linear fit on logarithmically transformed data. Error bars represent 95% CIs.

Despite the improvements to how FISB is calculated, it is important to note that it clearly does not fully capture the spread of flow levels, and the explanatory power of FISB varies between road conditions with R^2 values ranging between .56 for N_{Rd} and .84 for NMF_{Rd} (Figure 5.3). This variation is in part due to a drop in R^2 in conditions where the change in steering response to flow manipulation is small (N_{Rd}; see Figure 5.7), therefore fitting a line is problematic, and a rise in R^2 in conditions where flow manipulations cause distinct and consistent alterations to steering response (NMF_{Rd}, F_{Rd}, and MF_{Rd}; see Figure 5.7). Although this metric may be somewhat imprecise, it remains useful for facilitating comparisons across road conditions.

5.3 Results

Firstly, the steering measures (SB, RMSE, and SWJ) and derived measures (FISB) will be reported, then averaged trajectory plots (similar to those presented in Chapter 2) will be discussed in light of the steering measures. For each factor (Road and Flow) trends in the data will be presented through paired difference estimates relative to the control condition, with the precision of each estimated captured with 95% CIs (see Chapter 2 for validation of this approach).

5.3.1 SB

Figure 5.6A shows the positional bias for every flow level, across road conditions. In line with previous Chapters, there was a general trend to oversteering when flow speed was increased, and understeering when flow speed was decreased, and this effect varied according to the visible road segments. Figure 5.4 examines how steering response to flow varies across road viewing conditions in more detail by plotting the paired differences relative to FL_1.

For the control condition, NMF_{Rd} (Figure 5.4A), slowing flow speed by 25% caused understeering of ~3.6%RW (M_{diff}=-.11m [-.18, -.036], SEM=.034), and slowing flow speed by 50% caused understeering of ~9%RW (M_{diff}=-.27m [-.34, -.20], SEM=.032).

Conversely, *increasing* flow speed by 25% caused oversteering of ~1.5% (M_{diff}=.044m, [-.029, .1], SEM=.029), and increasing flow speed by 50% causes oversteering by ~4.2% (M_{diff}=.13m [.076, .17], SEM=.024). It is clear that slowing flow speed caused a larger steering response than increasing flow speed. In fact, for the same magnitude of change in either direction, decelerating flow causes just over double the positional change than accelerating flow.

This trend is borne out through all road conditions (Figure 5.4), although the magnitude of positional change varies. The most similar condition to NMF_{Rd} is F_{Rd} (Figure 5.4F). Whilst steering behaviour is more variable in F_{Rd}, the point estimates for the magnitude of positional change are remarkably similar: $FL_{.5=}$~9%RW; $FL_{.75=}$~4.5%RW; $FL_{1.25=}$~2.5%RW; $FL_{1.5}$=~4.4%RW. INV_{Rd} saw more variable behaviour still, but similar magnitudes of change to NMF_{Rd} and F_{Rd} were observed (Figure 5.4H).

It should be noted that NMF_{Rd}, F_{Rd}, and INV_{Rd} are the conditions with the largest changes in steering bias between flow levels. Conversely, N_{Rd} is the condition where changes in flow caused the smallest positional changes. Whilst the paired difference estimate for $FL_{.5}$ – FL_{1} (M_{diff}=-.13m [-.2, -.07], SEM=.032) are similar to NM_{Rd}, M_{Rd}, and NF_{Rd} (Figure 5.4), the paired difference estimates for $FL_{.75}$, $FL_{1.25}$, and $FL_{1.5}$ are substantially smaller and sit very close to zero.

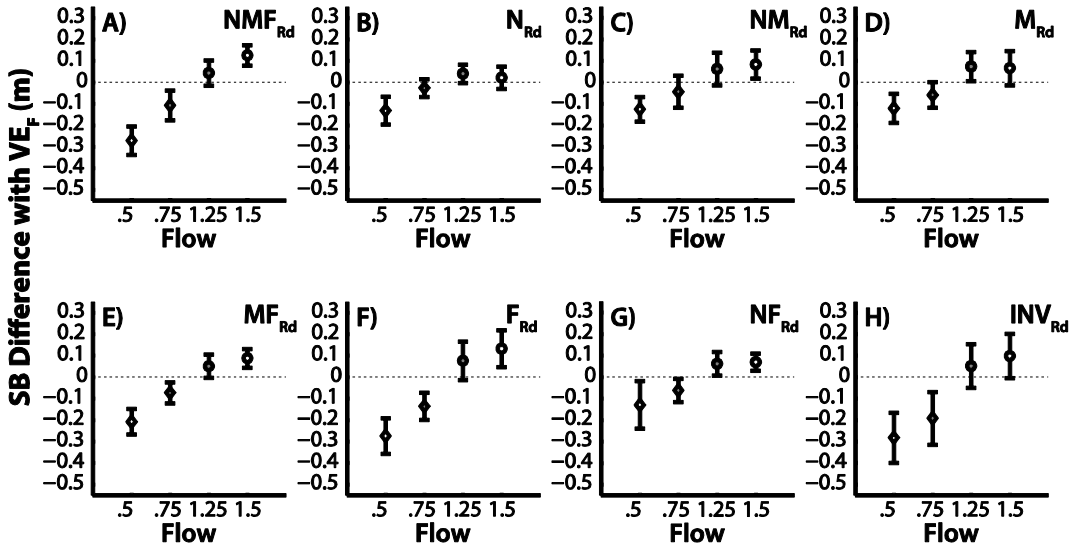

Figure 5.4 SB difference between the mean plots for comparisons across Flow levels for reach Road Level. Each point represents the paired difference between that particular Flow level and FL_1, the control condition. For all graphs a negative magnitudes indicates steering closer towards the outside edge of the bend than in FL_1, and a positive magnitude indicates steering closer to the inside edge. Error bars are 95% confidence intervals.

Figure 5.5 examines the trends across road conditions, for each level of flow. Under veridical flow conditions (Figure 5.5C) removing any road components caused understeering, although to different extents dependent on road component availability. The greatest understeering was observed when REs were removed altogether (INV_{Rd}; M_{diff}=-.29m [-.4, -.19], SEM=.05). When RE information was available, the most understeering occurred when only near road was available (M_{diff}=-.2 [-.26, -.15], SEM=.027). Adding the mid-road component reduced understeering (NM_{Rd}, M_{Rd}), as did adding the far road component (MF_{Rd}, F_{Rd}, NF_{Rd}), but neither components completely eliminated understeering compared to having the full road (NMF_{Rd}). The understeering-inducing effect of removing RE components is more pronounced at high Flow speeds (Figure 5.5D & E), than at low Flow speeds (Figure 5.5A & B).

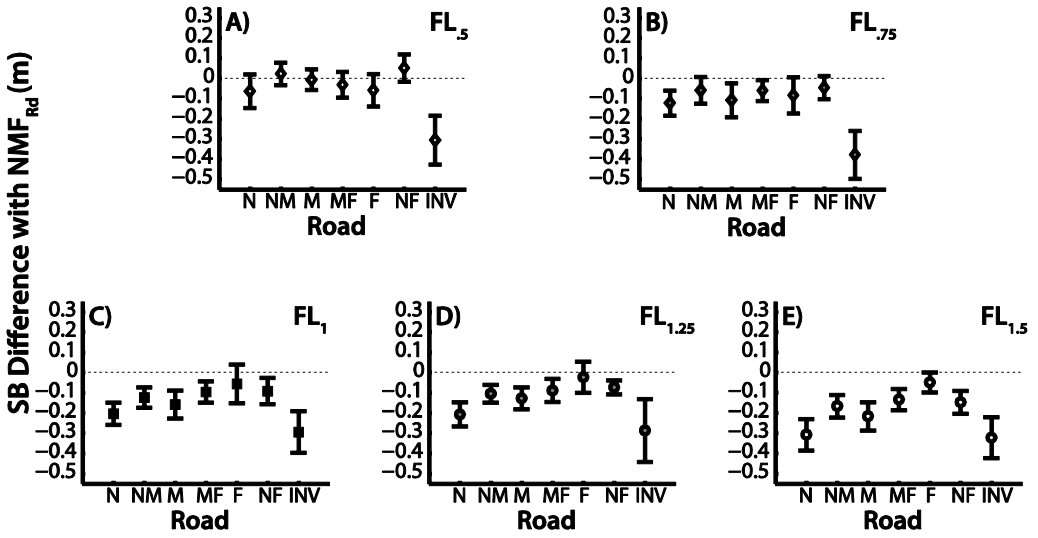

Figure 5.5 SB difference between the mean plots for comparisons across Road levels for reach Flow Level. Each point represents the paired difference between that particular Road level and NMF_{Rd}, the control condition. For all graphs a negative magnitudes indicates steering closer towards the outside edge of the bend than in NMF_{Rd}, and a positive magnitude indicates steering closer to the inside edge. Error bars are 95% confidence intervals.

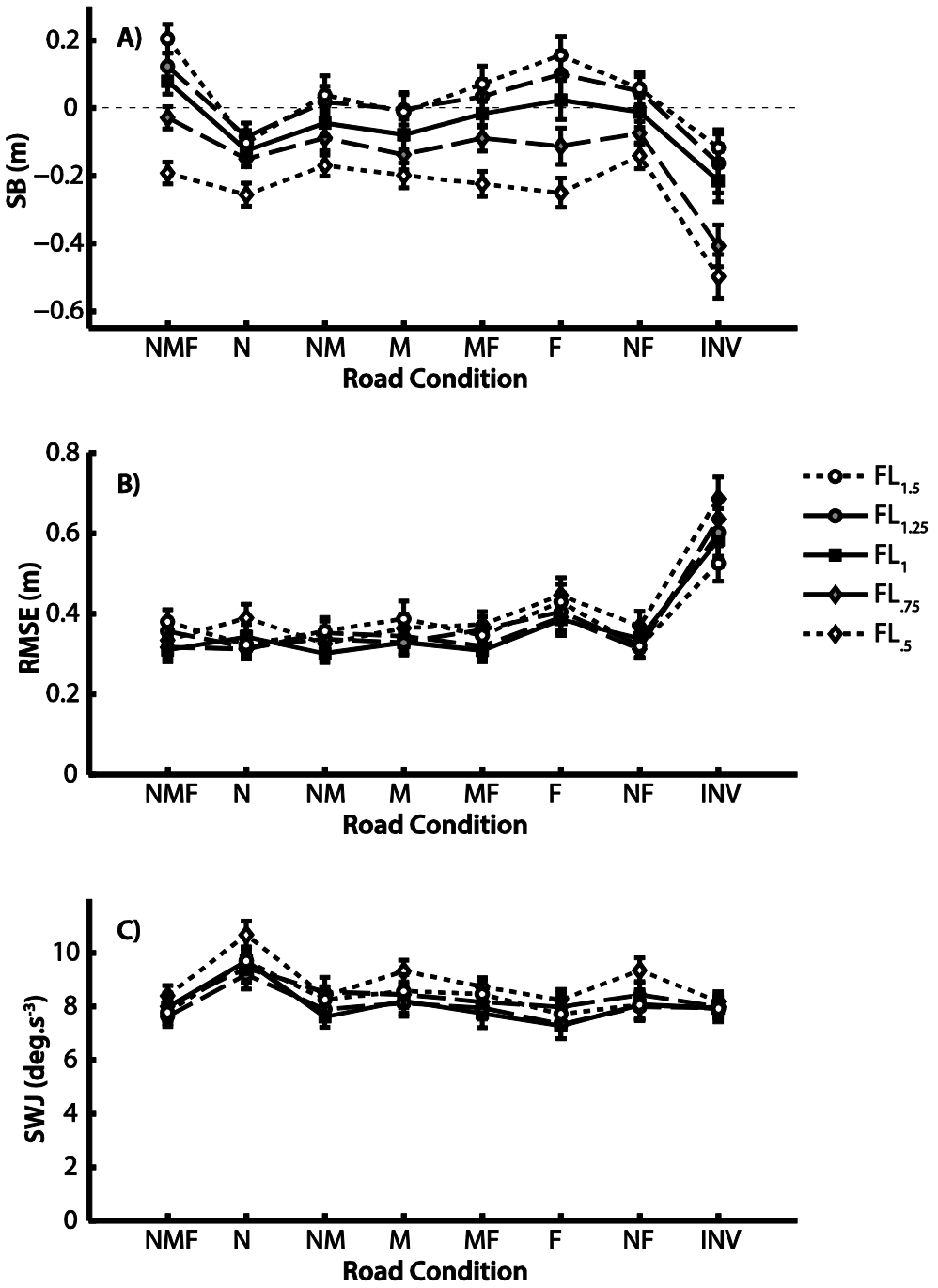

Figure 5.6 All steering performance measures across $FL_{1.5}$ (empty circles, dotted line), $FL_{1.25}$ (grey circles, dashed line), FL_1 (sold squares, solid line), $FL_{.75}$ (grey diamonds, dashed line), and $FL_{.5}$ (empty diamond, dotted line), showing A) Steering Bias, B) Root-mean-squared error, and C) Steering Wheel Jerk. Error bars represent standard error of the mean (SEM).

5.3.2 FISB

Steering bias is useful for precisely capturing positional changes in particular conditions. However, with 5 Flow levels for each road condition, it can be hard to assess general changes in flow sensitivity between road conditions. FISB provides a single value for each road condition (see section 5.2.4) that captures the extent steering was biased by flow, incorporating SB estimates for each flow level. As with previous Chapters, a larger FISB represents greater oversteering for faster-than-veridical flow levels, and understeering for slower-than-veridical flow levels.

Figure 5.7A shows average FISB for each road condition. It is clear that FISB is positive for every road condition, but the magnitude of FISB varies between Road presentations. Figure 5.7B examined how consistent these differences are within participants, and demonstrates that the road conditions can be grouped according to magnitude of FISB relative to NMF_{Rd}. Firstly, F_{Rd} (M_{diff}=.039 [-.144, .22], SEM=.08) and INV_{Rd} (M_{diff}=.045 [-.18, .27], SEM=.107) produced FISB values roughly equivalent to NMF_{Rd}, shown by paired differences centred near zero (Figure 5.7B). Secondly, FISB is reduced in MF_{Rd} to approximately 80% of NMF_{Rd} (M_{diff}=-.16 [-.32, 0], SEM=.08). Thirdly, at about 55% FISB of NMF_{Rd}, is NM_{Rd}, M_{Rd}, and NF_{Rd}. Lastly, N_{Rd} has the smallest FISB, about 42% of NMF_{Rd} (M_{diff}=-.47 [-.6, -.33], SEM=.063). The paired difference SB plots can be referred to for comparison (Figure 5.4); the road conditions with larger FISB (F_{Rd}, INV_{Rd}, and NMF_{Rd}) have a greater 'spread' of changes in SB across flow levels than road conditions with lower FISB (e.g. compare Figure 5.4F – F_{Rd} – with Figure 5.4B – N_{Rd}).

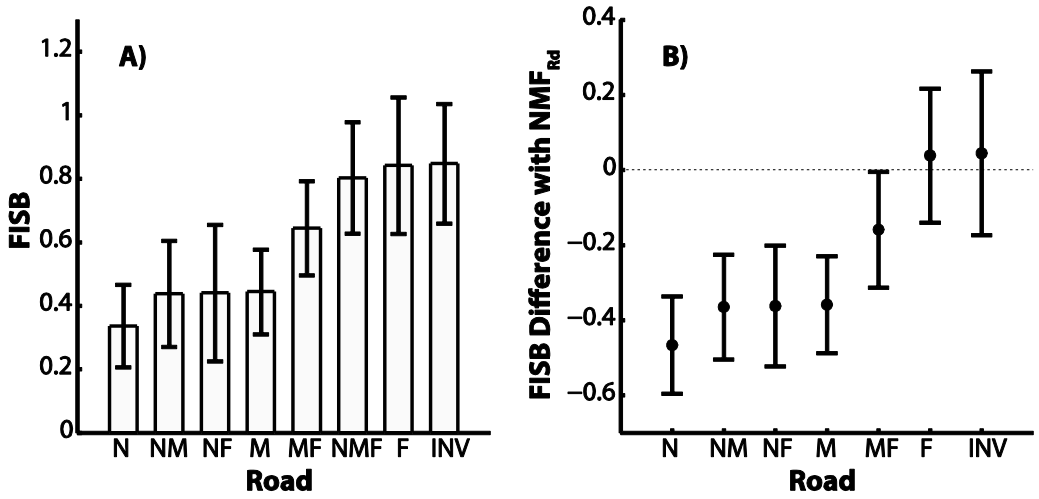

Figure 5.7 A) Average FISB scores for each road condition. B) Paired difference plots between each Road level and NMF_{Rd}. It is important to note that the order of road conditions have been determined by FISB magnitude (in order to more easily see the FISB 'groups') so are in a different order than other figures (with the exception of Figure 5.12). Error bars are 95% Confidence Intervals.

5.3.3 RMSE

Figure 5.6B shows average RMSE scores which demonstrate that deviation from the midline is fairly constant across road conditions, sitting at approximately .35m, with the main exception being the increase in error when all position-in-lane RE information is removed (F_{Rd}) and when RE information is removed altogether (INV_{Rd}). There do not seem to be systematic changes in RMSE due to changes in Flow speed, despite Flow manipulations causing clear positional changes (as shown by SB and FISB).

Changes across Flow levels are examined in more detail in Figure 5.8. There are some isolated biases that are consistent across participants, for example for NMF_{Rd} increasing flow speed by 50% ($FL_{1.5}$) caused a consistent small increase in RMSE. However, these are the exception rather than the rule. Generally, the paired differences compared to FL_1 sit around zero, or within .1m, suggesting that changes in error are small. One particular trend is that the point estimate for $FL_{.5} - FL_1$ is greater than zero

in all road conditions, although the 95% CI includes zero on five occasions (NMF_{Rd}, N_{Rd}, NM_{Rd}, M_{Rd}, and NF_{Rd}), indicating uncertainty as to the absolute magnitude of change. The increase in error for $FL_{.5}$ agrees with the SB results, where $FL_{.5}$ caused the largest positional change compared to FL_1 out of all the flow levels (Figure 5.4).

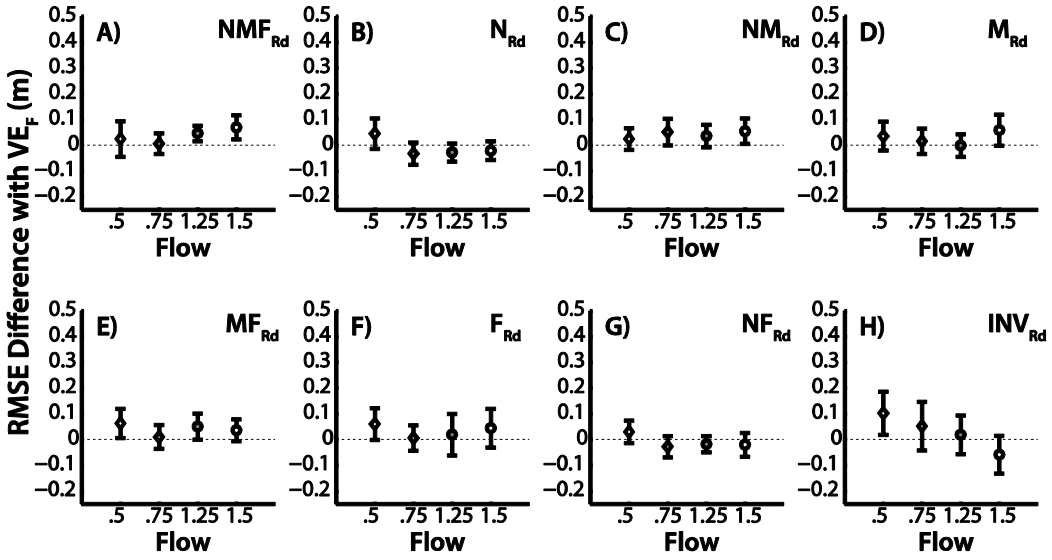

Figure 5.8 RMSE difference between the mean plots for comparisons across Flow levels for reach Road Level. Each point represents the paired difference between that particular Flow level and FL_1, the control condition. For all graphs a negative magnitudes indicate less deviation from the midline of the bend than in FL_1, and a positive magnitude indicates greater deviation from the midline. Error bars are 95% confidence intervals.

Changes across road conditions are examined in Figure 5.9. Under veridical flow conditions (Figure 5.9C), removing road components does not seem to increase error as long as the mid-road or near road segment remains, shown by paired differences estimates that sit close to zero for N_{Rd}, NM_{Rd}, M_{Rd}, MF_{Rd}, and NF_{Rd}. However, when only the far road segment remains, RMSE is consistently increased (M_{diff}=.076m [.013, .14], SEM=.03). Removing REs altogether causes the largest increase in total deviation from the road centre (M_{diff}=.27m [.17, .38], SEM=.05). This pattern is consistent across all flow levels. Interestingly, whenever flow speed is increased (Figure 5.9D & E), the road conditions N_{Rd} and NF_{Rd} seem to consistently reduce error compared to NMF_{Rd}.

Additionally, for $FL_{1.5}$ (Figure 5.9E) the error-inducing effects of INV_{Rd} is diminished compared to the other Flow levels (but still consistently increases RMSE; M_{diff}=.15m [.07, .22], SEM=.04).

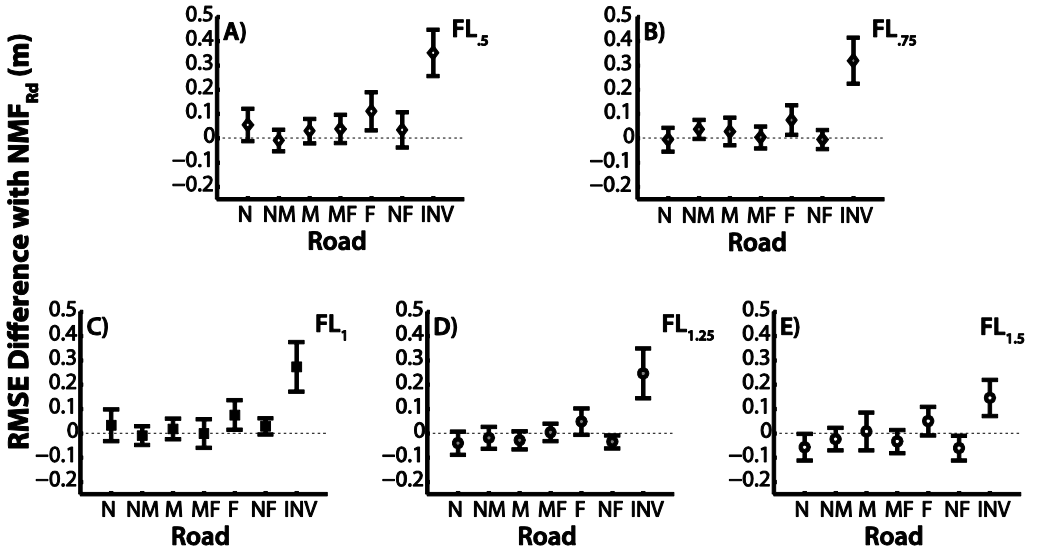

Figure 5.9 RMSE difference between the mean plots for comparisons across Road levels for reach Flow Level. Each point represents the paired difference between that particular Road level and NMF_{Rd}, the control condition. For all graphs a negative magnitudes indicates less deviation from the midline of the bend than in FL_1, and a positive magnitude indicates greater deviation from the midline. Error bars are 95% confidence intervals.

5.3.4 SWJ

Average SWJ scores are shown in Figure 5.6C. With a complete road, SWJ sits around 8deg.s^{-3} [6.83, 9.05], SEM=.52. Removing guidance RE information increases jerk by ~21.5% (M=9.69deg.s^{-3} [8.05, 10.31], SEM=.54). However, no other road condition produces a similar magnitude change in steering smoothness. It is not clear how altering flow speed impacted steering smoothness: $FL_{.5}$ seems to sit just above the other lines, indicating that people may have been particularly jerky when flow speed was lowest, but it is hard to see differences between the other flow levels.

Figure 5.10 examines how steering smoothness was affected by altering road components. Under veridical flow (Figure 5.10C), presenting only the near road component causes a large increase in jerk (M_{diff}=1.71deg.s^{-3} [.93, 2.49], SEM=.37). This increase is consistent across all flow levels. Additionally, presenting only the far road component causes a small *decrease* in jerk (M_{diff}=-.71deg.s^{-3} [-1.36, -.06], SEM=.31), although this consistent decrease is not present in non-veridical flow conditions. The paired difference estimates for all other road conditions sit around zero (Figure 5.10C).

Under non-veridical flow conditions, some differences between road conditions emerge that are not apparent under veridical flow: jerk is consistently increased for M_{Rd} in all non-veridical conditions, but particularly for $FL_{.5}$ (Figure 5.10A) and $FL_{1.5}$ (Figure 5.10E); under the slowest flow speed (Figure 5.10A), NF_{Rd} consistently increases SWJ compared to NMF_{Rd} (M=.94deg.s^{-3} [.28, 1.61], SEM=.32), this effect reduces in the other non-veridical conditions but the paired difference estimate is still positive.

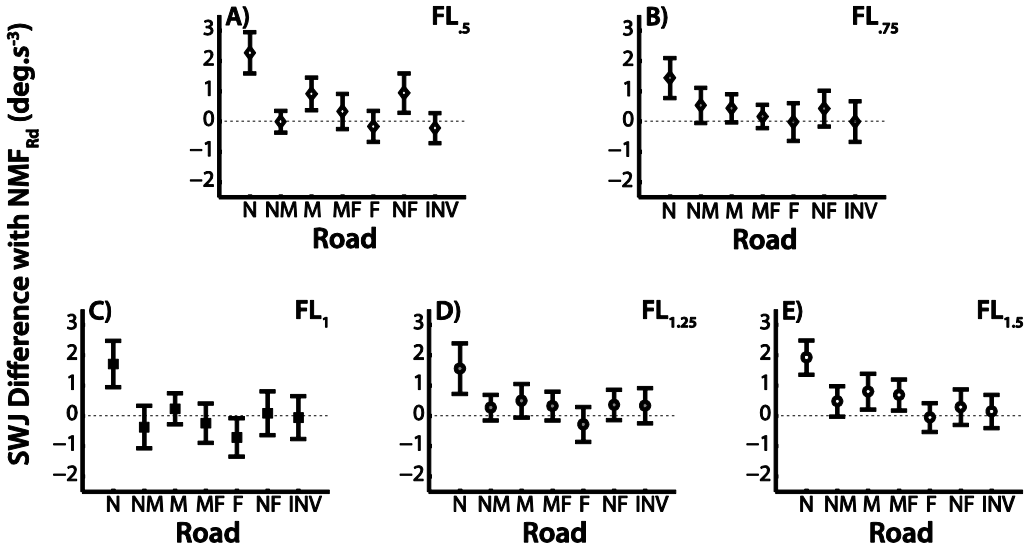

Figure 5.10 SWJ difference between the mean plots for comparisons across Road levels for each Flow Level. Each point represents the paired difference between that particular Road level and NMF_{Rd}, the control condition. For all graphs a positive magnitude indicates more steering corrections than in NMF_{Rd}. Error bars are 95% confidence intervals.

Figure 5.11 examines how steering smoothness was affected by changes in flow speed. Under full road conditions, manipulating flow speed does not seem to consistently change steering smoothness (Figure 5.11). The largest estimated difference is with $FL_{.5}$, but this effect is also the most variable and zero is well within the 95% CI (M_{diff}=.42deg.s^{-3} [-.31, 1.15], SEM=.35). However, for all other road conditions (with the exception of INV_{Rd}) the estimate of $FL_{.5}$ – FL_1 is consistently larger, at around 1deg.s^{-3}, suggesting that $FL_{.5}$ causes steering to be jerkier. Interestingly, this effect is diminished for INV_{Rd} (Figure 5.11E). The only other flow level that causes consistently increased jerk is $FL_{.75}$: F_{Rd} (Figure 5.11F) and NM_{Rd} (Figure 5.11B) have a paired difference estimate for $FL_{.75}$ – FL_1 of around .71deg.s^{-3} ([.15, 1.27], SEM=.27) and .91deg.s^{-3} ([.16, 1.67], SEM=.36) respectively, which is diminished in the other road conditions.

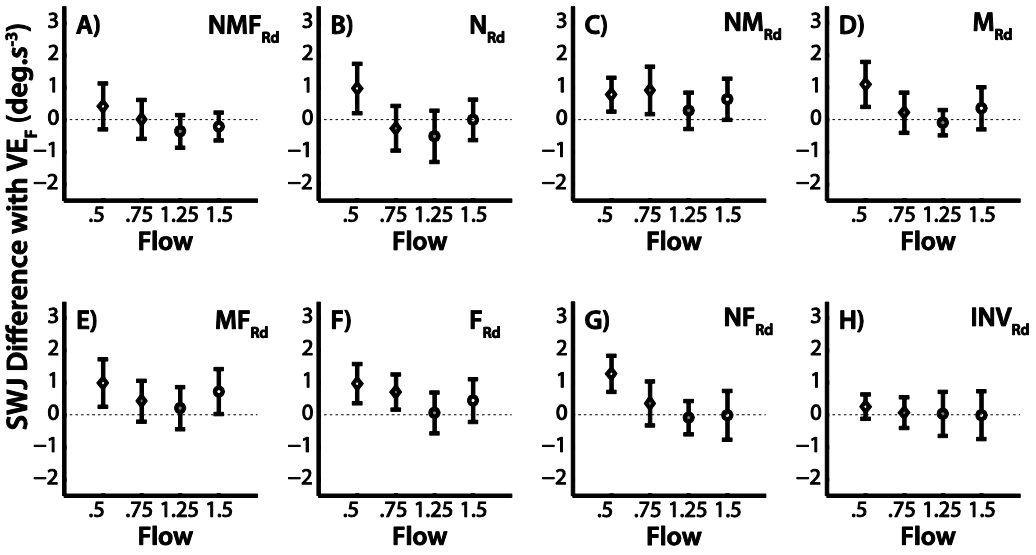

Figure 5.11 SWJ difference between the mean plots for comparisons across Flow levels for reach Road Level. Each point represents the paired difference between that particular Flow level and FL_1, the control condition. For all graphs a positive magnitude indicates more steering corrections than in FL_1. Error bars are 95% confidence intervals.

5.3.5 Analysing Trajectory Development.

As highlighted in Chapter 2 (see section 2.3.3), plotting an averaged 'typical' trajectory (Figure 5.12) is useful to develop a qualitative appreciation of steering behaviours. Here, averaged trajectories, with shaded error bounds, are presented for each road condition in order to see how road features affect steering responses to the various flow manipulations. Road conditions in Figure 5.12 are ordered by FISB magnitude (see Figure 5.7), and will be discussed with reference to the FISB 'groups' identified in section *5.3.2*.

It is important to first get an appreciation of the control condition (NMF_{Rd}), plotted in Figure 5.12F. Under veridical flow conditions (shaded green), participants enter the bend (after the initial 6m straight) slightly oversteering (present across all flow levels) which persists throughout the trial. Increasing flow speed by 50% ($FL_{1.5}$ = dark blue) causes oversteering to continue to develop before a gradual correction occurs ~2.2s into the bend, at which time position is shifted closer to the midline, but oversteering is not quite eliminated. This persistent oversteering is reflected in a larger RMSE than FL_1 (Figure 5.8A), but the gradual corrections mean the error does not result in jerkier steering (Figure 5.11A). Conversely, slowing flow speed by 50% ($FL_{.5}$ = red) causes the oversteering position to be eliminated quickly and understeering rapidly develops until ~2s, where maximal error is reached. Although understeering stops developing at this point, the offset causes understeering to persist throughout the remainder of the bend. The initial oversteering explains why RSME is not considerably greater than FL_1 (Figure 5.8A), despite spending a considerable larger time understeering (Figure 5.4A). Slowing flow by 25% ($FL_{.75}$ =o range) causes qualitatively similar steering behaviour to $FL_{.5}$, but on a smaller scale: understeering develops more slowly, but maximal error is reached around the same time point (~2s) before the understeering position is maintained. Increasing flow by 25% ($FL_{1.25}$ = light blue), however, causes a small amount of oversteering to develop later than its 50% counterpart ($FL_{1.5}$). There is considerable overlap between $FL_{1.25}$ and FL_1 (early in the trajectory) and $FL_{1.5}$ (later

in the trajectory). A similar overlap does not occur when Flow is slowed, which is reflected in larger magnitudes of change in SB for slower flow rather than faster flow (Figure 5.4A, see also section *5.2.4*).

F_{Rd} (Figure 5.12G) has qualitatively similar trajectories to NMF_{Rd}. All flow levels have similar shapes to NMF_{Rd}, but are simply more variable. This seems to be reflected in similar bias and jerk scores, but higher total deviation from the midline (Figure 5.6). Importantly, the similarity demonstrates that the equivalent FISB (Figure 5.7) captures qualitative similarities between the F_{Rd} and NMF_{Rd}. On the other hand, INV_{Rd} (Figure 5.12H) also has a similar FISB, but the trajectory plots show that behaviour in INV_{Rd} is qualitatively different to when true guidance information is available. Participants do not enter the bend with the initial oversteer present in F_{Rd} and NMF_{Rd}, instead participants enter the bend on the midline and understeering develops rapidly. Manipulating flow speed seems to determine the extent that this understeering stops developing and corrections start. For faster flow speeds, maximal error is reached around 1.5s, for slower flow speeds this value is around 2.25s. This results in a road condition with large understeering and large error, but low jerk (Figure 5.6). The high FISB value represents therefore varying degrees of understeering, not the pattern of faster-than-veridical flow causing oversteering and slower-than-veridical flow causing understeering, observed in F_{Rd} and NMF_{Rd}.

MF_{Rd} represents a 'transition' between the high-FISB and low-FISB conditions: it has lower FISB than NMF_{Rd} and F_{Rd} (Figure 5.12F & G), but higher FISB than NM_{Rd}, NF_{Rd}, and M_{Rd} (Figure 5.12A-D). This transition is demonstrated in the trajectory plot (Figure 5.12E). The steering response to a reduction in flow speed is qualitatively similar to NMF_{Rd} and F_{Rd}. However, the oversteering observed in NMF_{Rd} and F_{Rd} when flow speed is increased is not replicated in MF_{Rd}. Instead, the averaged trajectories for $FL_{1.25}$ and $FL_{1.5}$ sit roughly 'on-top' of FL_1, with considerable overlap, which is a characteristic of Figure 5.12A-D.

The next FISB grouping is NM_{Rd}, NF_{Rd}, and M_{Rd} (see Figure 5.7). The similar FISB values are reflected in almost identical trajectory plots (Figure 5.12B-D), characterised by an absence of the oversteering-inducing effects of increasing flow speed, and diminished understeering-induced effects of decreasing flow speed. These similarities are also reflected in comparable SB, RMSE, and SWJ between these conditions (Figure 5.6).

The final plot, N_{Rd}, has a unique profile (Figure 5.12A). The bend is entered with zero bias, and understeering develops rapidly, akin to INV_{Rd} (Figure 5.12H). However, unlike INV_{Rd}, the error is sharply corrected for and brought closer to the midline, resulting in jerkier steering but low RMSE (Figure 5.6). There is larger overlap between flow levels $FL_{.75}$, FL_{1}, $FL_{1.25}$, and $FL_{1.5}$, which explains the low FISB observed in Figure 5.7. However, $FL_{.5}$ still stands out from the other flow levels as inducing a consistent positional offset. This characteristic is shared throughout all road conditions (Figure 5.4).

To summarise, Figure 5.12 demonstrates that the FISB groupings identified in section 5.3.2 may also be grouped by qualitative similarities, with the exception of INV_{Rd} which has a unique trajectory development profile (Figure 5.12H). Generally, the presence of a far road component causes each flow level to develop more distinct trajectories (NMF_{Rd}, F_{Rd} and MF_{Rd}) than when F_{Rd} road is removed (N_{Rd}, NM_{Rd}, and M_{Rd}). Critically, trajectories for each flow level are most overlapping for N_{Rd}, when all guidance road edge information (the mid and far road) is removed. The exception to this pattern is NF_{Rd}, which is remarkably similar to M_{Rd} despite having both a near and far component (therefore according to Land and Horwood, 1995, it would have been expected for NF_{Rd} to be most similar to NMF_{Rd}).

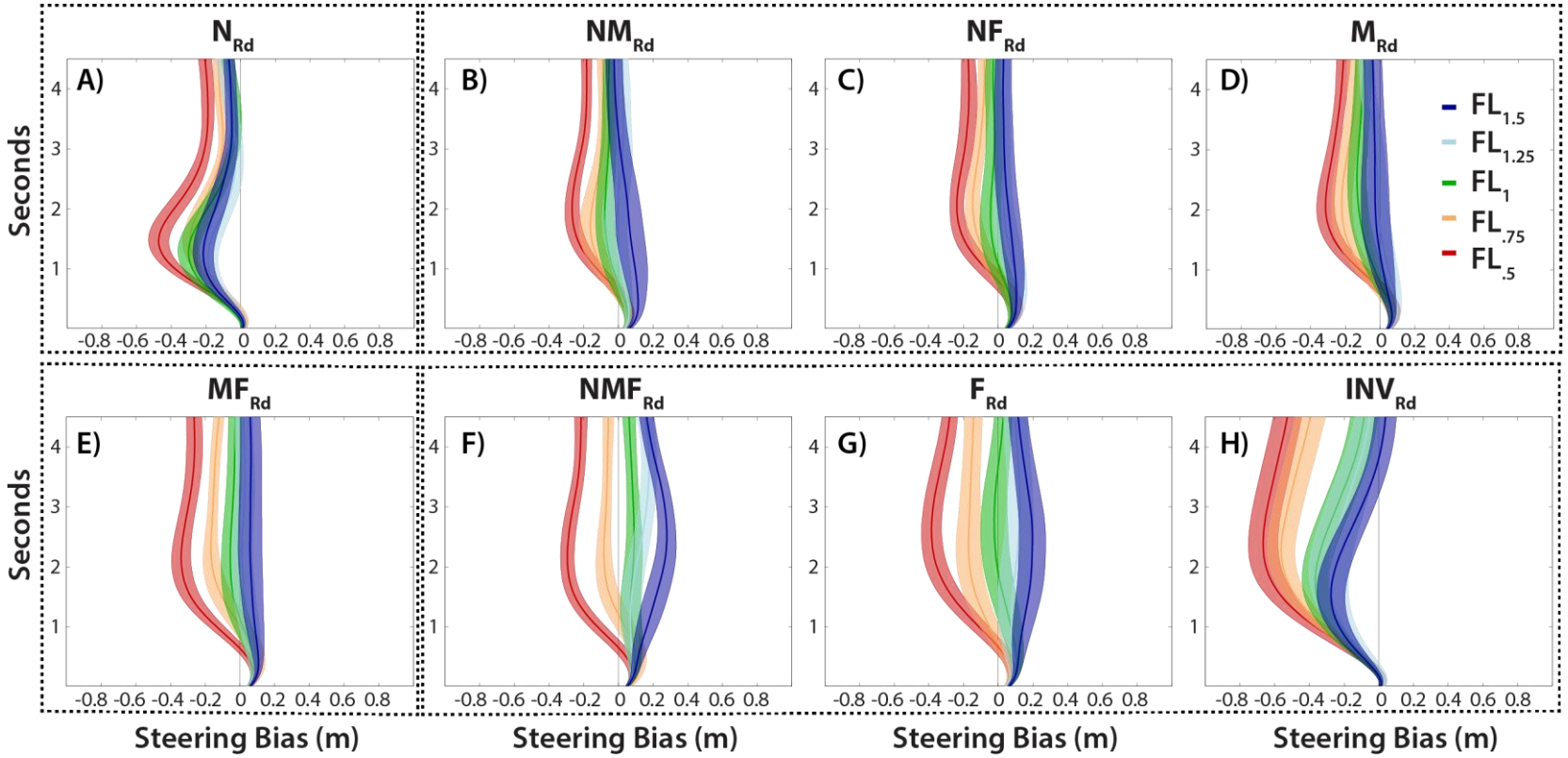

Figure 5.12 Average Trajectory plots showing Steering Bias over the course of a trial for all participants, with shaded bounds representing standard error of the mean. Plots are creating by averaging each Frame per participant, then averaging across participants and using this variability for the shaded error bounds. Plots are shown from the start of the bend, and are ordered A-H by their FISB magnitude, and dashed boxes signify groupings identified in section 5.3.2. Blue shades indicate Faster-than-veridical flow, and red shades indicate Slower-than-veridical Flow.

5.4 Discussion

The current experiment sought to examine the hypothesis proposed in Chapter 4 – that flow speed modulates a guidance level control signal – by systematically varying the amount of guidance and compensatory road edge information available. Generally, the results suggest that the presence of guidance level information is associated with increased influence of flow (with an interesting exception of NF_{Rd} – discussed later), which largely supports the hypothesis. FISB was least for N_{Rd} where position-in-lane information was available but all RE information giving cues as to the upcoming curvature requirements (the mid and far segments) were removed. Adding the mid road segment (which provides some guidance information; NM_{Rd}) increased FISB by approximately 30%, and adding the far road segment (NMF_{Rd}) increased FISB further by approximately 83%. The key determinant of the extent that flow influenced steering appears to be the presence of guidance level information. Additionally, a larger FISB was observed in INV_{Rd}, which as discussed in Chapter 4 appears to have commonalities with a guidance level task. Removing the near road from NMF_{Rd} caused a small change to FISB (reducing FISB by approximately 20%), but removing all compensatory information results in a FISB not markedly different from NMF_{Rd}. These trends support the hypothesis that the influence of flow speed is dependent upon a guidance level road edge signal.

The exception to the general pattern is NF_{Rd}. Under a simple additive two-level model (e.g. Salvucci & Gray, 2004), displaying both near and far components should produce similar steering behaviour to NMF_{Rd}. In the current experiment, however, NF_{Rd} is most similar to M_{Rd}. Looking at how the steering measures are altered by varying RE segment availability may explain why this might be the case. Jerky steering, with low error, are the classic characteristics of compensatory control (Land & Horwood, 1995; Land, 1998). Supporting this, removing all guidance information (N_{Rd}) caused a large increase in SWJ (Figure 5.6C). Conversely, smooth steering, but high positional error,

are the characteristics of guidance control (Land & Horwood, 1995; Land, 1998) – in the current results, RMSE is consistently increased when all compensatory information is removed (F_{Rd}; Figure 5.6B) but SWJ remains low (Figure 5.6C). N_{Rd} may be the only condition to induce large changes in jerk, but NM_{Rd}, M_{Rd}, and NF_{Rd} all show evidence of minor increases in jerk compared to a full road, at least in some flow conditions (Figure 5.5). Minor increases in jerk in NM_{Rd} and M_{Rd} would be expected due to the removal of the far road component, with the weakly informative mid road allowing smoother steering than in N_{Rd}. NF_{Rd}, however, contains both near and far components, which according to an additive two-stage model (e.g. Salvucci & Gray, 2004) would lead to similar steering behaviour to NMF_{Rd}. This is not what is observed: SWJ is increased for some flow levels (Figure 5.5), and the response to flow speed manipulations is not the same as NMF_{Rd} (Figure 5.12). Instead, levels of Jerk were similar to M_{Rd}. Moreover, the trajectory plots for M_{Rd} and NF_{Rd} were all but identical (Figure 5.12C & D), suggesting that they share qualitative as well as quantitative similarities that are not shared by NMF_{Rd}, which causes markedly different trajectory plots (Figure 5.12F). These measures suggest that NF_{Rd}, which under an additive framework should produce two strong compensatory and guidance level signals, instead produces control behaviours similar to a single weakly informative signal (M_{Rd}). In any case, it is clear that a full contiguous road is treated differently to 'broken' road boundaries, which disagrees with a simple additive combination of the two-levels (Land & Horwood, 1995; Saleh et al., 2011; Salvucci & Gray, 2004; a similar point is also made by Frissen & Mars, 2014).

The current findings allow the exploration of how guidance and compensatory RE signals are combined when gaze direction cues are controlled. To the author's knowledge, this is the first attempt to vary the amount of guidance and compensatory RE information in the scene whilst controlling for gaze direction (see limitations of Chatziastros et al., 1999; Cloete & Wallis, 2011; Land & Horwood, 1995 as outlined earlier). As previously highlighted, a shift to compensatory control is generally

identified by an increase in jerk (but low positional deviation), whereas a shift to guidance control is generally identified by high positional error but smooth steering (Land, 1998). Broadly, there is little change in RMSE and SWJ across road presentation conditions, with the only marked increases in RMSE or SWJ being exhibited by the 'extreme' conditions, where *all* guidance level information is removed (N_{Rd}; high SWJ) or *all* compensatory level information is removed (F_{Rd}; high RMSE). This is perhaps surprising; previous research has reported changes on instability and positional deviation measures that are yoked to the availability of compensatory and guidance level road edge information (Chatziastros et al., 1999; Land & Horwood, 1995). Instead, the current results support those of Cloete & Wallis (2011), who failed to find clear indicators of a shift in control strategies in response to changing RE information. The absence of real change in RMSE and SWJ in any road conditions apart from the extreme 'guidance-only' (F_{Rd}) or 'compensatory-only' (N_{Rd}) conditions suggests the visuo-motor system can cope with weakly informative guidance and compensatory RE signals (Land & Horwood, 1995; Neumann & Deml, 2011). One potential criticism is that constant curvature bends were used, and larger road segments were presented than in previous studies (Chatziastros et al., 1999; Cloete & Wallis, 2011; Land & Horwood, 1995). So it is possible that during a more demanding steering task, differences might emerge. Critically, since large differences are not observed with gaze constrained, it follows that differences observed in previous studies (Chatziastros et al., 1999; Land & Horwood, 1995) might be predominantly due to gaze behaviour changes across road conditions, rather than differences in road presentation per se. This is an important issue for future two-level steering work: a full description of how steering control solutions are obtained will not be achieved unless the interaction between gaze behaviours and guidance and compensatory RE signals is fully understood.

5.4.1 Comparing trends across Chapters 4 and 5

Chapter 4 demonstrated that flow speed had less influence over steering in N_{Rd} conditions than in F_{Rd}, NMF_{Rd} and INV_{Rd}. This same pattern is replicated in the current Chapter, despite subtle changes to road presentation (Chapter 5 cropped 'near' road at 6.71m and 'far' road at 13.41m, whereas Chapter 4 used 6m and 12m values), flow manipulation strength (Chapter 5 used $FL_{.5}$, $FL_{.75}$, $FL_{1.25}$, and $FL_{1.5}$, whereas Chapter 4 used $FL_{.66}$ and $FL_{1.33}$), and a different method of calculating FISB which was adapted to capture trends across all five flow levels. In order for the results to be directly compared to Chapter 4 (to be in the same units – metres), FISB was recalculated using the formula $(FL_X - FL_y) / 2$ (as per Chapter 4) for each flow manipulation magnitude used in Chapter 5. The replicative nature of the results can be exploited through a random effects meta-analysis (Borenstein, Hedges, Higgins, & Rothstein, 2009), in order to combine the two experiments to assess whether trends are consistent across experiments and across flow magnitudes. The estimates for the four duplicated conditions are shown in Figure 5.13. All the estimates for $FISB_{.25}$ are reduced compared to Chapter 4's estimates ($FISB_{.33}$). This reflects the smaller change in flow speed (25% shift in flow, rather than 33%). Similarly, all estimates for $FISB_{.5}$ are increased compared to $FISB_{.33}$, which reflects the larger change in flow speed (50% shift in flow, rather than 33%). These observations support the idea that the system responds precisely to flow speed magnitude (discussed in section 5.4.2). The meta-analytic estimates reinforce the trend that whilst there is a small amount of FISB for N_{Rd} (MA_N=.05m [.02, .07]), this increases for NMF_{Rd} (MA_{NMF}=.12m [.05, .2]). FISB is larger still for F_{Rd} (MA_F=.14m [.08, .21]) and finally for INV_{Rd} (MA_{INV}=.16m [.12, .21]). This reinforces the suggestion that different flow speeds cause larger steering biases when there is guidance level information (via far road or a fixation cross) present in the scene.

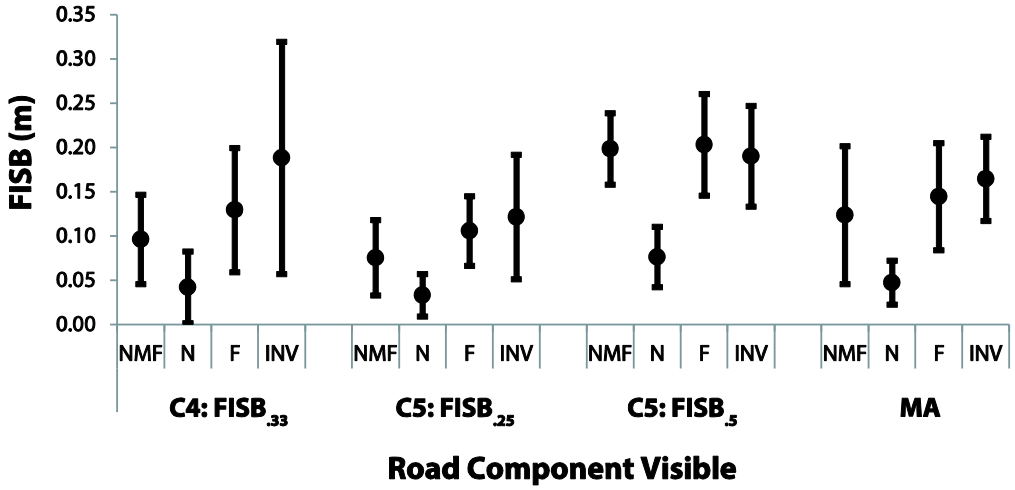

Figure 5.13 Flow influence was estimated using (FL_z – FL_y)/2, meaning that all estimates are in the same units (m). The estimates are combined using a random effects meta-analysis. Random effects was used, rather than fixed effects, because it does not assume that the same underlying effect is being estimated, thus estimates using slightly different parameters (i.e. of road component sizes and flow speed magnitudes) can be included. This allows assessment of whether trends are consistent across experiments and across flow magnitudes. Since Chapter 5 has two magnitudes of flow manipulations it provides two estimates to the meta-analysis (Chapter 4 only has one). The subscript on the x axis denotes the magnitude of the flow manipulation i.e. $FISB_{.25}$ would indicate the formula ($FL_{.75}$ – $FL_{1.25}$)/2. Error bars are 95% Confidence Intervals.

The meta-analytic estimates appear to suggest that FISB may be greater for F_{Rd} compared to NMF_{Rd}, which was not indicated by the FISB values reported in section 5.3.2 (Figure 5.7B). An increase of FISB when near or mid road is removed may indicate that the influence of flow speed is not wholly related to the presence of a guidance level signal, but also at least partially negated by the presence of compensatory signal. To assess whether this trend is consistent throughout both Chapters 4 & 5 a meta-analysis was conducted on the paired differences between NMF_{Rd} and F_{Rd} (Figure 5.14). The meta-analytic estimate is much more precise than the separate individual estimates, showing that each set of results are consistent.

Importantly, the combined estimate suggests that there is a reliable (albeit small) increase in FISB from NMF_{Rd} to F_{Rd} (M=.02m [.0, 0.04]). The main trends throughout Chapters 3, 4, and 5 suggest that the contribution of flow speed to steering is predominantly determined by guidance level signals, however, combining the results of Chapter 4 and 5 meta-analytically show that the modulation of flow by guidance level information may be simplistic – Figure 5.14 hints that the presence of compensatory information has the potential to negate the influence of flow speed.

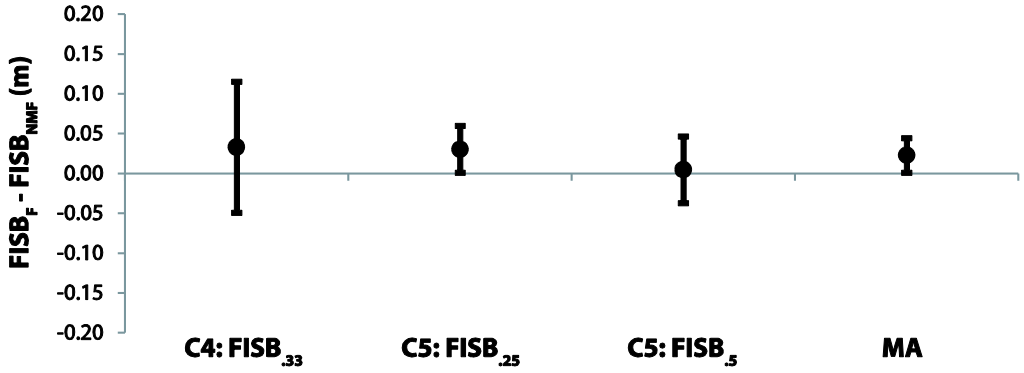

Figure 5.14 As per Figure 5.13 Flow influence was estimated using the formula (FL_X – FL_Y)/2. The paired difference between the means of FISB for NMF_{Rd} and F_{Rd} was estimated across experiments, and also across flow levels for Chapter 5 (where the design is expanded). These three estimates were then combined through random effects meta-analysis. Error bars represent 95% CIs.

5.4.2 Steering output is precisely specified by Flow speed magnitude

The current Chapter included five flow levels to assess whether steering response due to flow was proportional to input magnitude. The observed results suggest that it is, but not in a linearly proportional manner, as indicated in Chapter 2. Rather, there was a greater positional bias induced by slower flow levels than faster flow levels (Figure 5.4 & 5.12). There are two potential explanations for this. The first explanation is based on weber perception of flow speed (Authié & Mestre, 2012). The steering error caused by flow speed relies on a mismatch between the rate of movement of the REs (veridical

at 30mph) and the rate of flow (varied between 15mph, 22.5mph, 30mph, 37.5mph, or 45mph). If flow speeds are converted to weber fractions relative to 30mph (1, .33, 0, .2, and .33 respectively) it is straightforward to predict a greater degree of steering bias in response to the slow flow manipulations, as according to Weber's law the perceptual change is three times stronger. It can also be noted that the perceptual change of $FL_{.75}$ should be equal to $FL_{1.5}$. To approximate the degree of behavioural change caused by each flow speed manipulation, the grand mean of the change in steering position relative to 30mph was calculated. This grand mean was approximately equal for $FL_{1.5}$ (M=.085m) and $FL_{.75}$ (M=-.087m), smallest for $FL_{1.25}$ (M=.057m), and largest for $FL_{.5}$ (M=-.19m). Converting these values into fractions relative to 30mph (1, .45, 0, .3, and .44 for $FL_{.5}$, $FL_{.75}$, $FL_{1,}$ $FL_{1.25}$, and $FL_{1.5}$ respectively) demonstrates that whilst the magnitude of behavioural change does not *exactly* fit the weber fractions, the resemblance is close.

Whilst this explanation seems plausible, a competing explanation arises from the propensity to enter the bend in an oversteering position (Figure 5.12). As pointed out in Chapter 2, understeering causes errors to rise more quickly than oversteering. For this reason, understeering-inducing manipulations may be expected to produce larger errors than oversteering-inducing manipulations. This suggestion is reinforced by the Figure 5.12 plots, where understeering develops rapidly for $FL_{.5}$ in every road condition. However, this could also be due to the larger perceptual change compared to the other flow conditions (as previously discussed). Regardless of the underlying mechanism, the precise modulation of steering output due to flow speed magnitude shows flow speed has a functional and specifiable role in steering control.

5.4.3 Refresh rates and Steering Control

It is important to highlight that in Chapters 3 and 4 there were large increases in SWJ when either near or far RE components were removed. However, the computational demands of RE manipulations meant the update rate was reduced in these conditions.

Changes of the same magnitude were not observed in the current Chapter (update rate was constant at 60Hz): removing the near road did not increase steering jerk, and the increased in jerk in N_{Rd} was of a much smaller magnitude (around 21.5%, compared to a 90% increase in Chapter 4). It is likely that a proportion of the measured jerk in previous Chapters was caused by differences in update rates between conditions (Cloete & Wallis, 2011). Cloete & Wallis (2011) use a ten-fold increase in update rate (7.2Hz compared to 72Hz) to highlight this confound in Land & Horwood's study (1995), but the current evidence suggests instability effects can be found at much lower reductions in update rate (51Hz or 35Hz compared to 60Hz). There is no evidence that the lower update rate confounded the other steering measures of Bias and RMSE, with equivalent patterns observed across these other measures.

5.4.4 Implications for Two-Level Steering

There are no current steering models that capture the steering behaviours observed in the current experiment. Flow inspired steering models (e.g. Fajen & Warren, 2003; Wilkie & Wann, 2003a) have developed relatively independently of two-level steering models (Mars, 2011; Salvucci & Gray, 2004). The work of Chapters 3, 4, and 5 attempts to reconcile the two approaches by assessing whether flow speed information can be understood within a two-level framework (Donges, 1978). Indeed, the results suggest that flow speed is predominantly useful for guidance level control. The decision to investigate flow speed stemmed from previous work that found intriguing effects of flow speed when steering curved bends (Kountouriotis et al., 2013, 2015), however, modelling flow speed is problematic. Flow speed alone does not provide directional information, therefore cannot be directly used to adjust steering orientation which complicates simple feedback modelling solutions (such as using visual angle to a point to control steering e.g. Salvucci and Gray, 2004). However, there have been many steering models that incorporate directional information from flow, rather than speed information (Fajen & Warren, 2003; Warren et al., 2001; Wilkie & Wann, 2002). It is

currently unclear how flow direction information interacts with RE information, but throughout Chapters 3-5 a framework has been developed which allows systematic assessment of whether flow information can be captured within a two-level framework. The following Chapters use this framework to assess how flow direction information contributes to steering with road edges.

CHAPTER 6

FLOW DIRECTION AND TWO-LEVEL STEERING

6.1 Introduction

Recent studies have demonstrated that non-veridical global flow speeds can bias steering along curved roads (Kountouriotis et al., 2013, 2015). Chapters 2-5 of this thesis followed up these findings by assessing the role of flow speed within the framework of two-level steering control. It appears that flow speed predominantly affects steering when guidance level information is present in the scene. One interesting aspect of changes in flow speed that there is no change in the directional information provided by optic flow (accurate steering should cause similar vectors – they will just appear larger). In fact it remains unclear how the human visual system interprets the change in flow speed to produce the patterns of steering, though the results of Chapters 2-5 are consistent with modulating guidance level steering control. The original conception of optic flow by Gibson (1958) was that controlling orientation of steering control could be based around recovering directional information from optic flow information (rather than speed) to support locomotion (Warren, 1998).

Many studies have demonstrated that the direction of travel can be perceived from optic flow, on straight (Warren & Hannon, 1988) or circular paths (Cheng & Li, 2011; Kim & Turvey, 1998; Saunders & Ma, 2011; Warren et al., 1991), and gauging heading can sometimes be robust to eye-movements (Royden et al., 1994). However, the ability to recover a percept does not mean it is used for controlling locomotion, and the ubiquitous use of flow direction has been questioned (e.g. Harris & Rodgers, 1999). Rushton et al., (1998) asked participants to walk towards a target while wearing prisms that retinally displaced the entire visual scene sideways by 16 degrees. If one walks

toward a target whilst wearing prism glasses, the focus of expansion should still be centred on the target (the prism simply adds a single angular offset to the entire visual field), but the target will be offset (Figure 6.1).

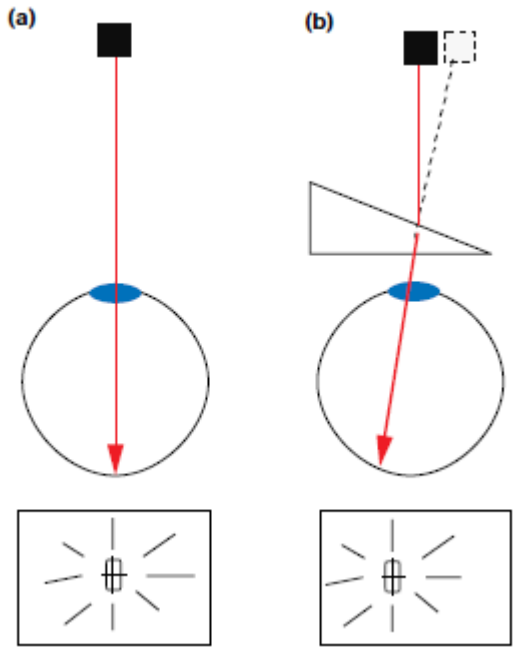

Figure 6.1 Retinal position of an object located straight ahead of the participants (a) without a prism and (b) with a prism. Lower panels show the instantaneous optic flow field corresponding to translation directly towards the target. The focus of expansion is centred on the target in both scenarios, but the retinal position of the target is offset in (b). Figure and caption adapted from Rushton et al. (1998).

Steering towards the target using egocentric direction would result in curved trajectories, due to orientation towards the retinally displaced target. Controlling steering by positioning the FoE over the target, however, should result in a straight line course. In Rushton et al. (1998), participants generally took curved paths to the target, providing strong evidence that egocentric direction (see Llewellyn, 1971, and section 1.4), instead of flow, might be used to control steering to a target. Supporting this, Harris and Bonas (2002) similarly found that participants modified their walking trajectories when walking whilst wearing prisms. Crucially, this modification was equivalent in well-lit conditions (where high quality optic flow is available), and dark

environments, suggesting that the addition of optic flow information did not negate the prism bias.

Whilst there have been a number of studies questioning the extent to which optic flow influences steering, the current balance of evidence suggests that both sources of information can be used. Wood et al. (2000) repeated Rushton et al.'s (1998) experiment, but varied the amount of additional information available. Participants were subject to either: i) a 10 degree restricted field of view; ii) a 35 degree restricted field of field and brown markings randomly distributed across the grassy plane; or iii) an unrestricted field of view with a grid-like pattern placed on the grass plane. When more cues where added to the environment, straighter trajectories were taken. Similarly, Warren et al. (2001) used a virtual environment to vary richness of information in the scene with displaced heading (by 10 degrees). They had four virtual environment setups, ranging from a simple target line with no flow to a doorway with textured walls, a doorway with walls and a ceiling, or a doorway with walls, a ceiling, and objects in the scene. Trajectories got successively straighter with richer flow information. Although studies suggest that flow information is combined with other sources based on availability and reliability (Wilkie & Wann, 2002, 2003a), when alternative information sources are strong, flow may only play a minor role in control (Rushton, 2004).

One issue with the studies outlined that examine walking/steering to a single target is that there are no constraints on trajectory choice. In principle participants could pivot on their foot to close down the visual angle and walk a straight line trajectory, or alternatively gradually close down the angle over time as the target is approached. Either solution is equally valid, but the underlying control solution involved in each strategy may be quite different (see Wilkie et al., 2011). In all cases, trajectories start with error in the direction of the prism bias, since flow is unavailable until one is moving. This initial error needs correcting for, but participants are free to do it in a

manner of their choosing. Therefore, a 'retinal flow' strategy (which is routinely assumed to be a straight-line course) could hypothetically produce curved trajectories if participants dampen their error-corrective manoeuvres. In short, in prism studies it is clear that strategies using egocentric direction would result in curved trajectories, but it is less clear that strategies using retinal flow would result in a straight line course. It is possible that the evidence in favour of a 'strong' egocentric direction account of locomotion when steering to a target (Rushton, 2004) might be too simplistic.

In these prism studies, the *goal* (target) is initially specified by egocentric direction alone (before the observer moves), but once the observer starts to move the course to the goal (trajectory to take) can be specified by either flow or egocentric direction. On a constrained path, both the goal and the trajectory to take are specified through egocentric direction sources, i.e. angular inputs from the lane boundaries (Land & Lee, 1994). It is unclear, in this case, whether directional information from flow would bias steering, since the task is clearly specified by road edges (although Chapters 2-5 have demonstrated that flow *speed* can bias steering with lane boundaries). One angular input from road edges is splay angle, which is defined as the optical angle of a road edge with respect to the vertical in the field of view and can be used to control lateral deviation (Warren, 1998). To test whether splay angle or flow information aided steering on straight road, Beall & Loomis (1996) had participants view road edges (where splay angle is available) or slalom gates (only motion parallax available) through small (1.15°) viewing windows placed near (6.4° down from horizon), medium (1.7°), or far from the viewer (.14°). Lateral perturbation was used to simulate a cross-wind, requiring constant steering adjustments. Adding ground texture to the slalom gate conditions significantly decreased RMS error, especially for viewing windows at farther distances where motion parallax information is weak. However, when road edge segments were available neither viewing proximity nor ground texture affected performance, consistent with controlling steering using splay angle. This

suggests that when directional information from REs is available, flow information may be superfluous.

More recently, Li & Chen (2010) have pointed out that Beall & Loomis's study used a small field of view monitor (~20° x 15°) and a relatively sparse flow field, which could have resulted in a weak flow direction signal. Li & Chen (2010) replicated Beall & Loomis's (1996) study using a large field of view (110° x 94°), and an added intermediate flow condition (they had 'no-flow', 'sparse-flow', and 'dense-flow). This time, adding flow information to displays with splay angle reduced RMS error, although there was not a reduction in RMSE from 'sparse' to 'dense' flow. This suggests that Beall & Loomis's (1996) results could be due to a narrow field of view reducing the quality of flow information. However, it is worth noting that the REs used by Li & Chen (2010) only subtend a vertical visual angle of 3.1°. It is possible that a larger road segment would provide multiple splay angle estimates with which to control lateral deviation, therefore with more road information available the control signal provided by the road edges might be stronger (i.e. more robust to noise) and flow direction information could remain unnecessary.

The studies examining the influence of splay angle and ground texture used straight roads with perturbing winds. Straight roads provide little anticipatory information, and splay angle is as salient at far distances as near distances (Beall & Loomis, 1996). As discussed in Chapter 1, straight and curved roads may require different control solutions. Successful steering on curved roads requires more anticipatory information due to changes in upcoming steering requirements (Donges, 1978), and gaze patterns reflect the need to obtain anticipatory information from the REs (Land & Lee, 1994; Lehtonen, Lappi, & Summala, 2012). Unfortunately, there have not been many studies assessing the role of a flow direction signal on steering control along curved paths. As highlighted in previous Chapters, Chatziastros et al. (1999) showed lane keeping performance is marginally improved on a curved course when ground texture is

added, across a range of road viewing conditions. However, this improvement was only found on a high contrast monitor screen; the lower resolution projector screen failed to find an improvement (presumably due to a weaker flow signal). Loomis & Beall (2003) report using scintillating random dot cinematograms with 1-frame lifetimes (SRDCs) to study steering along curved and straight paths with or without coherent optic flow information (i.e. SRDCs create conditions where the optic flow did not correlate with driver's movement). The SRDCs increased RMSE by 25% for straight paths and by 80% for curved paths, suggesting that optic flow information might contribute more strongly to steering on curved paths rather than straight paths, where simpler control strategies are available (Beall & Loomis, 1996).

It appears that the presence of a veridical flow direction signal can improve performance on curved paths. However, it is unclear how a flow direction signal can be incorporated into the popular two-level account of curved driving (Salvucci & Gray, 2004). To tackle this issue, this Chapter will follow the experimental framework established during Chapters 3, 4, and 5; direction as specified by flow and direction as specified by road edges will be purposely mismatched, and the availability of guidance and compensatory RE information will be manipulated. In Chapter 3, two competing hypothesis were presented: the Modulation Hypotheses (H1) and Weighted Combination Hypothesis (H2), each with their own mutually exclusive predicted patterns of results across road conditions.

In the current Chapter, both sources of information (flow direction or REs) can be used to adjust steering towards a goal in a feedback manner; therefore they are in *direct* conflict (as opposed to flow speed, which cannot be used to control steering by itself). When multiple sources specify similar outcomes, evidence suggests they are combined according to their availability or reliability (Wilkie & Wann, 2002): when one signal is weak, or removed, more weight will be attributed to the remaining signal. The pattern of results consistent with H2 is expected, reproduced here in Figure 6.2. If flow

direction contributes equally to both anticipatory and compensatory systems, more weight will be attributed to flow when either road segment is removed (H2C). However, if flow direction exclusively contributes to compensatory control (H2A) or anticipatory control (H2B) then flow will only increase when the near or far, respectively, road segment is removed.

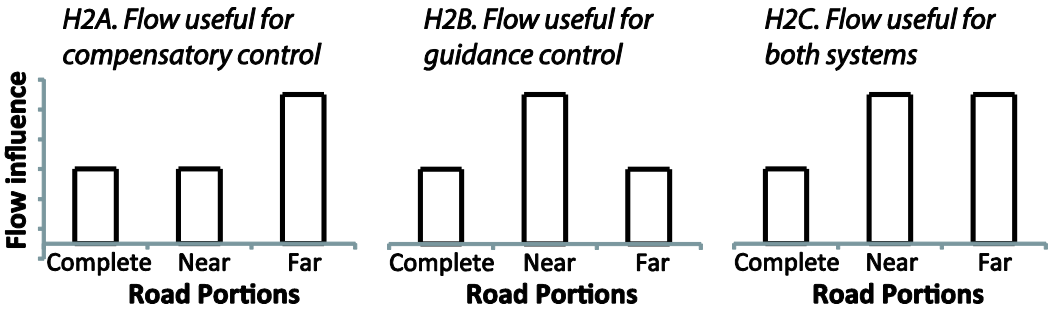

Figure 6.2 Weighted Combination pattern of results. If the weight attributed to flow depended on near road edges, the removal of near road edges would cause flow influence to increase (H2A). If flow competed with far road edges, flow influence would increase only when far edges are removed (H2B). Finally, if flow competes with RE information regardless of segment type, flow influence would increase whenever REs are removed (H2C).

The literature is currently unclear on which pattern would be expected. Chatziastros et al. (1999) demonstrated a similar influence of added ground texture across a range of single segment road viewing conditions, which might predict H2C. Alternatively, humans are able to perceive current direction of travel from flow over life-limited displays (Li et al., 2009, 2006), which suggests flow can be useful for immediate error-corrections (H2A). Supporting this, a couple of simulator studies have suggested that heading angle (which can be perceived from flow) is controlled in a continuous manner, whereas lateral deviation (in these cases, given by splay angle from road edges), is only controlled intermittently (McLean & Hoffman, 1973; Weir & Wojcik, 1971). Continuously correcting for error is characteristic of compensatory rather than

guidance control (Donges, 1978), so it might be expected that flow direction interacts with near road edges (H2A).

On the other hand, if one is looking to the future path, the path information necessary for guidance control may be extracted from flow (Kim & Turvey, 1999; Wann & Swapp, 2000). Although there is evidence that retinal flow information alone is insufficient to judge future circular path (Saunders & Ma, 2011), it is possible that even an uncertain judgement is useful to augment the information obtained from far road information (which may result in a pattern akin to H2B).

6.2 Methods

6.2.1 Participants

A sample of 18 University of Leeds Students (10 females, 8 males, ages ranged from 20 to 23, mean 21.3yrs), all having normal or corrected-to-normal vision, took part in Chapter 6. All held a full driving license (average time since test=3.1yrs) and did not take part in experiments presented in other Chapters. All participants gave written informed consent and the study was approved by the University of Leeds, School of Psychology Research Ethics Committee (Ref 13-0229), and complied with all guidelines as set out in the declaration of Helsinki.

6.2.2 Apparatus

The same apparatus as described in Chapter 2 was used in this experiment. Unfortunately, it was observed post-experiment that the update rate for N_{Rd} was 53Hz and for F_{Rd} it was 37Hz (for NMF_{Rd} and INV_{Rd} it was consistent at 60Hz). The issue of low refresh rates as a potential confound was addressed in Chapters 3 (section 3.5), Chapter 4 (section 4.4.2.1) and Chapter 5 (section 5.4.3), and it has been demonstrated that while the low refresh rates may be responsible for some increased jerk during N_{Rd} and F_{Rd}, they do not confound SB or RMSE measures.

6.2.2 Stimuli

The simulated virtual environment had a green tint ground texture, with a 3m wide road of constant curvature (60m radius) demarcated with white road edges (as in the previous Chapters; Figure 6.3A). Movement of the road edges was veridical to a driver speed of 13.41ms^{-1} (~30mph), therefore steering requirements relative to the road remain constant across all conditions and errors relative to the road edges develop at the same rate. Road edge cropping conditions were as per Chapter 4 (see Figure 4.2).

The movement of the ground texture was also matched to a driver speed of 13.41ms^{-1}. However, the ground texture could be manipulated so that additional texture motion orthogonal to the observer could be introduced into the scene (Figure 6.3B). The motion vector magnitude was constant throughout the entire trial, and either increased or decreased the inherent horizontal motion in the scene by 50% (.75ms^{-1}; calculated from a middle-of-the-road trajectory). The direction of this vector was determined by finding the nearest point on the midline to the observer and the angle between this point and the curve origin. This was updated every frame (so the introduced motion was orthogonal to the observer at each instant of motion). Whilst this method only results in 'perfect' orthogonal motion in the display if the observer's orientation is straight ahead relative to road edges, it means that the motion vector is consistent across participants. An alternative would be to match the motion vector to the locomotor axis of the observer, but this would result in very different rates of flow being introduced depending on the steering of the observer.

Simulations of the flow manipulation show that observers should perceive a trajectory from flow that is biased in the *opposite* direction of the ground texture shift (Figure 6.3C). For example, moving the ground texture towards the *inside* of the bend should cause flow to indicate that the participant is moving towards the *outside* of the bend (understeering; Figure 6.3C; red). In this case, it is predicted that when participants use flow they will correct for the (mis)perceived understeering by oversteering towards

the inside of the bend. Since the error specified from flow will be artificial, the correction would itself result in an error relative to the road edges. In short, if participants use flow direction information it is predicted that they would steer *in the same direction* as the ground texture shift: an inward shift causes oversteering; an outward shift causes understeering.

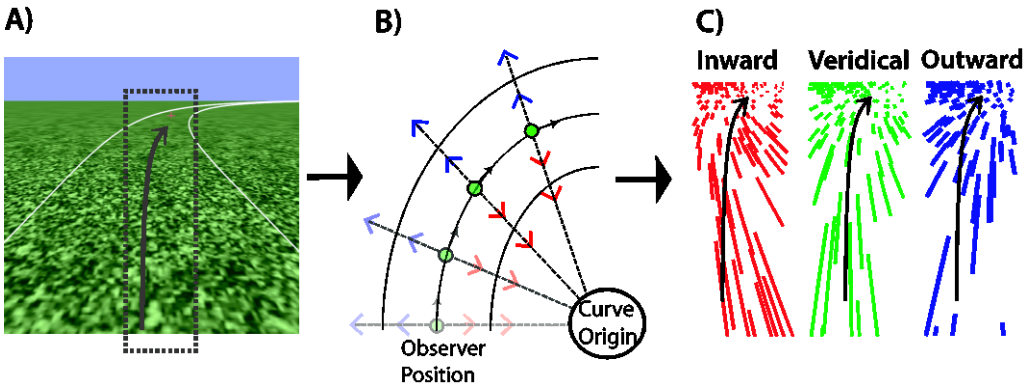

Figure 6.3 A) Screenshot of stimuli used, with boxed area representing the area displayed in panel C. B) As the observer moves through the bend, a motion vector orthogonal to the observer is introduced towards the inside or outside of the bend. C) Simulations show a flow trajectory moving towards the outside of the bend for the inward translation, and moving towards the inside of the bend for the outward translation.

It is possible that eye movements would interact with the flow manipulation (Regan & Beverley, 1982). For example, a gaze sweep towards the outside of the bend causes the flow field to shift towards the inside of the bend, therefore might 'cancel out' motion introduced towards the outside of the bend. Additionally, gaze patterns when steering a bend vary between individuals (Robertshaw & Wilkie, 2008) therefore differences in gaze patterns may cause inconsistent rates of flow being introduced. To avoid this confound the experiment was conducted with constrained gaze, with a fixation cross placed 16m ahead on the future path (1.2s, as per Chapters 4 & 5).

6.2.3 Procedure

Participants completed 8 practice trials (veridical flow, each road visibility condition, for left and right bends) to familiarise themselves with the simulator dynamics. Participants were instructed to 'attempt to steer a central trajectory, keeping to the middle of the road'; to steer 'as smoothly and as accurately as you can'; and to 'centre the wheel after each trial'. There were three flow manipulations (Figure 6.3C): flow with an inwards translation, veridical flow, and flow with an outwards translation, abbreviated to IN_F ('INward flow'), VE_F ('VEridical Flow'), and OUT_F ('OUTward flow'). There were also four road manipulations: NMF_{Rd}, N_{Rd}, F_{Rd}, and INV_{Rd} (see Figure 4.3). Trials were 6 seconds long with a .83s (50 frame) pause at the start of trials to give participants time to re-centre the wheel before motion commenced: the driving time was therefore 5.17s. There were six trials of each condition.

6.2.4 Analysis

Analysis was as per Chapter's 3 & 4. Positional data over time was recorded at 60Hz and the measures Steering Bias, RMSE, and SWJ were calculated. FISB was calculated using SB (IN_F – OUT_F / 2).

6.3 Results

Trends are analysed through plots showing paired difference estimates between the means of experimental conditions and the control condition (solid symbols; VE_F + NMF_{Rd}), with the precision of each estimate captured through 95% CIs. Additionally, the grouped and average measures are shown on line graphs with standard error bars.

6.3.1 SB

Average steering position relative to the midline is shown in Figure 6.5A. In the control condition (VE_F and NMF_{Rd}), participants showed slight oversteering (M=.037m [-.007, .081], SE=.02). Slight oversteering was also observed for F_{Rd} (M=.1m

[-.03, .24], SE=.064) and INV_{Rd} (M=.09m [-.039, .22], SE=.061). However, removing the far RE component caused slight understeering (M=-.056m [-.12, .007], SEM=.03). This is consistent with previous Chapters. The paired difference plots show that under veridical conditions F_{Rd} and INV_{Rd} cause slightly more understeering than $NMF_{Rd,}$ but that the magnitude of this effect was variable between participants, shown by large 95% CIs (Figure 6.4B). When a translation was added into the scene, F_{Rd} and INV_{Rd} showed consistently greater oversteering than NMF_{Rd}, by approximately .2m (Figure 6.4B). However, this effect collapses when an outward translation was introduced into the scene (Figure 6.4C).

It is clear from Figure 6.5A that adding IN_F produced systematic oversteering, whereas OUT_F produced understeering. This is in accordance with predictions from simulating the resultant flow field (Figure 6.3C). Moreover, the magnitude of this effect varies between road conditions. To assess how consistent trends were across participants, the paired difference estimates were explored with 95% CIs. Under complete road conditions (Figure 6.4D), an inside translation produced an oversteering shift of approximately 2.4%RW (M_{diff}=.072m [.031, .113], SE=.02). An outside translation produced a similar and opposite understeering shift of approximately 2.8%RW ($M_{diff=}$-.085 [-.12, -.05], SEM=.02). These magnitudes are highly consistent across participants, indicated by small 95% CIs in Figure 6.4D.

Similar oversteering and understeering magnitudes are observed for N_{Rd} (Figure 6.4E), however behaviour is more variable for OUT_F (M_{diff}=-.06m [-.15, .02], SE=.04). For F_{Rd} and INV_{Rd} the magnitudes are clearly much greater, but behaviour more variable. IN_F causes oversteering by approximately 6.7%RW, and similarly OUT_F causes understeering by approximately 6.7%RW (Figure 6.4F & G).

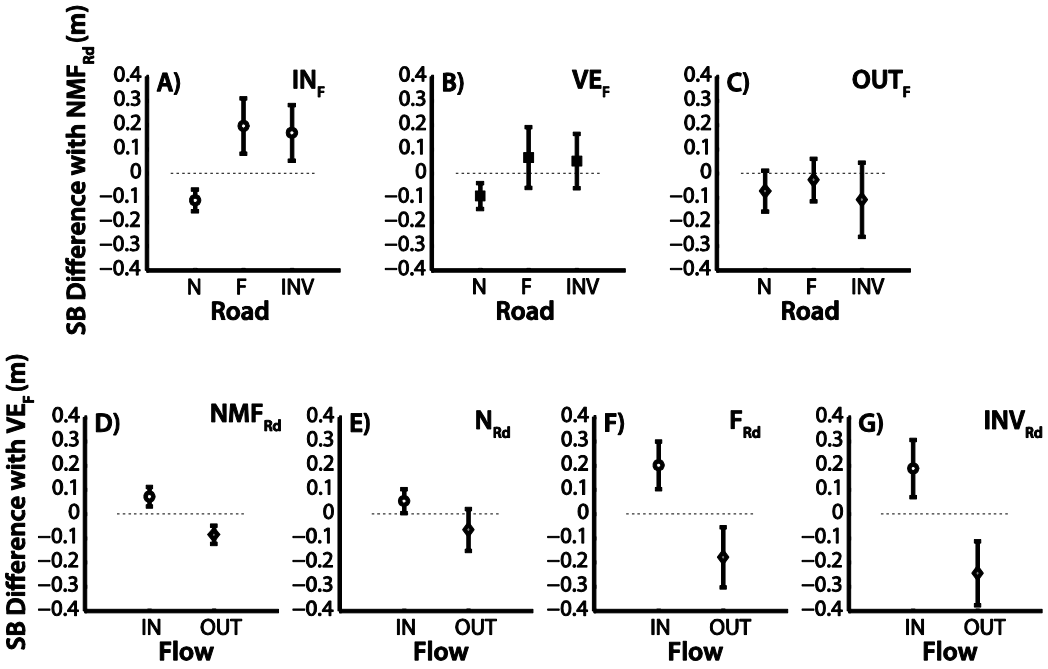

Figure 6.4 Steering Bias paired difference plots. Top Row: difference between means compared to NMF_{Rd} for A) IN_F, B) VE_F, and C) OUT_F. Bottom Row: difference between means compared to VE_F for D) NMF_{Rd}, B) N_{Rd}, and C) F_{Rd}. For all graphs a negative magnitude means steering further towards the outside edge (understeering) than the respective comparison condition, NMF_{Rd} or VE_F. Error bars are 95% confidence intervals.

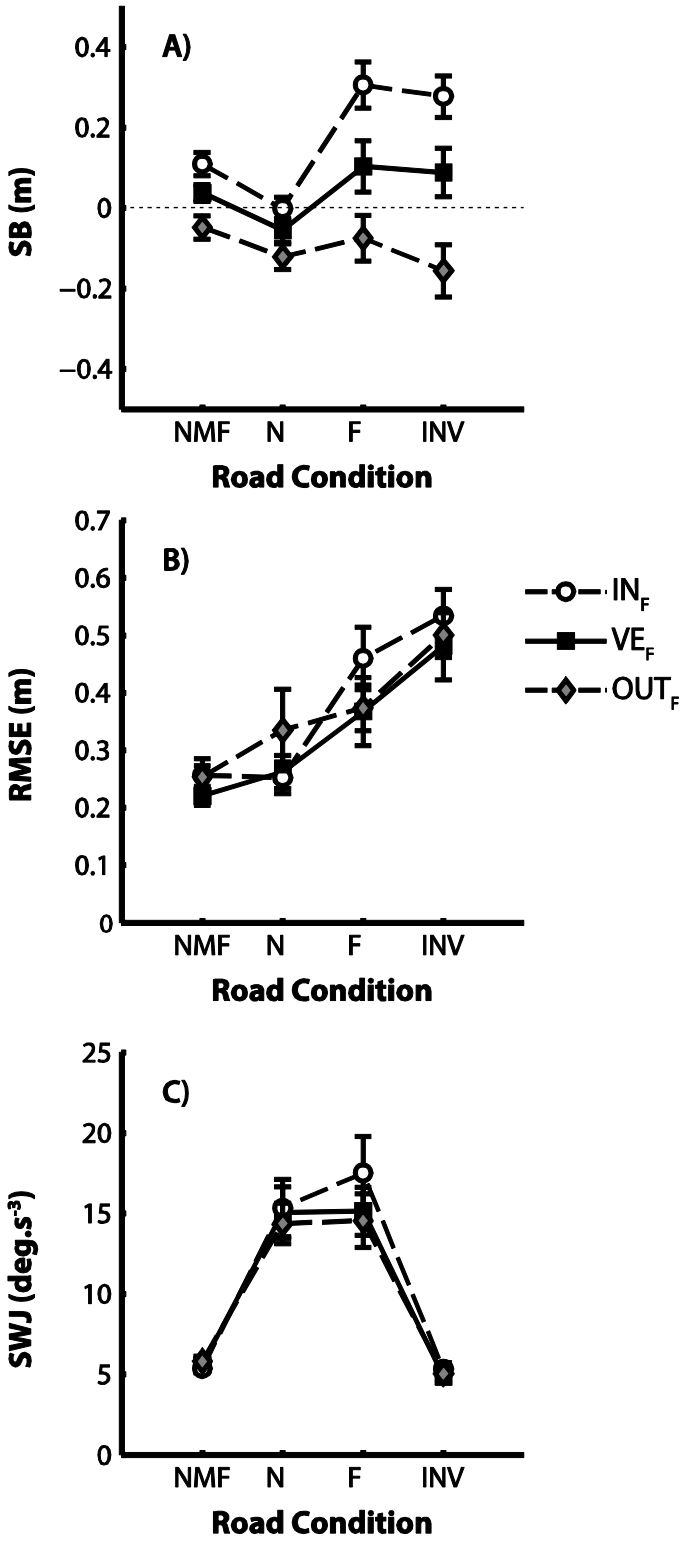

Figure 6.5 All steering performance measures across IN_F (empty circles, dashed line), VE_F (filled squares, solid line), and OUT_F (grey diamonds, dashed line), showing A) Steering Bias, B) Root-mean-squared error, and C) Steering Wheel Jerk. Error bars represent standard error of the mean (SEM).

6.3.2 FISB

Average FISB scores are shown in Figure 6.6A. FISB captures the extent that 'use' of flow changes across road conditions. Flow biased steering in every flow condition, shown by positive values. However, the FISB for N_{Rd} (M=.06m [.01, .11], SEM=.02) is similar to NMF_{Rd} (M=.08m [.05, .11], SEM=.01), but not F_{Rd} or INV_{Rd}. This is demonstrated by a paired difference estimate for NMF_{Rd} – N_{Rd} sitting around zero (Figure 6.6B), but the paired difference estimates for F_{Rd} and INV_{Rd} both being considerably and consistently larger, sitting around .11m ([.07, .15], SEM=.02) and .14m ([.08, .2], SEM=.03) respectively.

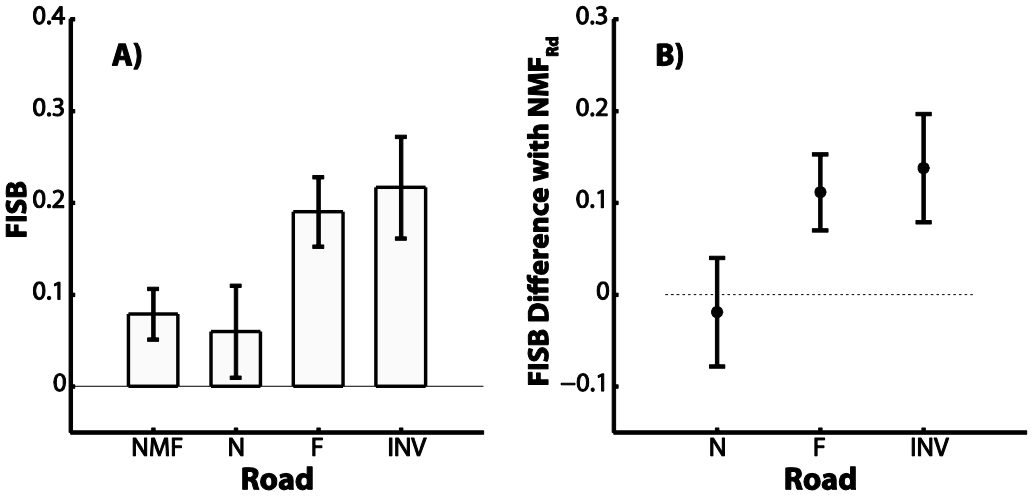

Figure 6.6 Average FISB scores for each Road Condition, a positive FISB indicates steering behaviour in line with predictions (oversteering for IN_F; understeering for OUT_F). B) Paired difference estimates between NMF_{Rd} and the other road conditions. All error bars are 95% confidence intervals.

6.3.3 RMSE

The average RMSE scores are shown in Figure 6.5B. Within each plot, a clear left-right increase is RMSE is readily apparent. Averaged across flow levels, the RMSE score for NMF_{Rd} is .24m ([-.2, .29], SEM=.02). This increases slightly to .28m ([.2, .37], SEM=.04) for N_{Rd}, to .4m ([.3, .5], SEM=.046) for F_{Rd}, and to .51m ([.42, .59],

SEM=.041) for INV_{Rd}. Systematic differences according to Flow manipulations are less immediately clear.

Figure 6.7 examines systematic trends in more detail. As discussed above, Figure 6.7B demonstrates that under veridical flow conditions a small, but consistent, increase in error was caused by removing far road information ($M_{diff=}$.04m [0, .08], SEM=.02); this increase more than doubles when compensatory information was removed (M_{diff}=.15m [.05, .24], SEM=.05); however, the greatest increase came when REs were removed altogether (M_{diff}=.26m [.17, .36], SEM=.05). This pattern is roughly consistent throughout all flow levels, with some slight nuances: removing the far road component does not increase error in INV_{Rd} (Figure 6.7A), but in OUT_F it increases error to a greater extent than in VE_F, although the steering response is more variable (Figure 6.7C).

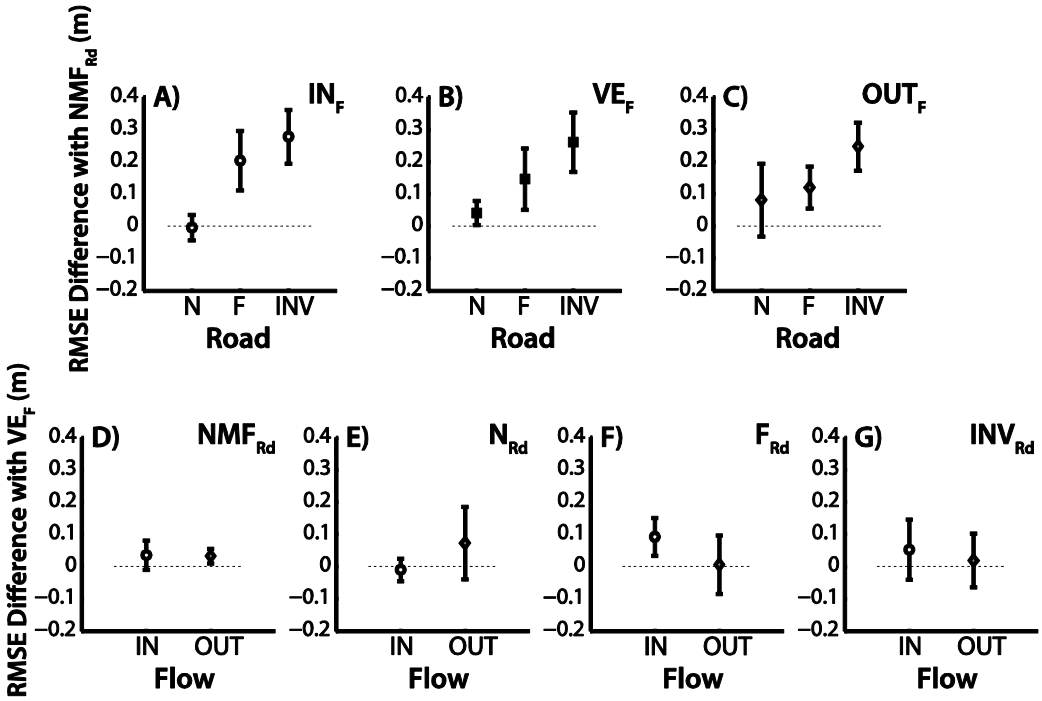

Figure 6.7 RMSE difference plots. Top Row: difference between means compared to NMF_{Rd} for A) IN_F, B) VE_F, and C) OUT_F. Bottom Row: difference between means compared to VE_F for D) NMF_{Rd}, B) N_{Rd}, and C) F_{Rd}. For all graphs a negative magnitude indicates less deviation from the midline, compared to the control comparison (NMF_{Rd} or VE_F), and a positive magnitude indicates greater deviation from the midline. Error bars are 95% confidence intervals.

The trends for flow manipulations are less clear (Figure 6.7D-G). Manipulating flow in either direction caused only a small increase in variable error: collapsed across road conditions, the average paired difference estimates for IN_F and OUT_F are .04m ([.011, .07], SEM=.01) and .03m ([.008, .056], SEM=.01) respectively.

6.3.4 SWJ

Average SWJ scores are shown in Figure 6.5C. There are clear alterations in steering smoothness due to road edges, but not due to flow. Under veridical conditions jerk is 5.6deg.s^{-3} ([4.89, 6.32], SE=.34), this value almost tripled for N_{Rd} (M=15.1deg.s^{-3} [11.67, 18.46], SEM=1.61) and F_{Rd} (M=15.1deg.s^{-3} [11.99, 18.3], SEM=1.5), but remained low for INV_{Rd} (M=4.85deg.s^{-3} [4.09, 5.61], SEM=0.36). Figure 6.8A-C show that these

differences are relatively consistent across flow levels. As discussed in section 6.2.2, some of the increase in SWJ in N_{Rd} and F_{Rd} is likely to be explained by low refresh rates.

Flow manipulations do not seem to have a large effect on steering smoothness. Generally, the paired difference estimates sit around zero Figure 6.8D-G, apart from an isolated case in F_{Rd}, were adding an inwards translation seems to make steering jerkier (M_{diff}=2.37deg.s^{-3} [-.15, 4.89], SEM=.67).

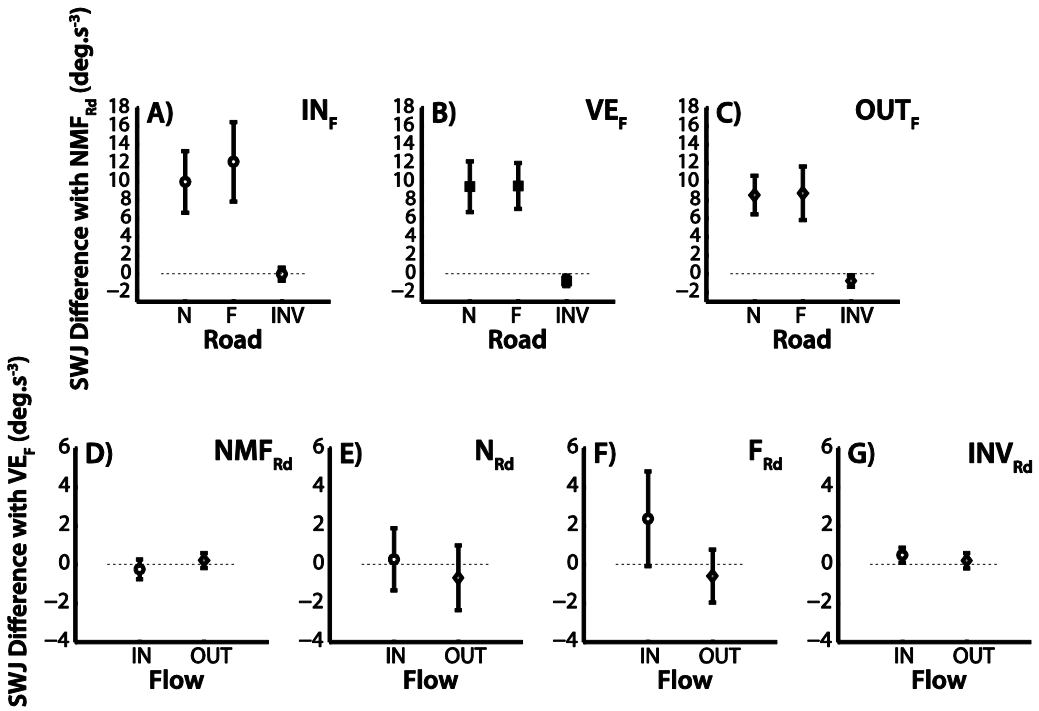

Figure 6.8 SWJ difference plots. Top Row: difference between means compared to NMF_{Rd} for A) IN_F, B) VE_F, and C) OUT_F. Bottom Row: difference between means compared to VE_F for D) NMF_{Rd}, B) N_{Rd}, and C) F_{Rd}. For all graphs a negative magnitude indicates less deviation from the midline, compared to the control comparison (NMF_{Rd} or VE_F), and a positive magnitude indicates greater deviation from the midline. Error bars are 95% confidence intervals.

6.4 Discussion

In the current experiment, flow information was manipulated to sometimes specify biased trajectories. If a driver is extracting directional information from flow to aid steering control, they will 'correct' for this perceived bias, resulting in systematic steering error (since actual locomotor path relative to the road edges was not biased). Crucially, the results demonstrate that the extent flow biased steering depends on road segment availability. This is the first research to show that use of flow direction information varies depending on which RE segments are available.

When no REs are available (INV_{Rd}), participants exhibit large biases due to flow. As discussed in Chapter 4, the fixation cross itself provides a potential control source (for example, if used to match curvature by cancelling target drift), so it is reasonable to assume the available cues of retinally-referenced direction and extra-retinal direction may constrain the influence of flow information (Wann & Wilkie, 2004) compared to having visual flow as the sole source of directional information. Therefore, the FISB magnitude in INV_{Rd} represents the 'maximum measurable' reliance on the flow direction signal in these displays. The extent that RE availability diminishes FISB has implications for how flow is weighted against each road segment.

When far road information was added into the scene, FISB did not reduce (Figure 6.6). The far road gives explicit guidance information, but participants are biased by flow information to a similar extent in INV_{Rd}, indicating that the availability of far REs does not negate use of flow any more than the presence of a fixation cross. On its own, this comparison suggests use of flow is not combined with guidance level information: if this was the case one would expect that a stronger guidance signal would result in less reliance on flow. Conversely, FISB magnitude is reduced by approximately half when near road, not far road, is available (N_{Rd}). In this condition, current position can be specified relative to near road edges. The reduced FISB shows that flow information is down-weighted in the presence of near road edges, suggesting that drivers use a near

road edge signal more than a flow signal when both are available. Critically, a similar magnitude of FISB is observed when a full road is available (NMF_{Rd}). Comparing NMF_{Rd} to N_{Rd}, and F_{Rd} to INV_{Rd}, shows that the addition of far road information to either a near road segment (N_{Rd}), or imprecise guidance level information (INV_{Rd}) does not alter the extent that participants rely on flow information. This allows hypotheses H2B and H2C to be rejected. Instead, FISB magnitude is largely related to the presence or absence of the near road component, resulting in a pattern most similar to hypothesis H2A: that flow direction is useful for compensatory control only.

Consistent with some previous research, the presence of near road edges did not completely negate influence of flow (Chatziastros et al., 1999; Kountouriotis et al., 2013; Li & Chen, 2010), strongly suggesting that lane following driver models (e.g. Salvucci & Gray, 2004; Mars et al., 2011) need to include a flow component. More generally, this experiment agrees with work suggesting that the use of flow is predicated on the reliability and availability of other cues in the scene (Warren et al., 2001; Wilkie & Wann, 2002; Wood et al., 2000). In the particular case of lane following, this experiment suggests that perceived direction from flow interacts with near road edges rather than far road edges, suggesting a flow direction signal could be combined with a compensatory RE signal in a weighted manner (Wilkie & Wann, 2002).

These findings can be contrasted with Chapters 3-5, where flow speed was demonstrated to be yoked to the presence or absence of a guidance level control signal. Taken together, Chapters 3-6 suggest that different components of flow map onto different components of steering control as formalised by a two-level steering control framework (Donges, 1978). Critically, it also seems that the nature of how each component (speed or direction) interacts with the respective road component (near or far road) also seems to differ. Flow speed seems to *modulate* a guidance signal, since it does not influence steering when guidance cues are removed. Conversely, Chapter 6 shows that directional information from flow seems to offer redundancy with position-in-lane information from near road edges since flow influences steering to a

greater extent when near road edges are omitted. Chapter 7 will examine this interaction in more detail by systematically degrading the amount of compensatory and guidance level information available in the scene.

CHAPTER 7

EXPLORING THE INTERACTION BETWEEN FLOW DIRECTION AND ROAD EDGES

7.1 Introduction

Chapter 6 examined the extent that steering was influenced by flow direction and whether this varied with road component availability. Crucially it was found that i) flow direction influenced steering to a greater extent when near road edges were absent, and ii) the extent that flow direction influenced steering was not affected by the presence or absence of far road edges. It was concluded, therefore, that a flow direction signal may be combined with near road edges in a weighted manner. This provides the first evidence that flow direction may be able to be incorporated into a two-level framework (put forward by Salvucci & Gray, 2004).

Whilst it is clear that flow direction influences steering, it is unclear how precisely steering is modulated by flow direction. For example, in Chapter 6 the flow direction bias resulted in a ~.07m steering bias when near road was present (NMF_{Rd} and N_{Rd}), and a ~.2m steering bias when near road was absent (INV_{Rd} and F_{Rd}). These values are only ~27% of the manipulated bias to flow direction for INV_{Rd} and F_{Rd}, and only ~9% of induced flow direction bias for NMF_{Rd} and N_{Rd}. It is unclear whether the observed steering bias magnitudes emerge due to the system responding to general impressions of perceived understeering or oversteering, or the system responding precisely to the magnitude of perceived trajectory error. As highlighted in Chapter 5, smooth steering can be modelled with crudely quantized inputs (Wilkie & Wann, 2003a). Chapter 6 only had one magnitude of flow direction bias, therefore it is unclear whether steering corrections were executed based on crude impressions (in which case, observed steering bias may not be yoked to flow direction magnitude manipulations) or precisely related to the magnitude of flow direction bias (whereby one would predict

that observed steering bias would be precisely altered by manipulating flow direction magnitude).

If the visual-motor system responds sensitively to flow direction magnitude it may be expected, in principle, that the observed steering bias would be ~.75m (i.e. 100% of flow direction bias) if flow information was the sole source of information available to control steering. However, the results from Chapter 6 suggest flow direction information is down-weighted by the presence of RE information. It follows that flow information may be down-weighted a little due to the presence of far road information or the fixation cross (causing steering bias to become 27% of the flow direction bias for F_{Rd} and INV_{Rd}), but down-weighted to a greater extent when near road information is present (causing steering bias to become only 9% for NMF_{Rd} and N_{Rd}). If the visual-motor system responds sensitively to flow direction magnitude then doubling the magnitude of flow direction bias would cause the observed steering bias to double, but the magnitude of steering bias would be weighted depending upon the availability of alternative information sources (such as near road information).

A third explanation for the observed steering biases being a relatively low proportion of the manipulated flow direction bias magnitude is that the amount of alternative task-relevant information available sets perceptual 'limits' on the amount of error accruable before steering corrections are executed. Models of general locomotor behaviour have treated obstacles as spring-like repellers (Fajen & Warren, 2003), whereby the penalty given to positional deviation increases the closer one strays to an obstacle. If this model is applied to steering with REs, it follows that a set amount of deviation towards a RE is allowed before some 'threshold' is reached, whereupon corrections occur in order to take position away from the obstacle (or RE). Similarly, some driver models have adopted a 'satisficing' approach, whereby a certain amount of error is acceptable given set boundaries and limits (see Markkula et al., 2014 for an overview of the Gordon & Magnuski, 2006, model). The idea of an 'invisible barrier' which limits the amount of accruable error can be applied to either the 'crude' or

'precise' hypotheses presented above. Chapter 6's results showed a greater reduction in flow influence when the near road is available compared to when only far road is available. This may be explained by the presence of the near road providing greater certainty about position-in-lane therefore imposing stricter limits on accruable error.

To tackle the issue of how flow direction magnitude maps onto steering output, the experimental design of Chapter 6 was expanded to include two extra magnitudes of flow direction bias (±1.5m). For the 'precise' hypothesis, one would predict that the observed steering response magnitude would be proportional to the step-change in flow direction bias magnitude. For the 'crude' hypothesis, similar values of steering response would be predicted for both the .75m and 1.5m flow direction bias magnitudes. Furthermore, if the presence of REs imposes 'limits' to the amount of accruable error, tighter limits may be imposed by near road edges compared to far road edges. Therefore, there may be little observable differences in steering response between 'crude' and 'precise' approaches when the near road is available (because the tight limits may prohibit a 1.5m flow direction magnitude biasing steering any further than a .75m flow direction magnitude), but differences would emerge when limits are relaxed (by removing near road edges).

Another outstanding issue is that it is unclear how the use of flow direction may be affected by a degraded compensatory signal. The current Chapter tackles this issue by using all 8 road combinations used in Chapter 5 – NMF_{Rd}, N_{Rd}, M_{Rd}, F_{Rd}, NM_{Rd}, MF_{Rd}, NF_{Rd}, and INV_{Rd} – to allow systematic investigation of how anticipatory and compensatory signals are combined in the presence of a biased flow direction signal. Chapter 6's results showed diminished FISB for conditions with a near road component present, and enhanced FISB when near road was absent. Near road provides explicit position-in-lane information, therefore can be thought of as a 'strong' compensatory signal. The mid road component still provides some position-in-lane information, but this information is more uncertain than that provided by near road so can be thought of as a 'weak' compensatory signal. It is unclear how the use of flow

direction would be affected by a degraded compensatory signal (i.e. if near road is removed but mid road remains). For example, there may a minimum amount of compensatory RE signal required for flow to be down-weighted. This 'threshold' may be reached by the mid road component, in which case FISB would decrease only whenever position-in-lane information (both the near and mid road components) is present, or the threshold may only be reached by the presence of near road signal information, in which case FISB would decrease only when the near road component was present. Alternatively, FISB may decrease or increase based on how strong or weak the compensatory signal is. If this is the case, a step increase in FISB would be observed when near road is removed and then again when mid road is removed.

7.2 Methods

7.2.1 Participants

20 participants (15 females, 5 males, ages 19 to 28, mean 20.3yrs), all having normal or corrected-to-normal vision, took part the experiment. None of these participants took part in any other experiments. 19 participants held driving licenses (average time since test=2.6yrs), the remaining participant was included in the analysis because their steering behaviour was not different to the rest of the group. All participants gave informed consent and the studies was approved by the University of Leeds, School of Psychology Research Ethics Committee (Ref 14-0225), and complied with all guidelines as set out in the declaration of Helsinki.

7.2.2 Stimuli

The same flow manipulation as Chapter 6 was used (see Figure 6.2). In Chapter 6, three flow levels were used: IN_F, VE_F, and OUT_F. The magnitude of the added horizontal texture motion was .75ms^{-1}. In the current Chapter, two additional levels are added at 1.5ms^{-1} (which is 100% of the inherent horizontal motion in the scene, given a middle-of-the-road trajectory). These are denoted IN_{100}, IN_{50}, VE_F, OUT_{50}, and

OUT_{100}. The flow strengths used in Chapter 6 are identical to IN_{50} and OUT_{50}. The road manipulations are as Chapter 5 (see Figure 5.1). Additionally, road manipulations did not impact on refresh rate (which was consistent at 60Hz).

7.2.3 Procedure

The procedure was similar to Chapter 5. All participants received the same written instructions, to 'attempt to steer a central trajectory, keeping to the middle of the road', to steer 'as smoothly and as accurately as you can', to 'centre the wheel after each trial', and to 'fixate on the fixation cross'. Participants completed 20 practice trials (2 minutes) of veridical flow, starting with four complete road trials and then being exposed to each road conditions for both left and right bends. There were six trials in each condition, each six seconds long, resulting in an experiment running time of 24 minutes. A brief (un-timed) rest break was inserted at the half-way point to alleviate fatigue.

7.2.4 Analysis

Throughout Chapters 2-6 the steering measures of SB (positional error), RMSE (quadratic deviation from the midline), and SWJ (steering smoothness) have been used to quantitatively capture steering behaviour – these measures are also used for the current experiment. Throughout Chapters 3-6 an additional metric, FISB, has been used to capture the extent flow influences steering in a single value to facilitate comparison across road conditions. Chapters 3, 4, and 6 had two experimental flow manipulations (excluding the control condition where flow was kept veridical), both predicting opposite directional effects. Therefore, the amount of positional change observed in either direction could be approximated by the simple formula $(FL_x - FL_y)/2$. Chapter 5 used an expanded design, with four experimental flow manipulations, allowing a more sophisticated FISB metric was calculated (section 5.2.4). The appropriateness of various fitting methods was assessed before settling on a logarithmic transform of weighted linear regression. A logarithmic transform was

investigated due to evidence suggesting that flow speed is perceived according to Weber's Law (Authié & Mestre, 2012) and also an experimenter observation that the magnitude of steering position change appeared to alter logarithmically across flow manipulations. There was no evidence suggest a similar transform might be appropriate in the current Chapter. Instead, a linear weighted regression (Equation 5.1) is compared to a simple linear fit (Figure 7.1). Although performing a weighted regression reduces the R^2 (compared to a standard linear fit) in three out of eight road conditions (NM_{Rd}, M_{Rd}, and INV_{Rd}; Figure 7.1), this reduction is small (on average, only reducing explained variance by 1.6%), and for the majority of road conditions a weighted linear fit increases R^2 (on average, increasing explained variance by 11.1%). Therefore, the β1 estimate from a weighted linear fit was taken as the FISB score.

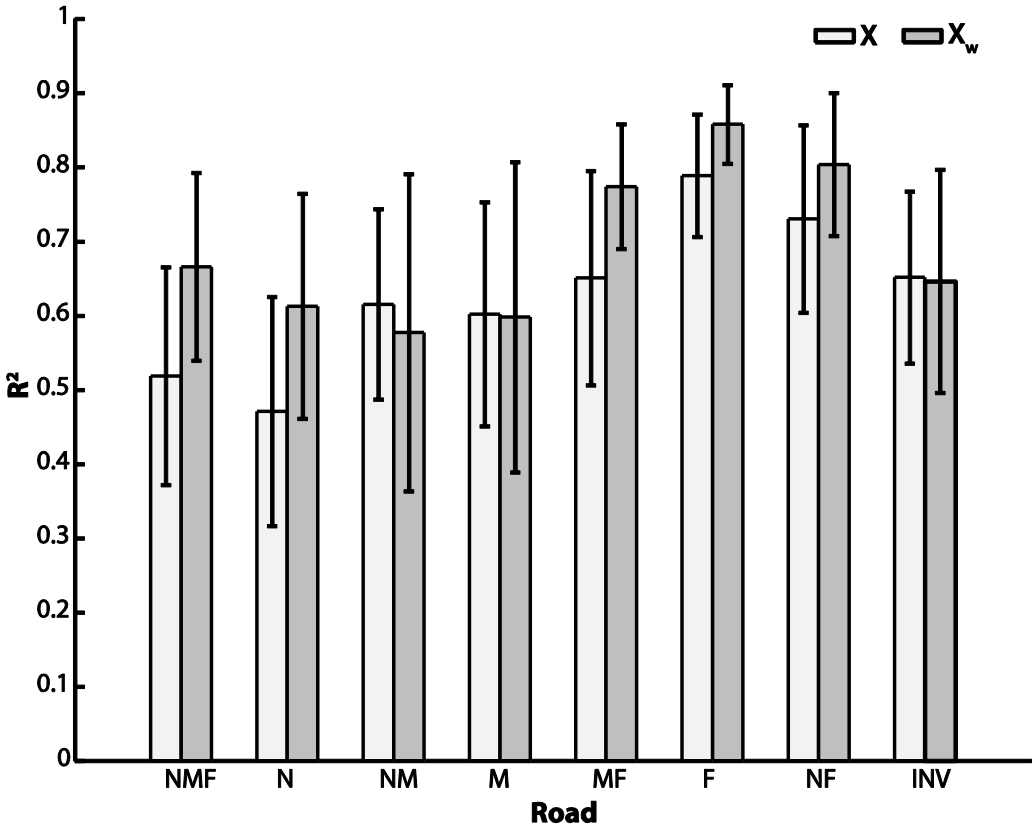

Figure 7.1 R^2 estimates are calculated per person, per condition, then averaged. The graph compares average explained variance for a 1) linear fit, and 2) a weighted linear fit. Error bars represent 95% CIs.

It is important to note that there was no formal threshold for defining an 'acceptable' R^2 value, and the amount of variance explained by FISB varies depending on road condition – ranging from 58% for NM_{Rd} and 86% for F_{Rd}. A similar range of values were observed in Chapter 5 (Figure 5.3). The capacity of a weighted linear fit to capture the spread of flow levels is in part determined by how evenly distributed the steering response is across flow manipulations. For example, the highest R^2 is for F_{Rd}, which (as shall be discussed later) is also the condition where steering response is most precisely and evenly modulated by flow direction (see Figure 7.10G). As highlighted in Chapter 5, although the FISB may be an imprecise metric for capturing the extent of flow influence it remains useful for facilitating comparison across road conditions if used in collaboration with other methods of capturing steering behaviour (e.g. quantitative

steering measures: SB, RMSE, and SWJ; and analysing trajectory development through averaged trajectories).

7.3 Results

Steering measures (SB, RMSE, and SWJ) and derived measures (FISB) are reported before averaged trajectory plots (similar to those presented in Chapters 2 & 5) are discussed in light of the steering measures. For each factor (Road and Flow) trends in the data will be presented through paired difference estimates relative to the control condition, with the precision of each estimated captured with 95% CIs (see Chapter 2 for validation of this approach).

7.3.1 Steering Bias

Figure 7.4A shows average positional bias for every flow level, across road conditions. Similar to Chapter 6, there was a trend to oversteering for inward translation of the ground texture (IN_{100} and IN_{50}), and to understeering for outward translation (OUT_{100} and OUT_{50}). However, it is also clear that the extent participants responded to flow manipulations varied between road visibility conditions. Figure 7.2 examines this in more detail by plotting the paired differences of each flow level relative to the control (VE_F), for every road level.

For the control condition, NMF_{Rd} (Figure 7.2A), adding inward motion caused marginal understeering of ~1.1%RW for IN_{50} (M_{diff}=.032m [-.028, .09], SEM=.029) and ~1.8%RW for IN_{100} (M_{diff}=.053m [-.027, .13], SEM=.038). Adding outward motion caused a slightly larger and opposite shift, in the direction of understeering, of ~3.2%RW for OUT_{50} (M_{diff}=-.095m [-.17, -.02], SEM=.037), which increased marginally to -4.8%RW (M_{diff}=-.14m [-.17, -.02], SEM=.03). The magnitude of SB change in response to adding inward motion (IN_{50} and IN_{100}) is smaller than adding outward motion (OUT_{50} and OUT_{100}). The same is true for NM_{Rd} (Figure 7.2C) where both the IN_{50} and IN_{100} paired differences to VE_F sit around .04m, whereas OUT_{50} –

VE_F sits at -.1m ([-.185, -.021], SEM=.023) and OUT_{100}- VE_F sits at -.14m ([-.19, -.08], SEM=.027). Similar (low) magnitudes of steering response to flow manipulations are observed in N_{Rd} (Figure 7.2B).

Whilst similar levels of understeering for OUT_{50} and OUT_{100} (as observed in NMF_{Rd} and NM_{Rd}) are also observed for M_{Rd}, MF_{Rd}, and NF_{Rd} (Figure 7.2D, E, & G), in the latter conditions there is a greater oversteering response to inward flow. Across all three conditions, the positional change induced by IN_{50} is ~.1m, and for IN_{100} it is ~.15m. When only the far road segment is visible (F_{Rd}), the steering response is larger still (Figure 7.2F). Participants exhibited oversteering by 6.6%RW for IN_{50} (M_{diff}=.2m, [.095, .3], SEM=.05) and 9.4%RW for IN_{100} (M_{diff}=.28m [.15, .41], SEM=.06). Participants exhibited understeering by 4.3%RW for OUT_{50} (M_{diff}=-.13m [-.21, -.051], SEM=.04) and by 8.6%RW for OUT_{100} (M_{diff}=-.26m [-.36, -.16], SEM=.04). Consistent with previous Chapters, INV_{Rd} (Figure 7.2G) caused the largest, and most variable, steering response to flow manipulations.

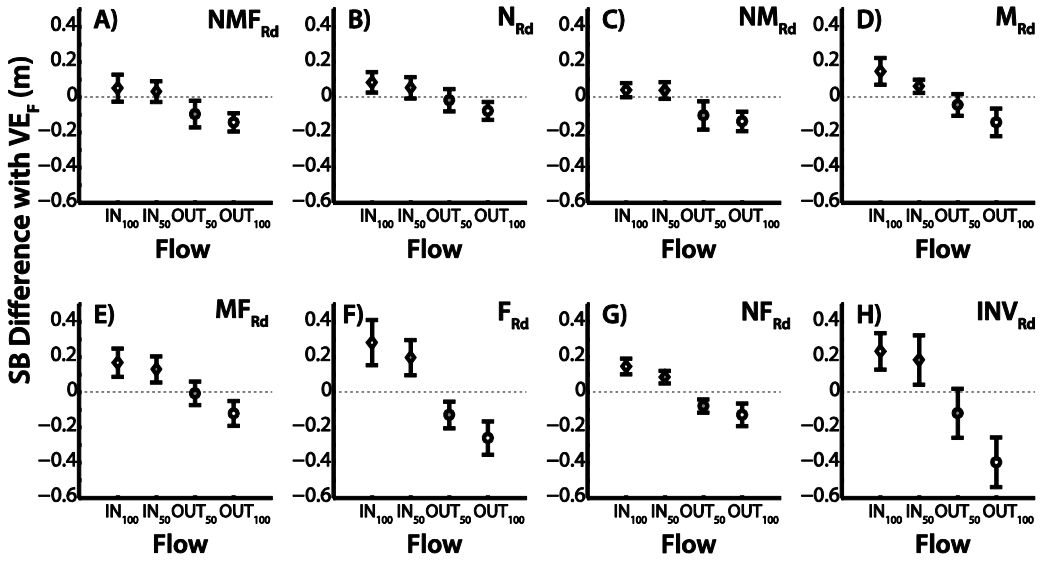

Figure 7.2 SB difference between the mean plots for comparisons across Flow levels for reach Road Level. Each point represents the paired difference between that particular Flow level and VE_F, the control condition. For all graphs a negative magnitudes indicates steering closer towards the outside edge of the bend than in VE_F, and a positive magnitude indicates steering closer to the inside edge. Error bars are 95% confidence intervals.

Figure 7.3 examines changes in SB due to changes in visible road components, within each level of flow. Under veridical flow conditions (VE_F; Figure 7.3C), removing road segments generally caused understeering (similar to Chapter 5), although to different extents according to which road segments are available. The smallest levels of understeering are observed in NM_{Rd} (which sits around zero), F_{Rd}, and NF_{Rd}. For NM_{Rd} and NF_{Rd}, the trend is fairly consistent throughout flow conditions, as the magnitude of the paired difference estimates sit within .035m for NM_{Rd} and .065m for NF_{Rd} for all flow conditions. However, the paired difference estimate of F_{Rd} – NMF_{Rd} varies between flow levels. F_{Rd} is the only road condition to produce noteworthy oversteering compared to NMF_{Rd}, in IN_{50} (M_{diff}=.11m [.06, .17], SEM=.027) and IN_{100} (M_{diff}=.18m, [.095, .26], SEM=.04). All other road conditions (N_{Rd}, M_{Rd}, and MF_{Rd}) tend to have caused understeering. Although there are slight fluctuations between flow levels, all magnitudes are within -.15m. INV_{Rd} is, again, the most variable, and causes the largest

positional change. Whilst the paired difference INV_{Rd} – NMF_{Rd} sits around zero in IN_{50} and IN_{100} (Figure 7.3A-B), removing road edges causes the largest understeering with each flow level for veridical flow (M_{diff}=-.19m [-.33, -.045], SEM=.07), for OUT_{50} (M_{diff}=-.21m [-.37, -.05], SEM=.08), and for OUT_{100} (M_{diff}=-.44m [-.63, -.26], SEM=.09).

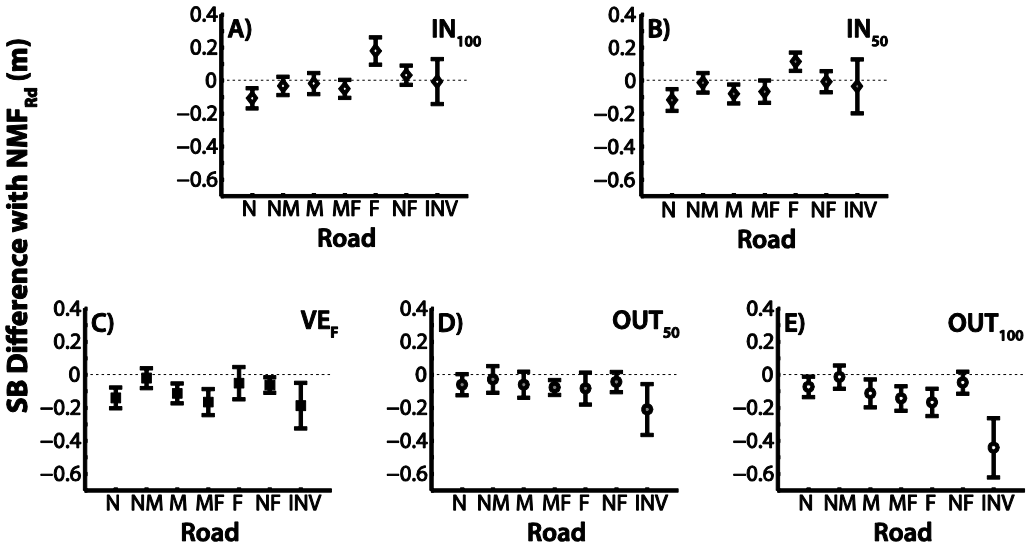

Figure 7.3 SB difference between the mean plots for comparisons across Road levels for reach Flow Level. Each point represents the paired difference between that particular Road level and NMF_{Rd}, the control condition. For all graphs a negative magnitudes indicates steering closer towards the outside edge of the bend than in NMF_{Rd}, and a positive magnitude indicates steering closer to the inside edge. Error bars are 95% confidence intervals.

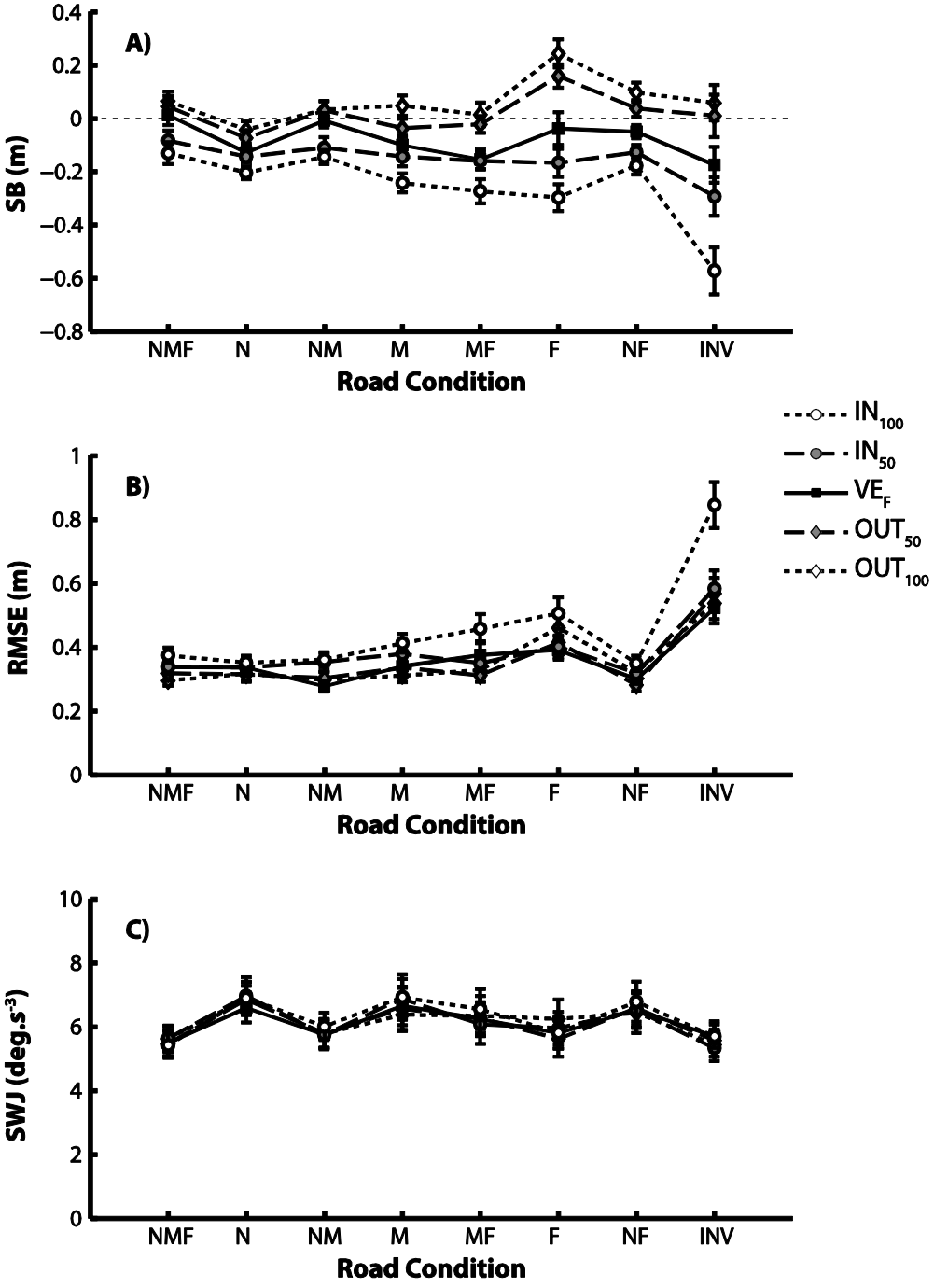

Figure 7.4 All steering performance measures across IN_{100} (empty circles, finely dashed line), IN_{50} (grey circles, thickly dashed line), VE_F (filled squares, solid line), OUT_{50} (grey diamonds, thickly dashed line), and OUT_{100} (empty diamonds, finely dashed line), showing A) Steering Bias, B) Root-mean-squared error, and C) Steering Wheel Jerk. Error bars represent standard error of the mean (SEM).

7.3.2 FISB

FISB provides a single value the captures the extent that flow manipulations influenced steering bias. As with Chapter 6, a positive FISB indicates oversteering for inward flow, and understeering for outward flow. Figure 7.5A displays average FISB scores for each road condition. For every road condition, FISB is positive, indicating flow influenced steering in all conditions. However, FISB magnitude varies between conditions. The lowest FISBs are observed in when compensatory ('near' and 'mid' road) but not guidance ('far' road) RE information is available: N_{Rd} (M=.16 [.09, .24], SEM=.04) and NM_{Rd} (M=.18 [.1, .33], SEM=.04). Alternatively, the highest FISBs are observed when only guidance RE information (F_{Rd}; M=.56 [.42, .69], SEM=.065) or no RE information (INV_{Rd}; M=.62 [.45, .8], SEM=.08) is available.

Figure 7.5B examines how consistent the differences between road conditions are, across participants, by showing paired differences of each road condition compared to NMF_{Rd} and constructing 95% CIs around this estimate. It is clear that F_{Rd} and INV_{Rd} have consistently larger FISB than NMF_{Rd}, although the magnitude is variable for INV_{Rd}, indicating that participants were variable in the extent they responded to flow in INV_{Rd}. The paired differences for all remaining conditions are close to zero, indicated by the 95% CI incorporating zero in N_{Rd}, NM_{Rd}, M_{Rd}, MF_{Rd}, and NF_{Rd} which suggests that for some participants FISB was fairly equal between NMF_{Rd} and these conditions. For N_{Rd} (M_{diff} =-.06 [-.13, .02], SEM= .04) and NM_{Rd} (M_{diff}=-.05 [-.14, .05], SEM=.05), the paired difference suggests FISB was consistently, but only slightly, smaller than for NMF_{Rd}. The paired differences for M_{Rd}, MF_{Rd} and NF_{Rd} were of a similar but opposite magnitude, suggesting a small increase in FISB (compared to NMF_{Rd}) of ~.5.

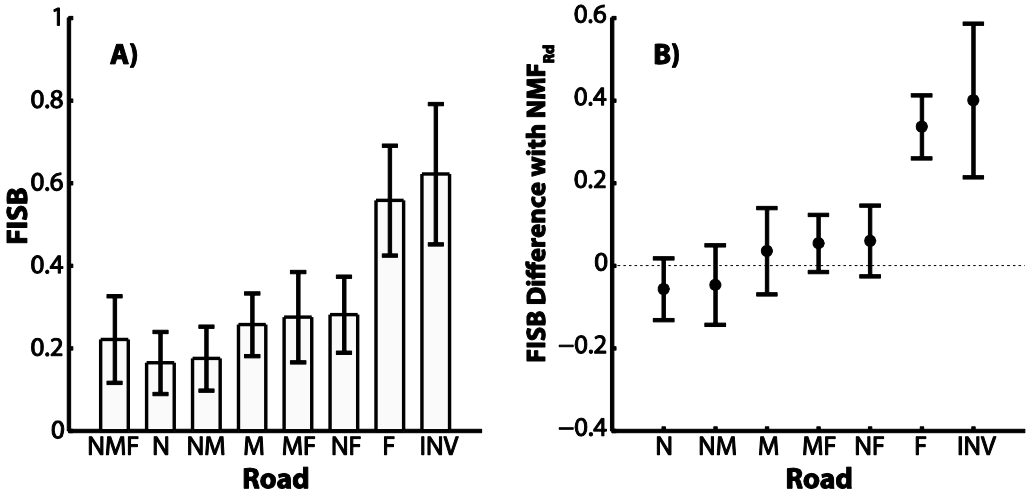

Figure 7.5 A) Average FISB scores for each road condition. B) Paired difference plots between each Road level and NMF_{Rd}. Road conditions are ordered in terms of magnitude. Note that the order of NF_{Rd} and F_{Rd} has been switched in comparison to the other graphs presented in this Chapter – this was done in order better observe trends. Error bars are 95% Confidence Intervals.

7.3.3 RMSE

Figure 7.4B shows average RMSE scores, which demonstrate deviation from the midline. Across all flow levels, RMSE for NMF_{Rd} is .33m ([.3, .36], SEM=.015). The only road conditions were there are clear changes to this 'baseline' error is F_{Rd} (M=.43m [.38, .49], SEM=.025) and INV_{Rd} (M=.61m [.52, .7], SEM=.04), where RMSE is increased. Broadly, there does not seem to be many differences between flow levels, with the exception of OUT_{100}, which generally sits 'above' the other lines, indicating increased error in this condition compare to the other flow levels.

Consistent changes across flow conditions are examined in Figure 7.6. OUT_{100} is the only flow level to cause substantial differences in error across a number of road conditions. In NM_{Rd}, M_{Rd}, and MF_{Rd}, the OUT_{100} - VE_F paired difference sits around ~.8m. For F_{Rd} this paired difference increases slightly in magnitude, but becomes more variable (M_{diff}=.11m [.01, .22], SEM=.05), and for INV_{Rd} the OUT_{100} – VE_F paired difference is the largest, sitting around .32m ([.2, .45], SEM=. 06). The other flow levels

(OUT_{50}, IN_{50}, and IN_{100}) tend to sit fairly close to zero, and all paired difference estimates are <.1m in magnitude.

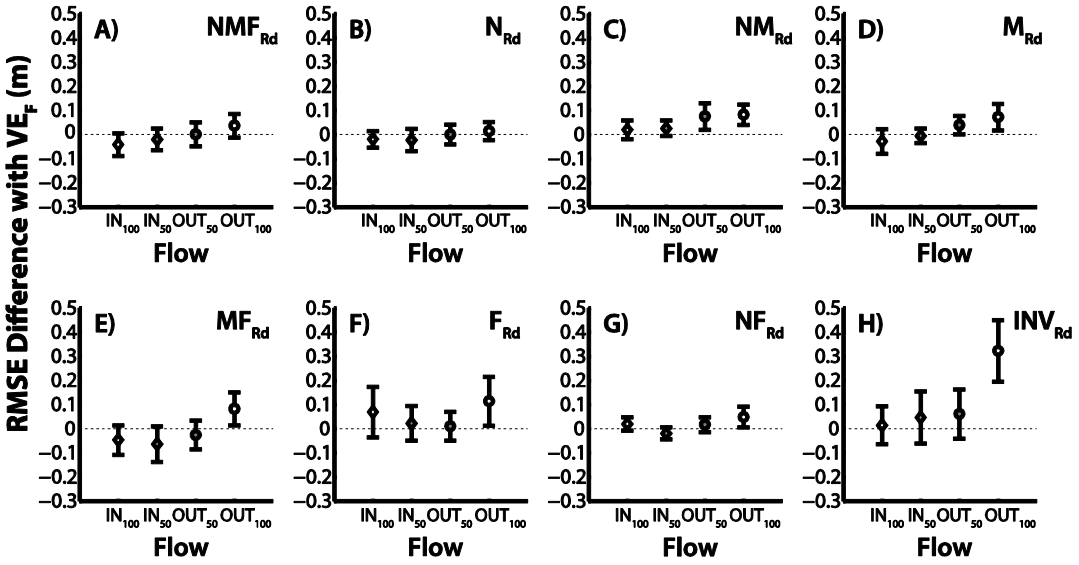

Figure 7.6 RMSE difference between the mean plots for comparisons across Flow levels for reach Road Level. Each point represents the paired difference between that particular Flow level and VE_F, the control condition. For all graphs a negative magnitude indicates less deviation from the midline of the bend than in VE_F, and a positive magnitude indicates greater deviation from the midline. Error bars are 95% confidence intervals.

Consistent changes across road levels are examined in Figure 7.7. Generally, removing road segments did not increase or decrease error, as long as the mid road or near road segment was visible, as shown by the paired difference estimates, compared to NMF_{Rd}, of NRd, NM_{Rd}, M_{Rd}, MF_{Rd}, and NF_{Rd}. For these road conditions, the only consistent differences are a small decrease in error for NM_{Rd} in VE_F (Figure 7.7C; M_{diff}=-.06m [-.1, -.02], SEM=.02), and a small increase in error for MF_{Rd} in OUT_{100} (Figure 7.7E; M_{diff}=.08m [-.01, .16], SEM=.04). When only far road is available, error is increased throughout all flow levels, ranging from a small magnitude in VE_F (Figure 7.7C; M_{diff}=.05m [-.01, .12], SEM=.03) to a larger magnitude in IN_{100} (Figure 7.7A; M_{diff}=.17m [.08, .25], SEM=.04). As with the previous measures of SB and FISB, removing all road edges consistently caused the largest (and most variable) magnitude of steering

response. The largest of which is observable in OUT_{100} (Figure 7.7E; M_{diff}=.47m [.34, .6], SEM=.06).

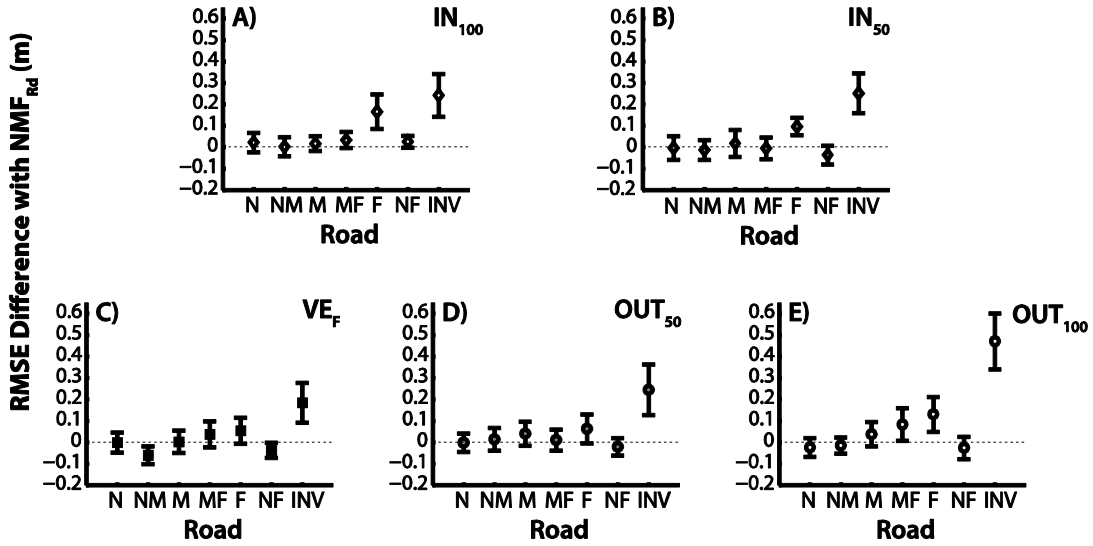

Figure 7.7 RMSE difference between the mean plots for comparisons across Road levels for reach Flow Level. Each point represents the paired difference between that particular Road level and NMF_{Rd}, the control condition. For all graphs a negative magnitudes indicates less deviation from the midline of the bend than in VE_F, and a positive magnitude indicates greater deviation from the midline. Error bars are 95% confidence intervals.

7.3.4 SWJ

Figure 7.4C shows average SWJ scores, which can be used as a proxy for steering smoothness. There is considerable overlap between the lines representing changes in flow levels, suggesting that adding a ground texture shift did not alter steering smoothness. Conversely, SWJ clearly fluctuates depending on road segment availability.

Figure 7.8 examines how steering smoothness was affected by manipulation flow direction. As suggested by Figure 7.4C, there are no systematic alterations in steering smoothness due to flow. Generally, the paired differences (compared to VE_F) sit

around zero. The maximum magnitude of the paired difference estimates is .44deg.s^{-3} (IN_{100} – VE_F for F_{Rd}; Figure 7.8F), which is very small.

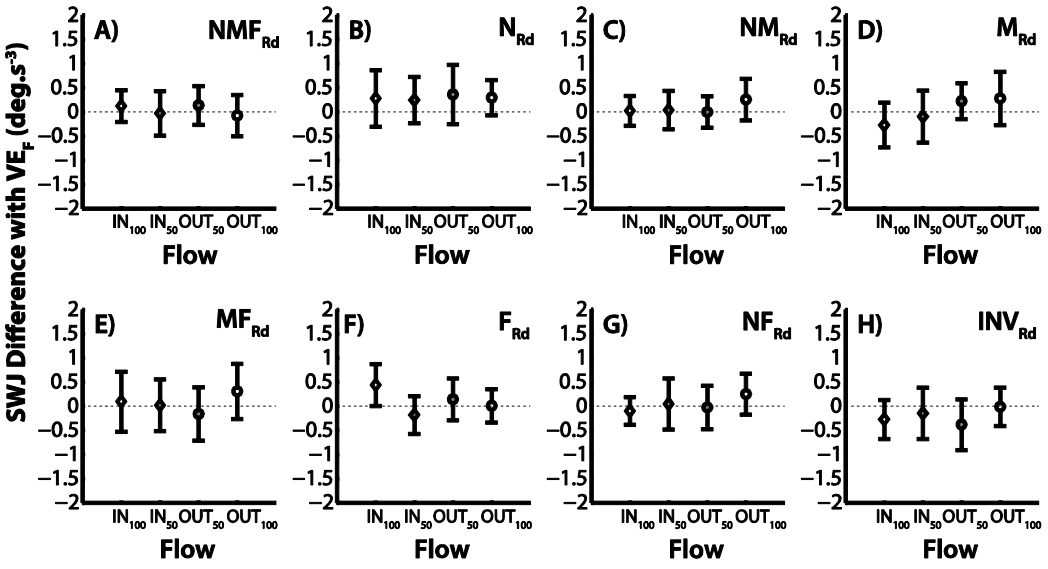

Figure 7.8 SWJ difference between the mean plots for comparisons across Flow levels for reach Road Level. Each point represents the paired difference between that particular Flow level and VE_F, the control condition. For all graphs a positive magnitude indicates more steering corrections than in FL_1. Error bars are 95% confidence intervals.

Figure 7.9 examines changes in steering smoothness according to road segment availability. Under veridical flow (Figure 7.9C) removing any road segment increases flow, but to different extents. The largest is seen in N_{Rd}, M_{Rd}, and NF_{Rd}, which all caused SWJ to increase by ~1.1deg.s^{-3} compared to NMF_{Rd}; MF_{Rd} caused an SWJ increase of ~.75deg.s^{-3} ([.24, 1.25], SEM=.24); the smallest increases are observed in NM_{Rd}, F_{Rd}, and INV_{Rd}, which have paired difference magnitudes of ~.25deg.s^{-3}. Whilst the magnitude and variability of these differences fluctuates slightly when a flow is manipulated (generally increasing rather than decreasing), the broad pattern remains the same.

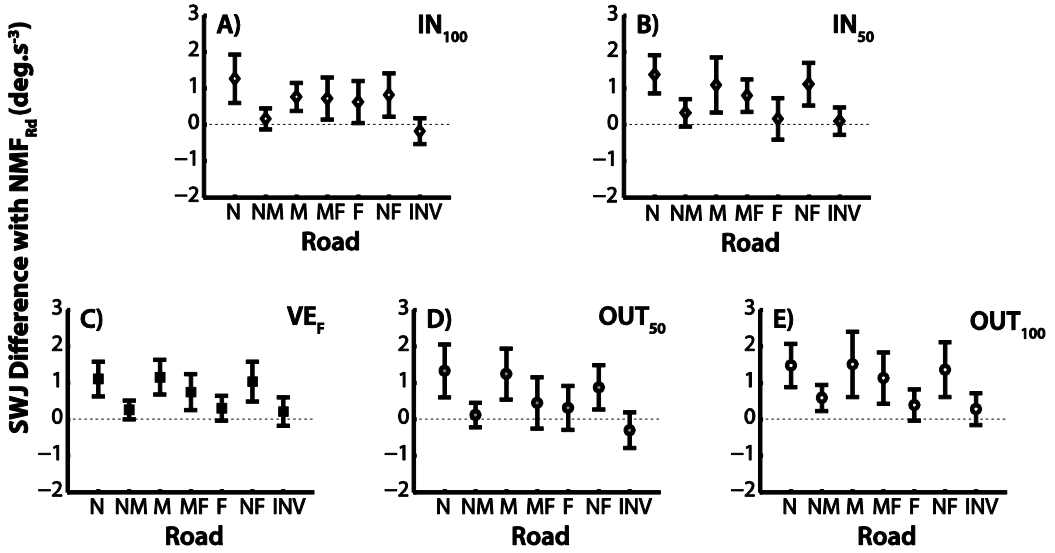

Figure 7.9 SWJ difference between the mean plots for comparisons across Road levels for each Flow Level. Each point represents the paired difference between that particular Road level and NMF_{Rd}, the control condition. For all graphs a positive magnitude indicates more steering corrections than in NMF_{Rd}. Error bars are 95% confidence intervals.

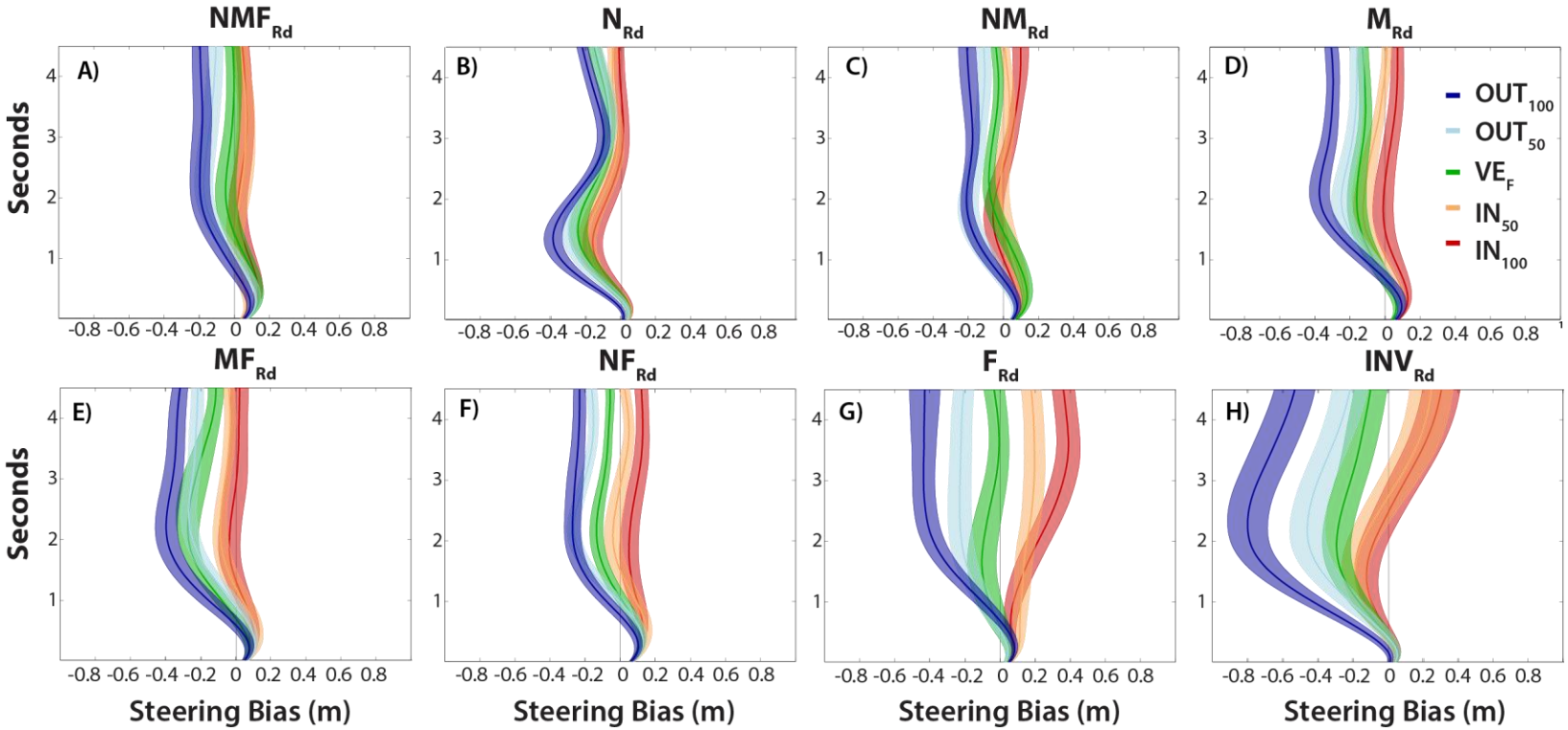

Figure 7.10 Average Trajectory plots showing Steering Bias over the course of a trial for all participants, with shaded bounds representing standard error of the mean. Plots are creating by averaging each Frame per participant, then averaging across participants and using this variability for the shaded error bounds. Plots are shown from the start of the bend. Blue shades indicate Faster-than-veridical flow, and red shades indicate Slower-than-veridical Flow. Note that the order of road conditions is identical to Figure 7.5.

7.3.5 Analysing Trajectory Development

Plotting averaged trajectories is a technique used throughout this thesis (see sections 2.3.3 & 5.3.5) in order to develop a qualitative appreciation of steering behaviours. Figure 7.10 shows averaged steering bias throughout a trial for the current experiment, with shaded error bounds indicating inter-individual variability for that particular frame.

The control condition is shown in Figure 7.10A. Regardless of flow manipulation, drivers entered the bend oversteering. Under veridical flow conditions (shaded green) the driver corrects for this initial error quickly, but overshoots, resulting in understeering at ~2s into the trial. Over time, the trajectory settles close to the midline. Due to the driver spending some time either side of the midline, bias is negligible (Figure 7.4A), but RMSE is not (Figure 7.4B). Shifting the ground texture towards the inside of the bend reduces the size of the correction for the initial oversteering, which causes oversteering to persist throughout the course of the trial. Although the changes in bias (Figure 7.2A) and RMSE (Figure 7.6A) are very small, Figure 7.10A demonstrates that these minor changes are a result of a consistent offset throughout the course of a trial. There is considerable overlap between IN_{50} (orange) and IN_{100} (red), suggesting that when a complete road is available increasing flow magnitude from IN_{50} to IN_{100} does not cause any additional shift in bias.

On the other hand, outward translation causes drivers to overcompensate for initial oversteering. Understeering develops gradually until ~.2s, at which time understeering plateaus. For OUT_{100} (blue), understeering error is not corrected for and persists, whereas for OUT_{50} position is brought slightly closer to the midline. The marginal difference in bias (Figure 7.4A) between OUT_{100} and OUT_{50} therefore emerges due to differences in the later stage of the bend. It is worth highlighting that despite differences in steering behaviour the flow manipulations did not affect steering smoothness (Figure 7.8A), suggesting that participants did not increase steering

corrections when biased due to flow (which may explain why errors persist once developed).

When the near road component is removed (MF_{Rd}) there are some clear differences in trajectory development (Figure 7.10E) compared to NMF_{Rd} (Figure 7.10A). For VE_F, OUT_{50} and OUT_{100}, understeering develops more rapidly during MF_{Rd} than in NMF_{Rd} (Figure 7.10A), so that although 'maximum' error is reached at roughly the same point (~2s) the magnitude of understeering is greater. At this point levels of understeering in both OUT_{50} and OUT_{100} keeps constant throughout the remainder of the trial, whilst VE_F is gradually brought closer to the midline, resulting in a clear dichotomy between flow conditions in the latter stage of the trajectory (but large overlap at early stages) which is reflected in the bias scores (Figure 7.2E). The steering response to IN_{50} and IN_{100} is similar to that observed for these flow levels in NMF_{Rd}: there is considerable overlap between the two conditions, and they both sit close to the midline. Although inward flow produces oversteering relative to the other flow manipulations, Figure 7.10E shows that this does not mean that drivers maintain an oversteering position throughout the course of the trial, rather they simply exhibit less understeering (Figure 7.4A). As with NMF_{Rd} these differences between flow conditions are not accompanied by changes in steering smoothness (Figure 7.8E)

Removing the near road segment increases uncertainty of position-in-lane, which seems to be reflected in greater variability between participants (shown by larger error bounds in Figure 7.10E compared to Figure 7.10A). Even greater variability than MF_{RD} is observed for F_{Rd} (Figure 7.10G), suggesting that the additional removal of the mid road component compounds position-in-lane uncertainty, leading to more variable trajectories. Crucially, the additional removal of the mid road component also increases the extent steering is biased by flow direction. Although initial oversteering is present with all flow manipulations, differences quickly develop. Whilst VE_F stays relatively close to the midline, the understeering-inducing effect of OUT_{50} and OUT_{100} (observed throughout all plots) is accentuated. Understeering develops rapidly and

persists once developed, for both OUT_{50} and OUT_{100} (as with MF_{Rd} and NMF_{Rd}). Critically, inward flow causes substantial oversteering, which gradually develops and plateaus late in the trajectory. The clear dichotomy between flow manipulations demonstrates that the high FISB in this condition reflects systematic, linear differences (see Figure 7.). It is worth comparing this to NMF_{Rd} and MF_{Rd}, who both had lower explained variance (Figure 7.). This is due to similar steering behaviour in IN_{50} and IN_{100}.

Variability is highest when there is no road edge information (INV_{Rd}; Figure 7.10H). As with Chapter 5, participants do not enter the bend in an oversteering position and understeering develops rapidly in every flow manipulation, causing the condition to be characterised by high RMSE in every flow condition (Figure 7.7). For IN_{50} and IN_{100}, the understeering is brought towards the midline relatively early (~.75s), eventually resulting in oversteering. With OUT_{100}, however, steering is brought towards the midline later (~2.25s), resulting in a trajectory with uniquely high levels of understeering and RMSE. Despite the high levels of RMSE, there is not an accompanying increase in steering corrections (Figure 7.9), which is consistent with Chapter 5's results. It is clear that despite the similar FISB, there are substantial qualitative differences between F_{Rd} and INV_{Rd}.

Removing the far road component (NM_{Rd}; Figure 7.10C) does not seem to alter the trajectories observed in NMF_{Rd} (Figure 7.10A) as drastically as removing near road information. Steering behaviour seems remarkably similar to NMF_{Rd}. Although characterised by an increase in understeering that is consistent throughout flow levels, the magnitude of this increase is very small (Figure 7.3). Similarly, removing far road increases jerkiness (which is characteristic of a switch to compensatory control) only a little (Figure 7.9), and does not increase RMSE (Figure 7.7). This suggests that mid road may provide enough guidance level information to supplement the removal of the far road component.

However, when the mid road component is removed (N_{Rd}; Figure 7.10B) trajectories take on a unique profile, similar to that observed in Figure 5.12A. Understeering develops rapidly upon entering the bend, which is consistent with a lack of preview (compare with INV_{Rd}; Figure 7.10H). However, the understeering does not persist, as is the case in other conditions; instead, the trajectory returns towards the midline. This 'inflection-point', where error ceases to build, happens at ~1.25s into the bend which is early then the ~2s observed for other road conditions. Interestingly, understeering begins to develop again later on in the trajectory for VE_F, OUT_{50}, and OUT_{100}, resulting in a unique 'snake-like' trajectory that results in low RMSE (Figure 7.7) at the expense of high jerk (Figure 7.9).

According to Land & Horwood (1995), adding a far road component to the near road (NF_{Rd}; Figure 7.10F) would result in similar behaviour to a complete road. However, the trajectory development for NF_{Rd} is more evenly separated between flow levels than in NMF_{Rd} (whilst this only results in a marginally higher FISB it means that the FISB metric explains more of the variance of the data; Figure 7.). Instead, the trajectory development in NF_{Rd} is similar to M_{Rd} (Figure 7.10D). These two conditions also share comparable SWJ scores (Figure 7.4C), which is increased relative to NMF_{Rd} (Figure 7.9). The observation that NF_{Rd} and M_{Rd} share qualitative similarities in steering behaviour is consistent with results reported in Chapter 5 (see Figures 5.12C & D).

To summarise, Figure 7.10 demonstrates that the removal of compensatory information is linked with more variable trajectories and a greater influence of flow direction, which is particularly observable in the latter stages of the trajectory. Despite the sometimes striking error caused by flow direction (for example, F_{Rd} - Figure 7.10G), this does not seem to be accompanied by an increase in steering corrections. There is considerable similarity in steering behaviour between conditions NM_{Rd}, NF_{Rd}, M_{Rd}, MF_{Rd}, and NMF_{Rd}, showing that the visual-motor system is flexible and can cope with degraded (but not removed) compensatory or anticipatory input (note that the mid road component provides weakly informative compensatory and anticipatory

information). Only in the extreme cases, where either source of information is completely removed (N_{Rd}, F_{Rd}, and INV_{Rd}), steering profiles develop unique characteristics.

7.5 Discussion

The current experiment examined the hypothesis that flow direction competes with a compensatory signal to inform two-level steering control. The results largely support this hypothesis. FISB was least in road conditions where the guidance level information was weak but compensatory information was strong (N_{Rd} and NM_{Rd}). Crucially, adding extra guidance signal (via the mid or far road) did not result in substantial increases to FISB, as long as position-in-lane information was provided by the near road (strongly informative), or mid road (weakly informative). FISB substantially increased (more than doubled) only when *all* position-in-lane road edge information was removed (in F_{Rd} and INV_{Rd}). These trends strongly support the hypothesis that flow direction is combined with a compensatory signal in a weighted combination manner. This discussion will first examine the evidence the current Chapter provides for how flow direction is incorporated into steering control, before examining the strength of the evidence across both Chapters 6 & 7, and finally the more general implications for two-level steering control will be discussed.

When no REs are present (INV_{Rd}) participants exhibit large biases due to flow. Consistent with Chapter 6, this does not substantially diminish when far road edges are present (F_{Rd} FISB is estimated to be around 90% of INV_{Rd} FISB), demonstrating that the presence of explicit path information provided by far road edges does not markedly negate flow use. This suggests that steering using predominantly guidance level information can incorporate flow direction as an input, and that the use of flow direction is independent of the amount of guidance level information present in the scene. Conversely, adding the 'mid' road component to either INV_{Rd} or F_{Rd} (M_{Rd} or MF_{Rd}) approximately halves FISB magnitude. The mid road is weakly informative

about position-in-lane, suggesting that providing some information about immediate position via road edges noticeably negates use of flow. When a strong position-in-lane signal provided by near road edges is added to guidance level information (NF_{Rd}, NMF_{Rd}), FISB is not negated further than when drivers have a weakly informative signal (M_{Rd} and MF_{Rd}). It is only when the far road information is removed, thus the task becomes predominantly a compensatory task, that FISB is reduced further, dropping by approximately another ~30%.

The reduction in FISB when near or mid road is added is large (Figure 7.5B), leaving little doubt that near or mid road avaiability reduces FISB. However, the reduction in FISB when far road is removed is small and 95% CIs bracket zero (Figure 7.5B) resulting in uncertainty about the directionality and magnitude of the error. Additionally, it has been conceded that FISB is an imprecise measure (Figure 7.1), adding further uncertainty to whether a reduction in FISB with the removal of far road is reliable. Since the experimental design had two separate flow magnitudes (IN_{50} and IN_{100}), an alternative method of assessing the extent of flow influence in a given road condition would be to use the formula used in Chapters 3, 4, and 5 – $(IN_x - OUT_x)/2$ – to calculate a FISB for each flow magnitude. These two estimates can then be combined via meta-analytic estimation, which will result in one FISB estimate for each road condition (per participant) which incorporates the extent flow caused changes in steering bias across both flow magnitudes. This can be used to compare with the FISB obtained through fitting a weighted linear model in section 7.3.2 (to avoid confusion, the FISB obtained through meta-analytic methods will be referred to as $FISB_{MA}$ and the FISB obtained through weighted linear regression will be referred to as $FISB_{WL}$). The group averages of the meta-analysis are shown in Figure 7.11A. Importantly, the pattern is remarkably similar to the $FISB_{WL}$ values shown in Figure 7.5A – $FISB_{MA}$ is largest for F_{Rd} and INV_{Rd}, and lowest for N_{Rd}. This suggests that although $FISB_{WL}$ is imprecise (Figure 7.), it captures the extent that flow influenced steering across each road condition fairly well.

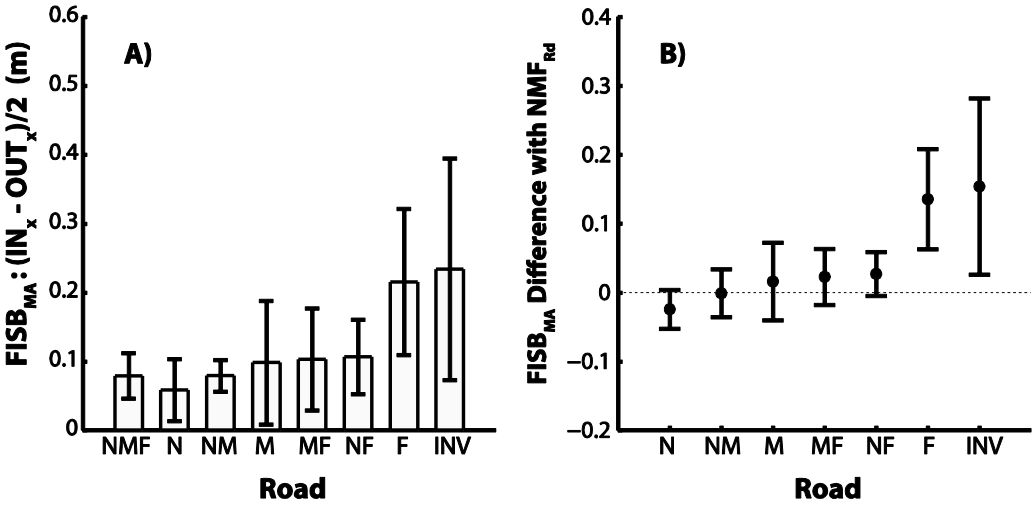

Figure 7.11 A) MA estimation of FISB, using (IN_x - OUT_x)/2 obtained from $FISB_{50}$and $FISB_{100}$. B) Difference between the means of each estimate and a full road. Note that the order of road conditions is identical to Figure 7.5. Error bars represent 95% CIs.

The critical reason for calculated $FISB_{MA}$ was to test whether the reduction in $FISB_{WL}$ from NMF_{Rd} to NM_{Rd} or N_{Rd} is reliable. Importantly, the $FISB_{MA}$ paired difference for NMF_{Rd}-NM_{Rd} sits on zero (Figure 7.11B), whereas same paired difference for $FISB_{WL}$ sat below zero (Figure 7.5B). This suggests that flow influence may not reliable reduce from NMF_{Rd} to NM_{Rd}. In contrast, the $FISB_{MA}$ paired difference for NMF_{Rd} – N_{Rd} sits below zero (Figure 7.11B), which corroborates the reported reduction for $FISB_{WL}$ (Figure 7.5B). This suggests that removing both mid and far road segments does indeed reduce FISB. The similarity of NM_{Rd} to NMF_{Rd} in Figure 7.11 is consistent with the proposal that the mid road segment provides enough compensatory or guidance signal for steering to not drastically differ when either the near or far road components are removed – substantial differences seem to only occur when *all* guidance signal (i.e. both mid and far road) or *all* compensatory signal (i.e. both near and mid road) is removed (see section 7.3.5).

The pattern of FISB from the current experiment strongly suggests that steering using feedback from near road edges relies less on flow direction than steering using feedback from far road edges. This builds on evidence presented in Chapter 6. By

combining the two studies via meta-analytic estimation (Figure 7.12), it is simple to observe that this trend is consistent across experiments and across magnitudes of flow. The estimates for the larger magnitude (1.5m, or 100%) are all enlarged, but the pattern is still consistent with the estimates for a .75m (or 50%) positional shift. This likely reflects the larger change in flow direction (1.5m rather than .75m), which supports a precise relationship between steering output and flow direction magnitude (discussed later). The precision obtained through the meta-analytic estimation shows that the pattern across experiments and across flow levels is one of high FISB for INV_{Rd} and F_{Rd} (MA_{INV}=.23m [.14, .31]; MA_F=.21m [.15, .27]) and reduced FISB for NMF_{Rd} and N_{Rd} (MA_{NMF}=.08m [.06, .1]; MA_N=.05m [.03, .08]), reinforcing the suggesting that adding the near road component reduces FISB. In particular, adding a near road component to INV_{Rd} causes FISB to reduce to ~24% of the original value, and adding near and mid component to far road causes FISB to reduce to ~37% of MA_F. An additional emergent characteristic of the meta-analytic estimation is the consistent trend of a reduction in FISB from NMF_{Rd} to N_{Rd} by about ~29%.

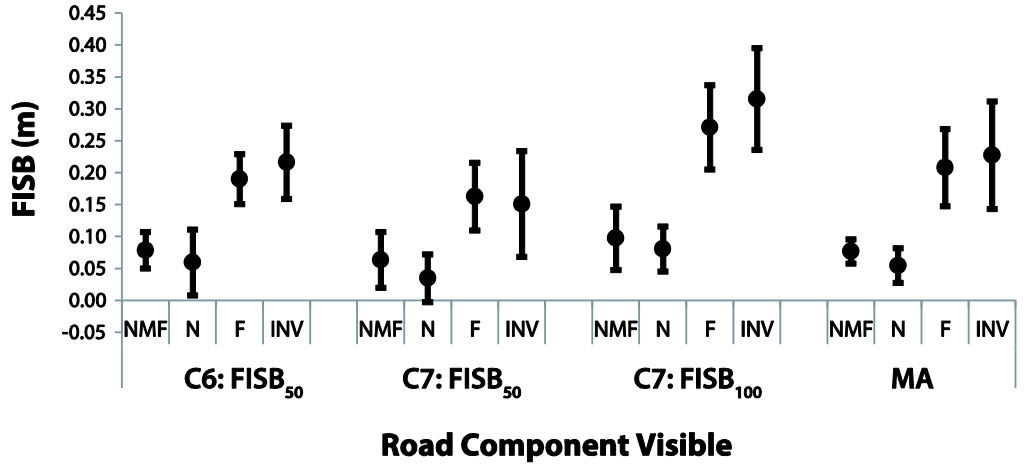

Figure 7.12 Flow influence was estimated using the formula (IN_X – OUT_x)/2, meaning that all estimates are in the same units (m). The estimations are combined using a random effects meta-analysis. Random effects was used, rather than fixed effects, because it does not assume that the same underlying effect is being estimated, thus estimates using slightly different parameters (i.e. of road component sizes and flow speed magnitudes) can be included. As with Chapter 5, the larger experiment provides two estimates, one for each magnitude of flow level, this allows assessment of whether trends are consistent throughout experiments and across flow magnitudes. The magnitude of FISB is denoted in the subscript on the x axis label. Error bars are 95% Confidence Intervals.

Crucially, the reduction of FISB from MA_{NMF} to MA_N demonstrates that FISB influence is further negated when the task becomes more reliant on near road information. As investigated in Figure 7.12B, two ways of calculating FISB both seem to suggest a reduction in FISB from NMF_{Rd} to N_{Rd} for the current experiment. To assess whether this difference is consistent throughout both Chapters 6 & 7, a meta-analysis was conducted on the paired differences between NMF_{Rd} and N_{Rd} (Figure 7.13). Individually the estimates are not conclusive because the 95% CIs are large so there is uncertainty about the direction and magnitude of the paired difference. The meta-analytic estimate is much more precise, which reflects that the same trend is exhibited across experiments and across flow levels. Critically, the combined estimate suggests

that there is indeed a reliable reduction in FISB from NMF_{Rd} to N_{Rd} (M=-.02 [-.05, 0.01]).

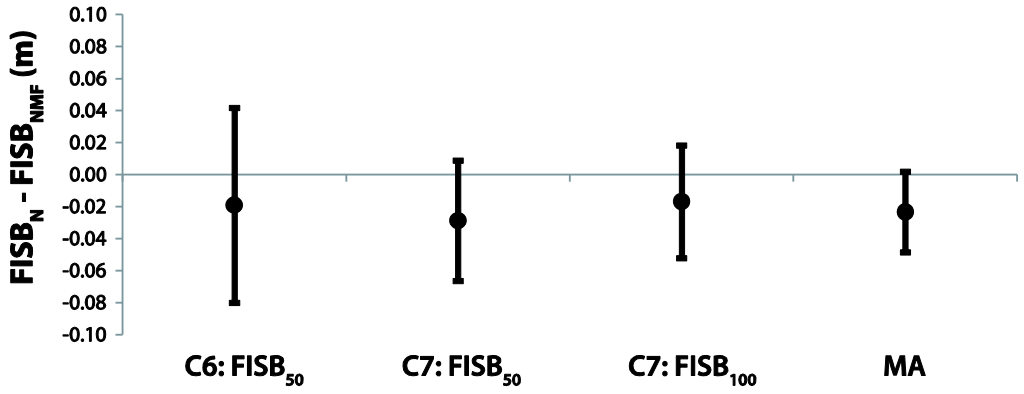

Figure 7.13 As per Figure 7.12 Flow influence was estimated using the formula (IN_X – OUT_x)/2. The paired difference between the means of FISB for NMF_{Rd} and N_{Rd} was estimated across experiments, and also across flow levels for Chapter 7 (where the design is expanded). These three estimates were then combined through random effects meta-analysis. Error bars represent 95% CIs.

7.5.1 Is steering output precisely modulated by flow direction magnitude?

The current experiment included five flow levels to assess whether the steering response to biasing flow direction was precisely yoked to the magnitude of the flow direction bias, or whether it was based on general impressions of understeering or oversteering. It was also discussed that the presence of task-relevant information in the scene may impose limits to the amount of accruable error before steering corrections were executed (e.g. Gordon and Magnuski, 2006; section 7.1).

The magnitude of flow direction bias was doubled from .75m (OUT_{50} and IN_{50}) to 1.5m (OUT_{100} and IN_{100}). If there was a precise relationship between flow direction and steering response then the magnitude of positional change for IN_{100} and OUT_{100} would be roughly double that observed for IN_{50} and OUT_{50}. In order to investigate this, Figure 7.14 plots the step-change in steering bias caused by each .75m change in magnitude of flow direction bias (e.g. from VE_F to IN_{50}, then again from IN_{50} to IN_{100}). Figure 7.10 demonstrates that steering response tends to settle in the latter stages of trajectory

development, so the values in Figure 7.14 were calculated from the last second of the trial. In Figure 7.14 paired bars of equal magnitude would indicate a steering response that is perfectly proportional to flow direction bias. There is particular evidence for this during F_{Rd}, where the steering response is large but increases an approximately equal amount for each .75m increase in flow direction bias (this can be usefully compared with the even spread of average trajectories in Figure 7.10G). This is evidence for a precise relationship between flow direction and steering response, suggesting that flow direction has a functional and specifiable role in steering control, and is not simply based on general impressions of understeering or oversteering.

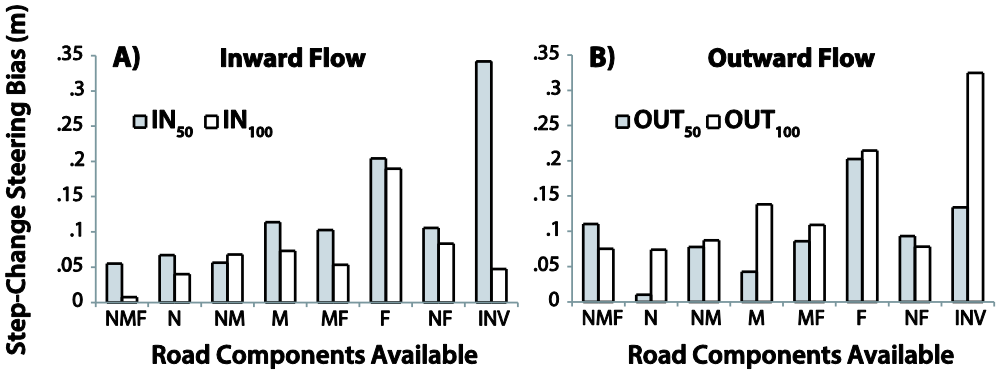

Figure 7.14 The step-change in steering bias (averaged over the last second of the trail) which occurs due to an additional .75m flow shift for A) Inward flow and B) Outward flow. These values are derived from group averages therefore there are no error bars. Note that the step change for OUT_{100} and IN_{100} is the magnitude of steering bias observed that *is not accounted for* by OUT_{50} or IN_{50}.

If the available task information imposed perceptual limits for error, it may be expected that the second flow direction step-change (e.g. from IN_{50} to IN_{100}) would be a smaller magnitude than the first. This may occur if the threshold for accruable error was reached during the first flow direction step-change (i.e. from VE_F to IN_{50}), or at some point a shortly after, thus constraining the magnitude of the second step-change. There is evidence for this for NMF_{Rd}, where IN_{100} does not produce greater oversteering than IN_{50} (Figure 7.14A; note also the overlapping trajectories of IN_{50} and IN_{100} in Figure 7.10A); however, the same pattern does not occur during outward

translation for NMF_{Rd} (Figure 7.14B). It appears that NMF_{Rd} may be an isolated case. Although it is common for the IN_{100} to produce less than double the magnitude of steering bias observed in IN_{50} (Figure 7.14A; despite a doubled flow direction bias magnitude), this does not appear to alter systematically with road component availability which would be expected if RE information imposed 'limits' to accruable error. Rather, it most likely reflects to propensity for oversteering to develop less readily in response to flow manipulations than understeering in these displays (consistent with Chapter 5's results; Figure 5.12); indeed, the step-change in flow direction bias from OUT_{50} to OUT_{100} tends to produce a *greater* understeering shift than the step-change in flow direction bias from VE_F to OUT_{50} (Figure 7.14B).

The evidence appears to suggest that flow direction is responded to in a proportional manner which varies in magnitude across road conditions. Flow direction therefore has a functional and specifiable role in two-level steering control.

7.5.2 Implications for Two-Level Steering Control

The current experiment used Chapter 5's road manipulations to systematically explore how guidance and compensatory RE signals are combined to support steering control. Consistent with the results reported in Chapter 5, the current experiment shows that NF_{Rd} and M_{Rd} share quantitative and qualitative similarities (see Figure 7.10D & F). This is not captured by the current additive two-stage model (Salvucci & Gray, 2004), which predicts that two 'strong' signals would produce equivalent behaviour to NMF_{Rd} (Land & Horwood, 1995). This is a non-trivial replication, as it reinforces the notion that the two-level framework needs developed in order to fully capture how the visual-system response to dynamically changing RE inputs.

The current experiments expanded Chapter 6's flow direction manipulation to investigate how flow direction was combined with RE inputs to support steering control. The findings support the proposals of Chapter 6 – that flow direction may be combined into the two-level framework through a weighted combination (as per

Wilkie & Wann, 2002) with a compensatory signal. Chapters 6 and 7 demonstrate that directional information from flow may have a specifiable role within two-level steering control, providing the first evidence that 'bridges the gap' between two-level steering control models (e.g. Saleh et al., 2011; Salvucci & Gray, 2004) and flow inspired models (e.g. Wilkie et al., 2008). Although these experiments do not provide a definite answer to *how* flow is used – e.g. whether heading (Warren et al., 1991) or path (Wann & Swapp, 2000) is recovered – they do provide an exciting avenue for future work into how humans combine multiple sources of information to support steering with road edges.

CHAPTER 8

GENERAL DISCUSSION

8.1 Review

For humans, vision is the predominant sense for perceiving the layout of the environment and thus identifying possible paths towards a goal. Although the exact nature of how visual information is used to identify paths and control steering is still debated, evidence suggests that humans are capable of combining multiple sources of visual information (Wilkie & Wann, 2002). Researchers who have considered the case of driving often treat road edges as the sole informational input for controlling steering, but this approach is not consistent with the notion that the human visual system adaptively uses multiple inputs to maintain robust control of steering. The experimental work reported here has primarily investigated how optic flow is combined with road edge information to support steering along constrained paths.

The first experiment developed a novel flow manipulation to try to generate predictable steering biases. It was important to have a method of quantifying reliance on optic flow, so that the flow contribution when steering could be assessed across different road conditions. Intriguing results have been presented by Kountouriotis et al. (2013) which suggest that drivers might respond predictably to global flow speed manipulations. This was subsequently confirmed in a follow-on experiment (Kountouriotis et al., 2015): increasing flow speed to levels faster-than-veridical appeared to cause oversteering and decreasing flow speed to levels slower-than-veridical appeared to cause understeering. Chapter 2 developed displays that differed from those in Kountouriotis et al (2013; 2015) in that they manipulated the entire flow field (as opposed to regions of texture either side of a road) and used explicitly

rendered white lines to denote REs (as opposed to a separately textured or coloured region used in Kountouriotis et al., 2013). This method would facilitate manipulating road information in later chapters. Crucially, this meant that 'use of flow' could be quantified from measuring the magnitude of directional deviation from the road centre (Steering Bias) throughout a trial – namely 'flow-induced steering bias' (FISB).

Chapter 3 created road conditions which varied the amount of guidance or compensatory road edge information available in the scene whilst also measuring FISB. Two frameworks were presented and used throughout the remainder of the thesis. The first framework – *Modulation Hypothesis* – considers road edge information to be the prime determinant of the steering control solution. In this case the contribution of flow information is restricted to acting upon a road edge signal (i.e. when a RE signal is absent, flow information is unable to contribute to the task), therefore optic flow offers complementary information which may *modulate* the control signal supplied by RE information. The second framework – *Weighted Combination Hypothesis* – considers that road edge and flow information combine to provide a steering control solution, therefore optic flow offers competing information which could be combined in a weighted fashion with RE information. In this case, when RE is absent (effectively zero weight), the contribution of flow information would increase (effectively 100% weight).

Chapter 3 also monitored gaze behaviours to document how manipulating REs affect eye-movements, which had not been documented in previous studies that vary RE information (Chatziastros et al., 1999; Cloete & Wallis, 2011; Land & Horwood, 1995). The pattern of flow influence across road conditions appeared to suggest that the influence of flow was dependent particularly on the presence of far road information. However, there were accompanying systematic changes in gaze. In particular, gaze was vertically relocated downwards when far road edges were removed and moved lower in the scene towards the remaining RE information (near road edges). This made it

difficult to conclusively determine whether the observed differences in steering behaviour were due to RE manipulations, or changes in gaze behaviours.

To address this issue, Chapter 4 reports the extent of steering bias when gaze was constrained to a far point. The results appear to support the hypothesis that flow speed influenced steering more when guidance information was present, and less when guidance information was removed. Additionally, some important comparisons were made between Chapters 3 and 4. In Chapter 3, when only near road was present (and gaze dropped to low in the scene) steering behaviour was characterised by high jerk, high error, and negligible FISB. For identical road conditions in Chapter 4, constraining gaze to a far point made steering smoother (although still jerky compared to a complete road), reduced steering error to similar levels as when a complete road was visible, and caused a small amount of FISB (in Chapter 3 there was no FISB). Simply moving gaze forward appeared to alter the steering response to flow manipulations and enabled the visual-motor system to successfully compensate for removing guidance RE information (i.e. steering was kept accurate at the expense of steering smoothness). This provides evidence that gaze may modulate how steering control responds to changing RE information which has implications for the interpretation of previous two-level studies (Chatziastros et al., 1999; Cloete & Wallis, 2011; Frissen & Mars, 2014; Land & Horwood, 1995). It also highlights the need to consider the role of gaze direction when analysing steering behaviours.

Chapter 5 sought to examine the hypothesis that flow speed modulates the guidance signal by investigating whether steering responses scale precisely with flow magnitude, and by assessing FISB over intermediate road manipulations. It was found that steering was indeed precisely modulated by flow speed, in a manner consistent with Authié & Mestre's (2012) suggestions that perception of flow speed falls under Weber's Law. Importantly, the magnitude of FISB was still broadly determined by the presence of guidance level information. There was an interesting exception to this rule: when the road was 'split' into a far and a near region behaviour was similar to when *only* a

middle region was displayed, and dissimilar to when a full road was available. This finding was later replicated in Chapter 7, and questions the simple additive process of combining compensatory and anticipatory modes of control, which is common amongst two-level models (e.g. Salvucci & Gray, 2004; Saleh et al., 2011).

In Chapter 6, a novel flow manipulation was used – instead of artificially altering flow *speed* the experiments manipulated flow *direction* instead. As previously, use of the flow information should cause predictable steering biases. In Chapter 2 an effect of global flow speed was expected (see Kountouriotis et al., 2013; 2015), however the literature was mixed on whether consistent effects due to flow *direction* were to be expected (see Li & Chen, 2010, and Beall & Loomis, 1996). The experimental design used in Chapter 4 was adapted to assess i) whether flow direction biased steering when road edges were present, and ii) whether this varied dependent on the type of RE information available. The results from Chapter 6 demonstrated that flow direction could indeed bias trajectories even with full RE information present. Interestingly, the pattern of FISB indicated that the presence of near road edges acted to diminish (but not remove) the influence of flow direction on steering, in a manner suggestive of a weighted combination of the two variables. In similar manner to Chapter 5, Chapter 7 sought to examine this hypothesis further. It was found that steering behaviour was precisely determined by flow direction magnitude, and that this was indeed yoked to the amount of compensatory information present in the scene.

Overall, the thesis has demonstrated that the contribution of flow to steering control can be understood within the context of two-level steering (Donges, 1978). More importantly, different characteristics of flow (i.e. speed or direction) appear to interact with RE information in different ways – flow speed acts indirectly through modulating RE signals, whereas flow direction acts directly by competing with RE signals. Both of these findings are novel, and should motivate future work into how multiple sources of information are combined with RE information to support steering control. An approach which emphasises robust control through combining multiple

informational inputs (e.g. flow information, road edges, and gaze direction) is vital if we are to fully understand how the visual-motor system solves the problem of steering along constrained paths.

8.2 Future Work

This thesis is the first attempt to systematically investigate how optic flow information is combined with road edge information whilst steering bends and the findings pose many questions for future research.

One issue is the role of gaze direction in steering control. The findings of Chapter 3 and Chapter 4 present compelling evidence that key aspects of steering control studied in this thesis – smoothness, precision, and the response to flow manipulations – can be altered merely by directing gaze farther forward in the scene. However, it is unclear whether the difference was due to extra-retinal direction cues, retinal direction cues (from the fixation cross), or some advantage of using flow information from 'looking where you are going' (as per Wann & Swapp, 2000). There is not a condition in the thesis where the participants are forced to look farther ahead but the fixation cross is removed (which should provide extra-retinal direction without retinal direction). This was done because without a fixation cross to stabilise gaze, fixation is likely to drift throughout a trial. An experimental work-around could be to display the fixation cross at the beginning of a trial, and perhaps once or twice more at intervals throughout the trial. This would mean that gaze is kept fairly stable and directed to a far point, but without the strong cues of retinal direction that the permanently visible fixation cross provides. Using this technique, it would be possible to look at fixations at various vertical gaze angles to systematically assess how extra-retinal direction cues interact with road edge information.

Another issue is that the flow manipulations used always manipulate the entire flow field, and that flow information was always rich (i.e. high contrast texture

information). In naturalistic scenarios, it is more common to have road edge information broken or occluded then it is to have sections of the flow field occluded but RE information present. However, it would be interesting to see if the usefulness of flow depended on the location or quality of flow information. One example where this research may be impactful is situations where visual input is disrupted. For example, in visual field loss drivers might not have access to the full, high quality flow field (Smith et al., 2015). How the removal or degradation of local flow information might impact steering control is not well understood, and is an important avenue to explore if this research is to be impactful and inform driving rehabilitation.

A major theme for future work is the explicit modelling of the emergent themes of the thesis. The two-stage approach of a guidance component that previews upcoming steering requirements, and a compensatory component that fine-tunes position-in-lane, has resulted in many control-theoretic models that capture various steering behaviours fairly well, for example lane-changing and car following (e.g. Markkula et al., 2014; Plöchl & Edelmann, 2007; for a review see Steen et al., 2011). However, these control-theoretic models tend to overlook the capabilities of the human sensorimotor system. The primary perceptually-inspired two-level model involves a simple additive combination of guidance and compensatory modes of control (Salvucci & Gray, 2004).

One avenue for modelling the role of flow speed and flow direction could be to use Salvucci & Gray's (2004) simple feedback model, and incorporate the multiple weightings approach adopted by Wilkie et al. (2008). The two models are conceptually similar, and the mathematics of reformulating the models to incorporate a dual-component model with multiple informational inputs is not difficult. Preliminary scripts that use genetic algorithms (Haupt & Haupt, 2004) to fit such a computational model to the trajectories observed in this thesis are in development, but are beyond the scope of this thesis. It appears that flow direction may be more straightforward than flow speed to incorporate into a computational model. Flow direction can be easily modelled in an input/output feedback relationship, in much the same way as RE

information, therefore easily lends itself to weighted combination techniques. Flow speed appears to inform steering control only indirectly. It is unclear, at this stage, whether flow speed would modulate guidance level information as part of a feedback loop, or act concurrently as part of more traditional 'open-loop' control (Donges, 1978).

The investigation of open-loop control is critical for future research. Open-loop control relies on internal models, and it is unclear how the perceptual variables involved in 'online' steering control (e.g. road edges, extra-retinal direction, and flow direction) are combined to tune up the internal models necessary for open-loop control. A theme of this thesis is that the simple additive combination of guidance and compensatory control (e.g. Salvucci & Gray, 2004) appears to be overly reductionist, as it does not appear to account for the steering behaviours observed in this thesis. It seems that to fully capture the response to flow, more sophisticated two-level models need to be developed. Development of techniques to investigate open-loop control could provide the sophistication needed to develop perceptually-grounded two-level models which capture a wide-range of steering behaviours.

Modelling steering behaviour is at an exciting stage. This thesis demonstrates that future steering models need to carefully consider the contribution of many informational inputs available to an observer. Although perceptually-grounded models are, at the moment, restricted to simple feedback models (Salvucci & Gray, 2004; Wilkie et al., 2008), there is scope to incorporate machine learning and control theory techniques which could help develop more sophisticated models that not only assess what informational inputs are being used during a bend but can also capture how steering behaviour is planned before bend entry. Such comprehensive modelling of steering behaviour is essential if the visual science literature is to keep up with recent advancements in shared automobile and human control (Abbink, Mulder, & Boer, 2012). For example, interesting advancements have been made by Frank Mars and colleagues, who have looked at combining Salvucci & Gray's (2004) two-level model

with an explicit neuromuscular model of actions on the steering wheel (Saleh et al., 2011; Sentouh et al., 2009). This holistic approach to steering modelling is essential for shared control, but as yet the visual science literature has not developed sophisticated enough steering models to hold up its end of the bargain.

Computer simulated locomotor control studies allow the precise manipulation of all visual variables available to an observer in a controlled and randomised fashion so provide robust estimates of the perceptual-motor capabilities and sensitivities of human drivers. Furthermore the road and flow manipulations used throughout the thesis would simply have been impossible to achieve in the real world. It should be acknowledged, however, that such displays lack the validity of observing behaviour in 'natural' real-world driving scenarios. That is not to say that the work does not translate to real-world conditions, but that this needs to be established through experiments informed by those in the in the laboratory where possible. The quality of flow information in natural scenarios varies, with 'low quality' flow information evident when driving at night or in fog, whereas 'higher quality' flow information would be available when driving along country lanes lined with hedges. The optic flow rate will be dependent on viewing characteristics such as eye-height, and will be subject to neuronal adaptation (as experienced during the 'coming off the motorway' scenario, where 30mph feels much slower after travelling at 70mph for a long period; Denton, 1976). It is clear that there are many real-world scenarios where flow signals may be unreliable, which according to my thesis will have ramifications for steering control. A potential avenue for investigating whether flow-inspired simulator predictions transfer to real-world driving could be to recruit Laser Scanning techniques which allow 3D modelling of natural environments (Otto Lappi – Personal Communication). It may be possible to scan a real-world environment and quantify the texture properties of the scene therefore allow modelling of various flow patterns produced by different trajectories and eye-heights. Using the findings of my experimental work, predictions could then be made about the steering responses of

drivers, and tested through observing real-world trajectories through the same environments. A combination of laboratory and real-world studies has proved to be powerful. For example, predictions about gaze behaviour (i.e. drivers should look where they want to go) which developed from controlled driving simulator studies (Wilkie et al., 2008; Wilkie & Wann, 2002, 2003b) have now been validated by real-world studies (Itkonen et al., 2015; Lappi et al., 2013). This cross-fertilisation is essential for the future of successfully modelling steering control.

REFERENCES

Abbink, D. A., Mulder, M., & Boer, E. R. (2012). Haptic Shared Control: smoothly shifting control authority? *Cognition, Technology & Work*, *14*(1), 19–28.

Authié, C. N., Hilt, P. M., N'Guyen, S., Berthoz, A., & Bennequin, D. (2015). Differences in gaze anticipation for locomotion with and without vision. *Frontiers in Human Neuroscience*, *9*(312), 1–16.

Authié, C. N., & Mestre, D. R. (2011). Optokinetic nystagmus is elicited by curvilinear optic flow during high speed curve driving. *Vision Research*, *51*(16), 1791–800.

Authié, C. N., & Mestre, D. R. (2012). Path curvature discrimination: dependence on gaze direction and optical flow speed. *PloS One*, *7*(2), e31479.

Ballard, D. H., & Hayhoe, M. M. (2009). Modelling the role of task in the control of gaze. *Visual Cognition*, *17*(6-7), 1185–1204.

Beall, A. C., & Loomis, J. M. (1996). Visual control of steering without course information. *Perception*, *25*(4), 481–94.

Bernardin, D., Kadone, H., Bennequin, D., Sugar, T., Zaoui, M., & Berthoz, A. (2012). Gaze anticipation during human locomotion. *Experimental Brain Research*, *223*, 65–78.

Billington, J., Field, D. T., Wilkie, R. M., & Wann, J. P. (2010). An fMRI study of parietal cortex involvement in the visual guidance of locomotion. *Journal of Experimental Psychology. Human Perception and Performance*, *36*(6), 1495–507.

Blouin, J., Gauthier, G. M., & Vercher, J. (1995). Internal representation of gaze direction with and without retinal inputs in man. *Neuroscience Letters*, *183*, 187–189.

Borenstein, M., Hedges, L. V., Higgins, J. P. T., & Rothstein, H. R. (2009). *Introduction*

to Meta-Analysis. Chichester, United Kingdom: Wiley.

Bridgeman, B., & Stark, L. (1991). Ocular proprioception and efference copy in registering visual direction. *Vision Research*, *31*(11), 1903–1913.

Brown, J. (1931). The visual perception of velocity. *Psychologische Forschung*, *14*(1), 199–232.

Chattington, M., Wilson, M., Ashford, D., & Marple-Horvat, D. E. (2007). Eye-steering coordination in natural driving. *Experimental Brain Research*, *180*, 1–14.

Chatziastros, A., Wallis, G. M., & Bülthoff, H. H. (1999). The Effect of Field of View and Surface Texture on Driver Steering Performance. In A. G. Gales, I. D. Brown, C. M. Haslegrave, & S. P. Taylor (Eds.), *Vision in Vehicles VII* (pp. 253–260). Amsterdam: Elsevier.

Cheng, J., & Li, L. (2011). Perceiving path from optic flow. *Journal of Vision*, *11(1)*(22), 1–15.

Cloete, S. R., & Wallis, G. M. (2009). Limitations of feedforward control in multiple-phase steering movements. *Experimental Brain Research*, *195*(3), 481–7.

Cloete, S. R., & Wallis, G. M. (2011). Visuomotor control of steering: the artefact of the matter. *Experimental Brain Research*, *208*(4), 475–89.

Cumming, G. (2012). *Understanding The New Statistics: Effect Sizes, Confidence Intervals, and Meta-Analysis*. New York: Taylor & Francis Group.

Cumming, G. (2014). The new statistics: why and how. *Psychological Science*, *25*(1), 7–29.

Denton, G. G. (1976). The influence of adaptation on subjective velocity for an observer in simulated rectilinear motion. *Ergonomics*, *19*(4), 409–30.

Denton, G. G. (1980). The influence of visual pattern on perceived speed. *Perception*,

9, 393–402.

Department for Transport. (2015a). Reported Road Casualties in Great Britain : Main Results 2014, (June).

Department for Transport. (2015b). Vehicle Licensing Statistics : Quarter 2 (Apr - Jun) 2015, (September).

Desmurget, M., & Grafton, S. (2000). Forward modeling allows feedback control for fast reaching movements. *Trends in Cognitive Sciences*, *4*(11), 423–431.

Dickinson, M. H., Farley, C. T., Full, R. J., Koehl, M. A. R., Kram, R., & Lehman, S. (2000). How Animals Move: An Integrative View. *Science*, *288*(5463), 100–106.

Donges, E. (1978). A two-level model of driver steering behavior. *Human Factors*, *20*(6), 691–707.

Duchon, A. P., & Warren, W. H. (2002). A Visual Equalization Strategy for Locomotor Control: Of Honeybees, Robots, and Humans. *Psychological Science*, *13*(3), 272–278.

Ernst, M. O., & Banks, M. S. (2002). Humans integrate visual and haptic information in a statistically optimal fashion. *Nature*, *415*(6870), 429–33.

Faisal, a A., Selen, L. P. J., & Wolpert, D. M. (2008). Noise in the nervous system. *Nature Reviews. Neuroscience*, *9*(4), 292–303.

Fajen, B. R., & Warren, W. H. (2000). Go with the flow. *Trends in Cognitive Sciences*, *4*(10), 369–370.

Fajen, B. R., & Warren, W. H. (2003). Behavioral dynamics of steering, obstacle avoidance, and route selection. *Journal of Experimental Psychology. Human Perception and Performance*, *29*(2), 343–362.

Fidler, F., & Loftus, G. R. (2009). Why Figures with Error Bars Should Replace *p*

Values. *Zeitschrift Für Psychologie / Journal of Psychology*, *217*(1), 27–37.

Fildes, B. N., & Triggs, T. J. (1985). The effect of changes in curve geometry on magnitude estimate of road-line perspective curvature. *Perception & Psychophysics*, *37*, 218–224.

Frissen, I., & Mars, F. (2014). The effect of visual degradation on anticipatory and compensatory steering control. *Quarterly Journal of Experimental Psychology*, *67*(3), 499–507.

Gibson, J. J. (1950). *Perception of the visual world.* Boston: Houghton Mifflin.

Gibson, J. J. (1958). Visually Controlled Locomotion and Visual Orientation in Animals. *British Journal of Psychology*, *49*(3), 182–194.

Gibson, J. J., Olum, P., & Rosenblatt, F. (1955). Parallax and perspective during aircraft landings. *The American Journal of Psychology*, *68*(3), 372–385.

Gordon, T., & Magnuski, N. (2006). Modeling normal driving as a collison avoidance process. *Proceedings of 8th International Symposium on Advanced Vehicle Control.*

Grasso, R., Prévost, P., Ivanenko, Y., & Berthoz, A. (1998). Eye-head coordination for the steering of locomotion in humans: an anticipatory synergy. *Neuroscience Letters*, *253*, 115–118.

Gray, R., & Regan, D. (2000). Risky driving behavior: A consequence of motion adaptation for visually guided motor action. *Journal of Experimental Psychology: Human Perception and Performance*, *26*(6), 1721–1732.

Gray, R., & Regan, D. M. (2005). Perceptual Processes Used by Drivers During Overtaking in a Driving Simulator. *Human Factors: The Journal of the Human Factors and Ergonomics Society*, *47*(2), 394–417.

Harris, J. M. (2001). The future of flow? *Trends in Cognitive Sciences*, *5*(1), 7–8.

Harris, J. M., & Bonas, W. (2002). Optic flow and scene structure do not always contribute to the control of human walking. *Vision Research*, *42*, 1619–1626.

Harris, J. M., & Rodgers, B. J. (1999). Going against the flow. *Trends in Cognitive Sciences*, *3*, 449–450.

Haupt, R. L., & Haupt, S. E. (2004). *Practical Genetic Algorithms* (Second Edi). Hoboken, New Jersey: John Wiley & Sons, Inc.

Higuchi, T. (2013). Visuomotor control of human adaptive locomotion: understanding the anticipatory nature. *Frontiers in Psychology*, *4*(277), 1–9.

Hoekstra, R., Morey, R. D., Rouder, J. N., & Wagenmakers, E.-J. (2014). Robust misinterpretation of confidence intervals. *Psychonomic Bulletin & Review*, 1–7.

Hoenig, J. M., & Heisey, D. M. (2001). The abuse of power: The pervasive fallacy of power calculations for data analysis. *American Statistician*, *55*, 19–24.

Hollands, M. a, Patla, a E., & Vickers, J. N. (2002). "Look where you're going!": gaze behaviour associated with maintaining and changing the direction of locomotion. *Experimental Brain Research*, *143*(2), 221–30.

Howard, I. P. (1982). *Human Visual Orientation*. Chichester, United Kingdom: Wiley.

Itkonen, T., Pekkanen, J., & Lappi, O. (2015). Driver Gaze Behavior Is Different in Normal Curve Driving and when Looking at the Tangent Point. *Plos One*, *10*(8),

Jagacinski, R. J., & Flach, J. M. (2003). *Control Theory for Humans: Quantitative Approaches to Modeling Performance*. Mahwah, NJ: Erlbaum.

Kandil, F. I., Rotter, A., & Lappe, M. (2009). Driving is smoother and more stable when using the tangent point. *Journal of Vision*, *9*, 1–11.

Kandil, F. I., Rotter, A., & Lappe, M. (2010). Car drivers attend to different gaze targets

when negotiating closed vs. open bends. *Journal of Vision*, *10(4)*(24), 1–11.

Kemeny, A., & Panerai, F. (2003). Evaluating perception in driving simulation experiments. *Trends in Cognitive Sciences*, *7*(1), 31–37.

Kim, N. G., & Turvey, M. T. (1998). Visually perceiving heading on circular and elliptical paths. *Journal of Experimental Psychology. Human Perception and Performance*, *24*(6), 1690–704.

Kim, N. G., & Turvey, M. T. (1999). Eye movements and a rule for perceiving direction of heading. *Ecological Psychology*, *11*, 233–248.

Kline, R. (2004). What's Wrong With Statistical Tests--And Where We Go From Here.

Kountouriotis, G. K., Floyd, R. C., Gardner, P. H., Merat, N., & Wilkie, R. M. (2012). The role of gaze and road edge information during high-speed locomotion. *Journal of Experimental Psychology: Human Perception and Performance*, *38*(3), 687–702.

Kountouriotis, G. K., Mole, C. D., Merat, N., Gardner, P. H., & Wilkie, R. M. (2015). Steering along curved paths is influenced by global flow speed not speed asymmetry. *Journal of Vision*, *15*(12), 416.

Kountouriotis, G. K., Shire, K. A., Mole, C. D., Gardner, P. H., Merat, N., & Wilkie, R. M. (2013). Optic flow asymmetries bias high-speed steering along roads. *Journal of Vision*, *13*(10), 1–9.

Kountouriotis, G. K., & Wilkie, R. M. (2013). Displaying optic flow to simulate locomotion: Comparing heading and steering. *i-Perception*, *4*, 333–46.

Land, M. F. (1971). Orientation by jumping spiders in the absence of visual feedback. *The Journal of Experimental Biology*, *54*(1), 119–139.

Land, M. F. (1998). The visual control of steering. In L. R. Harris & H. Jenkins (Eds.),

Vision and Action (pp. 421–441). Cambridge: Cambridge University Press.

Land, M. F., & Horwood, J. (1995). Which parts of the road guide steering? *Nature*, *377*(6547), 339–40.

Land, M. F., & Lee, D. N. (1994). Where we look when we steer. *Nature*, *369*, 742–744.

Lappe, M., Bremmer, F., & van den Berg, A. V. (1999). Perception of self-motion from visual flow. *Trends in Cognitive Sciences*, *3*(9), 329–336.

Lappi, O. (2014). Future path and tangent point models in the visual control of locomotion in curve driving. *Journal of Vision*, *14*(12), 1–22.

Lappi, O., & Pekkanen, J. (2013). Beyond the tangent point: Gaze targets in naturalistic driving. *Journal of Vision*, *13(13)*(11), 1–18.

Lappi, O., Pekkanen, J., & Itkonen, T. H. (2013). Pursuit eye-movements in curve driving differentiate between future path and tangent point models. *PloS One*, *8*(7), e68326.

Layton, O. W., & Browning, N. A. (2014). A unified model of heading and path perception in primate MSTd. *PLoS Computational Biology*, *10*(2), 1–20.

Lee, D. N., & Lishman, R. (1977). Visual control of locomotion. *Scandinavian Journal of Psychology*, *18*(1), 224–230.

Lehtonen, E., Lappi, O., Kotkanen, H., & Summala, H. (2013). Look-ahead fixations in curve driving. *Ergonomics*, *56*(1), 34–44.

Lehtonen, E., Lappi, O., & Summala, H. (2012). Anticipatory eye movements when approaching a curve on a rural road depend on working memory load. *Transportation Research Part F: Traffic Psychology and Behaviour*, *15*(3), 369–377.

Li, L., & Chen, J. (2010). Relative contributions of optic flow, bearing, and splay angle

information to lane keeping. *Journal of Vision*, *10*, 1–14.

Li, L., Chen, J., & Peng, X. (2009). Influence of visual path information on human heading perception during rotation. *Journal of Vision*, *9(3)*(29), 1–14.

Li, L., & Cheng, J. (2011). Heading but not path or the tau-equalization strategy is used in the visual control of steering toward a goal. *Journal of Vision*, *11*, 1–12.

Li, L., Sweet, B. T., & Stone, L. S. (2006). Humans can perceive heading without visual path information. *Journal of Vision*, *6*(9), 874–81.

Llewellyn, K. R. (1971). Visual Guidance of locomotion. *Journal of Experimental Psychology*, *91*, 245–261.

Longuet-Higgins, H., & Prazdny, K. (1980). The interpretation of a moving retinal image. *Proceedings of the Royal Society of London. Series B, Biological Sciences*, *208*(1173), 385–397.

Loomis, J. M., & Beall, A. C. (2003). Visual control of locomotion without optic flow. *Journal of Vision*, *3*(9), 132.

Macuga, K. L., Beall, A. C., Kelly, J. W., Smith, R. S., & Loomis, J. M. (2007). Changing lanes: Inertial cues and explicit path information facilitate steering performance when visual feedback is removed. *Experimental Brain Research*, *178*(2), 141–150.

Markkula, G., Benderius, O., & Wahde, M. (2014). Comparing and validating models of driver steering behaviour in collision avoidance and vehicle stabilisation. *Vehicle System Dynamics: International Journal of Vehicle Mechanics and Mobility*, *52*(12), 1658–1680.

Mars, F. (2011). Modeling the Visual and Motor Control of Steering With an Eye to Shared-Control Automation. *Proceeding of the Human Factors and Ergonomics Society 55th Annual Meeting*, 1422–1426.

McLean, J. R., & Hoffman, E. R. (1973). The effects of restricted preview on driver steering control and performance. *Human Factors*, *15*, 421–430.

Meehl, P. E. (1967). Theory testing in psychology and physics: A methodological paradox. *Philosophy of Science*, *34*, 103–115.

Mourant, R., & Rockwell, T. (1972). Strategies of visual search by novice and experienced drivers. *Human Factors*, *14*(4), 325–335.

Neumann, H., & Deml, B. (2011). The two-point visual control model of steering-new empirical evidence. In V. G. Duffy (Ed.), *Digital Human Modeling* (pp. 493–502). Berlin: Springer.

Owens, D. A., Wood, J., & Carberry, T. (2010). Effects of reduced contrast on the perception and control of speed when driving. *Perception*, *39*(9), 1199–1215.

Patla, A. E., & Vickers, J. N. (2003). How far ahead do we look when required to step on specific locations in the travel path during locomotion? *Experimental Brain Research*, *148*(1), 133–8.

Pelz, J. B., & Rothkopf, C. (2007). Oculomotor behavior in natural and man-made environments. In R. van Gompel (Ed.), *Eye Movements: A Window on Mind and Brain* (pp. 661–676). Amsterdam: Elsevier.

Plöchl, M., & Edelmann, J. (2007). *Driver models in automobile dynamics application. Vehicle System Dynamics* (Vol. 45).

Pretto, P., Bresciani, J.-P., Rainer, G., & Bülthoff, H. H. (2012). Foggy perception slows us down. *eLife*, *1*, e00031.

Readinger, W. O., Chatziastros, A., Cunningham, D. W., Bülthoff, H. H., & Cutting, J. (2002). Gaze eccentricity effects on road position and steering. *Journal of Experimental Psychology: Applied*, *8*(4), 247–258.

Regan, D., & Beverley, K. (1982). How do we avoid confounding the direction we are looking and the direction we are moving? *Science*, *215*(4529), 194–196.

Robertshaw, K. D., & Wilkie, R. M. (2008). Does gaze influence steering around a bend? *Journal of Vision*, *8(4)*(18), 1–13.

Rock, I., Goldberg, J., & Mack, A. (1966). Immediate correction and adaptation based on viewing a prismatically displaced scene. *Perception & Psychophysics*, *1*(5), 351–354.

Royden, C., Banks, M., & Crowell, J. A. (1992). The perception of heading during eye movements. *Nature*, *360*, 583–585.

Royden, C., Crowell, J. A., & Banks, M. (1994). Estimating heading during eye movements. *Vision Research*, *34*(23), 3197–3214.

Rushton, S. K. (2004). Egocentric Direction and Locomotion. In L. M. Vaina, S. A. Beardsley, & S. K. Rushton (Eds.), *Optic flow and beyond* (pp. 339–362). Dordrecht, The Netherlands: Kluwer Academic Publishers.

Rushton, S. K., Harris, J. M., Lloyd, M. R., & Wann, J. P. (1998). Guidance of locomotion on foot uses perceived target location rather than optic flow. *Current Biology*, *8*(21), 1191–4.

Rushton, S. K., & Salvucci, D. D. (2001). An egocentric account of the visual guidance of locomotion. *Trends in Cognitive Sciences*, *5*, 6–7.

Ryan, T. P. (2009). *Modern Regression Methods* (Second Edi). Hoboken, New Jersey: John Wiley & Sons, Inc.

Saleh, L., Chevrel, P., Mars, F., Lafay, J. F., & Claveau, F. (2011). Human-like cybernetic driver model for lane keeping. *Proceedings of the 18th World Congress of the International Federation of Automatic Control*, 4368–4373.

Salvucci, D. D., & Gray, R. (2004). A two-point visual control model of steering. *Perception*, *33*(10), 1233–48.

Saunders, J., & Ma, K. (2011). Can observers judge future circular path relative to a target from retinal flow? *Journal of Vision*, *11(7)*(16), 1–17.

Sentouh, C., Chevrel, P., Mars, F., & Claveau, F. (2009). A Sensoriomotor Driver Model for Steering Control. *Proceedings of the 2009 IEEE International Conference on Systems, Man and Cybernetics (SMC)*, (October), 2462–2467.

Shinar, D. (1977). Curve perception and accidents on curves: An illusive curve phenomenon? *Zeitschrift Fur Verkerhssicherheit*, *23*, 16–21.

Smith, M., Mole, C. D., Kountouriotis, G. K., Chisholm, C., Bhakta, B., & Wilkie, R. M. (2015). Driving with homonymous visual field loss: Does visual search performance predict hazard detection? *British Journal of Occupational Therapy*, *78*(2), 85–95.

Steen, J., Damveld, H. J., Happee, R., van Paassen, M. M., & Mulder, M. (2011). A review of visual driver models for system identification purposes. *2011 IEEE International Conference on Systems, Man, and Cybernetics (SMC)*, 2093–2100.

Summala, H., Nieminen, T., & Punto, M. (1996). Maintaining lane position with peripheral vision during in-vehicle tasks. *Human Factors*, *38*(3), 442–451.

Underwood, G., Chapman, P., Crundall, D. E., Cooper, S., & Wallen, R. (1999). The visual control of steering and driving: where do we look when negotiating curves? In A. G. Gale, I. D. Brown, C. M. Haslegrave, & S. P. Taylor (Eds.), *Vision in Vehicles VII* (pp. 245–252). Amsterdam: Elsevier.

van Leeuwen, P. M., Happee, R., & de Winter, J. C. F. (2014). Vertical field of view restriction in driver training: A simulator-based evaluation. *Transportation Research Part F*, *24*, 169–182.

Vansteenkiste, P., Cardon, G., D'Hondt, E., Philippaerts, R., & Lenoir, M. (2013). The visual control of bicycle steering: The effects of speed and path width. *Accident Analysis and Prevention*, *51*, 222–7.

Wann, J. P., & Land, M. F. (2000). Steering with or without the flow: is the retrieval of heading necessary? *Trends in Cognitive Sciences*, *4*(8), 319–324. Retrieved from

Wann, J. P., & Swapp, D. K. (2000). Why you should look where you are going. *Nature Neuroscience*, *3*(7), 647–8. http://doi.org/10.1038/76602

Wann, J. P., & Wilkie, R. M. (2004). How do We Control High Speed Steering? In L. M. Vaina, S. A. Beardsley, & S. K. Rushton (Eds.), *Optic flow and beyond* (pp. 371–389). Norwell, MA: Kluwer Academic Publishers.

Warren, W. H. (1998). Visually Controlled Locomotion: 40 years Later. *Ecological Psychology*, *10*(3-4), 177–219.

Warren, W. H., & Hannon, D. (1988). Direction of self-motion is perceived from optical flow. *Nature*, *336*(10), 162–163.

Warren, W. H., Kay, B. a, Zosh, W. D., Duchon, a P., & Sahuc, S. (2001). Optic flow is used to control human walking. *Nature Neuroscience*, *4*(2), 213–6.

Warren, W. H., Mestre, D. R., Blackwell, a W., & Morris, M. W. (1991). Perception of circular heading from optical flow. *Journal of Experimental Psychology. Human Perception and Performance*, *17*(1), 28–43.

Weir, D. H., & Wojcik, C. K. (1971). Simulator studies of the driver's dynamic response in steering control tasks. *Highway [Transportation] Research Record*, *364*, 1–15.

Wilkie, R. M., Kountouriotis, G. K., Merat, N., & Wann, J. P. (2010). Using vision to control locomotion: looking where you want to go. *Experimental Brain Research*, *204*(4), 539–47.

Wilkie, R. M., & Wann, J. P. (2002). Driving as night falls: the contribution of retinal flow and visual direction to the control of steering. *Current Biology*, *12*(23), 2014–7.

Wilkie, R. M., & Wann, J. P. (2003a). Controlling steering and judging heading: Retinal flow, visual direction, and extraretinal information. *Journal of Experimental Psychology: Human Perception and Performance*, *29*(2), 363–378.

Wilkie, R. M., & Wann, J. P. (2003b). Eye-movements aid the control of locomotion. *Journal of Vision*, *3*, 677–684.

Wilkie, R. M., & Wann, J. P. (2006). Judgments of path, not heading, guide locomotion. *Journal of Experimental Psychology. Human Perception and Performance*, *32*(1), 88–96.

Wilkie, R. M., Wann, J. P., & Allison, R. S. (2008). Active gaze, visual look-ahead, and locomotor control. *Journal of Experimental Psychology. Human Perception and Performance*, *34*(5), 1150–64.

Wood, R., Harvey, M., & Young, C. (2000). Weighting to go with the flow? *Current Biology*, *10*(15), 545–546.